EFFECT OF SURFACE ACTIVE AGENTS
IN
BOILING HEAT TRANSFER

EFFECT OF SURFACE ACTIVE AGENTS IN BOILING HEAT TRANSFER

By

S. NAGARAJA RAO, B.Sc., D.I.I.Sc.

A Thesis

Submitted to the Faculty of Graduate Studies

in Partial Fulfilment of the Requirements

for the Degree

Master of Engineering

McMaster University

April, 1967

MASTER OF ENGINEERING (1967) McMaster University
(Chemical Engineering) Hamilton, Ontario.

TITLE: Effect of Surface Active Agents in Boiling Heat Transfer

AUTHOR: Subbarao Nagaraja Rao, B.Sc., D.I.I.Sc. (Indian Institute of Science, Bangalore, India)

SUPERVISOR: Dr. T. W. Hoffman

NUMBER OF PAGES: xvii, 218

SCOPE AND CONTENTS: The boiling heat transfer phenomenon has presented a state of ambiguity regarding the role of solid-liquid-vapour interface in the mechanism of heat transfer. Recent studies (S1,M1) have given an indication to the possibility of the vapourization of a microlayer at the boiling surface as an alternative to the well-known theories based purely on the hydrodynamic factors. This study is an attempt to understand the boiling heat transfer mechanism at solid-liquid-vapour interface and to study the effect of interfacial properties like surface tension and contact angle on the maximum (critical) heat flux.

The present studies use the technique of changing the solid-liquid-vapour interface characteristics of water through the use of surface-active agent as additive, to study the boiling heat transfer under changed interface conditions. Four different surfactants were used at three levels of concentration in water. Surface tension and contact angle measurements were carried out

using the shadow photographs of pendant drops and sessile drops. Boiling heat flux measurements of these surfactant solutions in water were carried out using heat-flux meters which were made an integral part of the heat transfer surface. Experiments involving pool boiling and the boiling of thin liquid films were carried out over the transition and nucleate boiling regimes.

It has been observed that solid-liquid-vapour interface characteristics play a very important role in the boiling heat transfer mechanism. By a suitable choice of type of surfactant and concentration, the critical heat flux and heat transfer coefficient can be improved markedly.

It is suggested that the spreading wetting characteristic improves the heat transfer rate whereas the increased viscosity and decreased thermal conductivity of the liquid microlayer under the vapour masses may cause the heat flux to decrease. The present study shows significant possibilities for future studies in the nucleate boiling, transition boiling and film boiling regimes using surfactant solutions.

TABLE OF CONTENTS

APPENDICES

FIGURE INDEX

Appendices
Figure
Number

PLATE INDEX

TABLE INDEX

NOMENCLATURE*

A	area	$ft.^2$
a	dimensionless wave number	
C	specific heat	B.t.u./lb./$^oF.$
D	diameter	ft.
g	acceleration due to gravity	$ft./hr.^2$
g_c	gravitational constant	
G	mass flow rate per unit wetted perimeter	lb./hr./ft.
h	heat transfer coefficient	B.t.u./hr./sq.ft./$^oF.$
K	thermal conductivity	B.t.u./hr.sq.ft./(^oF/ft.)
n/A	number of nucleating sites per unit area	per sq. ft.
P	pressure	$lbs./hr.^2ft.$
Δ P	pressure difference	$lb./hr^2.$ ft.
Q/A	heat flux	B.t.u./hr./sq.ft.
$(Q/A)_{MAX}$	maximum or peak heat flux	B.t.u./hr./sq.ft.
r	radius	
R	radius of heat flux meter	ft.
t	time	hr.
T	temperature	$^oF.$

---

* Nomenclature of the variables used locally is given at its location. This nomenclature is for general considerations.

μ	viscosity	lb./ft./hr.
ΔT	temperature difference between heating surface and boiling liquid	$^{o}F.$
α	thermal diffusivity	$ft.^2/hr.$
δ, h	thickness of flowing liquid film	in., cm.
θ	contact angle	degrees
σ	interfacial tension	$lb./hr.^2$ or dynes/cm.
λ	latent heat of vapourization	B.t.u./lb.
ρ	density	$lb./ft.^3$
Γ	mass flow rate per unit width of channel	lb./hr.ft.

Subscripts

l, L	liquid
v, V	vapour
S	solid
MWR	minimum wetting rate
Cr	critical
SUR	surfactant solution
o	standard condition
H	superheated liquid
s, sat	boiling liquid
w	wall or heating surface
c	center
W	water

ACKNOWLEDGEMENTS

The author wishes to express his sincere and special thanks to Dr. T. W. Hoffman for his helpful suggestions, guidance and criticism.

The author also wishes to express his sincere appreciation to the helpful suggestions offered by the staff and graduate students of the Chemical Engineering Department. Special thanks is extended to Mr. Bob Dunn for his excellent suggestions and co-operation.

Sincere thanks to Mrs. Mary Petryschuk for her excellent co-operation and patience during the typing of this thesis.

The author appreciates the partial support granted by the Federal Department of Forestry.

1. INTRODUCTION

Boiling heat transfer is the transfer of heat associated with the vaporization of a liquid when this bulk fluid is at a temperature equal to or below the saturation temperature of the liquid. The principle characteristic of boiling is the high heat flux associated with a relatively small temperature difference between the heat transfer surface and the liquid.

There are a wide variety of operations which involve boiling, ranging from vapourization in the chemical process industries, generating steam in nuclear reactors or conventional systems, quenching and cooling in the metallurgical industries, transferring heat to cryogenic fluids, extinguishing forest fires, etc. This wide application of boiling heat transfer has stimulated great interest in the fundamental, underlying mechanisms associated with the vapourization phenomenon.

It is known that the amount of cooling, i.e. heat transfer, that can take place is limited by several hydrodynamic and surface factors of the system. Therefore, it is not surprising that a great effort has been directed to the task of understanding the effects of these hydrodynamic and surface factors on boiling over the entire range of heat fluxes. The present study is one such attempt.

2. LITERATURE REVIEW

2.1 Boiling Heat Transfer

The literature review which follows reports on and evaluates the theoretical and experimental work done to date to elucidate the fundamental mechanisms of boiling heat transfer. Since Dernedde[D1] has recently reviewed this subject, only those earlier references, which are pertinent and/or required for continuity, will be included here.

2.1.1 The Various Boiling Regimes

The regimes of boiling are best discussed with reference to a boiling curve, viz., a plot of the heat flux density (Q/A B.t.u./(hr.)(sq.ft.)) against the difference in temperature, (Δ T) between the heat transfer surface and the bulk liquid, (Figure 2.1). The boiling curve and the regimes in boiling heat transfer are characteristic of the boiling phenomenon. The actual shape of the curve is dependent on the liquid, the surface and hydrodynamic factors and the degree of subcooling.

The three basic regimes of boiling heat transfer are:

(i) nucleate boiling

(ii) transition boiling

(iii) film boiling

They have been discussed in detail by Westwater[W8], Rohsenow[R3] and Zuber[Z2]. These regimes can be visually observed but are most easily identified by the change of heat flux with the surface-

FIGURE 2.1

POOL BOILING CURVE OF WATER ON A HORIZONTAL PLATE

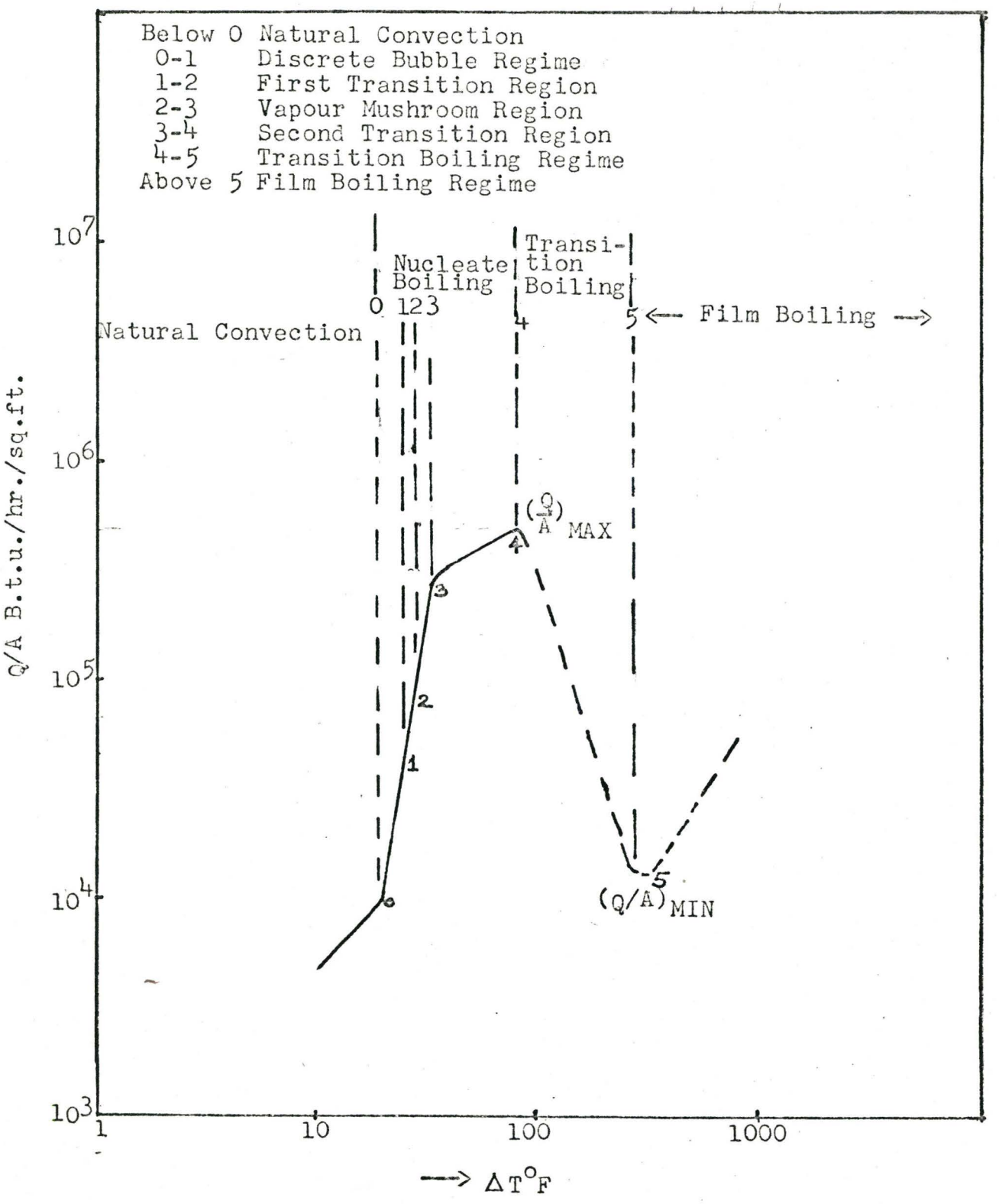

to-liquid temperature difference (Figure 2.1). In the last decade, research in nucleate boiling, with visual and photographic observations, has established a further classification (G1), viz.,

(a) discrete bubble region

(b) first transition region

(c) vapour mushroom region

(d) second transition region.

These regions have typical heat transfer characteristics within the nucleate boiling regime as shown on Figure 2.1 and cover the temperature difference region from the incipience of boiling to the maximum heat flux, $(Q/A)_{max}$.

2.1.2 Nucleate Boiling

Nucleate boiling is perhaps the most important boiling regime because of the high heat transfer rate observed at low temperature differences. The characteristics of vapour formation are different in all the four regions. An excellent description of the pool-boiling* and experimental results in pool-boiling which cover all the four regions of nucleate boiling has been given by Gaertner(G1). His observations for water are discussed below.

(a) Isolated bubble region

At the lowest heat fluxes (ca. 10,000 B.t.u./(hr.)(sq.ft.)), the main mode of heat transfer to the fluid is by natural convection. Further increase in surface temperature causes isolated

---

* The term 'pool-boiling' implies an absence of an externally induced-forced flow.

vapour bubbles to appear. Increasing the temperature further increases the number of nucleation sites and bubbles. In this isolated bubble region of nucleate boiling, the bubbles are essentially spherical until they leave the surface, when they become either bell-shaped or ellipsoid. The main mode of heat transfer seems to be the convection caused by the agitation of the bubbles.

Shadow photographs of the convection currents near the hot surface are presented by Gaertner[G1]. Studies of the wake behind the rising bubbles were conducted by Hsu and Graham[H4]. They found that the disturbances behind the rising bubble propagate up to one bubble diameter from the nucleating site which agrees surprisingly well with the studies on wakes behind moving liquid drops carried out by Hendrix[H2]. This also agrees with the assumption made by Zuber[Z5] in his analysis of nucleate boiling concerning the area of influence of each individual bubble. The increase in the heat flux with temperature difference may be obtained from the Gaertner equation[G2] in terms of active-site population (n/A):

$$\frac{Q}{A} = 181\ (n/A)^{2/3} \qquad \ldots(1)$$

and

$$n/A = \mathrm{Exp}\ \left(\frac{-K}{T_W{}^3}\right) \qquad \ldots(2)$$

where K is a constant and T_W is the wall temperature in ^{o}R, or in terms of the hydrodynamics and surface properties suggested by Rohsenow equation[R3]:

$$\frac{C_l \Delta T}{\lambda_l} = C_{sf}\left[\frac{\frac{Q}{A}}{\mu_l \lambda_l}\left(\frac{g_o \sigma_l}{g(\rho_l - \rho_v)}\right)^{0.5}\right]^{0.33}\left(\frac{C_l \mu_l}{K_l}\right)^{1.7} \quad \ldots(3)$$

where the following nomenclature is used,

C_{sf} = Coefficient of the equation which depends on the nature of heating surface-fluid combination

C_l = Specific heat of saturated liquid, B.t.u./lb./^oF.

μ_l = Viscosity of saturated liquid, lb./ft./hr.

K_l = Thermal conductivity of saturated liquid, B.t.u./hr./ft./^oF.

λ_l = Latent heat of vapourization of saturated liquid, B.t.u./lb.

ρ_l = Density of saturated liquid, lbs./ft.^{3}

ρ_v = Density of saturated vapour, lbs./ft.^{3}

σ_l = Surface tension of saturated liquid vapour interface, lb. force/ft.

g_o = Conversion factor, 4.17×10^8 (lb. ft.)/(hr.^{2} lb. ^oF.)

g = Acceleration due to gravity, ft./hr.^{2}

The agreement of the predicted values with those observed is quite good in some cases (R2, Z5) and poor in others (C3, Z2).

(b) First Transtion Region

Zuber[Z5] first observed that at a heat flux of about 46,000 B.t.u./hr./sq.ft., the character of the boiling changes. It was observed that this change takes place when the average bubble spacing becomes less than two bubble diameters. Under

these conditions bubbles interfere with each other. These interactions change the regimes of bubble removal and consequently affect the flow conditions adjacent to the heating surface. This observation was also confirmed later by Hsu and Graham[H4] from shadow photography of boundary layer. Moissis and Berenson[M4] and Zuber[Z5] derived equations for this transition region, based on hydrodynamic models. These equations predict Gaertner's experimental data[G1] quite well. Although the shape of the boiling curve does not seem to alter during this first transition region, the large temperature fluctuations in the thermal layer associated with the isolated bubble region are dampened out. A transition develops in the average bubble diameter at the break off and in the thickness of boundary layer[H4]. In the region of discrete bubbles the temperature through the thermal layer was a hyperbolic function of distance from the heating surface[H4]. After the predicted transition by Zuber[Z5], the temperature profile was of the exponential form as observed by Treschev[T1] and Colver[C2].

(c) Vapour Mushroom Region

At a heat flux of about 70,000 to 100,000 B.t.u./(hr.)(sq.ft.) coalescences of the vapour bubbles occur and large clouds of vapour attached to the heating surface only by numerous vapour spouts form. Analysis of this region with high speed photography[K3] has not yielded any quantitative information about the interface behaviour and thermal layer. So far we must be content to extrapolate the theoretical results for the lower heat fluxes into this region. The fact that experimental results show poor agree-

ment with theory is not surprising.

(d) Second Transition Region

The characteristic sharp change in the slope of the boiling curve of water (at point 3 in Figure 2.1) distinguishes this region from the others. This break occurs at a heat flux of about 300,000 B.t.u./(hr.)(sq.ft.). High activity in the vicinity of the heating surface poses a great problem in studying the interfacial phenomena occurring close to the heating surface even with high-speed photography(K3). It is believed that local vapour patches may be formed on the surface as a result of instabilities in the vapour mushrooms at certain nucleating sites. Therefore, at any given time less nucleating surface is available and hence the decreased slope on the boiling curve. The point at which this sharp change takes place is known as "Departure from Nucleate Boiling (DNB)".

2.1.3 Maximum Heat Flux

This maximum point on the boiling curve has excited considerable interest recently because of its importance, expecially in boiling-water nuclear reactors. It is aptly called the "burnout" point or "point of crisis". Just prior to this "burnout" point there is considerable interaction between the vapour leaving the surface and the liquid moving towards the surface. At the maximum heat flux this interaction causes the system to become unstable, so that further increase in temperature causes partial blanketting of the heat transfer surface at one instant and reversion to nucleate boiling during the next. The net result is

a lower heat flux. These ideas were formulated into a theoretical mathematical framework by Zuber and Tribus[Z6]. In this analysis, they coupled the hydrodynamic equation of Kelvin* with the instability theory of Helmhottz** to derive the expression.

$$\left(\frac{q}{A}\right)_{max} = \left(\lambda_1 \rho_v\right) \frac{\Pi}{24} \left(\frac{\sigma_1 (\rho_1 - \rho_v) g g_c}{\rho_v^2}\right)^{0.25} \left(\frac{\rho_1}{\rho_1 + \rho_v}\right)^{0.5} \quad \ldots(4)$$

Surface tension of the liquid plays a part only in determining the most probable unstable wavelength. The form of this equation agrees well with those determined by dimensional analysis[K5] and wave motion theory[C11]. Borishanskii[B11] extended Kutateladze's analysis[K5] to include the viscosity. He arrived at an additive correction factor due to viscosity, to the constant of proportionality in Kutateladze's equation[K5]. This effect is quite small in comparison to the deviations of the experimentaly observed critical heat flux from those calculated using equation (4). These predicted results are generally higher than those observed for pure liquids[T4]. In some cases, however, purely hydrodynamic

---

* i.e., $\lambda = 2\Pi \left[\frac{\sigma_1}{g(\rho_1 - \rho_v)}\right]^{\frac{1}{2}}$ where λ is the wave length, is based on the importance of surface tension as a stabilizing factor at interfaces of two superimposed fluids.

** i.e., with two flowing immiscible fluids, there is a maximum relative velocity above which a small disturbance will not be dampened out.

effects do not seem to determine completely the critical heat flux. For example, Costello and Frea[C17] found that the maximum heat flux increases, if the surface becomes contaminated; Adams[A5] found that the critical heat flux was directly proportional to surface tension.

Berenson[B10] suggests that all these differences can be explained by not having uniform surface conditions over the entire heat transfer surface. He claims that surfactants broaden the burnout point and that the maximum heat flux exists over a range of temperature differences by virtue of the nonuniform surface. The average behaviour of the surface will, therefore, indicate a lower, maximum heat flux. Even this suggestion does not seem to give a satisfactory explanation to discrepancies in the predicted maximum heat fluxes.

Rohsenow and Griffith[R4] proposed a modified equation based on the correlation of Forster and Zuber[F7], which employed the results of an analysis for bubble growth within an initially uniformly superheated liquid, for evaluating the bubble diameter at departure. This equation of Rohsenow et al[R6] given below, will not work for polar fluids, while the equation is quite good for non-polar fluids.

$$\left(\frac{Q}{A}\right)_{max} = K_{sf} \frac{\Delta T^{2.1} \; \Delta P^{0.75} \; \rho_l^{1.35} \; K_l^{8.55}}{\mu_l^{8.05} \; \rho_v^{1.1} \; C_l^{6.45} \; \lambda_l^{1.1} \; \sigma_l^{0.5}} \qquad \ldots(5)$$

where K_{sf} is a function of the heating surface and fluid combination

(determined by contact angle) and ΔP is the vapour pressure difference corresponding to ΔT.

Deissler[D7], employing a physical model of boiling mechanism at critical heat flux, obtains the following equation, without resorting to either dimensional analysis or vapour-liquid instabilities considered earlier.

$$\left(\frac{Q}{A}\right)_{max} = C_3 \frac{\theta^{\frac{1}{2}}}{C_D^{\frac{1}{2}}} \lambda_1 \rho_v^{\frac{1}{2}} \left[\sigma_1 g g_c (\rho_1 - \rho_v)\right]^{0.25} \quad \ldots(6)$$

where C_3 is a constant, C_D is the drag coefficient of the bubbles and θ is the contact angle. This equation is identical to equation (4), if the contact angle at breakoff and drag coefficient are considered constant. This analysis of Deissler is based on the postulate that the critical heat flux occurs when the rate of formation of bubbles just exceeds the rate at which they are carried away. Under these conditions the drag on the bubbles is sufficient for successive bubbles leaving the surface, to touch and coalesce.

Chang[C12] considers that the heat transfer in nucleate boiling is limited by the maximum rate of bubble generation from a unit area of the heating surface. He considers two extreme cases:

(a) low or no forced convection, where the final bubble size is not too small and bubble frequency not too high and

(b) high forced convection where the bubbles are extra fine and their concentration is very large. He considers the stability for a bubble growing or moving in an intensively tur-

bulent fluid, where the surface tension force gives a stabilizing effect but the dynamic force tends to destabilize the motion. His analysis of critical heat flux based on the above consideration in terms of Weber number and Reynolds number yielded the following equation for burnout in saturated pool boiling:

$$\left(\frac{Q}{A}\right)_{max} = 0.0206 \sqrt{\rho_v \rho_l}\ \lambda_l \cdot \beta_l \left(1 - EXP(-C_3^{\frac{1}{4}} V / \beta_l)\right) \quad ...(7)$$

where

$$\beta_l = \beta \cdot \frac{\sigma_l}{\mu_l} \quad ...(8)$$

$$V = \frac{g \sigma_l (\rho_l - \rho_v)}{\rho_l^2}^{\frac{1}{4}} \quad ...(9)$$

Here β and $(C_3)^{\frac{1}{4}}$ are system parameters which are to be determined from experiments. This bubble agglomeration effect was experimentally observed by Costello[C13]. This prediction depends on the assumptions:

(i) there exists some statistically mean values of the final bubble size, bubble frequency and number of bubble sites per unit area of heating surface

(ii) bubbles are spherical

(iii) at the critical condition, the bubble on the heating surface has developed to its departure size under hydrodynamic and thermodynamic equilibrium.

2.1.4 Transition Boiling

In this regime, one observes the anomolous decrease in heat transfer rate with increasing temperature as shown in Figure 2.1. The decrease in the boiling heat flux with increased surface temperature results from the large unstable vapour patches that

cover the surface. The extent of these patches increases as the surface temperature is increased. For this reason this regime is sometimes referred to as the "partial film-boiling regime".

Theoretical analysis of this regime has been presented by Zuber[Z6], Berenson[B5] and others[B4,D3,S3]. Zuber[Z4] considers a vortex sheet which oscillates under the influence of surface tension. Applying Taylor - Helmholtz instability criteria, he arrives at the following equations for transition boiling,

$$C^2 = \frac{\sigma_l \, m}{(\rho_l + \rho_v)} - \frac{\rho_l \, \rho_v}{(\rho_l + \rho_v)^2} (U_1 - U_2)^2 \qquad \ldots(10)$$

and

$$\frac{q}{A} = \frac{\Pi}{24} \lambda_l \, \rho_v \, \frac{\lambda}{\tau} \qquad \ldots(11)$$

$$\lambda = 2 \Pi \left(\frac{\sigma_l}{g(\rho_l - \rho_v)} \right)^{\frac{1}{2}} \qquad \ldots(12)$$

where $m = 2\Pi/\lambda$ is the wave number, C is a real number for stable transition boiling and U_1 and U_2 are the constant velocities in the positive X direction of the vapour and liquid phase respectively. The gross liquid velocity U_2 is usually less and the wave length λ, period τ and velocity U_1 of the vapour are interrelated. However due to the Taylor - Helmholtz instability, where a definite geometrical configuration can be expected, the geometry is characterized by disturbances with wave length in the spectrum

$$2\Pi \left[\frac{\sigma_l}{g(\rho_l - \rho_v)} \right]^{\frac{1}{2}} \leq \lambda \leq 2\Pi \left[\frac{3\sigma_l}{g(\rho_l - \rho_v)} \right]^{\frac{1}{2}}$$

where the diameter of the vapour slugs was approximated by $D = \lambda/2$. According to Zuber[Z4] the interface takes the form of spikes and bubbles. In their downward fall, the spikes approach the heated surface and rapid evaporation occurs. A spheroidal state similar to the Leidenfrost phenomenon is expected. This assumes that no solid-liquid contact exists. As liquid evaporates from the spikes, vapour flows in the region in between two spikes. Therefore a release of bubbles at regular intervals occurs. As a row of bubbles is released due to vapour thrust effect, an unstable interface is again formed. Because of the downward flow of the liquid again a new spike beneath the bubble forms. Thus a thermally stable, but hydrodynamically unstable situation was suggested by Zuber[Z4]. Similar analysis with modified criteria for vapour thrust effect and instability was considered by Berenson[B5]. Westwater's high-speed movie pictures[D5] indicated the higher stability of vapour-liquid interface during transition boiling when surfactants were added to boiling isopropanol. Berenson[B10] observed during transition boiling that the heat transfer rate was increased by the presence of wetting agent.

2.1.5 Minimum Heat Flux

At the point of minimum heat flux the unstable vapour films become stable and a continuous vapour blanket forms over the heat transfer surface. Hosler[H3], Zuber[Z4] and Bankoff[B4] have successfully applied Taylor - Helmholtz instability theory to obtain an expression for the heat flux at this minimum point. In this case, the stability of a two-fluid system is considered where

the lighter fluid is below the heavier one. By utilizing assumption concerning critical wave lengths, Zuber[24] derives the equation:

$$\left(\frac{Q}{A}\right)_{min} = \frac{\Pi}{24} \lambda_1 \rho_v \left[\frac{\sigma_1 g(\rho_1 - \rho_v)}{(\rho_1 + \rho_v)^2}\right]^{\frac{1}{4}} \qquad \ldots(14)$$

This equation predicts experimental data reasonably well.

2.1.6 Film Boiling

The point of minimum heat flux signals the beginning of stable film boiling. Increasing the temperature of the heat transfer surface increases the heat flux partly because of increased conduction across the vapour film and partly because of the increasing contribution by radiation.

The vapour film is disturbed continuously by the departing bubbles which break away from the vapour film. The amplitude of the waves formed by the departing bubbles has been discussed in detail by Hosler and Westwater[H3]. Their experimental work substantiates Zuber's equation (14). They conclude that the minimum interbubble distance at departure is the critical wave length and the average distance the most dangerous one.

The equation derived on this basis for the film-boiling heat flux is given below in terms of the bubble parameters:

$$(Q/A)_{film} = V_B f n \rho_v h_v \qquad \ldots(15)$$

where f is the frequency of bubble formation, V_B is the volume of the bubble, n is the number of bubbles per square foot, h_v is

the enthalpy of the vapour. Zuber[Z6] and Hosler[H3] present the details for determining f, V_B and n in their papers.

2.1.7 Forced Convection

The addition of forced convection to the boiling phenomenon adds another complexity to an already complex problem, since now different effects will be observed depending upon the flow system. For example, in the case of flow inside closed conduits, the amount of vapour present will determine the flow regime of the two-phase system, which, in turn, should effect the heat transfer process (B13,C9,H8). The effect of forced flow on the burnout heat flux is shown in Figure 2.2.

To date the most successful attempt at correlating boiling heat transfer in forced flow systems is through the approach just suggested by Rohsenow[R3]. Rohsenow[R3] recommended that the heat transfer rate under forced flow conditions could be found by adding each contribution separately as indicated in equation (16).

$$\left(\frac{Q}{A}\right)_{\text{Total}} = \left(\frac{Q}{A}\right)_{\substack{\text{Forced}\\ \text{Convection}\\ \text{(Single Phase)}}} + \left(\frac{Q}{A}\right)_{\substack{\text{Pool}\\ \text{Boiling}}} - \left(\frac{Q}{A}\right)_{\substack{\text{Incipient}\\ \text{Boiling}}} \qquad \ldots(16)$$

This equation is quite conservative if applied to the entire tube. This method worked quite well at low flow rates and vapour qualities. It requires a knowledge of the pool boiling characteristics of the heat transfer surface in question and since, in forced-convection boiling, boiling effects are far more significant than forced convection, this represents a serious drawback.

FIGURE 2.2

EFFECT OF SUBCOOLING AND FORCED CONVECTION

ON MAXIMUM BOILING HEAT FLUX OF WATER - REF: (G8)

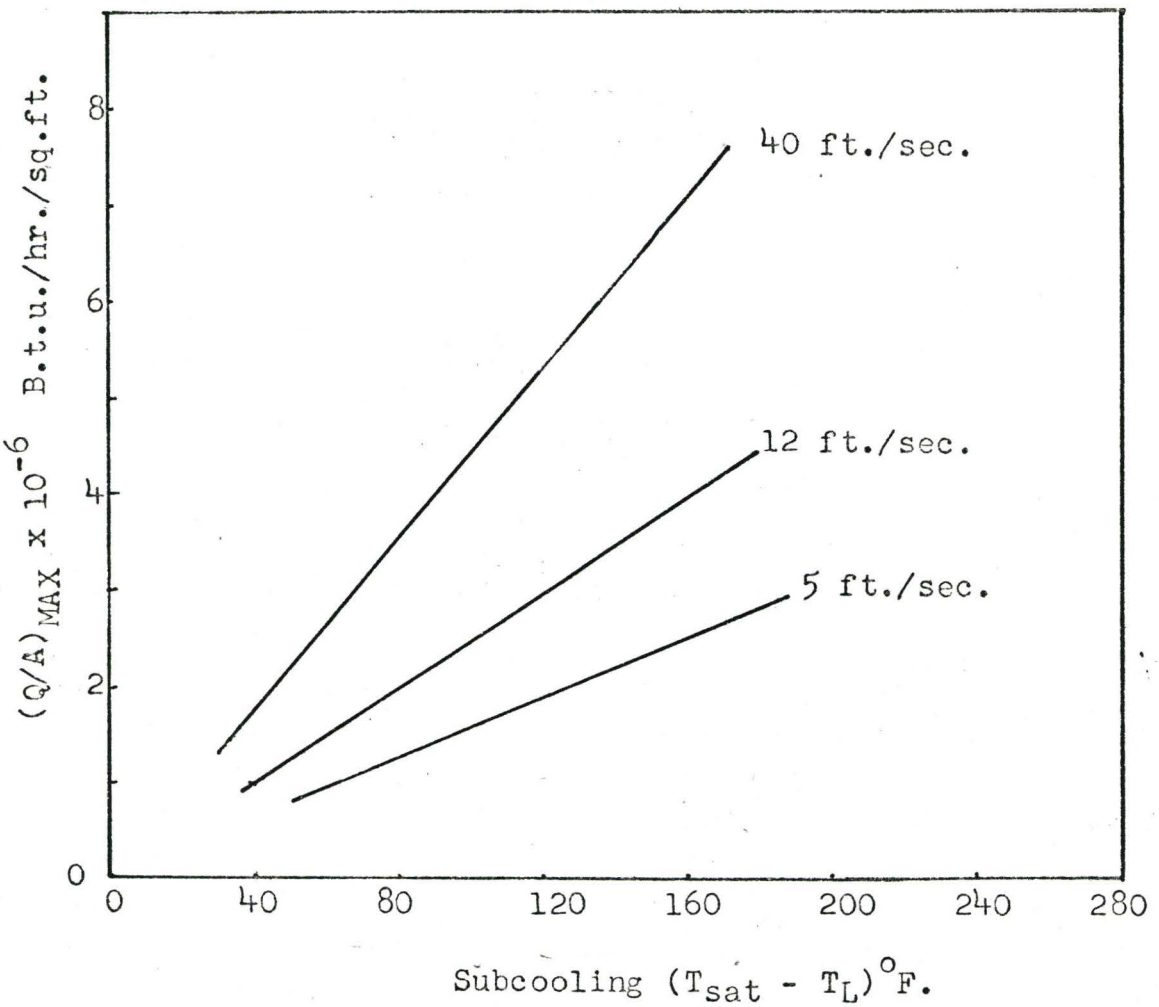

Chen[C3] presented a method based on this idea but claimed to correct for the effect of forced-flow on the boiling phenomena by including a bubble suppression factor (< 1) and for the effect of boiling on forced flow by multiplying the forced flow heat transfer coefficient by a factor (> 1) which was correlated against two-phase flow parameters. The main criticism of this work is that he used a pool boiling correlation of Forster and Grief[F8] which had been shown to be accurate only for very limited situations. Nevertheless Chen's correlation[C3] represents the best available for predicting boiling heat flux at the present time. He was able to demonstrate that his correlation predictions agreed well with all available experimental results from over the entire world. This correlation serves a purpose but is quite unsatisfactory, since it is essentially empirical in nature.

The problems of burnout in forced convection boiling have received a lot of attention. In this case the phenomenon depends on the stability and dynamics of a thin liquid film moving along on the inside of the hot tube wall (T3). More will be said on this stability problem in section (2.4)

2.1.8 Subcooling

Subcooling is of great significance in heat transfer on account of large heat fluxes (of the order of 10,000,000 B.t.u./ hr./sq.ft.) observed in subcooled forced convection boiling systems. Figure 2.2 shows the effect of subcooling on peak heat flux. There are many excellent studies on the heat transfer mechanism in subcooled boiling. Perhaps the most interesting ones are by Gunther[G8],

Forster and Grief[F8], Ellion[E1] and Sharp[S8]. Growth and collapse of a bubble is characteristic of subcooled boiling. Bubble size will be less but bubble population will be large. Bubbles were found to be hemispherical and coalescence and collapse were common characteristics. At lower subcooling, the fluid temperature being high, bubbles may be larger in size and may have enough momentum to detach itself from the heating surface. Forster and Grief[F8] suggested a pumping mechanism in the thermal boundary layer to account for large heat fluxes. Bankoff[B9] suggested that the condensation at the top of the bubble may be a significant contribution. Zuber[Z3] and Hsu and Graham[H4] analyzed the bubble growth and thermal boundary layer. Zuber[Z3] suggested an equation for subcooled boiling peak heat flux, which agrees well with experimental data.

Heat transfer seems to increase significantly in transition and film boiling regions. Theoretical studies have been done by Cess and Sparrow[C8]. Experimental studies have been done by Bromley and Motte[B12].

2.2 Summary of Phenomenological Approach to Predicting Boiling Heat Transfer

In the previous section, discussion has centered on the phenomenological description of the various regimes of boiling. The equations which have been derived based on either a particular hydrodynamic model or a dimensionless-group-empirical approach have indicated the large number of variables that influence the boiling phenomenon. To date there has not been either a full description of the boiling process nor have there been satisfactory

semi-empirical equations available to the design engineer to predict boiling behaviour under any given conditions. This is especially true in the nucleate boiling regime. This situation suggests that considerably more effort must be directed to the fundamental studies of the mechanism which affect boiling in all regimes. The following section reviews some of the investigations which have been carried out to date on all aspects.

2.2.1 Nucleation

There is no completely satisfactory theory for nucleation in boiling heat transfer, though many theories have been proposed.

By performing a force balance on a vapour bubble of radius, r, it can be easily shown that the vapour pressure inside a bubble must be greater than the pressure in the surrounding liquid by $2\sigma/r$. If the bubble is in equilibrium with its surroundings then the liquid must be superheated for the bubble to exist at all. This simple analysis cannot be extended to the size of bubble nuclei but does point out that some degree of superheat is required for nucleation.

Spontaneous nucleation within a liquid is different from nucleation at a heat transfer surface. For the latter situation, there will be many nuclei of trapped gas and/or vapour on the surface. Rohsenow[R3] has indicated how surface tension of the liquid can affect the existence of nucleating sites on a heat-transfer surface. Ellion[E1] has presented a nucleation equation which predicts quite well the experimental superheat required for nucleation. It is based on Laplace's, surface tension-curvature,

equation and the Clapeyron equation relating vapour pressure and temperature. Free vapour nuclei arising in the bulk of the liquid by virtue of molecular fluctuations or cosmic radiation are not important as nucleation centres in the boiling process.

Griffith and Wallis[G6] carried out nucleation experiments with cavities formed from needle tips of a given shape. They demonstrated that Ellion's equation predicted nucleation quite well. Hsu and Graham[H4] suggested a method for calculating the superheat required for nucleation under any flow condition. This model assumes a linear temperature gradient at the heat transfer surface and a hemispherical bubble. Ellion's nucleation equation is assumed to hold for this situation. Nucleation is predicted to occur, i.e. the vapour bubble in the cavity grows, if the hemispherical bubble is completely immersed in a fluid, the temperature of which is greater than that predicted by Ellion's nucleation equation for the hemispherical bubble radius. Bergles [B6] extended this to forced convection. His experiments agree exceptionally well with the predicted results.

2.2.2 Bubble Growth

When a bubble is nucleated, there is an initial period of rapid growth (R3) followed by a much longer period when the bubble grows at a rate proportional to time (K3) to a size where the buoyancy forces exceed the surface forces holding it to the heat transfer surface. Prior to reaching this departure volume, the gas bubble may coalesce with another bubble, etc. Although the theoretical investigations of the bubble growth rate of an isolated

bubble in a superheated isothermal liquid provide some appreciation of the importance of the physical properties, these growth rates are not realized at a heat transfer surface because of the proximity of the wall and the severe temperature gradients which exist in this region. Indeed, Westwater[W7] feels that an analytical solution to this problem will probably never be obtained because of the extreme complexity of all the phenomena occurring simultaneously. It is important to note, however, that the fraction of the heat that is transferred in boiling, which results in vapourization, i.e. the formation of vapour bubbles, is less than 10%. However this does not rule out the vapourization process as one of the most important ones occurring, since according to Bankoff's analysis[B9], vapour can be formed at the bubble base and then condense on those surfaces removed farthest from the heat transfer surface.

To understand the factors which affect the growth rate next to a heating surface, one must consider the mechanism by which heat is transferred during boiling.

2.2.3 Boiling Heat Transfer Mechanisms

Some of the earliest ideas about the heat transfer mechanism associated with boiling are attributed to Jakob[J1], Clark and Rohsenow[C4] and Gunther and Kreith[G7]. They suggest that the high heat transfer rates can be attributed to the agitation caused by the growing (possibly collapsing) and departing bubbles. This agitation is thought to create considerable turbulence (microconvection) in the regions next to the surface. The area over which

this agitation has influence is known as the area of influence of a bubble.

Forster and Grief[F8] suggested that a more efficient heat transfer mechanism occurs when the growing bubble displaces the superheated liquid layer completely from the heating surface, thus allowing the neighbourhood cooler liquid to move into the immediate vicinity of the hot wall. The heat transfer mechanism would be the continuous displacement of hot fluid. Mixon et al[M2] performed heat transfer experiments in which air was blown through a heat transfer surface. Although the heat transfer rate was increased, the bubble agitation did not account for the much higher heat fluxes experienced in boiling systems.

A profoundly different mechanism had been suggested by Snyder[S7] and Edwards[E2] on the basis of their experiments; they suggested that evaporation occurs directly from the base of the growing bubble or from a thin film of liquid which existed under most of the bubble during bubble formation. Credulence to this idea was obtained indirectly by Moore and Mesler[M1] and Sharp[S1]. Moore and Mesler measured the surface temperature directly under a growing bubble and noted an exceedingly high temperature drop which occurred almost instantaneously. This drop was then followed by a relatively slow rise in temperature until the temperature had recovered to its original value. The rapid drop and rise repeated according to bubble frequency. This temperature drop corresponded to heat fluxes that were approximately twenty times the average measured heat flux for the entire surface.

These high heat fluxes could not be accounted for by the quenching theory or the microagitation theory, but could only be explained on the basis of a microlayer of liquid under the bubble. All of this heat does not manifest itself as vapour as the experiments of Clark and Rohsenow(C4) attest. Probably most of the vapour produced at the base is condensed on the bubble surface, leaving only 1 - 2% of the total heat as vapour bubbles (C4). The remainder is convected away by the agitation of the bubbles and produces vapour at the free liquid surface.

Direct experimental proof that the drop in temperature coincided with the bubble formation over the thermocouple was provided by Sharp and Hendricks(S8). Sharp(S1) actually observed and measured the microlayer under a growing vapour bubble by an ingenious high-speed photographic and interferometric technique. He concluded that the cooling at the bubble base accounted for more than 50% of the heat transferred. He also analyzed the effect of the thermal capacity of the heating surface and concluded that experimental observations by many investigators supported the microlayer theory.

All these experiments were conducted at low heat fluxes but the same mechanism is expected to pertain at higher fluxes. Whether other effects exist, such as those arising out of strong Marangoni forces which might exist because of the large temperature gradients in the vicinity of the wall and bubble, is still a matter of conjecture. Certainly other factors such as surface material and roughness, surface thickness, additives to the liquid and

the hydrodynamics associated with the liquid and vapour interact with the basic boiling mechanism. These factors may even override others, for example, the hydrodynamic factors at the critical heat flux.

2.2.4 Bubble Departure

When the buoyancy or other forces on a bubble become greater than the surface forces holding the bubble on the surface, the bubble breaks away and a gravitational or forced flow field leaves the vicinity of the heat-transfer surface. Sharp and Hendricks[S8] have shown that at this point the temperature under a bubble reaches a minimum. They further show that when the surface temperature recovers, another bubble is nucleated and the process repeats itself at a fairly constant frequency. The actual bubble motion and shape at the heating surface depends on the temperature of the boiling surface (heat flux) and the particular solid-liquid combination.

The earliest work on this aspect of boiling was done by Jakob[J1] and Fritz[F2]. In this work they report that the product of bubble diameter at break off and the frequency of bubble formation is a constant (Figure 2.3(a)). This observation was made in the region of isolated bubbles; the situation becomes much more complex at higher heat fluxes as indicated on Figures 2.3(b) and 2.3(c).

There are a number of excellent studies reported in the literature (J1,Y1,K3,W1,Z3,F3,R3,D4) on the bubble growth, bubble frequency and bubble diameter at departure. A number of these in-

FIGURES 2.3

BUBBLE DEPARTURE

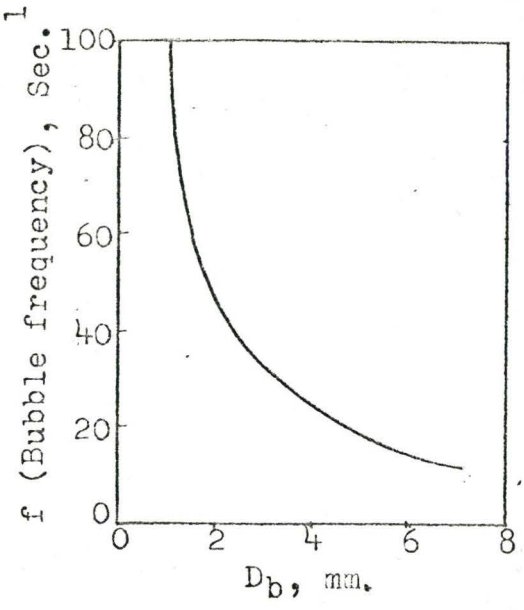

Figure 2.3a

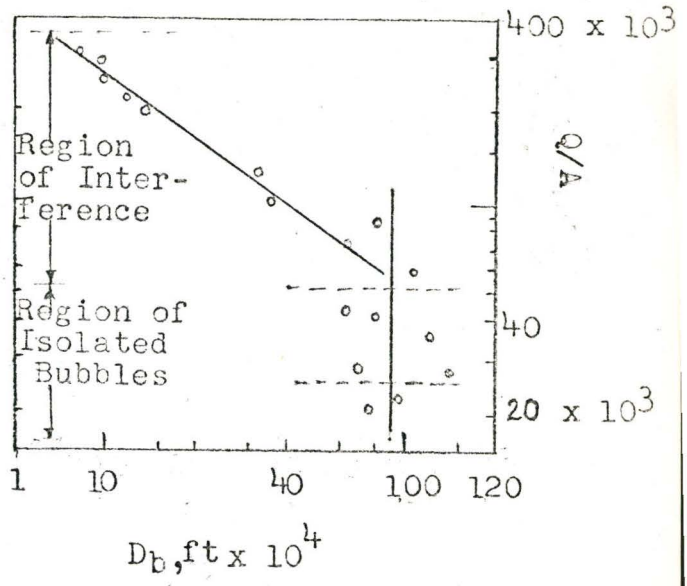

Figure 2.3b

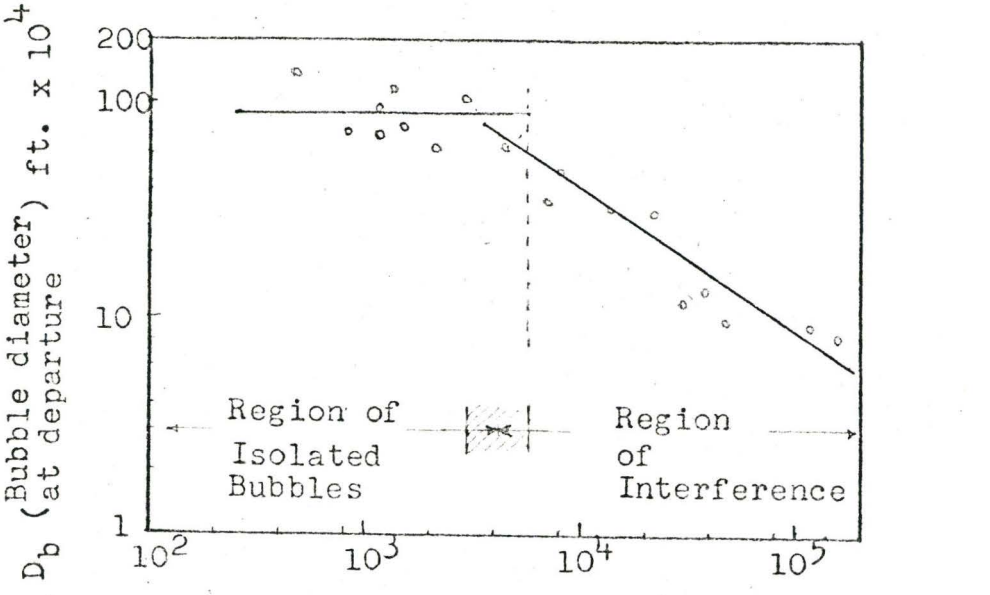

Figure 2.3c

clude an extensive review of earlier work. A selected review of the subject is presented below.

2.2.5 Shapes of Bubbles

One of the earliest descriptions of the shapes of bubbles in boiling was presented by Yamagata et al(Y1). Zuber(Z5) concluded that the shapes of bubbles in boiling were no different from those generated at orifices, as reported by Anick and Davidson (A2). Figure 2.4 illustrates the various bubble shapes considered by Zuber(Z5), Sharp(S1), and Kirby and Westwater(K3). The shape changes from type I through to type III as the heat flux is increased.

At very low heat fluxes, the small bubbles are essentially spherical. The diameter of the bubbles in this region can be calculated by balancing buoyancy and adhesive forces. Fritz's analysis of this problem indicated that the bubble diameter at departure should be given by:

$$D = 0.021\ \theta\left(\frac{\sigma_l}{g(\rho_l - \rho_v)}\right)^{0.5} \qquad \ldots(17)$$

is the bubble contact-angle in degrees. The equations of Zuber (Z7) and Plesset(P2) differ only by the constant of proportionality.

The bubble shape and the boundary layer thickness depend on the hydrodynamic conditions in the liquid as well as on the interface phenomenon at the triple interface of vapour-liquid-solid as reported by Zuber(Z2). The bubbles are normally isolated.

At intermediate heat fluxes, bubbles grow and interact

FIGURES 2.4

SHAPES OF BUBBLES

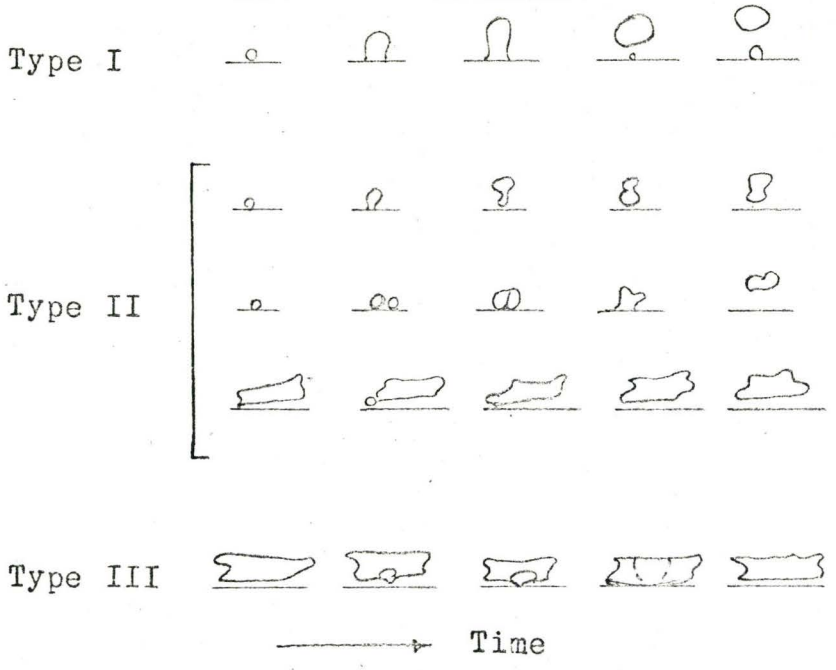

Figure 2.4a - IMAGINED BUBBLE SHAPES OF GROWING BUBBLES (K-3)

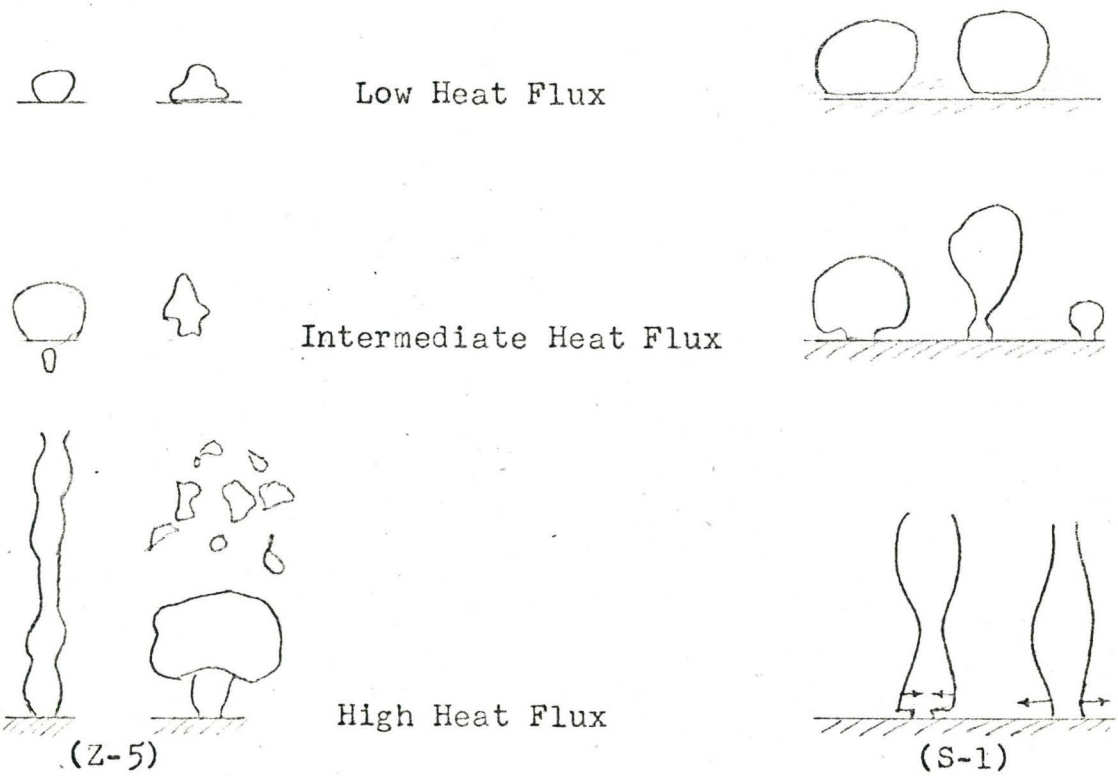

Figure 2.4b - BUBBLE SHAPES IN BOILING (Z-5 and S-1)

with other bubbles, thus causing coalescence and bubbles of non-uniform size. They have been described as precession or tandom-type by Yamagata et al[Y1] and as mushroom-type by Kirby[K3] and Gaertner[G5]. The actual shapes depend on the liquid-solid combination and on the density of nucleating sites. For this reason, studies of the type reported by Mesler[M6], which are based on hydrodynamics only, may not provide an adequate description.

At high heat fluxes, above 50% of the maximum, type III bubbles and vapour mushrooms are common along with the continuous swirling vapour columns or jets (S3,J1). Sharp[S1] suggests a pulsating vapour column which rests on a thin micro-layer of liquid at the base. At lower heat fluxes he feels that this column pinches off to form individual bubbles. Kirby and Westwater[K3] photographed bubbles from below a transparent heating surface and observed type III shaped bubbles and considerable dry-spot formation as well. They suggested that irregular vapour masses rather than individual bubbles lie above a thin liquid layer. These vapour masses are held to the surface by the sizeable dry spots which are probably associated with the nucleating cavities. This observation contrasts the small dry spots observed by Sharp[S1] and Moore and Mesler[M1].

The transition boiling regime is comprised of unstable regions of nucleate and film boiling and therefore bubble dynamics are associated mainly with the hydrodynamic instabilities that arise under these conditions.

The preceding discussion has attempted to provide the

reader with an appreciation of the variables which are important in the boiling process. In summary, these can be classified as those variables affecting the hydrodynamics and the heat transport phenomena and those associated with the nucleation and surface phenomena. There obviously is an interaction among these variables and also there are situations when one phenomenon controls the entire process.

In this study, the interest is focused on the interfacial and surface phenomena, in particular, on the effect of surface active agents on the boiling of flowing liquid films and a pool of liquid. The discussion which follows considers this aspect in greater detail.

2.3 Surface Effects in Boiling

The heat transfer surface and its condition have been observed to alter the boiling process in two ways: (i) by altering the bubble shape, size and frequency and (ii) by changing the degree of superheat required to initiate the bubble growth for a given heat flux. The earliest attempts to characterize the nucleating surface were by Jakob[J2] and Fritz[F2]. As indicated earlier, Rohsenow[R3] in deriving his model for boiling for his correlating equation utilized the earlier observation by Fritz[F2] concerning, fD = constant, which involved a surface tension functionality and allowed the coefficient in the equation to vary with liquid-solid combination, presumably to account for wettability of the surface. He claimed the equation was applicable to metals that were obtained from normal manufacturing processes and, in this

way, claimed to circumvent the problem of surface condition.

From the previous discussions we can conclude that the surface material and condition is going to affect the nucleating characteristics of the surface, the bubble shape (and therefore growth characteristics) and the frequency of departure of the bubbles. Since this covers the entire boiling process, there is obviously going to be strong interaction between surface variables and the hydrodynamic effects and transport properties. Moreover, a method has not been developed where the surface under consideration can be characterized for the boiling process. Couple this with the extreme difficulties associated with direct observation (even with high-speed cameras) and it is not surprising that a number of factors are still unknown concerning surface effects in boiling. Furthermore, the gas-liquid interface may play a considerable role in determining the boiling characteristics of a given system. Some of the studies related to these points are discussed below.

2.3.1 Nucleation Effects

The extreme complexity of the boiling heat transfer phenomenon, associated with the great difficulty in measuring surface characteristics has restricted considerably the study of the effect of surface variables. Nevertheless, many significant studies regarding the effect of nucleation sites on boiling have been made (A3,A4,B5,B14,C5,G6,K6,S3,C6). Gaertner(G1,G2) reviews the various studies which have been made on the nucleation phenomenon to 1965.

The earliest attempts to characterize the nucleating vari-

ables were by Yamagata[Y1], Jakob[J1] and Fritz[F2]. Corty and Foust[C5] studied various surface variables and concluded that there is a very significant effect of contact angle, surface roughness and surface material on boiling heat transfer. Their observation that a rough surface yielded a higher heat flux than a smooth one at a given temperature difference and for a given surface-liquid combination has been well substantiated now. This factor has been analyzed by Griffith and Wallis[G6] who also carried out extensive and controlled experiments. They attributed Corty's and Foust's observation to the various cavity sizes (nucleating sites) and their effect on the nucleation phenomenon. They also studied active-site population, type and size of cavities and contact angles. They concluded that nucleation occurs from preexisting, gas-filled cavities and generally only width is sufficient to characterize them. Kurihara[K7,K6] studied extensively the effect of surface roughness and superheat on boiling coefficients. He observed that (Q/A) is not proportional to nucleation site density (n/A), as Jakob[J1] observed, but is proportional to $(n/A)^m$ where m is a constant. He also observed a greater number of bubble columns in a rough surface and derived a relation relating the temperature difference driving force and the number of active centers.

Westwater and Gaertner[W6] utilized a novel electroplating technique to study active site population. They measured population densities up to 1130 sites/sq.in. at 317,000 B.t.u./(hr.)(sq.ft.) for aqueous solutions. The Corty and Foust[C5] studies only in-

volved site densities of 60 per sq. in. Other studies (K7,N1) were limited to lower heat fluxes as well. Gaertner[G10] later had limited success in his high-speed photographic study of the nucleating site population. His analysis of the problem (G1,G2) suggested the following relationships for water between nucleating site population (n/A), heat flux (Q/A) and wall temperature in the range of heat flux of 317,000 B.t.u./(hr.)(sq.ft.)

$$(Q/A) = 181(n/A)^{2/3} \qquad ...(18)$$

$$(n/A) = C_n.\exp(-K/T_w^3) \qquad ...(19)$$

where C_n and K are constants which depend on the heat flux range. Kurihara[K6] obtained a value of 0.55 for the exponent for the identical system. Kirby and Westwater[K3] obtained an exponent of 0.73 for a glass surface.

Bonilla, Grady and Avery[B15] conducted some excellent experiments on the effects of scratches. Copper surfaces were polished with successively finer grades of emery paper from #2/0 to a fine finish. Scratches 2400 to 3500 microns wide and 120 to 68 microns deep were put in the heating surface. They observed that the scratches should be spaced approximately at $2.5\sqrt{\sigma_l/(\rho_l - \rho_v)g}$ for maximum effectiveness and the depth may be about 25 microns. They also observed better improvement with liquid metals.

Some very interesting studies have been conducted in this area by Young and Hummel[Y2]. They obtain nucleating sites by sticking small teflon spots onto the heat transfer surface and

obtain well-controlled nucleation in this way. These treated surfaces yield higher heat fluxes for a given temperature difference and given material. Similarly Gaertner[G2] treated surfaces with teflon and silicon grease. In this case, a lower maximum heat flux and larger bubbles which easily formed vapour blanket were observed. Studies with silicate spots, which have good wetting properties and low thermal conductivity yielded improvement in boiling heat transfer.

Costello and Frea[C17] studied the boiling of tap water and observed that the coating of the deposits on the heating surface allowed extremely high heat fluxes. They reported a 50% increase in peak heat flux by using a coated 0.125 inch diameter cylindrical heater.

Averin[A3,A4] during his studies on the effect of materials and machining of surface observed significant effects of nucleating sites and thermal conductivity of heating surface on the boiling heat transfer rate. Berenson[B5] in his studies with Copper-Pentane boiling observed that roughness had no effect on critical heat flux rates and film boiling regimes but had considerable effect in the transition and nucleate boiling regimes. Stock[S3] treated his heating surface with various coatings and observed that though there was considerable change in nucleating sites, critical heat flux rate remained essentially the same.

The only experimental support for the hydrodynamic instability analysis of the peak heat flux was that obtained by Stock[S3] and Berenson[B5], (Figure 2.5). Surface material, roughness and con-

FIGURES 2.5

EFFECT OF SURFACE MATERIALS

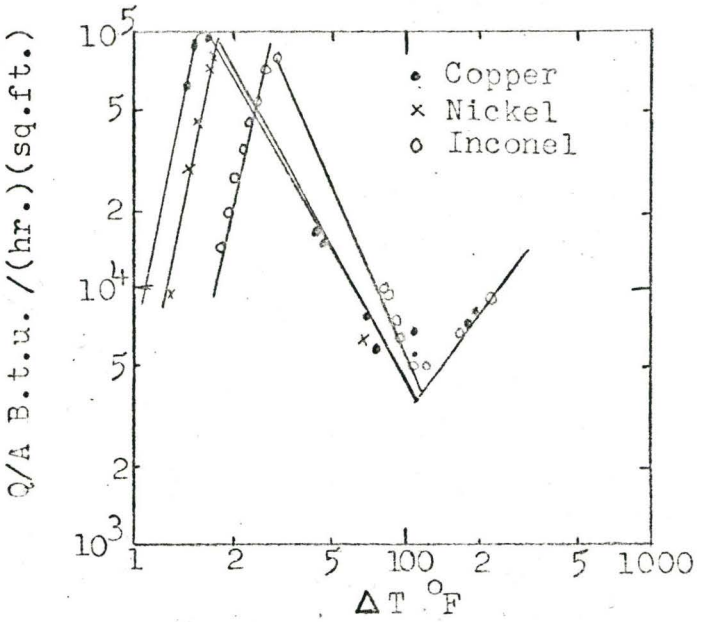

Results of Effect of Materials
(Copper-Pentane System)

(Ref. B5)

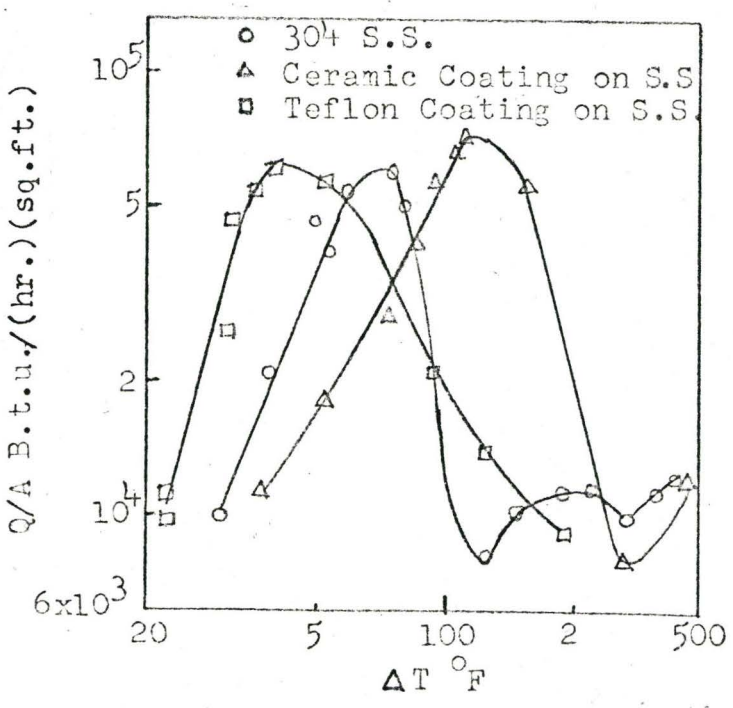

Boiling of Freon-11 on Various Surfaces

Ref (S3)

tact angle do not seem to influence the peak heat flux.

Costello[C15] suggested that the experiments may have been conducted in the region where the cohesive energy of the bubble* is negligible. Since the cohesive energy depends on wettability, type and number of nucleating cavities and surface tension, the effects may have been compensating. These questions still remain unanswered.

2.3.2 Thermal Effects in the Heat Transfer Surface

The interest in the heat transport effects within the heat transfer surface have only recently received some attention. This lack of interest can be traced to the success of the hydrodynamic studies; its recent interest arises out of the proposed mechanism and experimental temperature measurements of Moore and Mesler[M1].

Sharp[S1], during his experimental studies on the microlayer vaporization found that the thermal capacity and conductivity of the heat transfer surface was very important in determining boiling dynamics. He found that the surface material with the highest ratio of thermal conductivity to the square root of thermal diffusivity exhibited the steepest boiling curve. He also concludes on the basis of the microlayer vapourization theory and the experimental data of Bonilla and Perry[B16] and Berenson[B5], that a greater degree of superheat is necessary for materials with decreasing $K/\sqrt{\alpha}$ values. All situations which did not agree with this rule could be attributed to differences in active-site dis-

---

* i.e. adhesive energy at the solid-liquid-vapour interface due to the force $W_{S/L} = \sigma_l(1 + \cos\theta)$

tribution in different metals when they were given the same polish. For example, he shows boiling curves for smooth and roughened platinum in which the roughened surface required a higher wall superheat than a polished surface for the same heat flux. He concludes that site distribution alone is not sufficient to account for observed surface effects. Sharp also considers the effect of thin heat transfer surfaces and problems of temperature recovery after bubble detachment.

Some of these preceding effects have been observed experimentally. Carne and Charlesworth(C14) studied the boiling of n-propanol at atmospheric pressure on various metal strips (monel, inconel, mild steel, beryllium-copper and copper). They observed that the critical heat flux increased by a factor of two when the element conductance, Kt*, increased from 4.5×10^{-6} to 1680×10^{-6} watt/°C. Bernath(B14) and Ivey and Morris(I1) reviewed critical heat flux data for water and observed that the critical heat flux from horizontal cylindrical elements decreases as the thickness and the diameter of the test pieces are decreased. The data also indicated an asymptotic critical heat flux for thick elements. Carne (C16) found a similar dependence of critical heat flux on thickness for a number of organic liquids. Carne et al(C14) explained these effects as arising out of the large variations in local heat flux. These variations were considered by him to be due to local variations in nucleating site characteristics due to roughness, surface energy and contamination. The local variations

---

* t is the thickness of the metal strip

in heat flux caused local variations in temperature which permitted the thermal conduction to neighbouring microscopic areas on the heater surface. They assumed that for a fixed fluid condition, the local maximum heat flux can never exceed some characteristic maximum value.

2.3.3 Effect of Surface Tension and Interface Characteristics

It is a well-known fact that the most significant variable in the formation, shape and size of a bubble is the surface tension. This is borne out by Ellion's derived expression which relates the minimum degree of superheat required to the size of cavity, the surface tension and other fluid properties. Similarly the coalescing properties of bubbles at high heat fluxes is going to be influenced by surface tension effects. The semi-empirical correlations on boiling heat transfer fail to agree on the effect of surface tension. As equations (4) and (5) indicate, correlations based on purely hydrodynamic considerations predict a direct dependence to the 0.25 power (Z5), whereas those based on bubble agitation (R3) indicate an inverse dependence to the 0.5 power. The former correlations do not include any interfacial effect; the latter imply such an effect by requiring a coefficient which depends on the solid-liquid combination. This state of affairs suggests that the whole area of surface effects requires investigation and probably the development of new experimental techniques.

The discussion up to this point has indicated that it is impossible to separate surface tension and interfacial effects for

a particular solid-liquid combination. Moreover it is very difficult to determine the interface characteristics. Perhaps the only way of changing the interface characteristics is by using liquids of varying wetting characteristics.

So far, there has not been an experimental study on boiling heat transfer which has completely characterized the solid-liquid-vapour interface. Most of the studies have looked into the effect of surface tension of pure liquids. Dunskus and Westwater(D5) conclude from their studies that consideration of only the surface tension is a gross over-simplification. Although Griffith and Wallis(G6) were the only ones to measure surface tension and interface characteristics (contact angle) under controlled conditions, they indicated that they experienced extreme difficulties in determining contact angle under boiling conditions.

Some of the studies to date have reported observations and have accumulated data on the effect of varying surface properties through the addition of surface active agents. Most of these are at low heat fluxes (R5,M5,F2,W6,E1,J1,Y1); only a few experiments have been carried out at high heat fluxes (L4,D5,C1,E1). Many of these indicate conflicting results: for example, Costello and Adams(C1 reports burn-out heat fluxes for water containing wetting agent in which these fluxes varied as the 0.3 power of surface tension on stainless steel, as the 0.55 power on smooth graphite and as the first power on rough graphite. All observers agree that solutions containing surfactants do not exhibit the same boiling characteristics as pure liquids. They also agree that present

correlations are grossly inadequate in this respect. Explanations based on volatility, molecular weight and viscosity effects have been too specific and inconsistent and hence do not offer any general explanation. These experimental programs are reviewed below.

Yamagata et al[Y1] observed that bubbles eminating from a solution containing surface active agents tend to be smaller in diameter and that the ratio of pausing time to generating time was smaller than in the pure liquid. Indeed, vapour columns or jets and vapour mushrooms begin at much lower fluxes with the surfactant solutions. They attributed their observations on bubble characteristics to evaporation from the surface of the bubbles. These investigators also observed that, with these solutions, the spots of bubble formation were liable to be shifted during continuous bubble generation. Roll[R5] reports essentially the same observations as Yamagata. He also observes a large density of smaller bubbles which coalesced and drifted their nucleating sites.

Myers[M3] also reports a higher bubble frequency with solutions containing surfactants. Rather surprisingly, he finds that the bubble frequency-bubble volume product is constant for any given concentration. The constant varies with the concentration of the Tergitol* solutions, but remains constant over a wide concentration of Aerosol* although the surface tension varies considerably with concentration in both cases. Myers feels that the

---

* These are industrial trade names of surface active agents. A complete description may be found in (R5).

effect of these surfactants is not related to the break-off dimensions of the bubbles.

Dunskus and Westwater[D5] report on a study of surfactants in the boiling of isopropanol. Figures 2.6 to 2.8 show their results. They studied the effect of the molecular weight, concentration, volatility and viscosity of the additives on the boiling characteristics. They observed that the molecular weight of the additive had a significant effect, the higher the molecular weight, the higher the heat flux for the same concentration of additive at a given temperature difference. Low molecular weight additives at low concentrations caused the heat flux to be lower than the pure isopropanol. They attributed this effect to the ability of the molecule to diffuse away from the interface. They believed that the increased mobility associated with low molecular-weight material reduces the build up in the vicinity of the heat transfer surface. They suggested that this reduced build up altered the surface viscosity so as to reduce the boiling heat transfer. Increasing the volatility of the additive, greatly increases the peak heat flux. The peak heat flux approximately doubled as the concentration of one surfactant was increased. Dramatic changes also occurred in the transition boiling regime. This unstable region became much more stable in the presence of surfactants.

The effect of surface active agents on bubble growth has been studied by Ellion[E1]. He also conducted boiling studies with subcooled liquids containing Aerosol surfactant. He found that the critical heat flux was lower for solutions than for pure water over the entire range of subcooling from 10 to 140°F. At

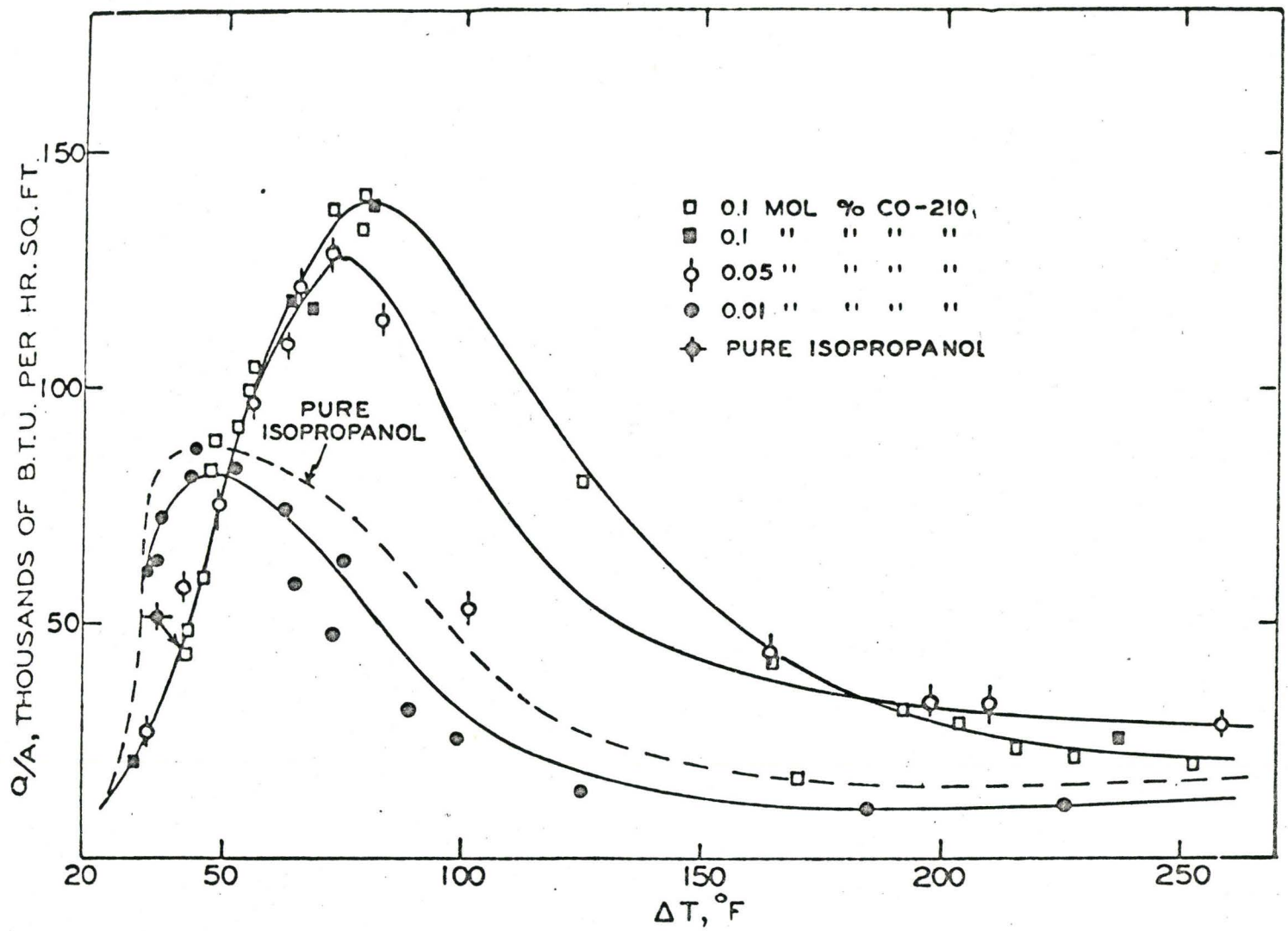

Figure 2.6 - Effect of concentration, boiling curves for isopropanol with various amounts of Igepal CO-210.

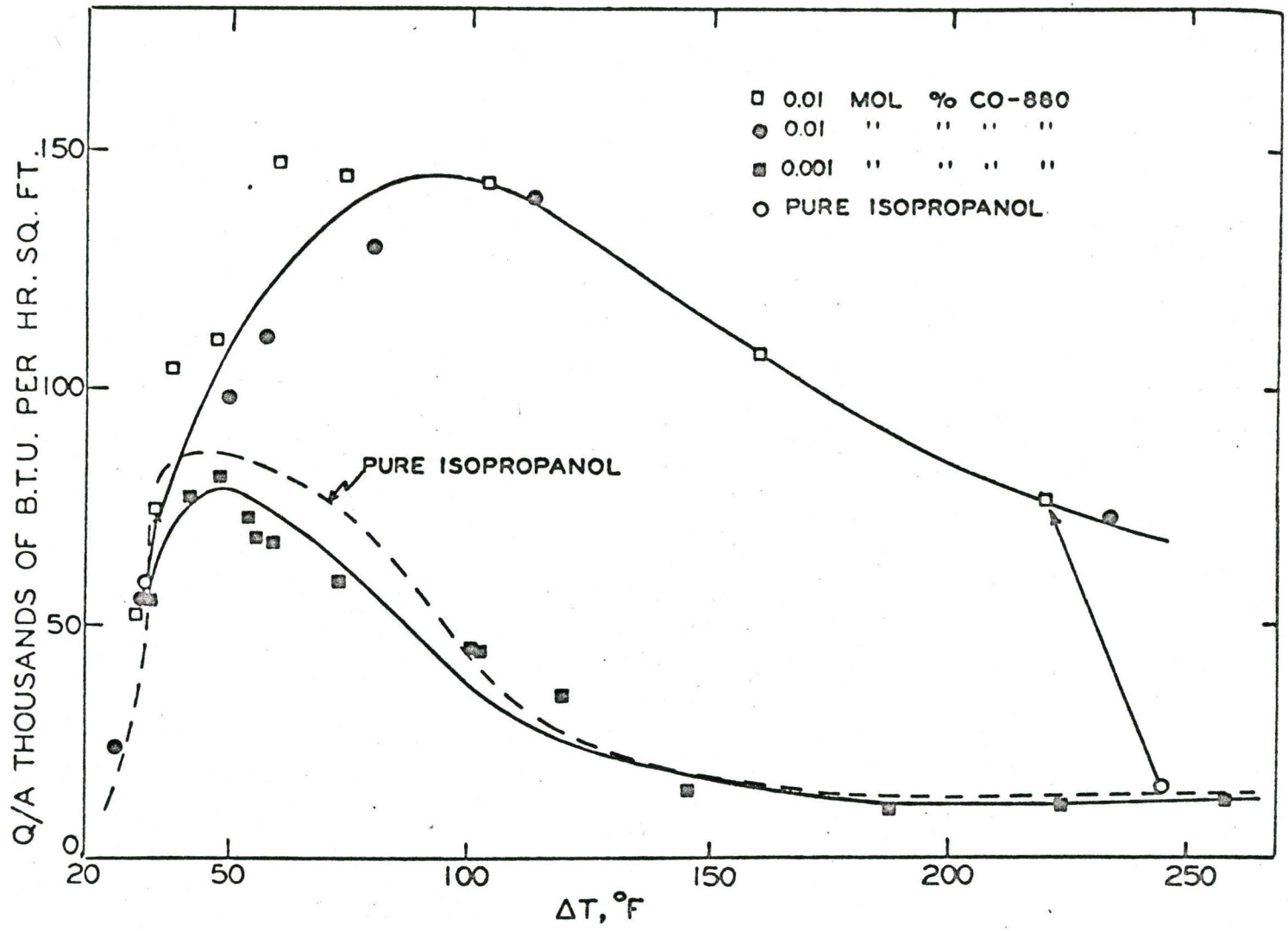

Figure 2.7 - Effect of high molecular weight additive, isopropanol with small amounts of Igepal CO-880.

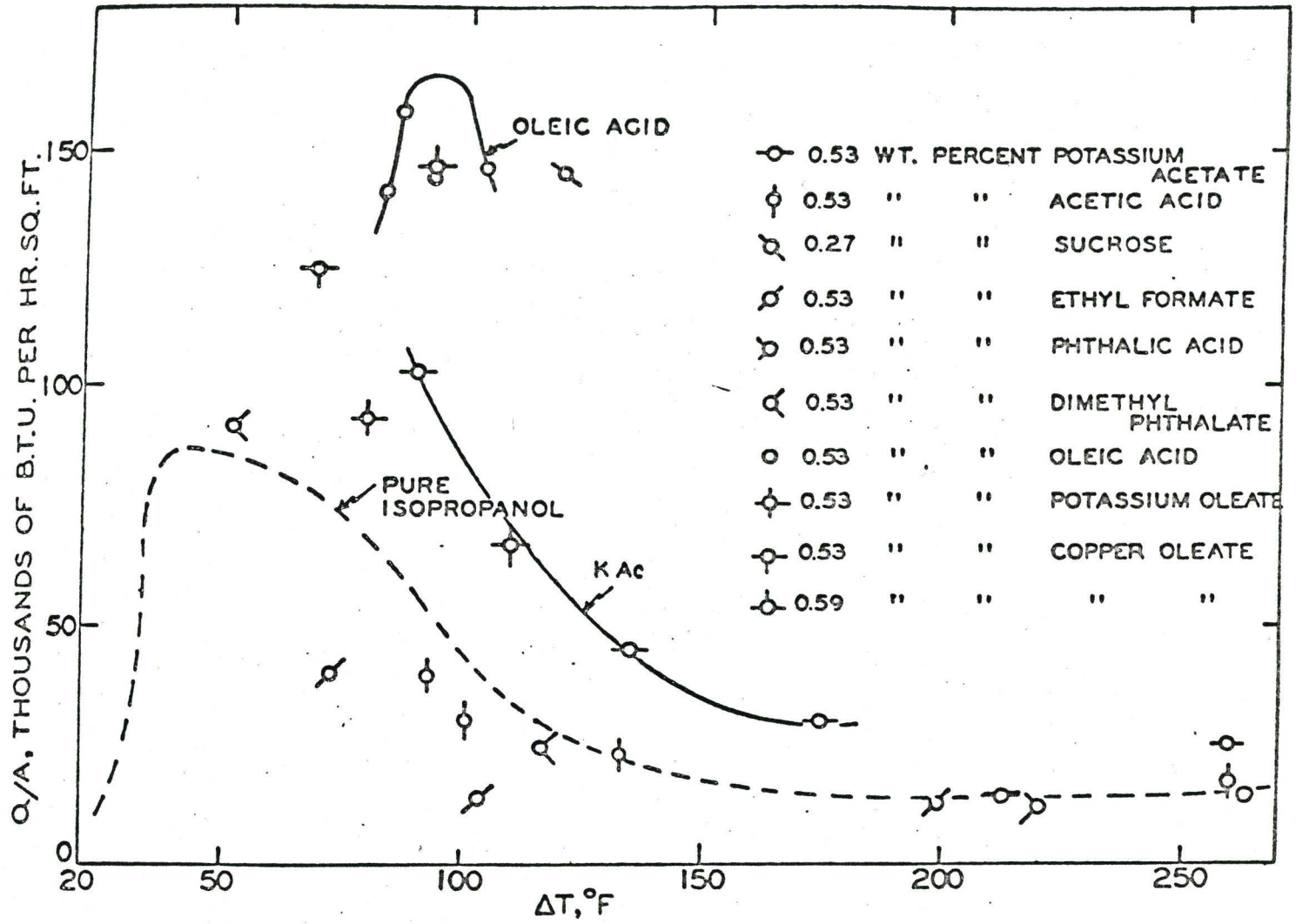

Fig. 2.8 - Effect of volatility of the additive, isopropanol with an approximately constant weight percent of nine additives.

saturation there was no significant difference in maximum heat flux.

Sabersky[S6] suggested that a liquid with low thermal diffusivity should have a lower growth rate. He used Ellion's results for an Aerosol solution and carbon tetrachloride which have equal surface tensions but different thermal diffusivities. The observed bubble growth rates corresponded to the predicted results.

Leppert et al[L4] studied the effect of adding small amounts of alcohol to boiling water. They observed that with about 1% isopropanol or 2% methanol (by weight), the nucleate boiling heat transfer coefficient was unaltered or slightly improved. However, the average and maximum bubble size was greatly reduced. Although these studies were conducted in forced-convection flow normal to a single tube, they do point up some of the perplexing problems associated with these studies.

This discussion indicates the need for more experiments to try to solve some of the mysteries in this area and also to improve our understanding of the basic mechanisms in boiling heat transfer.

2.4 Liquid Films in Boiling Heat Transfer

Interest in the boiling of flowing liquid films arises from recent developments in the metallurgical industry, boiling in nuclear reactors and cooling of rocket motors. Moreover, in any boiling, two-phase system in a closed conduit, most of the boiling usually takes place in the annular flow regime.

2.4.1 Film Flow

The earliest investigations on film flow were in the studies on mass transfer in wetted-wall columns and on heat transfer in condensing systems. An extensive review of the film flow phenomenon has been presented recently by Fulford(F6), so that only the essential details will be discussed here.

Analogous to the film flow in pipes, film flows may be laminar or turbulent depending on the magnitude of the film Reynolds number, $\frac{4\Gamma}{\mu_l}$. Films are definitely in turbulent flow if this Reynolds number is greater than 1600. The flow is not truly laminar, i.e. free from waves, unless the Reynolds number is < 10. In the intermediate range the flow is usually wavy-laminar unless stabilizers are present.

At low flows, surface forces become of the same order or higher than viscous forces and surface tension has a stabilizing influence. The approximate relationship between average thickness and Reynolds number is given by Fulford(F6).

The gas velocity affects film flows when it is high enough. Dukler (D6) observed considerable effect in his studies; whereas

Knuth[K8] and Kinney et al[K9] observed a lesser effect. There are a number of other studies (H8,B13,C9,D6) on film flow inside conduits which are not of real interest here. Dernedde's study of the boiling of liquid films in this laboratory (D1) has not observed any effect of the shear exerted by the "stagnant" gas on one side of the film (H10).

2.4.2 Film Instability

Instability of the film may not by itself be harmful, so long as the conditions of flow and heat transfer are not appreciably affected. A flowing film is considered unstable when its flow patterns change and then break-up occurs. Instabilities in film flow can, in general, be attributed to hydrodynamic or thermal causes (temperature gradients). Surface tension effects are included in both. Extensive studies have been reported in the literature (B13,B17,C7,C10,C9 ,02) on both types of instability. Berenson and Stone[B17] have made a photographic study of heat transfer to flowing films in a two-phase flow system and concluded that liquid films formed dry spots on the surface because of vapourization and not because it was hydrodynamically unstable. In this case, however the flowing gas may have had a stabilizing effect.

2.4.3 Hydrodynamic Instability

Ostrach[02] has given a description of the various hydrodynamic instabilities that can occur as a result of shear, surface, buoyancy and inertia forces and presents criteria for film break-up. These instabilities are characterized by Reynolds, Froude and

Weber numbers.

2.4.4 Stability Due to Surfactants

The fact that surface active agents can stabilize the flow of a liquid film has been known for a long time. Whitaker[W2] has extended Benjamin's analysis (B 8) of instability of film flow to include the effect of surface active agents. He shows that surface tension and surface viscosity can dampen only very small disturbances and that the stabilization results from what he calls surface elasticity. Surface elasticity arises out of gradients in surface tension which, in turn, arises from surfactant concentration gradients along the interface. These surface tension gradients introduce a tangential surface force (from high to low surface tension) which acts to stabilize any wavy interface. Therefore, the rate of mass transport of surfactant to the fresh interface will determine, in part, the stability of the film. It can then be said that the dynamics of a flowing film of a liquid containing surfactant will depend on the Surface Elasticity number $(\frac{\partial\sigma / \partial c}{C_o \rho \; u^2 \; h})$, Weber number $(\frac{\sigma}{\rho u_o^2 \; h})$, Reynolds number $(\frac{h \; u_o \rho}{\mu})$, Schmidt number $(\frac{\mu}{D \rho})$, Froude number $(\frac{g}{\rho \; U_o^2})$ and the equilibrium concentration of the surfactant. The regime of flow and chemical in the system will determine which of these groups are dominant. Berg[B1], Whitaker[W2] and Whitaker and Jones[W3] present the results of their computer studies to indicate under what conditions instability can be expected. Figures 2.9 and 2.10 are taken from their papers

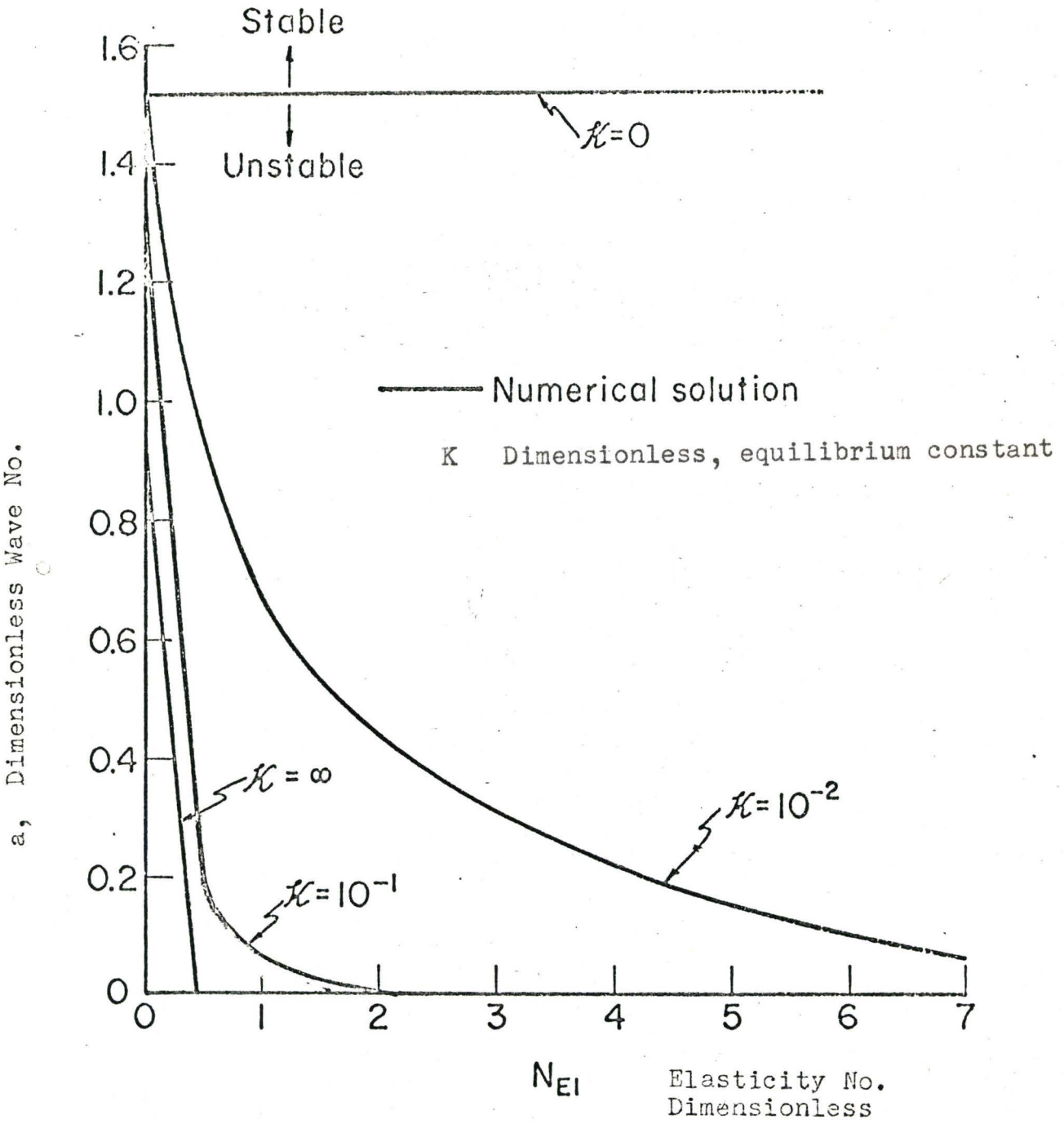

Fig. 2.9 - EFFECT OF MASS TRANSPORT ON THE CRITICAL WAVE NUMBER (Ref. W3)

FIGURES 2.10

EFFECT OF SURFACTANTS ON NEUTRAL STABILITY OF FILMS

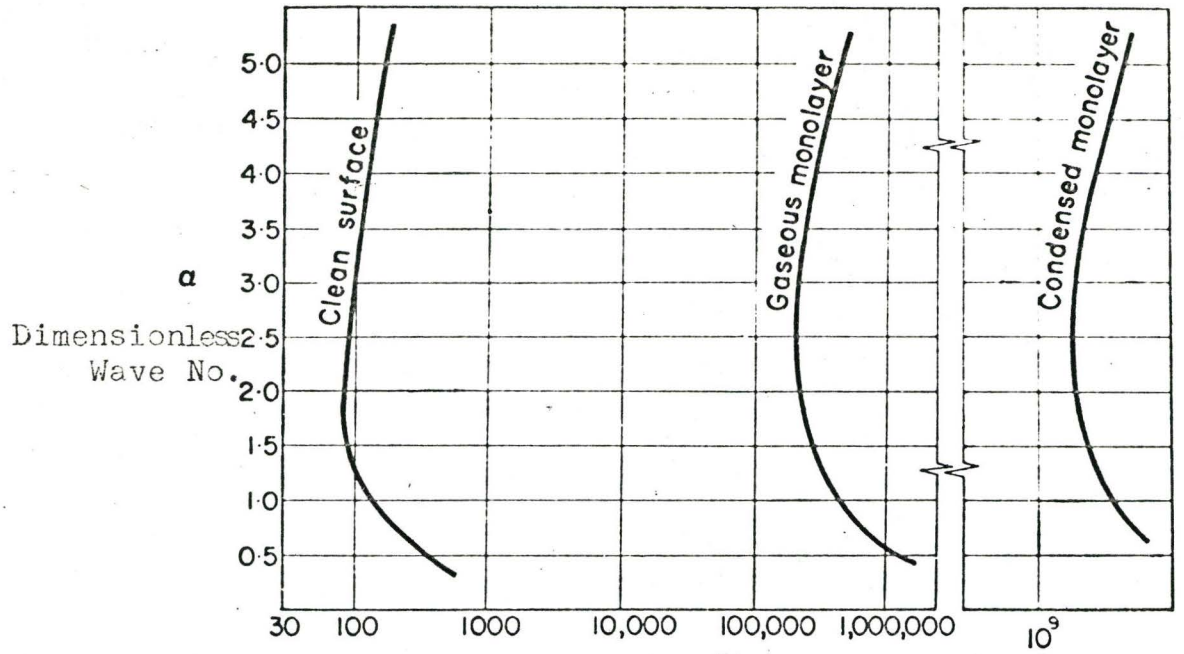

Neutral stability curves showing the effect of surfactants (isothermal bottom). (Ref. B1)

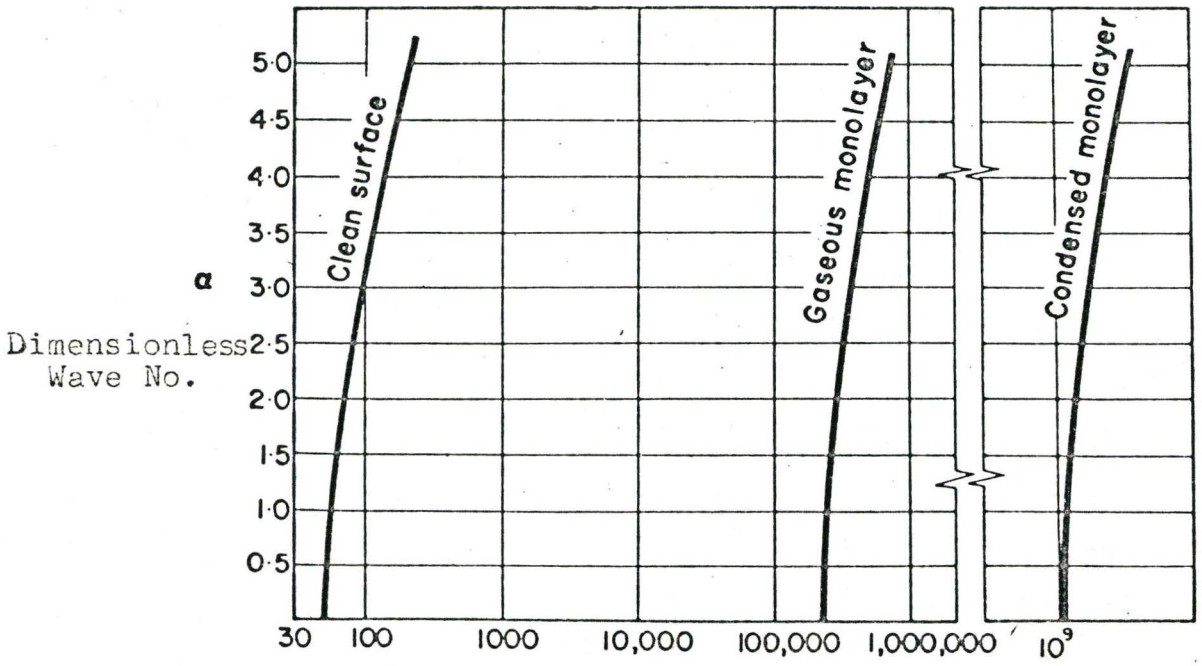

Neutral stability curves showing the effect of surfactants (constant flux bottom). (Ref.B1)

$$B = -(\partial\sigma/\partial T_o)\,\beta h^2/\mu\alpha$$

β = Grad T_o

(B1,W3). They indicate the type of results that have been obtained. In Figure 2.9 the effect of mass transport of surfactants on stability is given; in Figure 2.10 the stability curves are shown for surfactant solutions in which temperature effects exist. Unfortunately, there is no work done on the stability of liquid films under varying conditions of liquid-solid-gas interfaces.

Most surface active agents exhibit a tendency to approach an asymptotic surface tension as concentration is increased. Therefore the effect of surfactants on stability is expected to become small at high concentrations.

2.4.5 Thermal Stability

The earliest studies on thermal instability date back to 1836, when Varley[V1] "observed strange and curious motions in fluids undergoing evaporation". This motion which is not normally visible to the naked eye received serious attention by the turn of the century by Benard[B18] who found a systematic hexagonal pattern of convection cells in a layer of liquid heated from below. This is the famous "Benard Thermal Instability" and is the most common one. Pearson[P3] in 1958 analyzed this problem considering the temperature varying layers and ascribed the motion to surface tension effects (Marangoni forces) rather than to buoyancy forces, whenever the depth of the liquid is less than 1 cm.

Many experiments later indicated the importance of interfacial contamination. Langmuir and Langmuir[L5] noted that monolayers of several surfactants eliminated the convection which normally accompanies the evaporation of aqueous ether solutions.

Bell[B7] demonstrated that silicone monolayers prevented the occurrence of Benard cells. Berg and Acrivos[B1] have done an extensive study of stabilizing this "Benard Thermal Instability" by using surface active agents; Figure 2.10 shows the stability curves.

Some of the recent studies on thermal instabilities have been conducted by Hsu et al[H9], Staub and Zuber[S9] and Ostrach and Koestel[02]. These are essentially a combination of the hydrodynamic instabilities and Benard instability.

Many authors have their own system of classification of thermal instability (S9,H9,02). One such interesting classification is by Staub and Zuber[S9]. They consider the film break up and dry patch formation in liquid film flow boiling heat transfer as due to three causes,

(i) thermo-capillary effect

(ii) vapor thrust effect and

(iii) bubble growth effect.

An excellent description of this has been recently given by Dernedde[D1]. An extensive study of the film break up and dry patch formation criteria is given in (03,S9,H9,D1). None of these seems to consider the difference between liquid-vapour interface and liquid-solid-vapour interface in detail.

2.4.6 Minimum Wetting Rate

In flow systems, the combination of hydrodynamic and thermal instabilities is more obvious. This necessiated both experimental and theoretical studies on minimum wetting rates needed to avoid

film break up and dry patch formation. Some of the excellent studies on minimum wetting rates are by Norman and McIntyre[N2] and Ostrach et al[O3]. Minimum wetting rate depends on the liquid temperature and temperature of the tube surface. The minimum wetting rate is less at higher than at lower temperatures. Norman and McIntyre[N2] correlated their results for thin continuous films, in terms of average film thickness at the point of break down and the product ($\sigma \cdot \Delta\sigma$), where $\Delta\sigma$ is the difference between the surface tension of the liquid in equilibrium with tube surface temperature and the bulk liquid surface tension. They observed a sharp increase in heat transfer coefficient at the point of film break up. During boiling the minimum wetting rate decreases considerably and therefore dry spot formation is reduced when boiling takes place. The minimum wetting rates for water reported in the literature are very scattered. Hartley and Murgatroyd[H7] attempted to predict the minimum wetting rate both from heat energy principle and from a force balance. The former was not generally applicable especially to thin interfacial films. Here the meta stable condition exists and the sum of potential energy and surface energy may not have a minimum. The latter was based on the force balance to form dry spots.

Hsu et al[H9] extended this dry spot theory. Figure 2.11 shows the schematic representation of the liquid film analyzed by Hsu and also shows the temperature profile assumed for the analysis. The temperature depends on the heating the film has undergone. The dry spot formation depends on the temperature and the thickness

FIGURES 2.11

DRY SPOT FORMATION OF FLOWING LIQUID FILMS

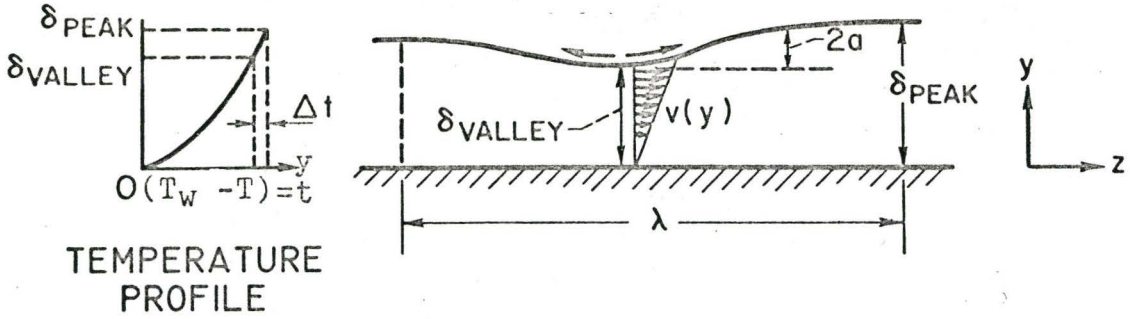

a - Thermocapillary motion at the film surface. (Ref. H9)

y - Direction Normal to heating surface
x_f - Length from the inlet in the direction of flow
λ - wave length
a - Amplitude of wave

Effect of Contact Angle and Thermocapillary motion

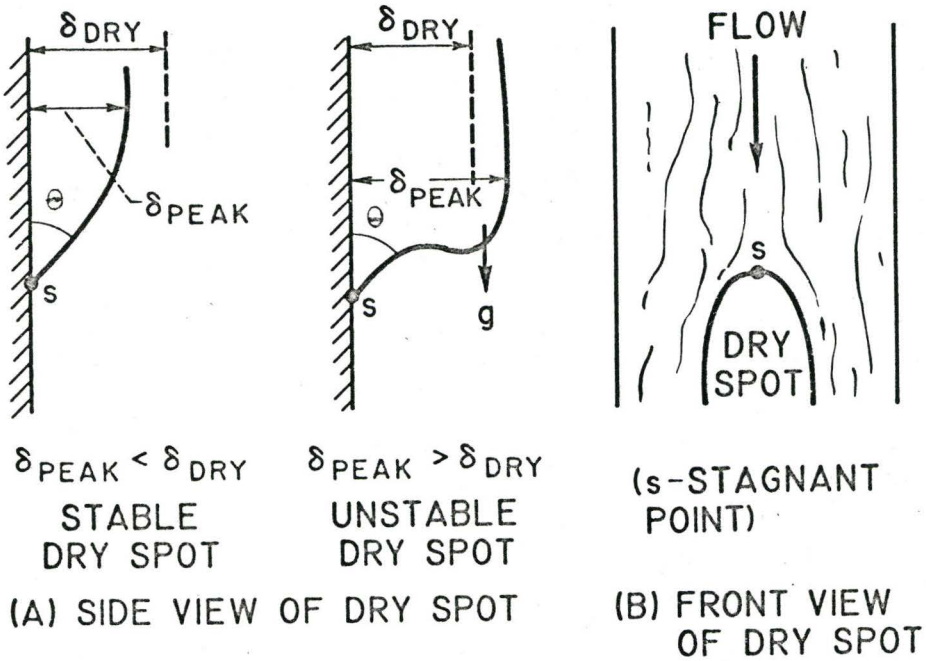

b. - Stability of a dry spot. (Ref. H9)

FIGURE 2.12

EFFECT OF HEATING LENGTH ON DRY SPOT FORMATION

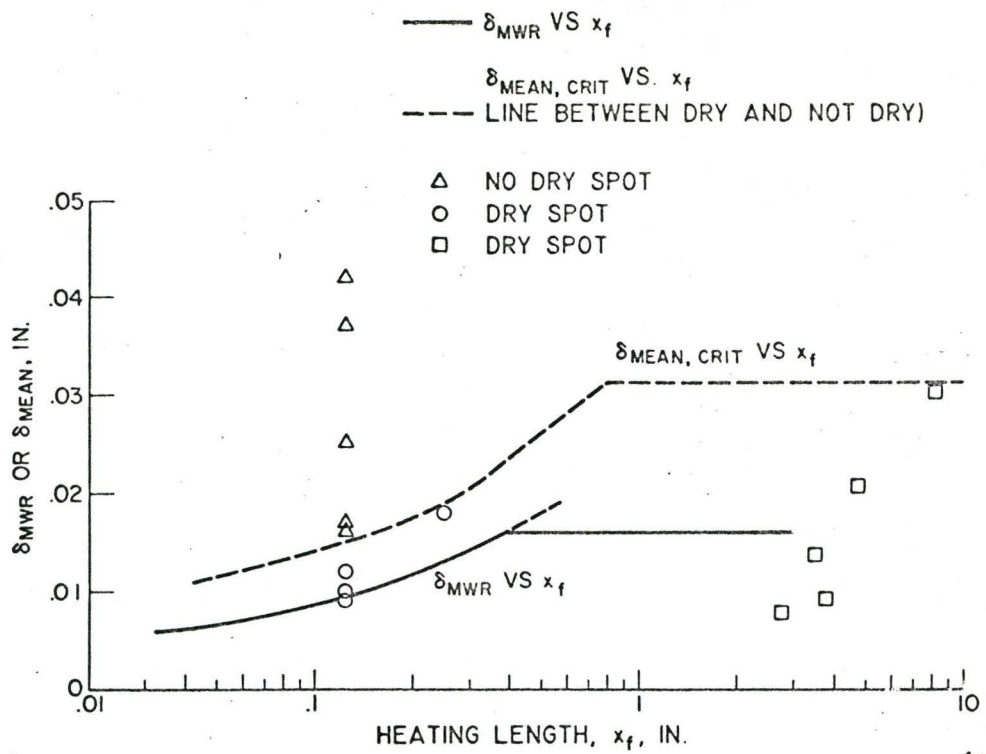

a - Comparison of δ_{mean} (experimental) with δ_{MWR} (theoretical) at various heating lengths. (Ref. H9)

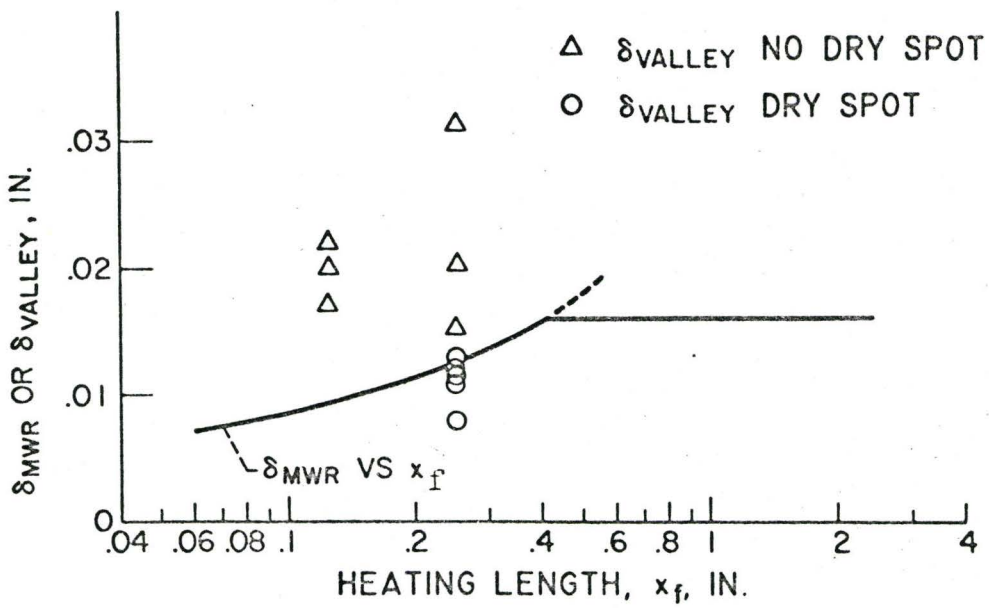

b - Comparison of δ_{valley} (experimental) with δ_{MWR} (theoretical) at various heating lengths. (Ref. H9)

of the film. Thus he considers thickness at minimum wetting rate, δ_{MWR}, for each heating length, instead of the minimum wetting flow rate criteria discussed earlier. He derives an expression for δ_{MWR}, based on the thermal boundary layer at the entrance region. The results of his theoretical studies on the δ_{MWR} are reproduced in Figure 2.12. He proposes a critical thickness, δ_{cr}, for a stable dry spot based on the wetting properties of the heating surface and compares with δ_{MWR} in the same Figure 2.12. The minimum thickness of a wavy film is at its valley (Figure 2.11). He compares his experimental data of thickness of the film at the valley, δ_V with δ_{MWR} for various heating lengths. Thus any study on film flow boiling heat transfer needs a consideration of this dry spot formation of a flowing film. It is better to have liquid flow rates so as to have a film thickness greater than δ_{MWR} and preferably greater than δ crit. There is no study so far on the minimum wetting rate and critical dry spot thickness of surfactant solutions.

2.5. Wetting Effects in Boiling

The effect of wetting in boiling heat transfer, especially at high fluxes, has received very little attention and yet direct observation, as shown on Plate 1, has indicated how surface contamination, roughness and surface material can change the boiling process. Gaertner[G2] has shown the effect of non-wetting teflon on boiling; Jakob[J1] has mentioned that a thorough study of contact angle is necessary for further development of the theory of

PLATE 1A

EFFECT OF CONTAMINATION ON BOILING SURFACE

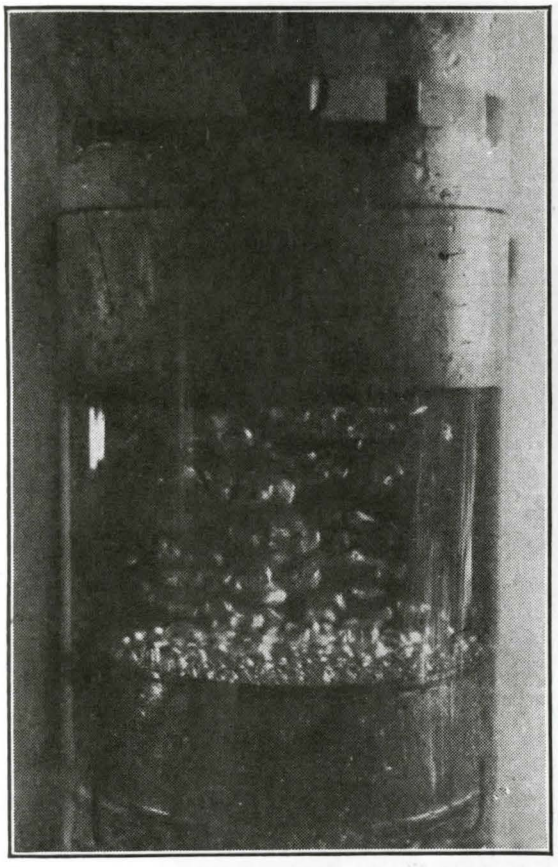

a Boiling of water on a horizontal surface covered with oil.

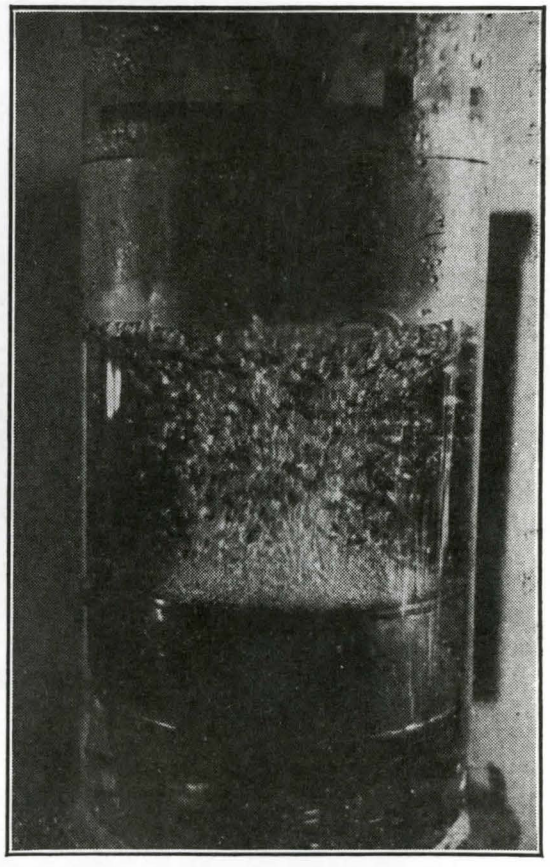

b Boiling of water on a clean horizontal surface.

Ref. (J1)

(Q/A) = 19,000 B.t.u./(hr.)(sq.ft.)

Time of Exposure = 1/200 sec.

(a) Surface Unwetted

Small no. of Large Bubbles
Bell or Tandem Type

(b) Totally Wetted

Large Number of Small Globular or Oval Bubbles, and Vigorous Activity.

PLATE 1B

EFFECT OF SURFACE ROUGHNESS AND MATERIAL

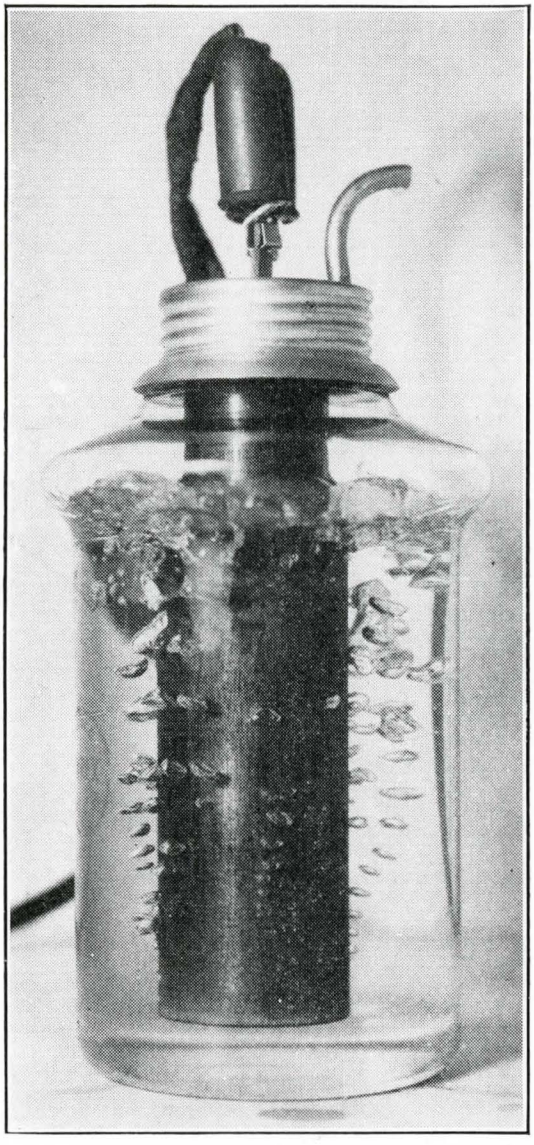

Boiling of water on a smooth vertical surface.

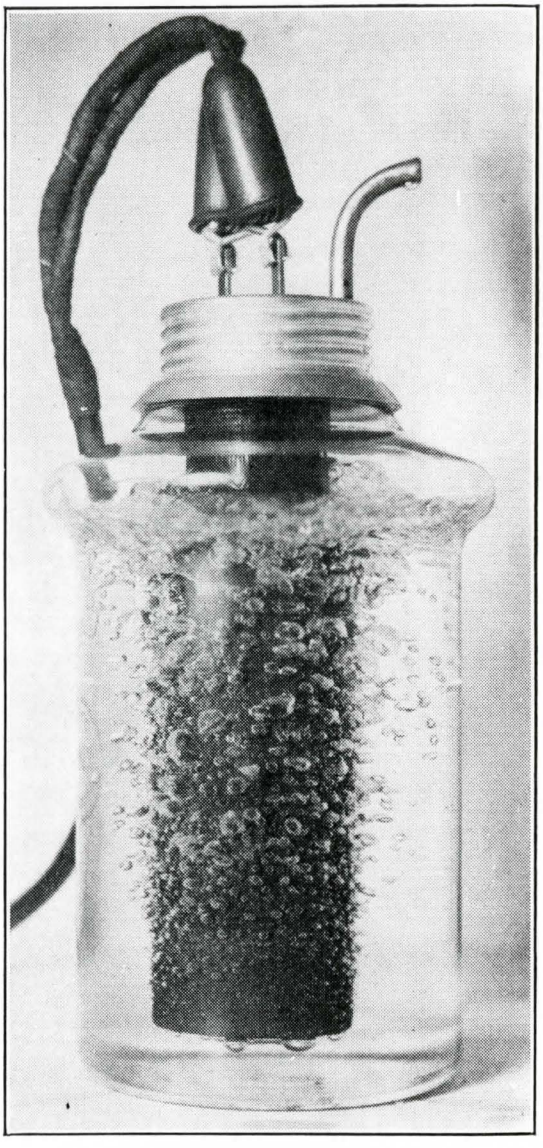

Boiling of water on a vertical surface painted with a graphited mass.

Ref. (J1)

(Q/A) = 19,000 B.t.u./(hr.)(sq.ft.)

Boiling Surface is $1\frac{1}{2}$" O.D. Steel Boiler Tube

Time of Exposure: 10^{-5} sec. by light of 16,000 V. Spark

(a) Nucleation at a few places, large bubbles

(b) Nucleation at large number of places, smaller bubbles

nucleate boiling. Most investigators consider the contact angle of water* as constant for any surface. Jakob(J1) assumes 50°, Gaertner(G1) 60°. Direct measurements have shown it to vary from 50 to 90° on a copper plate (B2, O1) depending on the surface roughness, contamination and ionic properties of the surface.

Certainly some dramatic effects have been observed to occur as a result of wetting. By adding 0.04 percent of potassium to mercury Lozhkin(L1) has found an increase of 200% in the boiling heat transfer coefficient. This was attributed to the greater wetting power of the potassium amalgam.

Although more quantitative data on the effect of wetting are not available, the existence of a microlayer and its part in the mechanism of nucleate boiling have demonstrated the importance of wetting and other thin-film properties. Since surface active agents affect these properties they are expected to have a considerable affect on the boiling process. The review that follows considers some of the fundamental properties of interfaces and surface active agents.

2.5.1 The Interface

Since the following discussion is centered on interfacial phenomena and properties it is worthwhile considering what is meant by an interface.

Mathematically, we always consider an interface as a plane

---

* Defined on page 67.

when in essence it is a fuzzy boundary extending over several molecular layers. Forces will exist over this region which will be quite different from those in the bulk. These will manifest themselves in certain properties such as surface tension, viscosity and elasticity. In other words, this region can be thought of as a region occupied by a fluid of quite different physical properties. In some cases these properties become very important in determining the overall behaviour. Surface active agents or surfactants play a large role in changing the properties of the material "in the interface". The following discussion considers this interfacial behaviour.

2.5.2 Surface Active Agents

Substances are called surface active agents when the surface tension decreases as the bulk concentration of the substance increases. This lowering of the surface tension is proportional to the concentration of the solute raised to some fractional power. This can be expressed by Freundlich's equation (F5)

$$\Delta\sigma = kc^{1/n} \qquad \ldots(20)$$

Furthermore, the concentration of the substance is different at the interface relative to the bulk of the solution. Usually a larger concentration of surfactant is observed at the interface and this concentration increases as the bulk concentration increases, at least for dilute solutions. The distinct dependence of concentrations at equilibrium is indicated by Stucke's equation (S4)

$$-\frac{d\sigma_\infty}{dc} = \text{constant} \qquad \ldots(21)$$

and $$\sigma_i - \sigma_\infty = -c_\infty \frac{d\sigma_\infty}{dc} \qquad \ldots(22)$$

where σ_i and σ_∞ are the surface tensions at the interface and bulk concentrations respectively and c_∞ is the concentration of surfactant in the bulk.

Considerable time is required for the concentration to change at the interface after a new surface is formed. The time to reach equilibrium concentrations depends on the nature and concentration of the solute. As a result of this time lag, surfaces of different ages will have different concentrations and hence regions of different surface tension. Such a situation gives rise to Marangoni forces which cause movement of liquid from points of high to those of lower surface tension. This coupled with similar effects that arise out of temperature differences leads to a very complex, interacting flow phenomena. Therefore any accurate and complete study of the effect of surfactants on the boiling phenomenon must necessarily consider the equilibrium and non-equilibrium characteristics of the solid-liquid-gas interface. Unfortunately, the development in the knowledge of surface forces at an interface is still not complete enough to study the equilibrium/non-equilibrium aspects of this problem (D2).

2.6 Interfacial Films and Forces

The preceding discussion has indicated the importance of the heating surface in determining the boiling heat-flux. The existence of an evaporating microlayer of liquid under a vapour

bubble has underlined the importance of the wetting characteristics of a liquid on any given solid surface. One can visualize a complex interaction between the hydrodynamics of the system and its interfacial characteristics. Associated with this probelm are the difficulties in measuring the physico-chemical properties of thin films and the solid-liquid interface (F1,W3).

Since the depth of the microlayer film cannot be more than 50-100 molecules, the surface forces of the solid are expected to influence considerably the behaviour of the thin film. Studies on colloidal stability by Zisman(Z1) and Deryagin(D2) have shown that the effect of the forces exerted by a solid surface may extend several molecular layers. Moreover, with such thin liquid films properties such as surface viscosity, elasticity and others, which may be a function of the orientation of the molecules at the surface, will become important in establishing stability, flow, vapourization, etc. More sophisticated experimental techniques are obviously required to measure the properties of these thin liquid films. One can only hope that the measurements (such as contact angle) with larger quantities and thickness of liquids on solids are directly related to the behaviour of thin films. A discussion of some of the fundamentals and experimental measurements follows.

2.6.1 The Disjoining Pressure of Thin Liquid Films

The studies reported by Fuks(F1) on the resistance to thinning exhibited by surface films may have some direct bearing on the dynamics of the microlayer. In these experiments, the kinetics of thinning were studied by measuring the time of thinning

of liquid films contained between two parallel discs. The time of thinning (t) can be related to the measured variables in the experiment by the Stefan-Reynolds equation:

$$t = \frac{3\pi\mu}{4F} r^4 \left(\frac{1}{h_i^2} - \frac{1}{h_f^2}\right) \qquad \ldots(23)$$

where F is the applied force, h_i and h_f are the initial and final thicknesses respectively, r is the radius of the disc. Problems arose when an attempt was made to extend the experiments to zero final thickness. Fuks found that low molecular-weight hydrocarbons could be extruded completely, whereas solutions of mineral and fatty acids could not. His data show that the residual film-depth of a solution and the resistance to thinning depend, not only on the force applied but also on the solute, the solvent and the solid body. The equilibrium factor which determines this residual film depth for any given system is the disjoining pressure. It is defined as the negative of the derivative of the system free energy with respect to film thickness. It refers only to equilibrium surface forces normal to the interface. The disjoining pressure is a property of a particular solid-liquid combination; it shows up only in thin liquid films and hence must be related to interfacial forces. Some thermodynamic considerations of disjoining pressure are discussed below.

Thermodynamics of ordinary systems considers that the ordinary surface or interface phenomenon arise from an excess of free energy or some other thermodynamic potential, which is pro-

portional to interfacial area. The theory of these effects developed by Gibbs(G 9) is only applicable to systems of moderate dimensions. Thus this theory is only strictly applicable to systems with dimensions greater than 10^{-4} cm., above which the surface tension is independent of dimensions (r). In recent years, many developments (D2,S2) have been made to extend the Gibbs Theory, so as to allow for the dependence of surface tension on "r". These studies in Russia (D2,S2,F1) have shown that departures from the additive distribution of free energy or other potentials over the component parts, whose dimensions fall below a certain limit (film depth "h" or bubble or drop radius "r" equal to 10^{-5} cm.) cannot be accounted only by a single term for surface energy in the bulk. Thus they introduced some new terms. These are not characteristic of the surface of the drop or bubble or film alone but refer to the whole structure. Thus with the knowledge of these factors it may be possible to extend the treatment to cover small objects, in which a separation into surface and bulk components cannot be made.

This effect of dimension of the thin film was observed by Scherbakov(S2) and Deryagin(D2) while working on the Adhesion Pressure or Disjoining Pressure. They found that equilibrium hydrostatic pressure in thin liquid films exceeds the normal hydrostatic pressure.

Indeed, Scherbakov(S2) derived an expression for the disjoining pressure as given below:

$$P = P_{\infty} \quad \text{Exp} \left(\frac{V^{l}}{RT} \quad \left(\frac{2\sigma}{r} + \frac{\partial \sigma}{\partial r} \right) \right) \qquad \ldots(24)$$

where P is the Disjoining or Adhesive Pressure

P_∞ is the Hydrostatic Pressure in the bulk

V^l is the volume of a bubble or vapour mass

R is the gas constant

σ is the surface tension

r is the depth of film from the surface.

The superheat of the boiling surface needed for the microlayer vapourization may thus be different compared to the superheat needed in normal systems, where normal hydrostatic pressure is assumed to be the factor controlling the superheat.

With future progress in theoretical and experimental studies on residual film thickness, disjoining pressure, surface elasticity and surface viscosity, criteria for microlayer vapourization and superheat may be possible.

2.6.2 Wetting

When a liquid is placed on a solid surface, the bare surface of the solid adsorbs the vapour of the liquid until the fugacity of the adsorbed material is the same as that of the vapour and liquid. The adhesive force between a liquid and solid is that existing between the liquid and adsorbed layer on the solid.

The meaning of the term wetting is only a matter of definition and, in general, indicates the relative magnitude of adhesive forces at the interface, i.e. the wetting of a liquid on a solid is a measure of the adhesive force between the liquid and solid relative to the adhesive force between two liquid masses.

When small drops of liquid are placed on the surface of a

FIGURES 2.13

WETTING OF SESSILE DROPS

a - Wetting of small sessile drops

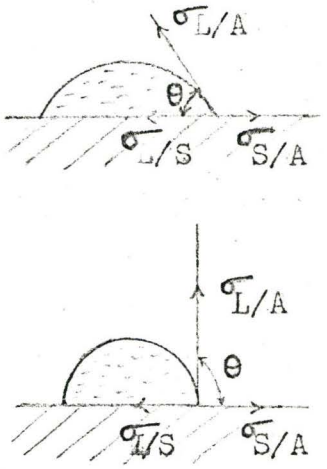

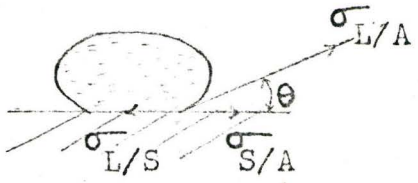

b - Wetting and Non-Wetting Sessile Drops (Large)

solid they do not spread completely but form a segment of a sphere. Larger drops form segments of ellipsoids; still larger masses spread over the surface. Wetting is usually defined in terms of the contact angle formed at the liquid-solid-gas interface shown in Figure 2.13. The solid is completely wetted if this angle is zero and considered to be non-wetting if the contact angle is 180°.

There are a number of methods for experimentally measuring contact angle. Each has certain advantages and disadvantages. Some of the most widely-used methods, their limitations and the choice for the present study, are given in Appendix III.

The contact angle can be related to the liquid-vapour interfacial (surface) tension through the interfacial tension of the solid-liquid and solid-vapour ($\sigma_{S/L}$ and $\sigma_{S/V}$ respectively) by the equation:

$$\text{Cos } \theta = \frac{\sigma_{S/V} - \sigma_{S/L}}{\sigma_{L/V}} \qquad \ldots(25)$$

If the calculated cos θ > 1, the measured contact angle will be zero and wetting is considered to be complete.

To achieve complete wetting, cos θ should tend to 1, $\sigma_{S/V}$ should be large and $\sigma_{S/L}$ and $\sigma_{L/V}$ should be small. Often $\sigma_{S/L}$ is large in practical systems, especially if the surfaces are rough or particulate. Thus cos θ can be increased by lowering the liquid-vapour interfacial tension through the addition of surface active agents. With most surfactants, the wetting is further improved because the liquid is able to penetrate and wet some of the

unwetted areas of the solid surface and thereby reduce $\sigma_{S/L}$. Furthermore since surfactants concentrate at the interface the free energy of the solid-liquid interface will be affected by virture of these other species being present. These foregoing characteristics work to improve the wetting characteristic of any liquid.

There are three types of wetting which may occur depending upon the magnitude of the free energy changes which take place in the entire system and the manner by which they are brought about. They are described as adhesional wetting, spreading wetting and immersional wetting. The first two are of interest in boiling phenomena.

(a) Spreading Wetting

Spreading wetting is referred to as the process which occurs when a layer of liquid spreads over a solid and displaces the gas or vapour, i.e. in the case of a liquid film, a given area of solid-gas interface disappears and is replaced by equal areas of the solid-liquid and gas-liquid interfaces. Spreading wetting is obviously important as the liquid moves in behind the departing vapour bubbles on a heat transfer surface.

It is possible for spreading to be essentially spontaneous as a result of interfacial forces only. Often mechanical or chemical forces may influence spreading although interfacial free energies may still be the dominant factor. The tendency for spreading of a liquid is measured by the spreading coefficient, S. It is a measure of the Free Energy change accompanying spreading

and is given by

$$S = \sigma_{V/S} - \sigma_{L/V} - \sigma_{L/S} \qquad \ldots(26)$$

where $\sigma_{V/S}$, $\sigma_{L/V}$ and $\sigma_{L/S}$ are the interfacial tensions of the vapour-solid, liquid-vapour and liquid-solid interfaces. If S is greater than zero, spreading is spontaneous and the driving force is given by S. However most liquids invariably show negative S-values and highly negative coefficients mean less wetting of the solid surface (D2).

Surface active agents influence spreading wetting by their effect on the interfacial tensions. The values of S will reveal their influence in the wetting process. This is visualized better by writing the spreading coefficient in terms of the contact angle, viz:

$$S = \sigma_{L/V} (\cos \theta - 1) \qquad \ldots(27)$$

This equation strictly applies to equilibrium contact angles.

There are many relatively easy methods for measuring spreading wetting. For liquids with positive "S" values, direct measurements have been made using monolayers of the liquid. If stable sessile drops are easily formed, the spreading coefficient should be calculable with reasonable accuracy from the measurements of contact angle and surface tension.

(b) Adhesional Wetting

When a state of equilibrium exists between liquid, solid and gas at a three phase boundary, there is certain resistance offered to the liquid when it is displaced from the solid by the

gas. The driving force by the liquid to overcome such a resistance is what is known as Adhesive Force, $W_{L/S}$ and is given by:

$$W_{L/S} = \sigma_{L/V} + \sigma_{V/S} - \sigma_{L/S} \qquad ...(28)$$

where again σ represents the interfacial tension between the phase indicated by the subscripts (L is liquid, V is gas and S is solid). In terms of contact angle this can be conveniently expressed as:

$$W_{L/S} = \sigma_{L/V}(1 + \cos \theta) \qquad ...(29)$$

Adsorption of surface active agents at interfaces, generally reduces interfacial tension and consequently affects the degree of adhesive wetting. It is to be noted, however, that the lower the surface tension the lower will be the work of adhesion and the easier it will be to displace liquid from the solid by the gas. On the other hand, the smaller the contact angle, the higher will be the work of adhesion and the greater effort will be necessary to disjoin liquid by the gas.

Adhesive wetting is expected to influence the vapour formation and departure from the solid surface during the boiling process. Although some preliminary work has been done on this aspect (H1,Y1,G1,S1) direct studies on this variable have not been made. This situation exists because of the complexities of the interactions and the need for new experimental techniques.

Some preliminary suggestions for the effect of wetting on boiling can be obtained from the criteria for adhesive joints (G3). They are

(i) the surface free energy of the solid should be high,

(ii) the liquid vapour interfacial tension or free energy should be intermediate, not too high, not too low,

(iii) the solid-liquid interfacial tension or free energy, $\sigma_{S/L}$, should be low,

(iv) generally solid and liquid should possess similar polarity. The surface free energy of the solid and solid-liquid interfacial free energy are the most important properties. It can be seen from preceding studies that higher critical heat fluxes have been observed in the case of high energy heating surfaces (Sl). In principle this can be done by cleaning or etching or attacking with polar reagents. Roughness increases the available area and thus increases the surface free energy. However, in practice it is very difficult to prepare a clean rough surface which will allow liquid contact of the entire area. In practice it is also very difficult to select the solid-liquid combination which give low interfacial tension for high energy surfaces.

As already indicated, surface-active agents may improve the wetting characteristics of any surface by lowering the surface tension. Many of the best wetting agents have irregularly-shaped molecules which very rarely pack into micelles but usually concentrate at interfaces because of the different affinity that various functional groups in the molecule have for the solvent. This characteristic probably accounts for the large effects of relatively small concentrations. For this reason the ionic character (anionic or cationic) becomes very important in determining the effect on the wetting. For example, silica and glass are always wetted by

water containing anionic surfactants, whereas they become non-wetted by very low concentrations of cationic agents. At higher concentrations of this latter material, wetting occurs again. Figure 2.14 shows the effect of increasing the concentration of surfactant and ionic character on the wetting behaviour.

A property of liquids containing surface-active agents which is important in heat transfer studies is the so-called Krafft point. This is the temperature at which the surfactant molecules agglomerate to form micelles. As expected, at this temperature a significant change in surface tension is observed.

Many surfaces are not wetted by liquids because of the roughness of the surface, or when wetting occurs significant changes in contact angle are observed because of this factor. Roughness has the effect of making the contact angle greater than the smooth-surface contact angle if it is already greater than 90° and vice versa for systems with contact angles less than 90°. For example, water on rough paraffin wax exhibits a contact angle of 132°, whereas on smooth wax it is 110°. Similarly water on smooth copper indicates a contact angle of 80° and 50° on a rough surface. Wenzel[W4] has expressed many of these ideas quantitatively. When making experimental measurements of contact angle much of the scatter of data will arise because of the variations in surface roughness or contamination over the surface.

There is a critical wetting temperature for many surfaces above which $\theta = 0$. Rideal[R1] has presented a procedure to calculate this from the energy of mixing of the molecules. Similarly

FIGURES 2.14

EFFECT OF IONIC CONCENTRATION ON WETTING AND CONTACT ANGLE

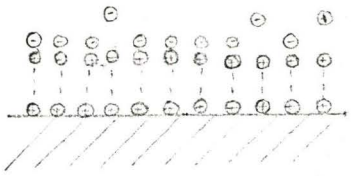

a. A bimolecular layer at the interface adsorbed from high concentration of surface active agents, reducting S/L to a very low value. Surface becomes wetted

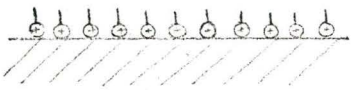

b. A monolayer at low concentrations of surface active agents. σ S/A is reduced more than σ S/L result in non-wetting.

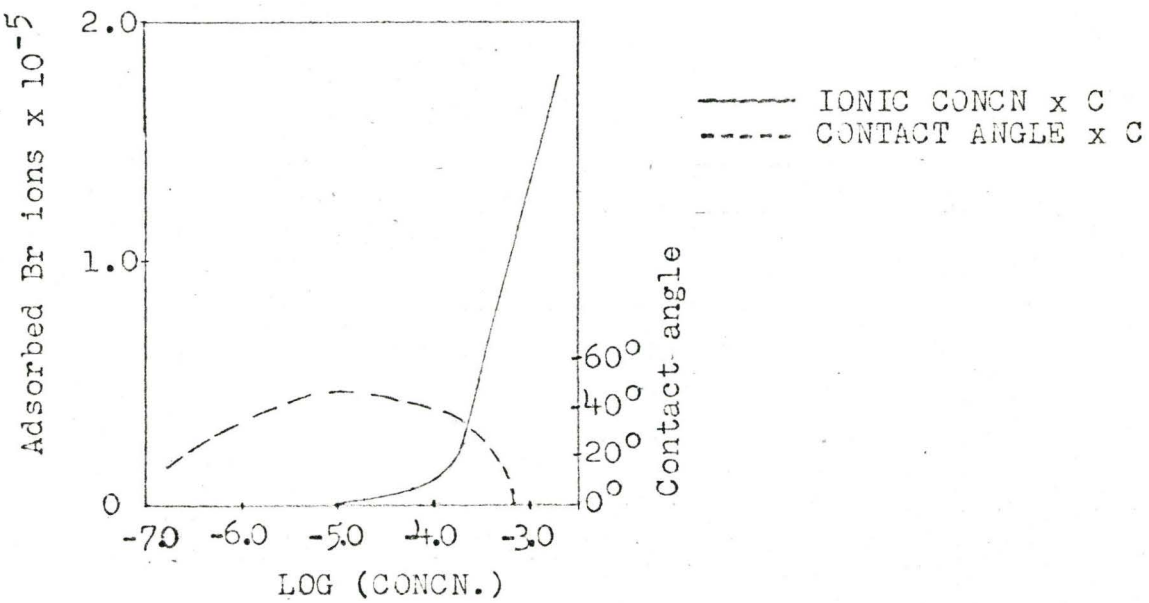

c - Effect of Ionic Concn.

it is neither unusual nor difficult to make a surface non-wetting. In practice a contact angle greater than 90^{o} is a sufficient criterion for non-wetting.

All the interfacial phenomena previously discussed will be important in boiling heat transfer; however additional effects are going to arise in very thin liquid films. These effects are discussed below.

The adhesive or disjoining pressure which was discussed earlier is directly related to the adhesive wetting behaviour of a liquid-solid system. This adhesive wetting can be related to the thickness of the residual film (Fl). Some of the properties of the residual film can be obtained by considering the effect of various solutes on the thickness of this film. It has been observed that the minimum thickness of the film at any pressure can be expressed by the equation:

$$h_{min} = k_1 + k_2.f \text{ (Molecular weight)} \qquad \ldots(30)$$

k_1 is a constant and is equal to the depth of the residual film for any solvent; it decreases as the adhesive energy decreases. This constant can be zero or almost zero, in which case the residual film can be easily stripped from the surface. This probably leads to easier dry patch formation and possibly a lower critical heat flux. k_2 is also a constant which depends only on the properties of the solvent. The characteristics of the surfactant additive are contained in the functional relationship which seems to be dependent only on the molecular weight of the solute.

Therefore by introducing a suitable surfactant (i.e. choice of molecular weight and hydrophobic character) it should be possible to vary the residual film thickness to a considerable extent.

Some of the interesting effects of temperature on this residual film have been observed by Fuks[F1] and Deryagin[D2]. They observed that the residual depth of the film is unaffected by a rise in temperature at very low temperatures. However, at higher temperatures the effect of temperature becomes considerable. At still higher temperatures (within a very small range) the film softens and this softening temperature increases as the molecular weight of the dissolved substance increases and film depth decreases. This softening point is always lower than the melting point of mono-molecular film.

There seems to be an excellent analogy between the dry patch formation from microlayer vapourization in boiling heat transfer and softening and melting behaviour of thin films. The studies on temperature, residual film thickness, resistance to thinning and adhesive pressures gives a preliminary understanding of solid-liquid-vapour interface behaviour (S3,D2,F1). All the preceding discussion point to the fact that the orientation and firmness of bonding of molecules of solute in film, diminish in moving away from the solid surface and gradually pass over into the disorganized state which is characteristic of bulk. The structure and behaviour of microlayer may thus hold a clue to high-flux boiling heat transfer.

2.6.3 Transient Effects in Wetting

The effect of time during wetting as applied to the boiling phenomenon, is very complex. In general, there can be long-range time effects, known as aging, and short-time transients effects, known as the dynamic effects of wetting. Changes in the solid-surface characteristics take place over a long period of time when these changes occur by chemical attack, erosion, etc. The only reported study of this aging behaviour in boiling heat transfer is by Rohsenow[R3]. Higher surface temperatures were recorded for a given heat flux. This was attributed to either scale deposit, or to oxide formation or to chemical reaction which may cause the cavities to shrink.

More important to the fundamental mechanism of boiling are the dynamic effects of wetting which, in general, can be attributed to two main factors, viz the surface roughness and the dynamic surface tension. The dynamic surface tension is the instantaneous value of the surface tension during expansion and contraction of surfaces. Most of the discrepancies in the measurement of contact angle can be attributed to surface roughness and contamination which affect the attainment of equilibrium by the interfacial forces. During the time spreading wetting occurs, equilibrium may not be attained as well because of the dynamic surface effects and the considerable time required to attain equilibrium.

The time to attain equilibrium of the interfacial forces has even more significance when surfactants are involved. This

situation arises because of the time required to reach an equilibrium interfacial concentration of surfactant after fresh surface has been formed. Obviously then equilibrium is going to require considerably more time to attain in the liquid film on the solid. Dynamic surface tension has been observed to be greater than the static value when the surface is being extended and is less than the static value when the surface contracts. Temperature changes in the surface cause similar effects. Similarly if the contact angle was measured while the liquid was in motion the contact angle is invariably higher when the liquid was advancing than when the surface was receding. The cleaner and smoother the surface the smaller this hysteresis effect (R1).

Time effects are more pronounced at low concentrations where relatively large amounts of surfactant must be taken up by the interface. At high concentrations a considerable number of molecules is at the interface already and hence these effects are less pronounced.

3. APPARATUS

3.1 Introduction

The overall system is basically the same as that used earlier by Dernedde[D1] in his study of boiling of flowing films of pure liquids. It is shown diagramatically on Figures 3.1 and 3.2; a photograph of the boiler is shown in Plate 2. However, considerable modifications in boiler, heater, piping and pool boiling apparatus are made. Liquid is fed from an overhead tank through a rotameter and heater to the boiling apparatus. Some evaporation occurs as the liquid passes over the hot surface. The bulk of the liquid flows back to a hold-tank located at the inlet to a gear-pump. The pump transfers this liquid back to the constant-head tank. Coolers and heaters are located in this transfer line.

The apparatus used in this study can be resolved into four separate parts, each serving a distinct function:

(i) The heat-transfer surface with its electrical heat supply.

(ii) The feed preparation system for supplying measured flows of aqueous solutions of surfactants at predetermined concentrations and temperatures.

(iii) The specific devices such as heat-flux meters and surface thermocouples to measure heat-flux and surface temperature continuously in any given situation.

(iv) The devices for measuring surface tension and contact angle of the solution on the heat-transfer surface so that

FIGURE 3.1

POOL BOILING APPARATUS

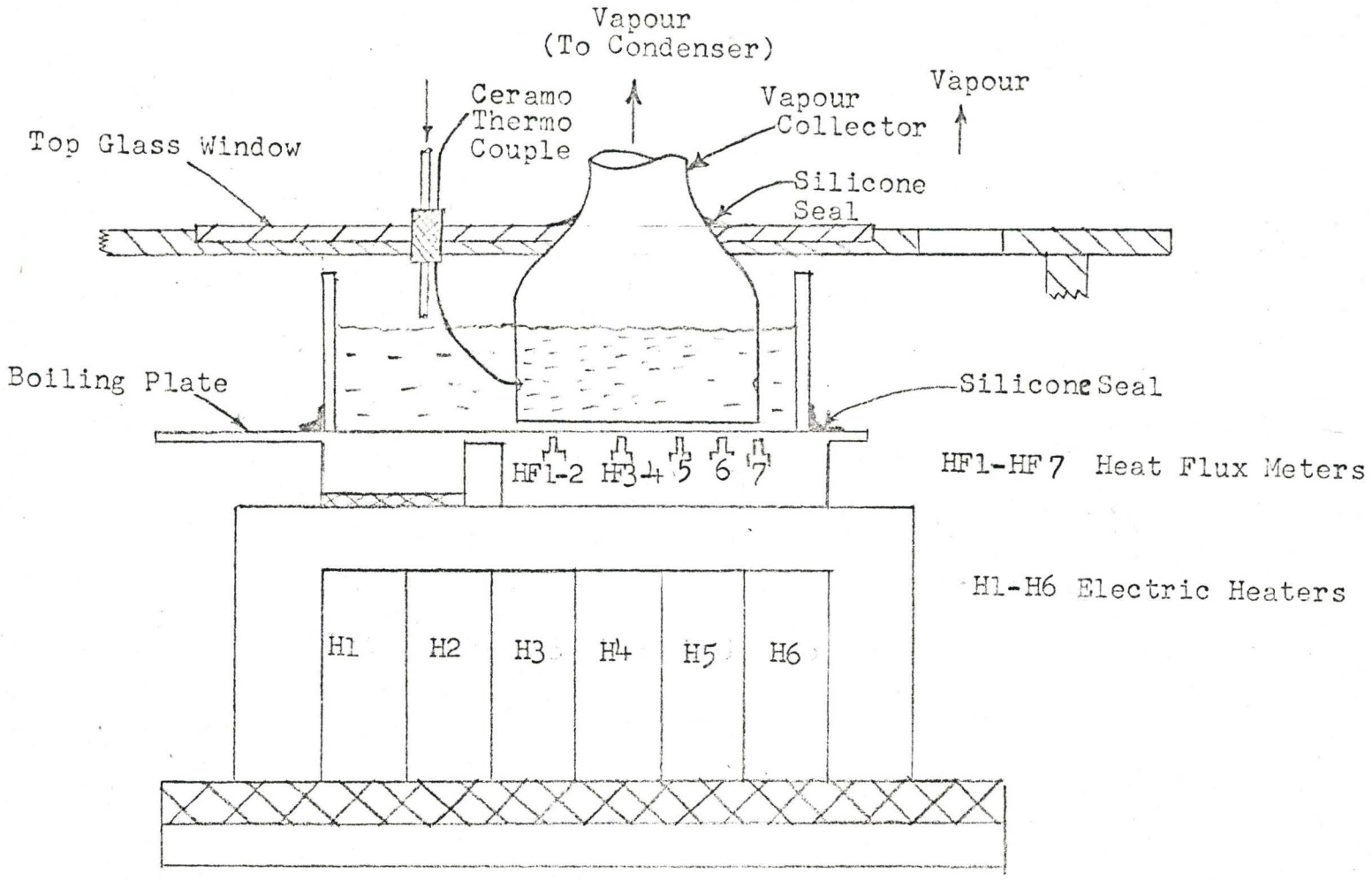

FIGURE 3.2

FEED PREPARATION SYSTEM

(FORCED CIRCULATION BOILING)

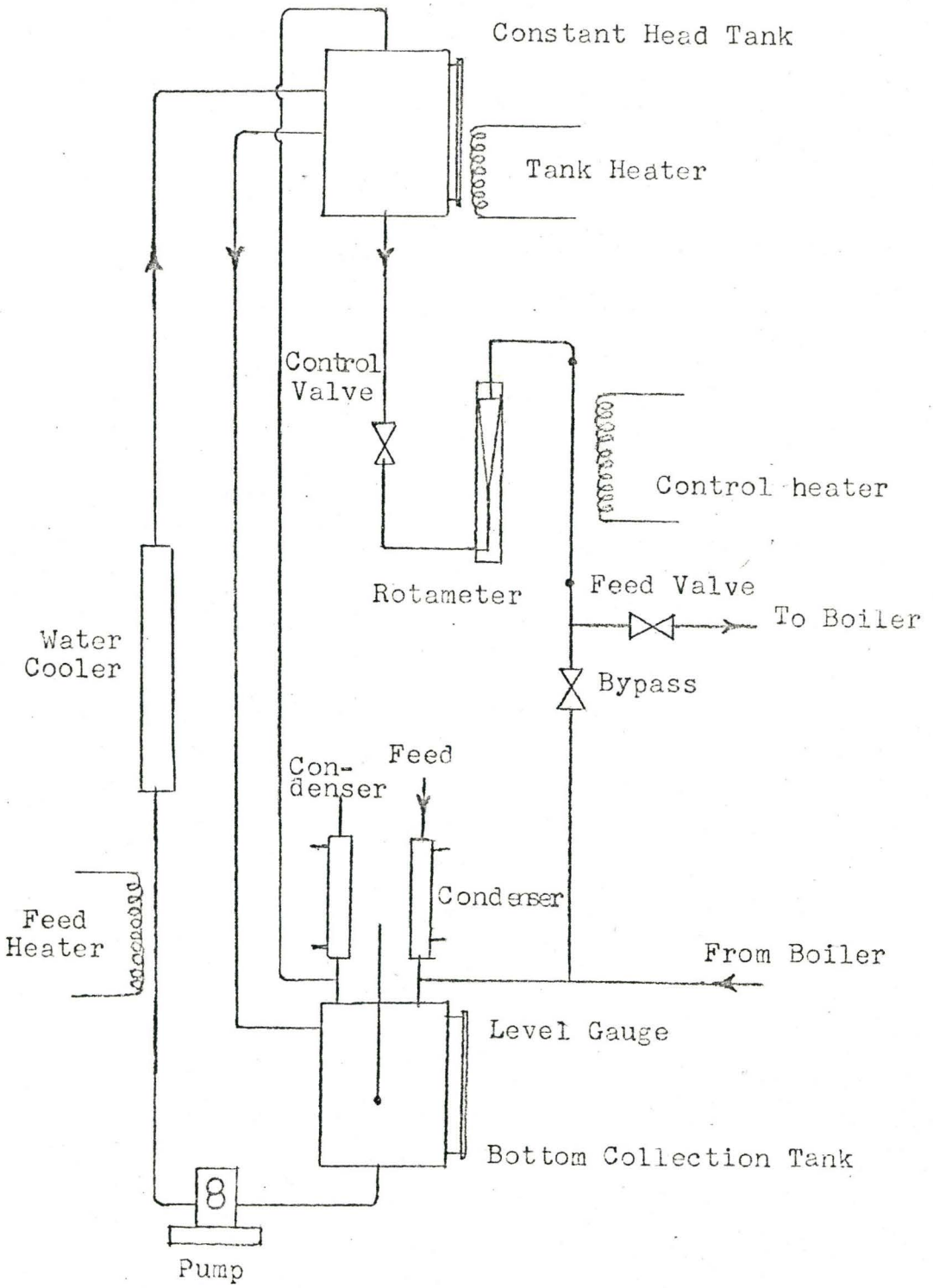

the heat-transfer surface could be characterized at any time.

3.2 The Feed Preparation System

The feed in the present studies consisted of degassed distilled water or aqueous solutions of various surface active agents. The feed system was different for the two different types of experiments that were performed, i.e. for the pool boiling or for the boiling of flowing liquid films. The former experiments were carried out under steady-state or unsteady-state surface-temperature conditions while the latter were all unsteady-state experiments.

(a) Pool Boiling - The equipment details can be seen in Plate 2 and Figure 3.1. The steady-state pool-boiling equipment requires a continuous addition of water at or near its boiling point during the entire run. Since heater capacity limited the steady-state heat fluxes to those less than 100,000 B.t.u./(hr.)(sq.ft) relatively small addition rates were required in this case. During the unsteady-state experiments, in which the entire system is cooled from a relatively high temperature, considerably more liquid feed was necessary (ca. 2 litres). This feed was made and kept in a 5 lit. stainless steel vessel at 90 to 95°C. From time to time it was transferred to a 1500 c.c. glass flask. An electrical heater maintained the liquid at or near its boiling point. A stopcock on the outlet from the flask allowed the flowrates to be controlled in order to maintain essentially a constant liquid depth in the boiler.

PLATE 2

APPARATUS FOR BOILING HEAT TRANSFER

1 Boiler System

2 Heater for Feed

3 Feed Storage in Pool Boiling

4 Camera with the Extension Tube

5 Visicorder

6 Pre-amplifier

7 12 pt. Honeywell Recorder

8 Vapour Collection end

9 Liquid inlet end

10 Potentiometer

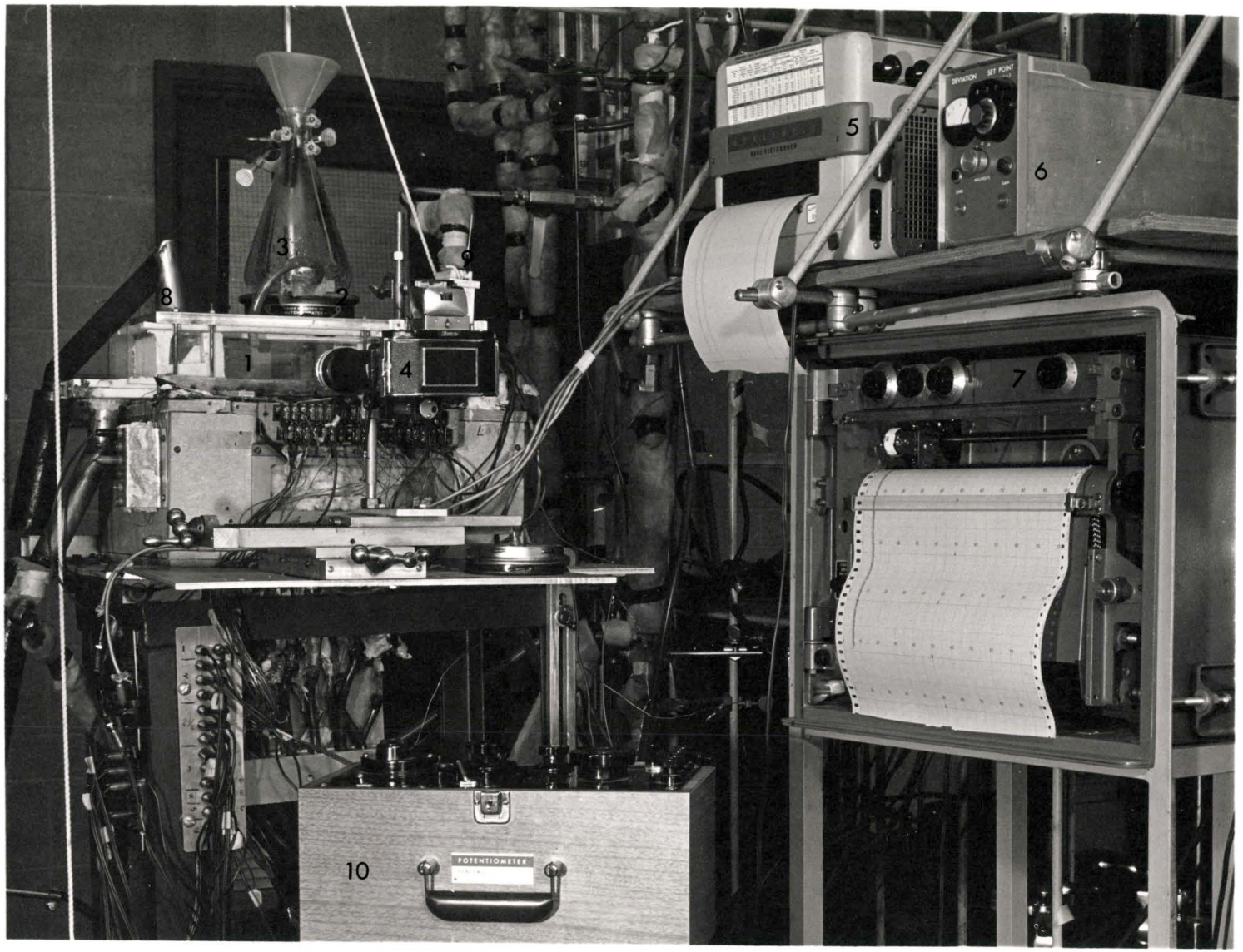
1
2
3
4
5
6
7
8
9
10
DEVIATION
SET POINT
POTENTIOMETER

(b) Liquid-film boiling - Figure 3.2 shows the feed system for the forced-convection, subcooled or saturated liquid-film boiling experiments.

Distilled water or surfactant solution was charged to the collector tank at a known concentration and the system was filled by circulating the liquid through the entire system. Solutions of surface-active agents were made up in the system by charging the appropriate amounts of distilled water and concentrated solution. The heaters and coolers were adjusted to provide a predetermined inlet temperature to the boiler. The by-pass system allows better control. The liquid was distributed over the flat heat-transfer surface by an adjustable slot at the inlet followed by a 3 inch length of wire mesh which was placed flat on the inlet section prior to the heat transfer surface. The flow was measured by a calibrated rotameter; it was maintained constant throughout any experiment.

3.3 Boiler and Heat Supply

The boiler consists essentially of a large copper block 8 inches long by 6 inches wide by 6 inches deep in which electrical heating strips have been imbedded (Figure 3.1). The upper surface is the heat transfer surface in which heat-flux meters and thermocouples have been placed. To allow these devices to be accurately made and located and to allow relative ease in manufacture, the upper 1 inch of the block had to be removed from the lower heated section. This upper piece was later bonded

to the lower section by tin-lead solder. The upper section was further cut up by removing a $\frac{1}{4}$ inch deep by 6 inch long by 3-7/8 wide section from the upper plate. After the heat-flux meters were manufactured and the thermocouples installed this plate was silver-soldered into the thicker block.

The layout of the heat flux meters and the surface thermocouples is given in Figure A.2. Surface thermocouples are made from 0.013 inch insulated and sheathed constantan wires. Details of their construction are given in section 3.4. The heat flux meters are similar to those used by Dernedde[D1], a modification of those first introduced by Gardon[G4]. They are made by cutting holes in the copper block to leave a thin copper disc on the heat transfer surface which has accurately known dimensions. Constantan wires (0.005 in. dia.) are silver soldered into accurately located holes at the center and on the periphery of the disc. There are seven heat flux meters of 0.078 inch radius. Two of these are referred to as thin (0.010 in. thick), and five others are thick (0.030 in. thick). Further details are provided in section 3.4.

The heater block has slots 6 inches long by 0.125 inches wide by 3 inches deep cut into it, into which Kanthal heater strips, 0.75 inches wide by 0.015 inches thick are placed as indicated in Figure A.1. These heaters are held in place inside these slots by high temperature, electrical insulation (Hiloset cement manufactured by the Kaiser Manufacturing Co.). Outside the block the heaters are electrically insulated by fiberglass high temperature insulating sleeves. The power is supplied from

the 3 phase 230 V. mains through a powerstat auto-transformer to 10:1 stepdown transformer to provide a continuously varying voltage from 0-25 V. The heaters are separated into six independent supply systems, three are 7.5 k.w. and three are 3.0 k.w. Details are given in Appendix I.

The upper heat transfer surface was carefully machined in the hope of providing a uniform surface and one that would be similar to that of Gaertner[G1]. It was finished by 600 emery paper to 10.0 micro inches as measured by a profilometer. This treatment and surface finish is almost identical to Gaertner's. The upper surface of the boiler is enclosed in a teflon and glass cover. The bottom is housed in a transite box filled with glass-wool.

The arrangements of the boiler surface for pool boiling and forced-convection experiments were entirely different.

(a) Pool boiling - The details of the equipment for steady and unsteady state pool boiling can be seen in Plate 2 and Figure 3.1. About a 1½ ins.depth of liquid was maintained on the horizontal surface by inserting 1/16 inch thick brass, end-plates at the inlet and outlet of the heated plate. A glass, goose-necked, bell-shaped vessel was placed over the heating surface (Figure 3.1) to act as a vapour collector over a known-area. The bell-shape extended below the free liquid surface but about a ¼ inch above the heating surface. It was assumed that this arrangement did not disturb the boiling process but did collect all the vapour which was generated by the heat that was trans-

ferred over the bell area. The heat-flux meters were located in the central regions of the bell.

The condensate from a shell-and-tube condenser was collected in a 100 c.c. graduated cylinder. A slight vacuum was applied to the receiver to facilitate the vapour flow to the condenser.

(b) Forced-convection Liquid-film boiling - In this case, the brass-plates were removed and the entire apparatus could be tilted to any desired angle between 0° and 90°. Liquid flowed from the slot at the entrance over a 3 inch length of teflon plate (over which was placed the 100 mesh screen), onto another 3 inch entrance section of unheated copper plate, onto the heated copper plate. A ½ inch length of this heat transfer surface was made thin to minimize heat flow upstream and to provide control over the point of break-up of the liquid film. The unevaporated liquid is removed by a 1" dia. s.s. tube back to bottom collection tank afte it passes over the heated surface. This liquid is recirculated to the constant head tank. Flexible hose connections allow the apparatus to be tilted to the desired angle and back to the horizontal with the minimum of delay. This practice is necessary since the heat transfer surface was characterized by "contact-angle" measurements before and after each run.

3.4 Heat Flux Meters and Surface Thermo-Couples

(a) Heat Flux Meters - Heat flux meters are the most delicate, sensitive and complicated parts of the boiling surface. There are seven heat flux meters all with the same radius (0.078 in.) Two of them are 0.010 in. thick, the other five are 0.030 in.

thick. Each heat flux meter had three constantan wires of 0.005 in. diameter silver-soldered into 0.006 inch diameter holes. The line joining the three heat flux meter thermocouples, was perpendicular to the direction of the liquid flow. The layout of the heat flux meters is given in Figure A.2. The details of the heat flux meters are given in Figure A.3. The underside of the copper disc of heat flux meter is insulated by sauereisen cement (Sodium Silicate) so as to minimize the heat flow from or to the underside. Except for the final 0.25 inch length, the constantan wires were contained in a magnesium oxide insulation covered with a 0.04 inch diameter stainless steel sheath. The wires were thinner and the insulation thicker than those used in earlier experiments (D1). Conduction error was therefore minimized and responses were faster.

(b) Surface thermocouples - The layout of the surface thermocouples is given in Figure A.2. Surface thermocouples were made from 0.013 inch diameter constantan wires which had a thin magnesia insulation and a copper sheath of 0.032 inch diameter. About 15 inches of this sheathed wire was filed flat at one end and was polished with a fine emery paper. After proper cleaning with dilute hydrochloric acid followed by wash water, the tip was electro-plated in a dilute copper cyanide solution for about 45 minutes at $\frac{1}{2}$ volts d.c. at about 70°C. (equivalent to about 20 amps/sq.ft). A cone shaped lucite shield placed 0.25 in. above the tip, was very useful in preparing a satisfactory surface thermocouple. Electroplating of 0.035 in. was done. This included sufficient allowance for metal removal during the surface finish

of heating surface and shrinkage during testing. The surface thermocouple was slowly heated in a bunsen flame to high temperature oxidation and was tested for continuity. Eleven surface thermocouples were prepared and tested using the method detailed above and were joined to the boiling plate by silver soldering in a suitably sized hole.

3.5 Contact Angle and Surface Tension Apparatus

Contact angle was measured using a shadow photograph of a sessile drop. The apparatus for the shadow photograph consisted of an Exacta Camera equipped with a 100 mm lens and a 10 inch extension tube to give a magnification of 2.5 times. A Sylvania No. 2, super flood lamp in combination with a condenser was used to provide the parallel beam of light for the shadow photograph. A microlitre syringe and a ministat pipette were used to form a sessile drop of fixed volume. Details regarding apparatus used and choice of methods are given in Appendix II The shadow photograph of the sessile drop was magnified to give an overall magnification of 35 times. The camera was set up on a bed which could be adjusted in two directions. This facilitated the exactness in the location of sessile drop on any of the heat flux meter positions. The temperature control of the boiling surface was possible by using a fine control of input to heaters. The glass box over the boiling surface was used for providing an atmosphere of air saturated with H_2O vapour.

Surface tension of the surfactant solutions was determined

using the pendant drop method. Here a suitably sized drop (of about 40 μlitre) was formed on a specially made teflon tip at the end of a microsyringe (or in some cases at the tip of ministat pipette) as a pendant drop and photographed using essentially the same lighting and camera arrangement as described before. The pendant drop was allowed to form at the tip of a syringe which was well stabilized otherwise, the least disturbance would cause the pendant drop to fall down. Temperature around the pendant drop was maintained at required level by enclosing the pendant drop in the closed space formed by glass walls on the boiler. An atmosphere of air saturated with water vapour was provided for high temperature measurements. The pendant drop was magnified to 35 times and essentially the same procedure as given by Andreas et al (A1) was used to determine the surface tension.

3.6 Instrumentation

The instruments of the system mainly consist of a Honeywell Visicorder, a Honeywell multipoint recording potentiometer, a preamplifier and an Exacta camera with 100 mm lens and an extension tube for still photography. However, to study the film flow, a pentax camera with 50 mm lens and high speed (400 ASA) film were used.

The Honeywell Visicorder 906C, which is a recording oscillograph, was used to give the traces of the two heat-flux meter outputs and outputs of the two edge-thermocouples of the same heat flux meters. More sensitive M-40-350A galvanometers were used

for heat flux meter outputs in the range of 0.0 to 2.00 millivolts for heat flux measurement. Two other less sensitive M-100-350 galvanometers were used for temperature measurement from edge thermocouples. One M-1000 galvanometer was used in combination with preamplifier to record the output of heat flux meter for heat flux measurement during steady state pool boiling. Chart speed was adjusted at 0.4" per sec. though for occasional checks in liquid film boiling higher speeds of 10 inches/sec. and 2 inches/sec. were tried. Details of the connections and calibrations are given in Appendix I.

The Honeywell Multipoint Temperature Recorder was mainly used to measure in 0 to 10 millivolts range, temperatures of the feed, the copper block and surface temperatures of the boiling plate from surface thermocouples. This recorder provided an excellent check with the visicorder readings. It was also used for measurement of surface temperature distribution by heat flux meter and surface thermocouples. The saturation temperature of the boiling liquid in pool boiling was also measured in this recorder. The recorder is adjusted to a chart speed of one inch per minute. The Honeywell single point recorder was used to get occasional tracings of edge thermocouple temperatures during unsteady state pool boiling and liquid film boiling experiments. This was necessary to facilitate the comparison of edge and centre thermocouples of heat flux meter.

Preamplifier was used only to get the traces of output of heat flux meter in steady state pool boiling of water. Output

is taken to M-1000 galvanometer of the visicorder through a 220 ohms resistance in series. The input was within 0.3 mv and the output was about 3 volts.

An Exacta camera with 100 mms lens and extension tube and Pentax camera with 50 mms lens and extension tube were used for still photography of the flowing films, sessile drops and pendant drops. High speed films of 125 ASA and 400 ASA were used. Details of the apparatus including lighting and magnification ranges are given in Appendix II.

4. EXPERIMENTS

4.1 Scope and Objectives

The objective of this study was to find out qualitatively and quantitatively the effect of surface active agents in boiling heat transfer of water with the heat flux meters and boiling system described in Chapter 3. The type and concentration range of surface active agents and the choice of experiments were such as to give maximum information regarding the boiling heat transfer mechanism and the effect of surfactants on high heat-flux rates (especially the maximum heat flux).

4.2 Selection of Surface Active Agents

Four surfactants, two manufactured by the American Cynamid Co., under the trade name of Aerosols and two manufactured by the Wyandotte Chemicals Co., under the trade name of Pluronics were selected. The four surface active agents were

(i) Aerosol - OT

(ii) Aerosol - OS

(iii) Pluronic - L-62

(iv) Pluronic - F-68

The important properties and characteristics of these surface active agents are given in Tables 5.1 to 5.4. The variation of many of these properties with the type of surfactants is shown in Figure 5.5.

The main criteria in the selection of the surface active agents

were, molecular weight, hydrophobic and ionic character. These agents were also used in earlier boiling heat transfer studies (E1,R5,J3) and are employed in the treatment of boiler feed water for corrosion inhibition.

Aerosols are among the very well known surface active agents of low molecular weight and high wetting characteristics. Aerosol OT is nonionic by nature and produces a very low surface tension and high wetting properties even at very low concentrations. Aerosol OS has a similar hydrophobic character but it is anionic by nature; it produces the lower surface tension and high wetting property (similar to Aerosol OT) but at very high concentrations.

Pluronics have a much higher molecular weight than Aerosols. They are non-ionic by nature and, unlike the Aerosols, are highly soluble in water. Pluronic L-62 has a low molecular weight compared to Pluronic F-68 and exhibits high wetting characteristics. Pluronic F-68 has high dispersing characteristics, i.e. it does not allow salts to adhere to solid surface and keeps them in solution. Compared to L-62 it has poor wetting characteristics. Figure 5.5 and Tables 5.1 to 5.4 indicate these comparisons.

4.3 Choice of Concentration Range

The range of concentrations was mainly limited by

(i) Solubility

(ii) Micelle formation

(iii) Concentration ranges used in previous studies or practice

(iv) Experimental difficulties regarding formation of foam and surface contamination.

The concentration range was limited by the performance of the surfactant solution and the availability of time. The solubility was not a problem in the case of pluronics. Above 1.0% by weight, it was very difficult to dissolve aerosols in water. Micelle formation was possible at higher concentrations in the case of high molecular weight pluronics. The concentration range of previous experimental studies and industrial practices indicated that a high concentration of 1% by weight was required. Similarly the lower limits were set at 0.1 to 0.01% by weight. However, on the basis of preliminary experiments, a concentration range of 0.01% to 1.0% by weight for pool boiling studies and 0.01% to 0.1% for the liquid film boiling studies, were selected to avoid excessive foaming and contamination of the surface.

4.4 Choice of Experimental Studies

The choice of experimental studies was limited to mainly three different type of experiments with distilled water and solutions of surface active agents:

(i) steady-state pool boiling of water

(ii) unsteady-state pool boiling of water and surfactant solutions,

(iii) unsteady-state forced convection liquid-film boiling of water and solutions of surface active agents.

The choice of these experiments was mainly based on the design

of the boiler and heat-flux meters. Similar studies by Dernedde[D1] simplified the choice of experiments.

Steady-state pool boiling and liquid-film boiling studies were greatly limited by the performance of heaters (which developed very high resistances at the joints because of oxidation). In addition, the center thermocouple of the thin heat flux meters became disengaged from the plate quite early in the experimental program and could not be used. In all about 50 pool-boiling runs and 30 liquid-film boiling runs were made with water and surfactant solutions.

4.5 Experimental Procedure

4.5.1 Steady-State Pool Boiling

About 500 c.c. of degassed distilled water were added to the boiling chamber to produce a height of about 1.5 inches above the heat transfer surface. This height was maintained by feeding boiling, distilled water continuously from the feed-preparation system. An overflow disposed of the slight excess. The heat input to the boiler was controlled by setting the auto transformers for a given voltage output from the step-down transformers. Steady state was indicated by the constancy of the temperature over a ten minute period. The amount of condensate collected was measured in consecutive five minute intervals; the total volume collected was about 100 c.c. Plate temperatures and the temperature differences from the heat-flux meters were measured by potentiometer and visicorder. Six runs of condensate collection were made for each of the seven heat-flux levels in the range from

10,000 to 100,000 B.t.u./(hr.)(sq.ft). This range was about twice that attained earlier by Dernedde[D1] with this apparatus. However, this was still not sufficient to reach the higher heat fluxes of the nucleate boiling regime.

During these tests, the differences in temperature indicated by all the plate temperatures, including those on the edge of the heat-flux meters, were recorded.

4.5.2 Unsteady-State Pool Boiling

Unsteady-state pool boiling experiments are carried out by heating the entire apparatus to a high temperature (ca 450°F.) and then flowing water or surfactant solution was allowed into the boiling chambers to yield a depth of approximately 1.5 inches. As the entire system cooled down, all boiling regimes could be visually observed on the surface. Heat-flux meters continuously monitored the boiling system as these different boiling processes occurred and provided a record of heat-flux versus plate temperature. In spite of the local variations in temperature during boiling, the visicorder continuously traced out the variations in heat flux as the plate temperature changed. Dernedde[D1] had shown earlier that this process can be considered as quasi-steady state.

4.5.3 Unsteady-State Liquid-Film Boiling

Unsteady-state boiling in this case refers to the experiment in which the block is heated to approximately 450°F. and then cooled by a flowing film of water or solution containing surfactants. As the plate cools the point of destruction of the film moves

down the plate and over the heat-flux meters. The region of destruction occurs over a region of 1/4 to 3/8 inches over which violent nucleate boiling can be observed. The heat flux meter then records the heat-flux for all boiling regimes and the edge thermocouple also allows measurement of the plate temperature. Dernedde[D1] has shown that this meter allows a fairly accurate measurement of heat-fluxes which are in agreement with those reported in the literature.

Only the thick disc (0.030 inches thick) was used in these experiments. Each experiment lasted about one minute, somewhat less for subcooled liquid.

Essentially the same hydrodynamics were maintained throughout all the surfactant tests by maintaining a flow rate of 10 lb./min., the same angle of inclination of the plate and the same inlet temperature conditions. At this flow rate complete wetting of the plate was maintained, the system operated without difficulty and excellent control was possible. Dernedde[D1] showed that the angle of inclination does not have a pronounced effect on the boiling process. Small changes in viscosity that may have resulted for the surfactant solutions were considered to have a negligible effect on the heat transfer process.

Three runs with subcooled boiling and three repeated runs for saturated boiling at each concentration of any given surfactant constituted a set of experiments. Later runs included only saturated boiling because the plate cooled too fast with subcooled liquid. Some difficulties were experienced with the higher con-

centrations of surfactants because of excessive frothing of these solutions.

Characterization of the boiling surface was done before and after each set of experiments with a particular type of surfactant. This was done by measuring the contact angle of water on the plate and carrying out a cooling experiment with water.

4.5.4 Measurement of Contact Angle and Surface Tension

The wetting and interfacial forces of the surfactant solutions can, in general, be characterized by surface tension and contact angle measurements. The details of the apparatus for measuring these are described in Chapter 3 and App. II and III. The choice of methods and their reliability are also discussed there. The difficulties in the measurement resulted from:

(i) high wetting achieved by medium and lower surface tension liquids on high-energy surfaces like copper and

(ii) aging and evaporation of surfactant solutions.

The experimental procedure for determining contact angle was relatively simple. Boiling liquid, the contact angle of which was to be measured, was taken up in a 0.1 c.c. syringe and a known volume of liquid was carefully placed on the surface at the point where the surface was to be tested. The boiling surface was maintained at a temperature of 214 $\pm$ 2^{o}F. by controlling the heaters and placing other patches of water around the sessile drop. This procedure allowed sufficient time to photograph the droplet.

In some instances there were problems of evaporation and aging. These were overcome by careful washing of the surfactant

contaminated surface and by taking the pictures very shortly after the drops were formed (ca. one minute)

Surface tension measurements of the solutions were measured by the pendant drop method already described. Liquid was taken up in a 0.1 c.c. syringe and then allowed to form a pendant drop on the end of a teflon tip. When the drop was almost breaking off the tip, a shadow photograph was taken. Measurements were made on photographic enlargements (ca. 35 X).

These measurements were made at or near the boiling temperature by performing these measurements with the drop in a steam atmosphere. Surface tension ratios of water to surfactant solution remained almost the same thus confirming the observations made by Roll[R5].

4.5.5 Special Precautions in Experimental Procedure

The heat-flux meter provides a quick and convenient way of ascertaining the effects which are under investigation here. The need for fast experiments arises because of the problems of increase in concentration and deposition (contamination) on the surface with surface-active agents or their decomposition products. By performing any given liquid film flow experiment within the 30-60 sec. time span, these effects should be minimized. Moreover, to obviate the effects of contamination after each set of experiments with solutions of a given surfactant, the apparatus was flushed for two to four hours with tap water and then an amount of distilled water equivalent to four times the system hold-up was pumped through in stages. Furthermore, after the cleaning

before each test, the boiling surface was tested to insure the same condition by measuring the contact angle. Tests with pure water were carried out to ensure reproducibility of the surface conditions; only when reproducibility similar to that of water was established were new tests carried out. The problems of increase in concentration, cleaning and testing on the surface were less in pool boiling compared to liquid film flow experiments, but essentially the same procedure for cleaning and testing was used. Here cleaning and testing of the surface in between runs with water were possible. It was found that after the initial breakin period of the apparatus, the surface conditions as indicated by the above tests remained essentially constant.

5. EXPERIMENTAL OBSERVATIONS

5.1 Surface Properties of Water and Aqueous Surfactant Solutions

The previous discussion in section 2.5 has indicated how contact angle, surface tension, molecular weight and hydrophobic character of the surfactant may influence various types of wetting and interfacial film thickness and stability. Indeed, surface tension and contact angle are the only properties that can easily and conveniently be measured in situ. The assumption is made that these properties are a direct function of those properties which effect the basic mechanisms of the boiling process. Moreover, all measurements are made at equilibrium conditions. Since the boiling process is a dynamic one, the shortcomings of these measurements are obvious; ways to circumvent this difficulty are not. Plate 3 shows two photographs of sessile and pendant drops.

Measurements of contact angle of good wetting liquids like water and aqueous surfactant solutions on a high energy surface like copper are very susceptible to errors because of contamination, roughness, method of placing droplets and evaporation. With good control and standardization of time, temperature and volume, reproducibility within $\pm 4^{\circ}$ in the range of 30 to 80° and $\pm 2^{\circ}$ in the range of 15 to 30° was possible. Details of the contact angle measurements are given in Appendix III. Standardization of the procedure was made by measuring the contact

PLATE 3

SESSILE AND PENDANT DROPS FOR SURFACE TENSION AND CONTACT ANGLE MEASUREMENT

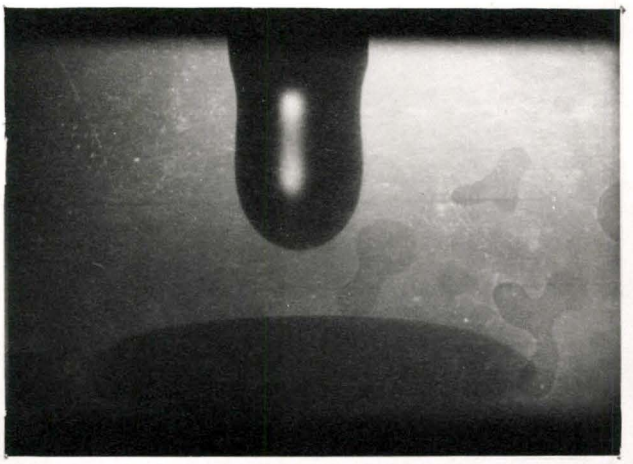

(Aerosol-OT, 0.025 Wt. %)

(Pluronic L-62, 0.1 Wt. %)

angle of doubly distilled water; values of 66° to 72° were observed. Observations of the various surfactant solutions are shown on Figure 5.4.

The reliability of the pendant drop method for measuring surface tension was demonstrated by the measurements for pure water, viz 71.0 to 72.0 dynes/cm. at 25°C. However, as expected the surface tension of the surfactant solutions varied considerably with time and temperature. A constant value was indicated only after an initial non-equilibrium situation. For this reason, pictures were taken after approximately 1 min. of the drop formation (based on the initial studies with a solution of 0.01% by wt. Pluronic L-62). Accuracy of measurement is suggested to be ± 2%; Appendix II contains the details of the surface tension measurement. The results for the measurement of surface tension for the various surfactants at several concentrations are shown on Figure 5.3.

The preceding measurement of contact angle and surface tensions were used to predict the spreading coefficient (Figure 5.22), interfacial tension (Figure 5.24), and adhesive wetting (Figure 5.23).

Data on the molecular weight and hydrophylic tendency of the surfactants were obtained from various references (W5, F4,R1,K2). These data are tabulated in Tables 5.1 to 5.4; the variation of the various characteristics of surfactants with hydrophile concentration is shown in Figure 5.5.

TABLE 5.1*

PROPERTIES OF SURFACTANT, PLURONIC L-62

Composition	80% Hydrophobic Units (polyoxypropylene glycol) on a base of 20% hydrophyllic Units (Polyoxyethylene)
Molecular Weight	2500
Appearance	Thick transparent liquid
Specific Gravity	1.04 (at 25/25°C.)
Cloud Point	< 0°C.
p^H	6-8 Non Ionic
Solubility in Water	> 10 gms./100 ccs.
Viscosity	400 c.p. (but negligible effects in aqueous solutions up to 1% by weight)
Wettability	78 secs. in Draves wetting test at 25°C. at 0.1% concentration
Foamability	35 mms in dynamic foam tester at 120°F. and at 0.1% concentration at a flow rate of 400 ccs/min.
Toxicity	Non toxic, oral LD_{50} > 5 gms/kgm

* This data was compiled from Technical Bulletin of M/S Wyandotte Chemicals (W5)

TABLE 5.2*

PROPERTIES OF SURFACTANT, PLURONIC F-68

Composition	80% Hydrophyllic Unit (Polyoxyethylene) and 20% Hydrophobic Units (Polyoxypropylene Glycol) as base
Molecular Weight	8350
Appearance	Hard, milky white flakes
Melting Point	50°C.
Cloud Point	> 100°C. in 1% Aqueous Solution
P^H	6-8 (Non Ionic)
Solubility in Water	> 10 gms/100 ccs.
Viscosity	Negligible effects up to 1.0 gms/100 ccs.
Wettability	> 1800 secs. in Draves wetting test at 25°C. at 0.1% concentration
Foamability	> 600 mms. in dynamic foam tester at 120°F. and 0.1% concentration at a flow rate of 400 ccs/min.
Toxicity	Relatively non toxic, oral LD_{50} > 35 gms/kgm

* This data was compiled from Technical Bulletin of M/S Wyandotte Chemicals (W5)

TABLE 5.3*

PROPERTIES OF SURFACTANT, AEROSOL OT (A-345)

Composition	Sodium Dioctyl Sulfo Succinate. Mostly hydrophobic in nature.
Molecular Weight	444
Appearance	Viscous, transparent liquid
Specific Gravity	1.05
Cloud Point	< 20°C.
p^H	6-8 Non ionic
Solubility in Water	Low, 1.6 gms/100 ccs. of water at room temperature
Viscosity	Negligible effects in solutions up to 7.5 gms/100 ccs.
Wettability	30 secs. (max) in Draves text at 0.025 % solids

* This data was compiled from Refs. (K2,F4,R1).

TABLE 5.4*

PROPERTIES OF SURFACTANT - AEROSOL OS (A-35⁴)

Composition	Sodium Isopropyl Naphthalene Sulfonate
Molecular Weight	Not known, ($\geq$ 400)
Appearance	White, free flowing powder
Cloud Point	> 100°C. for 1.0% Aqueous Solution
pH	9 $\pm$ 1.0 (Alkaline)
Solubility in Water	1.43% at room temperature
Viscosity	Negligible effects up to 1.0 gm/100 ccs.
Wettability	Low
Foamability	High

* This data was compiled from Refs. (F4, K2, R1)

FIGURE 5.1

STEADY STATE POOL BOILING OF WATER

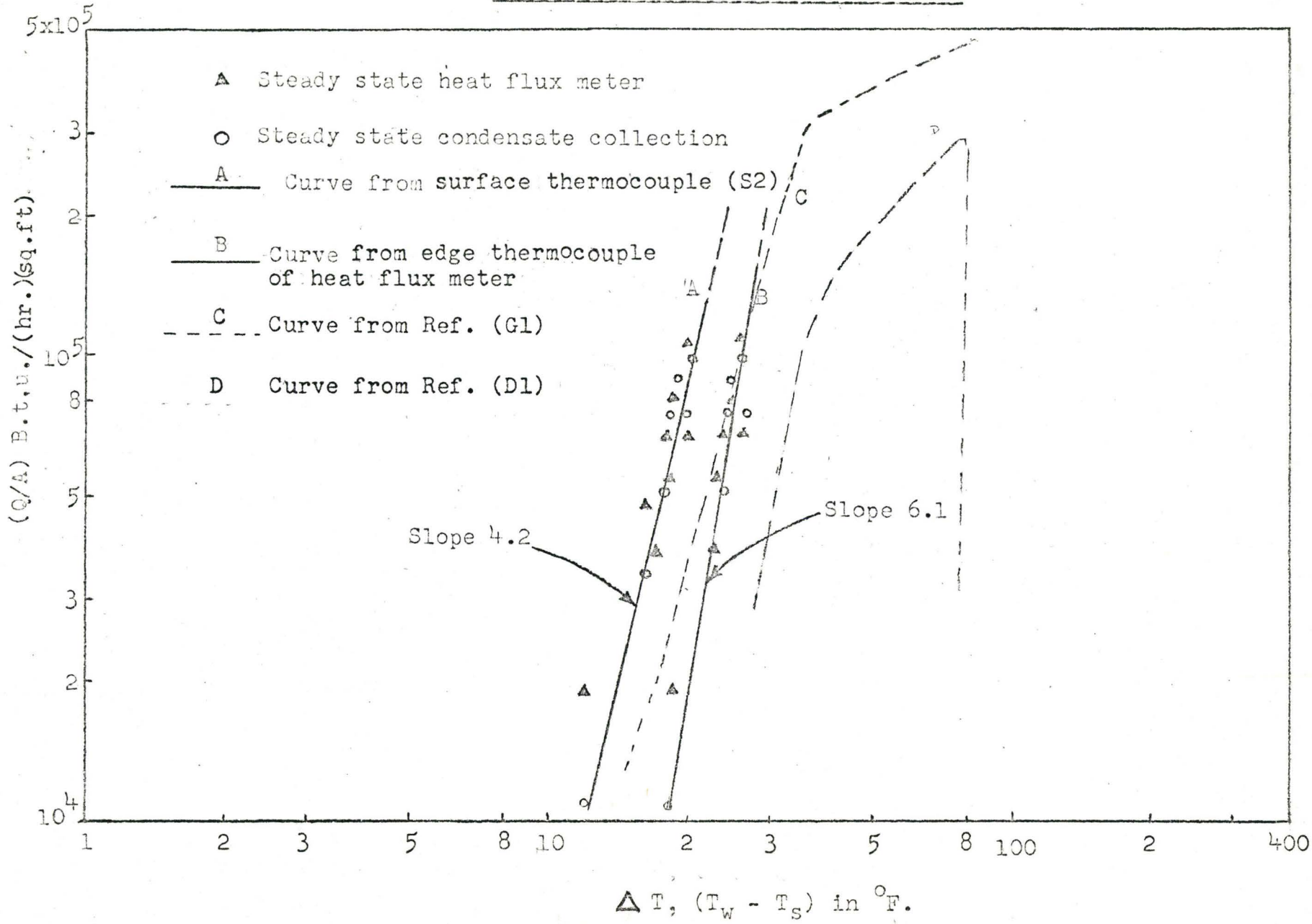

FIGURE 5.2

POOL BOILING CURVE - WATER

(UNSTEADY STATE)

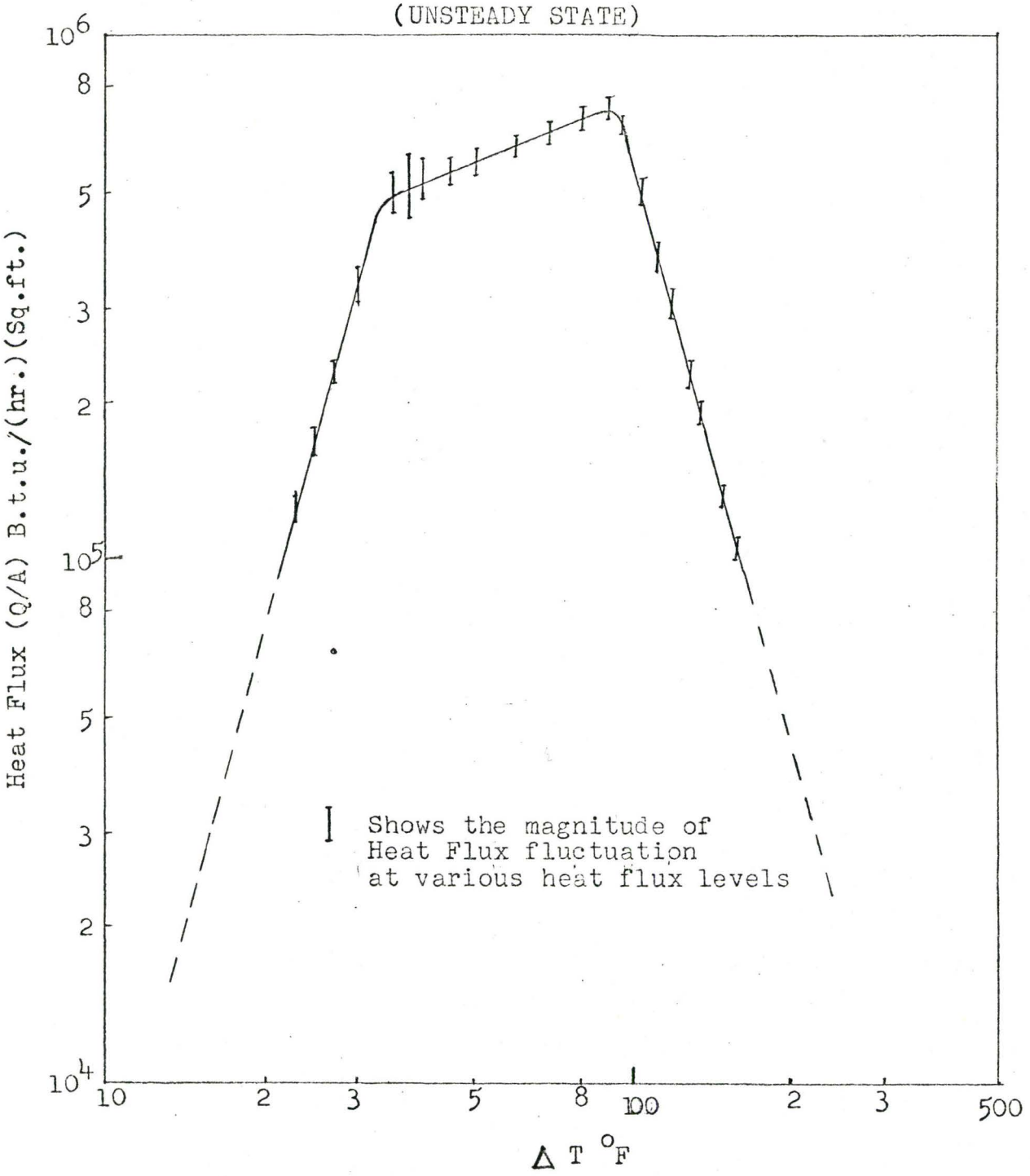

FIGURE 5.3

SURFACE TENSION OF SURFACTANT SOLUTIONS

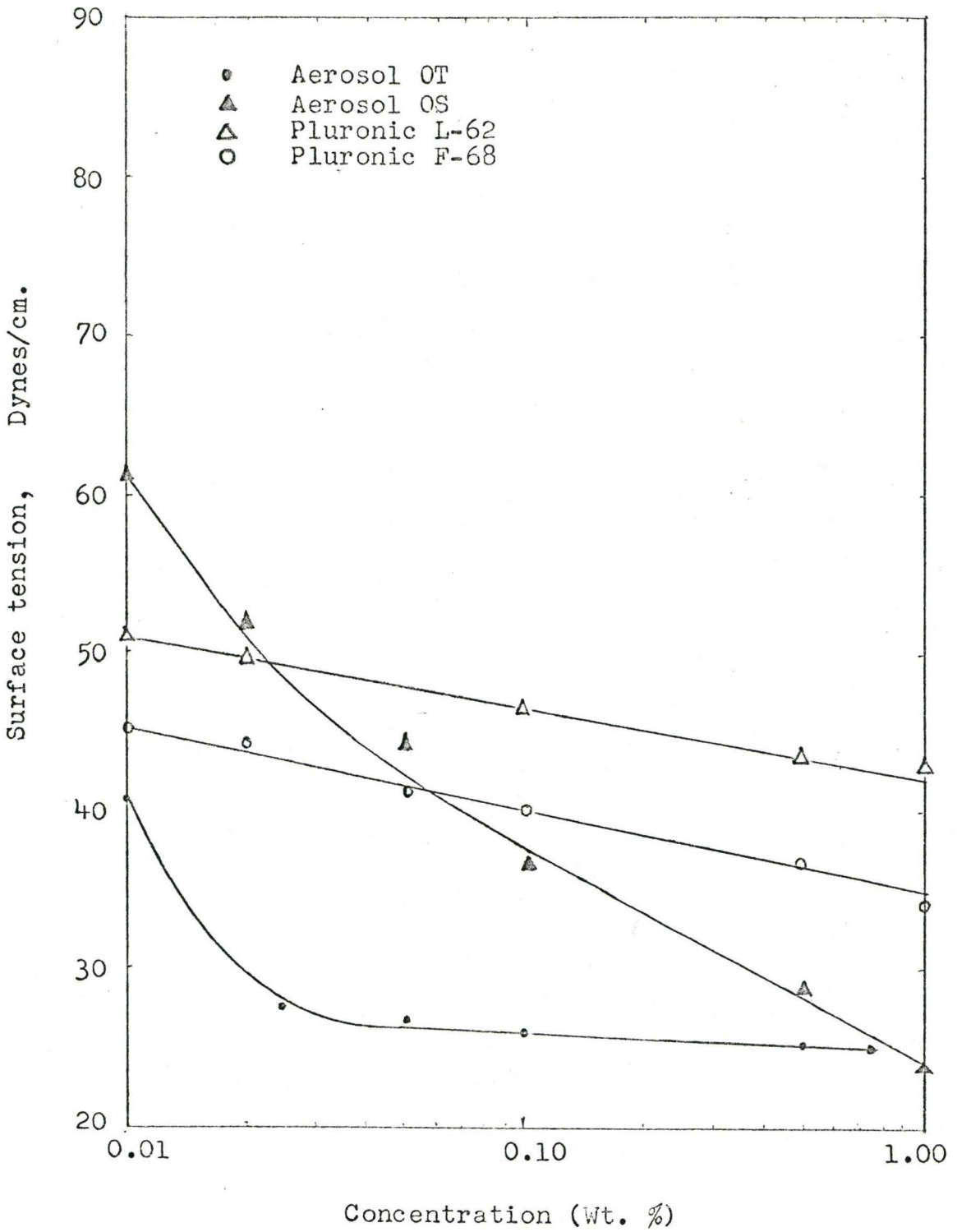

FIGURE 5.4

CONTACT ANGLE OF SURFACTANT SOLUTIONS

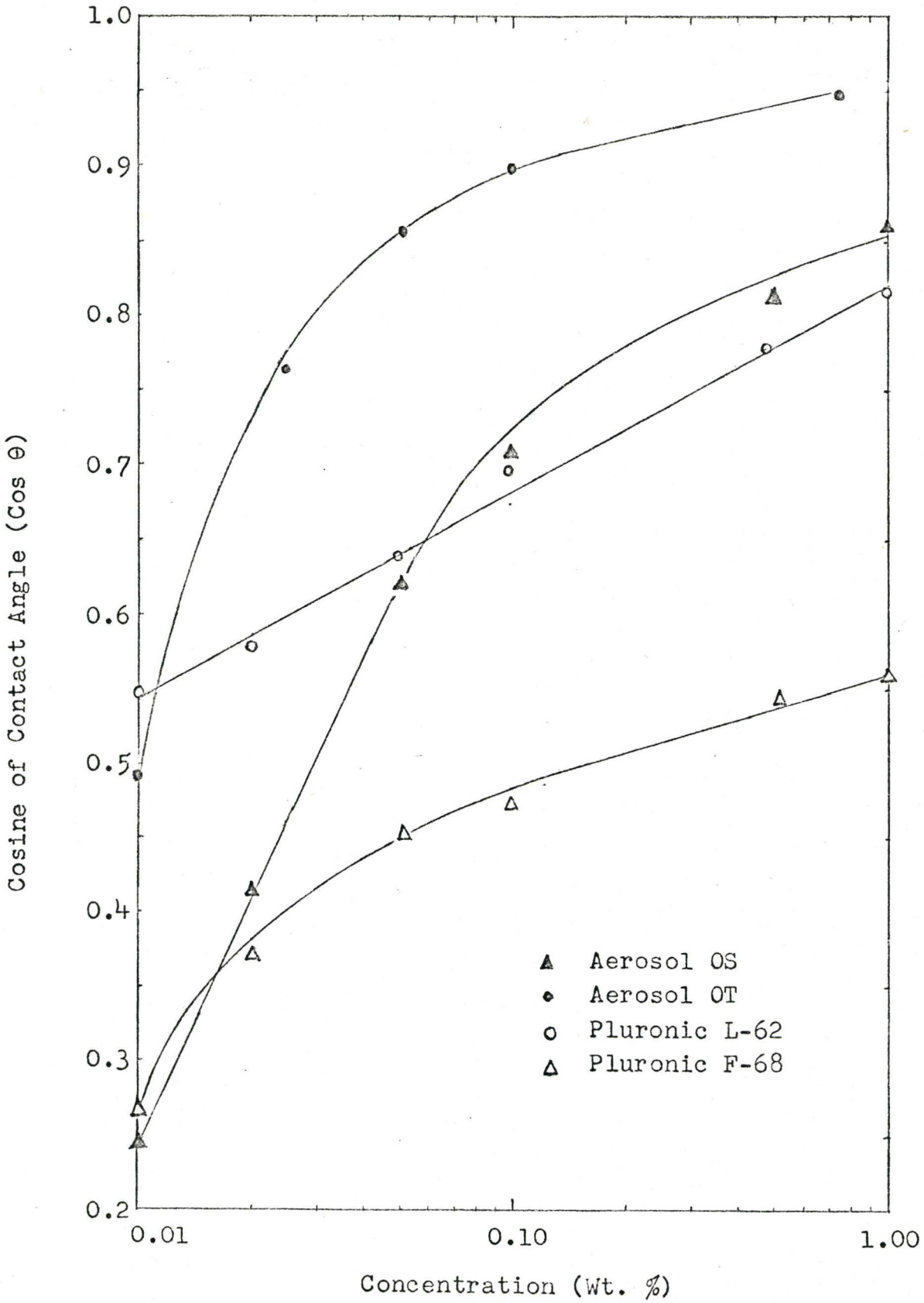

FIGURES 5.5

EFFECT OF HYDROPHILE CONCENTRATION

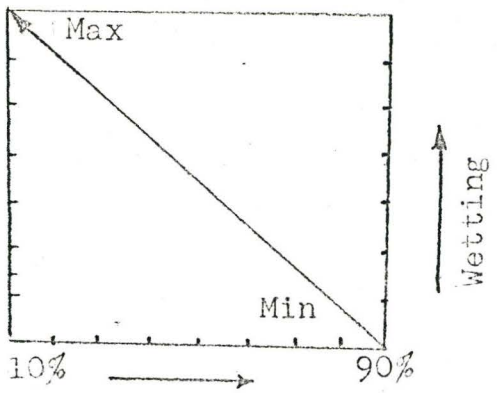

Figure 5.5a

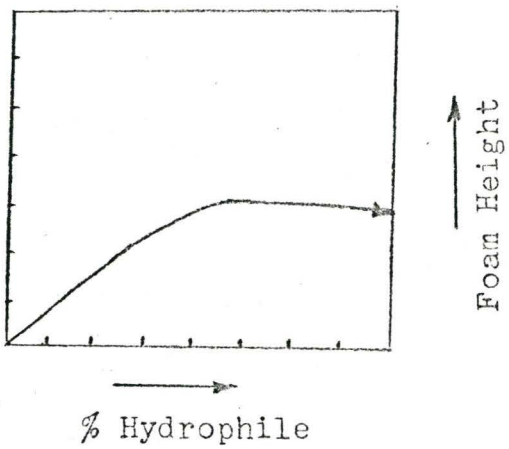

Figure 5.5b

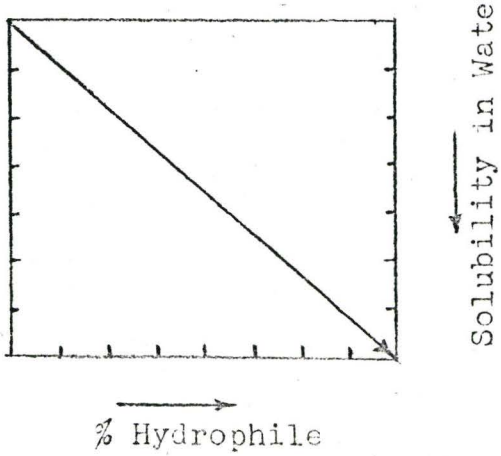

Figure 5.5c

5.2 Steady-State Pool-Boiling

(a) Heat-flux meter calibration

The steady-state pool-boiling experiments were performed with degassed distilled water to calibrate the heat-flux meters. The calibration was achieved by measuring the heat-flux in two ways:

(i) from the rate of condensation of the vapours produced by the boiling within a known area, and

(ii) from the temperature difference between the centre and periphery of the heat flux meter.

The heat flux was calculated from the two-dimensional equation (Equation A5) assuming constant heat flux over the entire disc.

The comparison of the heat fluxes is shown on Figure 5.1 as a regular boiling curve plot. Two experimental curves are shown; the difference is associated with the measurement of surface temperature. In one case (curve B) temperature as indicated by the thermocouple at the edge of the disc is assumed to be the temperature of the entire heat transfer surface. Curve A shows the boiling curve which results when the temperature as indicated by the surface thermocouple at the centre of the heat transfer area is used as the wall temperature. Figure A.11 shows the variations in surface temperature that were indicated by the various thermocouples in this study. Such a difference is unexpected in a copper plate of this thickness and with the present heater distribution and design. The attachment of the thermocouples to the plate is suspected as the cause of the

difference.

The heat flux as calculated from the condensate rate is consistently higher than that indicated by the heat-flux meter. The operation of the heat-flux meter under boiling conditions is analyzed in section A.1.2. The thick-disc meter was quite insensitive at heat-fluxes below 30,000 B.t.u./(hr.)(sq.ft.); however, the fluxes indicated by the two discs agreed to within ± 10% at the higher fluxes. Unfortunately only one heat-flux meter (0.030 in. thick) remained active during the liquid-film boiling experiments.

The results of Gaertner[G1] and Dernedde[D1] are plotted on the same figure. The materials and surface finish in Gaertner's experiments were identical to those used here; Dernedde used the identical apparatus but did not control his surface finish and therefore is unknown. The differences among these measurements may be fundamental to the boiling process or may reflect the experimental errors involved in these studies.

(b) Bubble Dynamics

The experimental observations shown as data points on Figure 5.1 correspond to operation in the isolated bubble region, the first-transition region and vapour-mushroom region of the nucleate boiling regime.

At a heat-flux of 11,000 B.t.u./(hr.)(sq.ft.), isolated bubbles could be clearly observed but the bubble departure at any particular site was quite rapid. At 34,000 B.t.u./(hr.)(sq.ft) bubble interference was quite apparent. It was impossible to

control the heaters to adjust the heat flux exactly to the flux corresponding to the upper limit of the isolated-bubble region. At 50,000 B.t.u./(hr.)(sq.ft.), there was vigorous formation and break-up of large bubbles. These bubbles corresponded with the mushroom-shaped bubbles observed by Gaertner[G1].

At 100,000 B.t.u./(hr.)(sq.ft.), the root of the vapour release was not visible. However large vapour bubbles of Type II suggested by Kirby[K3] were observed. Further visual observations were not possible due to the high bubble activity and turbulence.

5.3 Unsteady-State Pool Boiling

(a) Water

The measurements of the heat-flux as the copper block was cooled by the pool-boiling of water served a dual purpose:

(i) the agreement between the steady-state and unsteady-state boiling curves (Figure 5.2) demonstrated the quasi steady-state behaviour of the boiling system and indicated that extrapolation of the calibration of the heat-flux meters to higher fluxes was reasonable, and

(ii) it provided a convenient datum point for comparing the effects of surfactants on the boiling process over the entire range.

It will be noted that the heat-fluxes recorded here all seem to be higher than those previously observed by other workers.

The temperature differences required for a given heat flux are in the range of earlier observations. The fact that Gaertner observed variations of ± 20% from run to run at high heat fluxes whereas the present work indicates ± 5% reproducibility may have a bearing on these differences. It must be remembered that Gaertner's were direct measurements whereas the present ones are indirect and without a calibration of the heat flux meter at or near these high heat-fluxes; therefore, some question of absolute accuracy still remains. However, it is expected that the relative performance of these devices will indicate the effect of surface active agents on the boiling process.

Some discussion of the method of treating the output signal from the heat-flux meter thermocouples is warranted. The phenomena associated with boiling lead to considerable fluctuation in surface temperature, the magnitude and duration depending upon the surface material and the boiling regime. The fluctuations recorded by the heat-flux meter are sizeable, amounting to ± 15% in some cases (see Figures 5.15 to 5.21). In all cases the average temperature was determined by averaging the Visicorder trace by eye; this temperature is the one reported here. The maximum variation of the heat-flux is shown on Figure 5.2 for the various regimes. Further discussion on these fluctuations is included in section 5.5.

(b) Aqueous Surfactant Solutions

Results of the high-flux pool-boiling studies of the

FIGURE 5.6

EFFECT OF CONCENTRATION OF SURFACTANTS

(Pool Boiling)

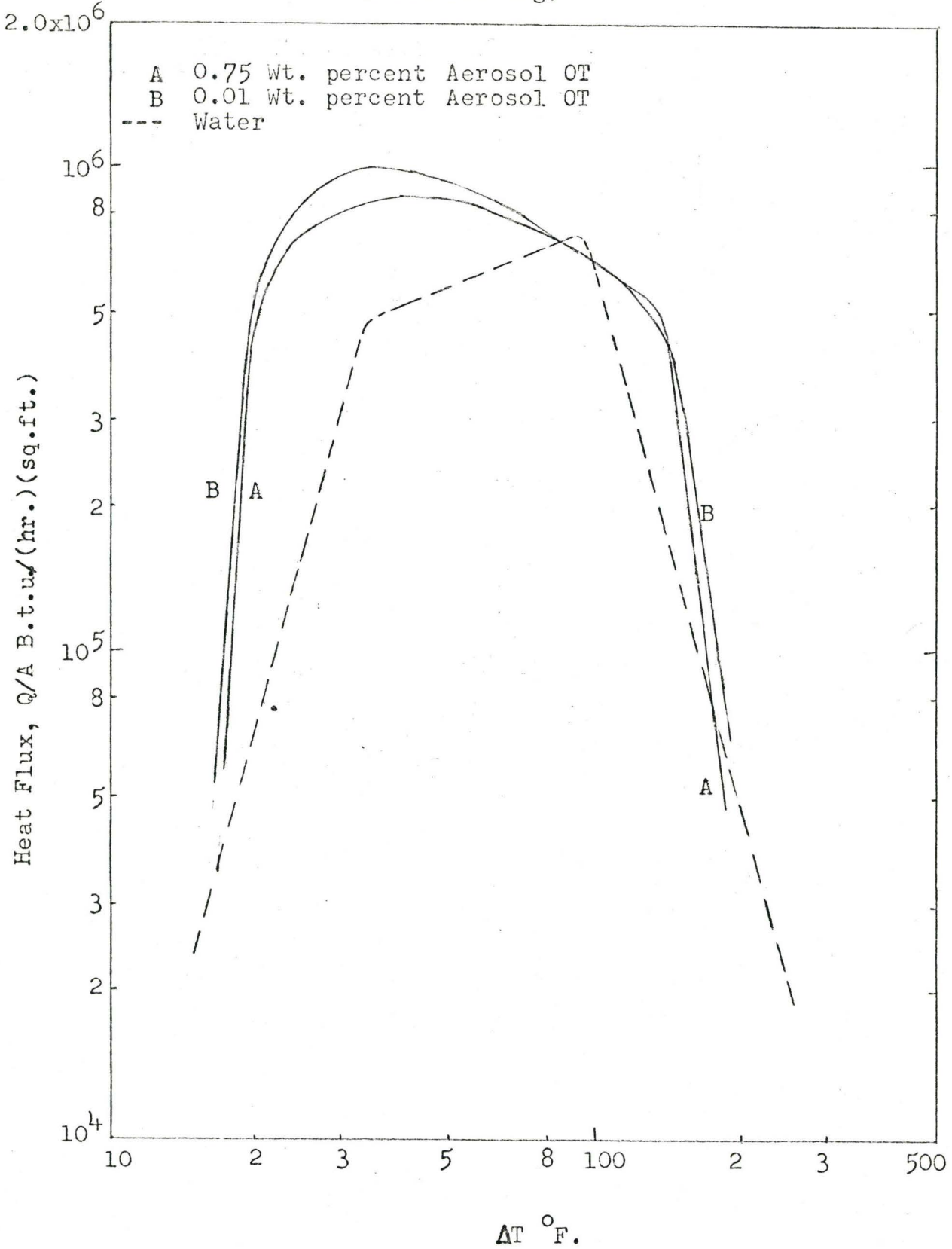

FIGURE 5.7

EFFECT OF CONCENTRATION OF SURFACTANTS

(Pool Boiling)

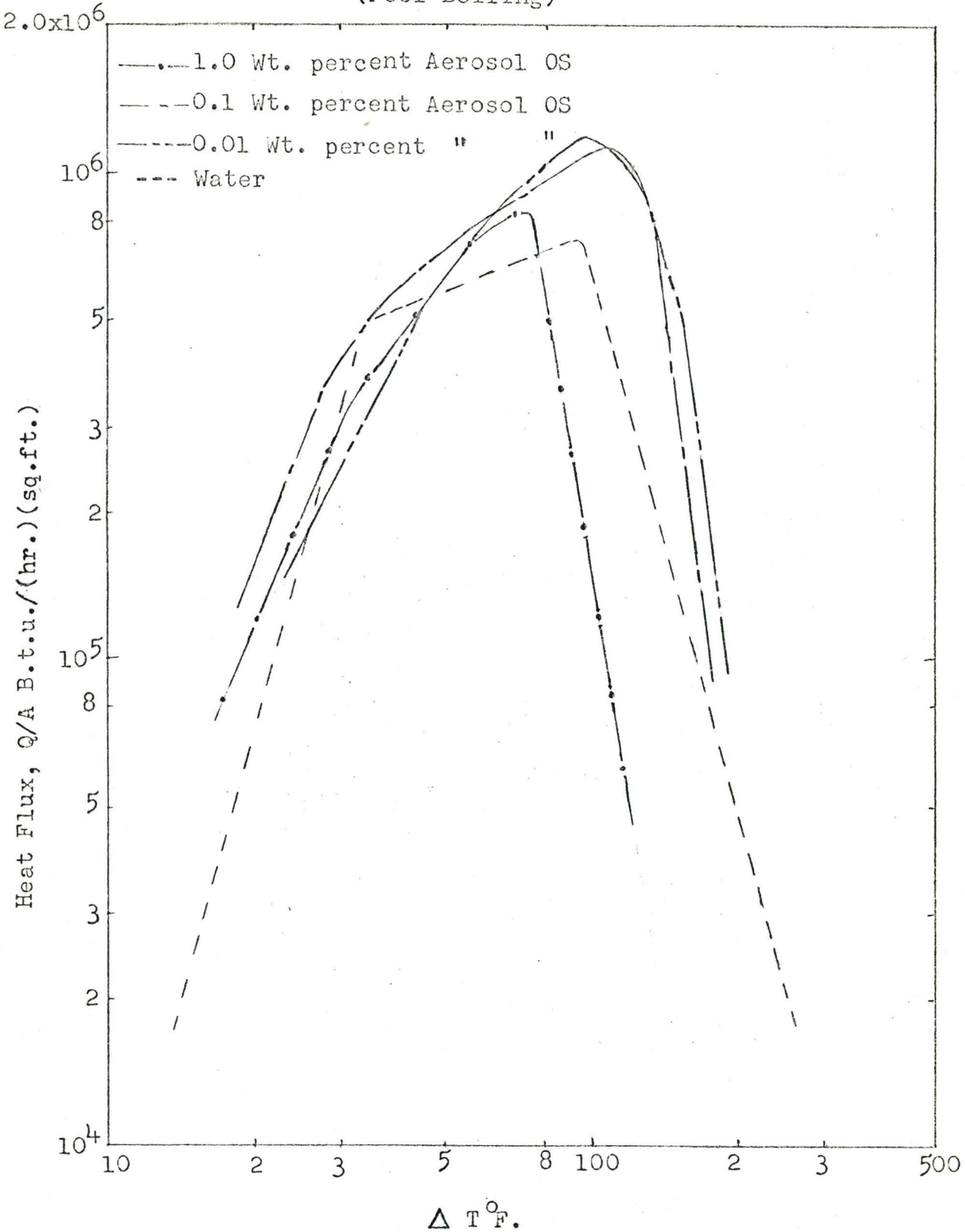

FIGURE 5.8

EFFECT OF CONCENTRATION OF SURFACTANTS

(Pool Boiling)

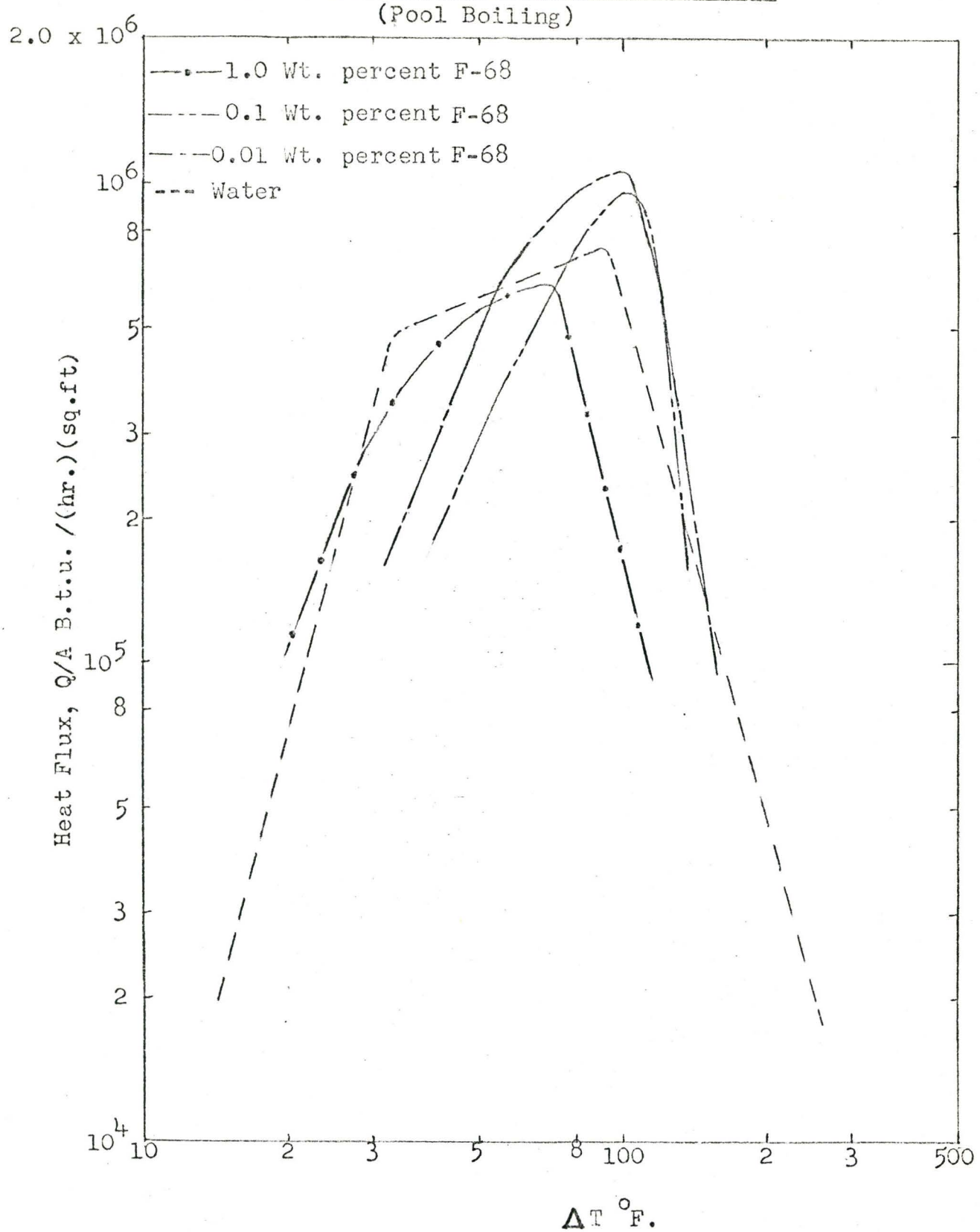

FIGURE 5.9

EFFECT OF CONCENTRATION OF SURFACTANTS

(Pool Boiling)

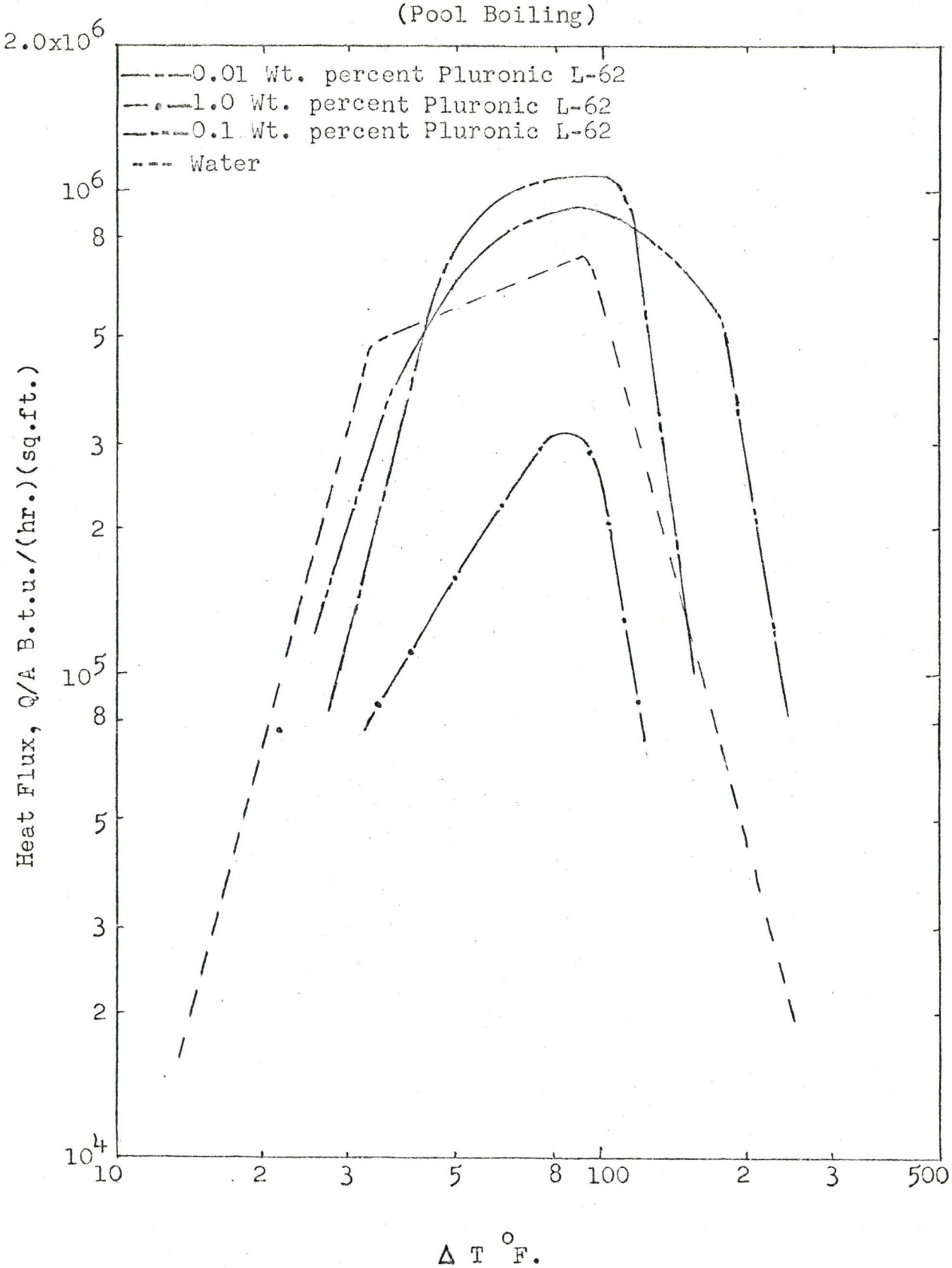

FIGURE 5.10

EFFECT OF CONTAMINATION BY THIN INTERFACIAL FILMS

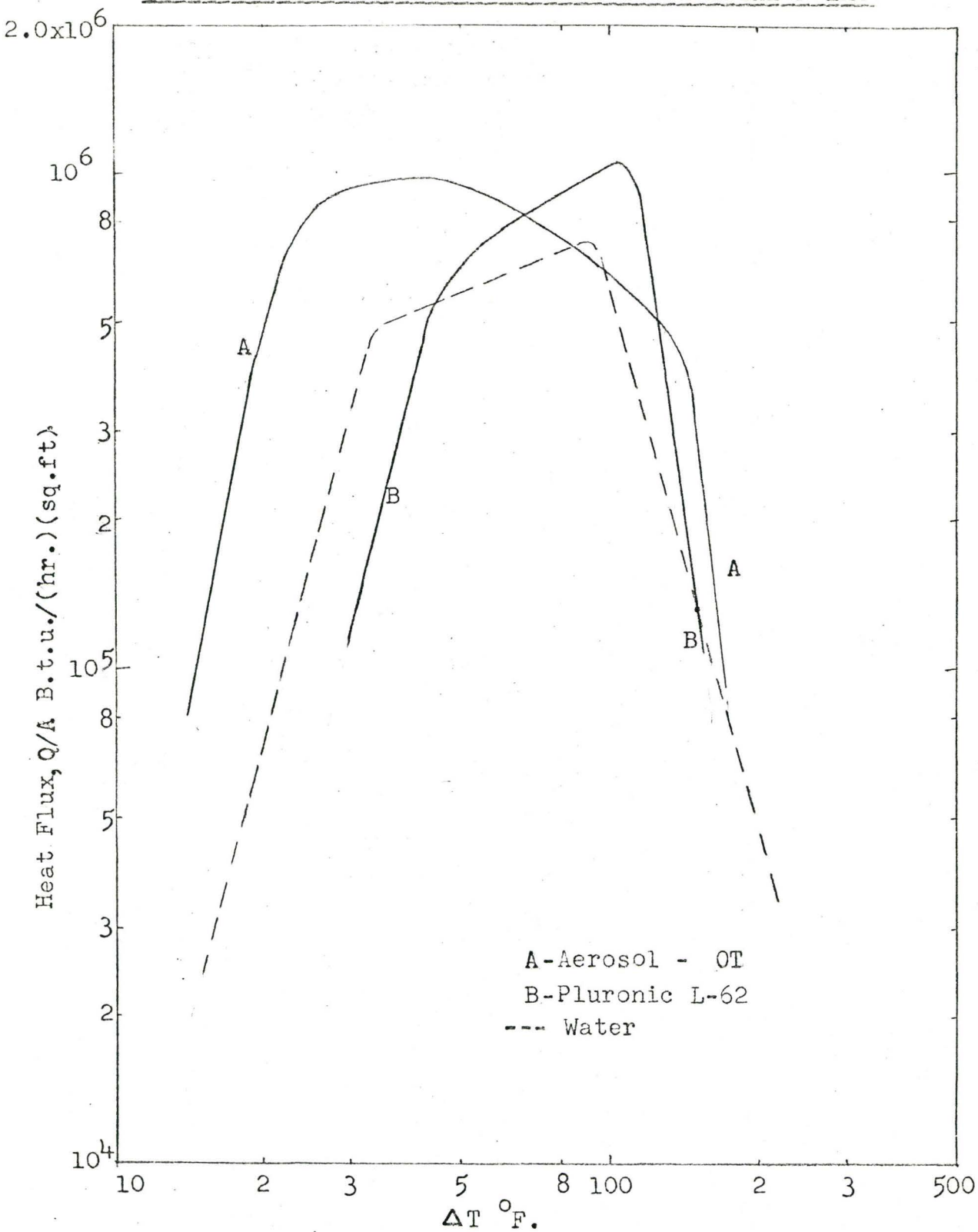

solutions of surfactants are given in Figures 5.6 to 5.10. The most striking result is the variation of the peak heat flux compared to water. In some the heat flux increased considerably while in others it indicated an appreciable decrease. Very significant and consistent variations of maximum heat-flux with concentration, molecular weight and the hydrophobic character of the surfactants were observed. The fact that the peak heat flux changed by as much as $\pm$ 50% is in direct opposition to existing theories regarding the effect of contact angle and surface tension, first with respect to the magnitude and secondly with respect to the direction of change.

5.4 Unsteady-State Liquid-Film Boiling

Since the type of experiment may play a role in producing the effects observed, unsteady-state experiments with water and surfactant solutions were carried out at one flow rate (10 lb./min.) and plate-angle (30^{o}). The results of these studies are shown on Figures 5.11 to 5.15.

It is to be noted that the heat fluxes indicated in these tests for pure water are much higher than those suggested for forced-convection subcooled boiling films (G8) or those measured by Dernedde[D1] with similar heat-flux meters, although they are in line with those observed by Leppert et al[L4]. The reasons for this difference may be associated with the heat-flux meter construction as discussed in section A.1.2. Here again the relative changes in heat-flux brought about by the surfactant solutions

FIGURE 5.11

SATURATED LIQUID FILM BOILING OF WATER

(Unsteady State)

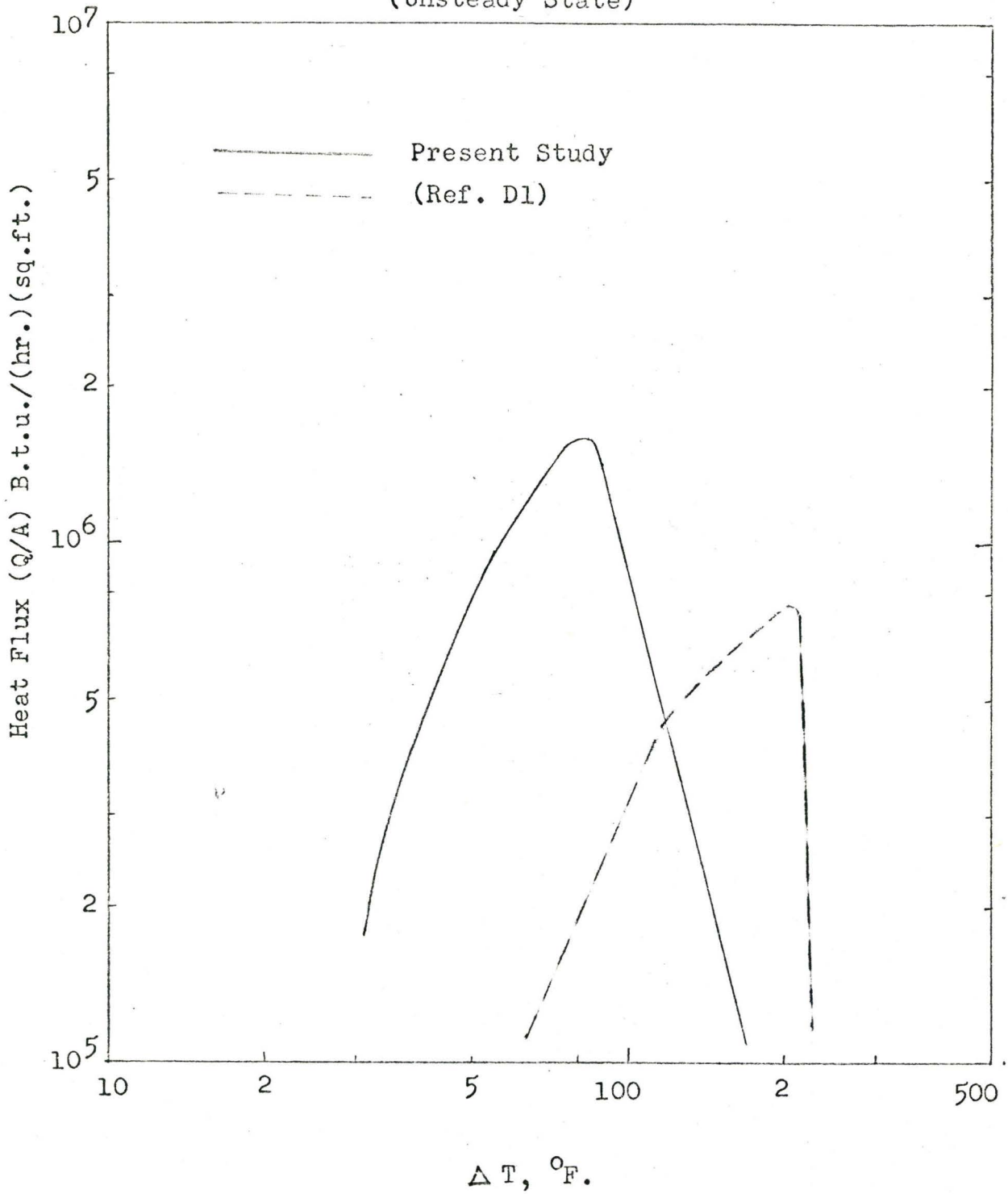

FIGURE 5.12

EFFECT OF CONCENTRATION OF SURFACTANTS

(Saturated Liquid Film Flow Boiling)

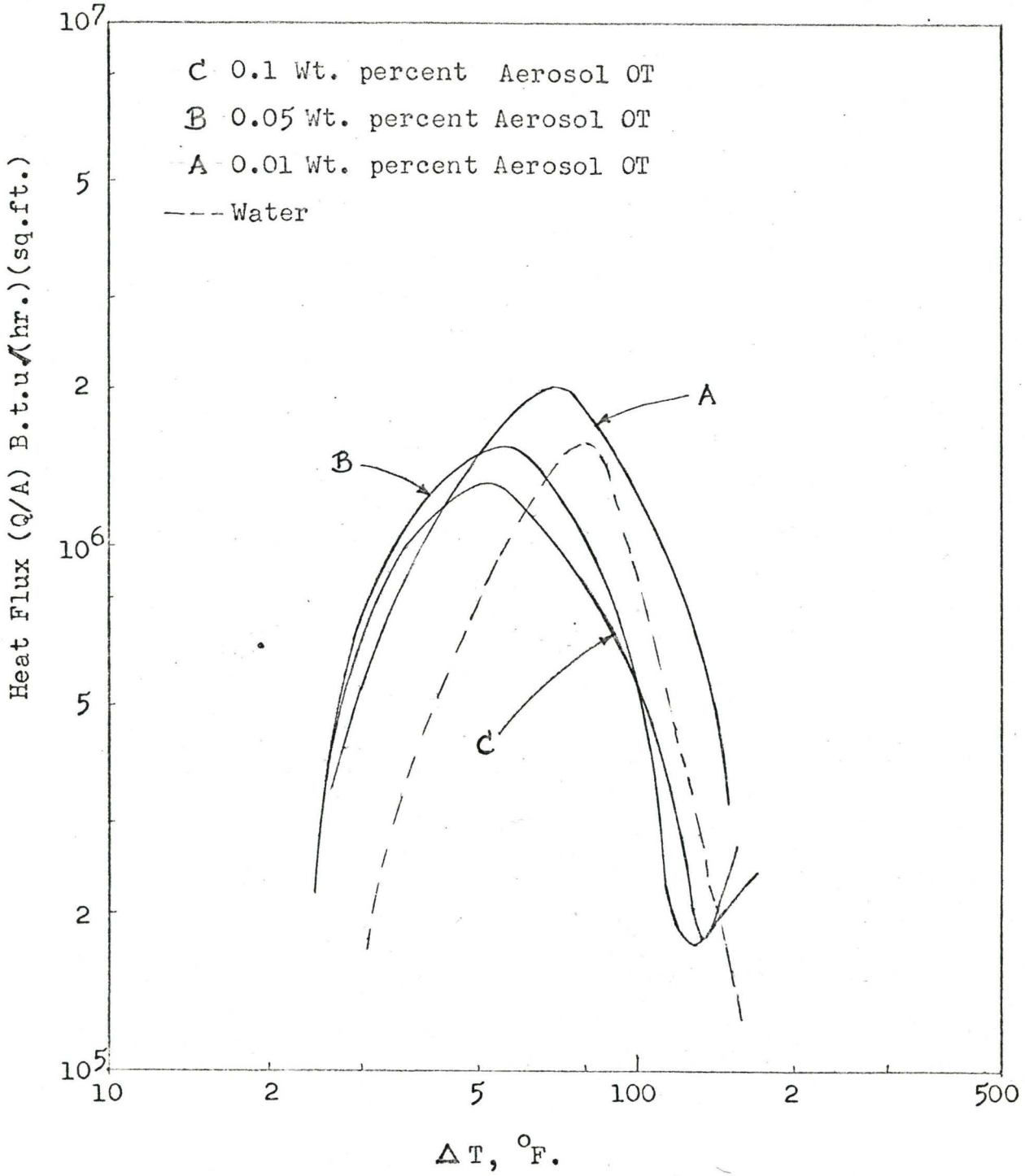

FIGURE 5.13

EFFECT OF CONCENTRATION OF SURFACTANTS

(Saturated Liquid Film Flow Boiling)

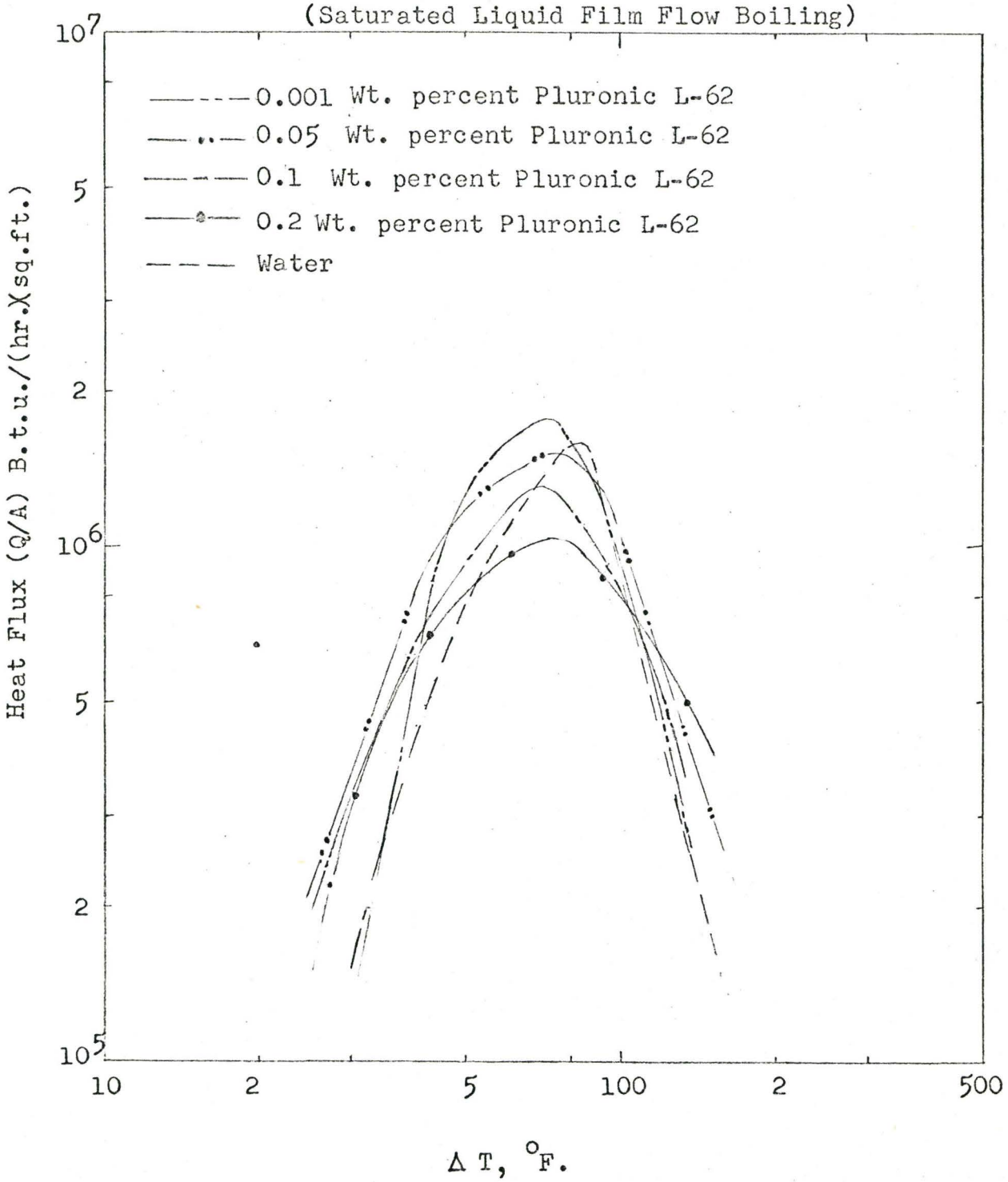

FIGURE 5.14

EFFECT OF CONCENTRATION OF SURFACTANTS

(Saturated Liquid Film Flow Boiling)

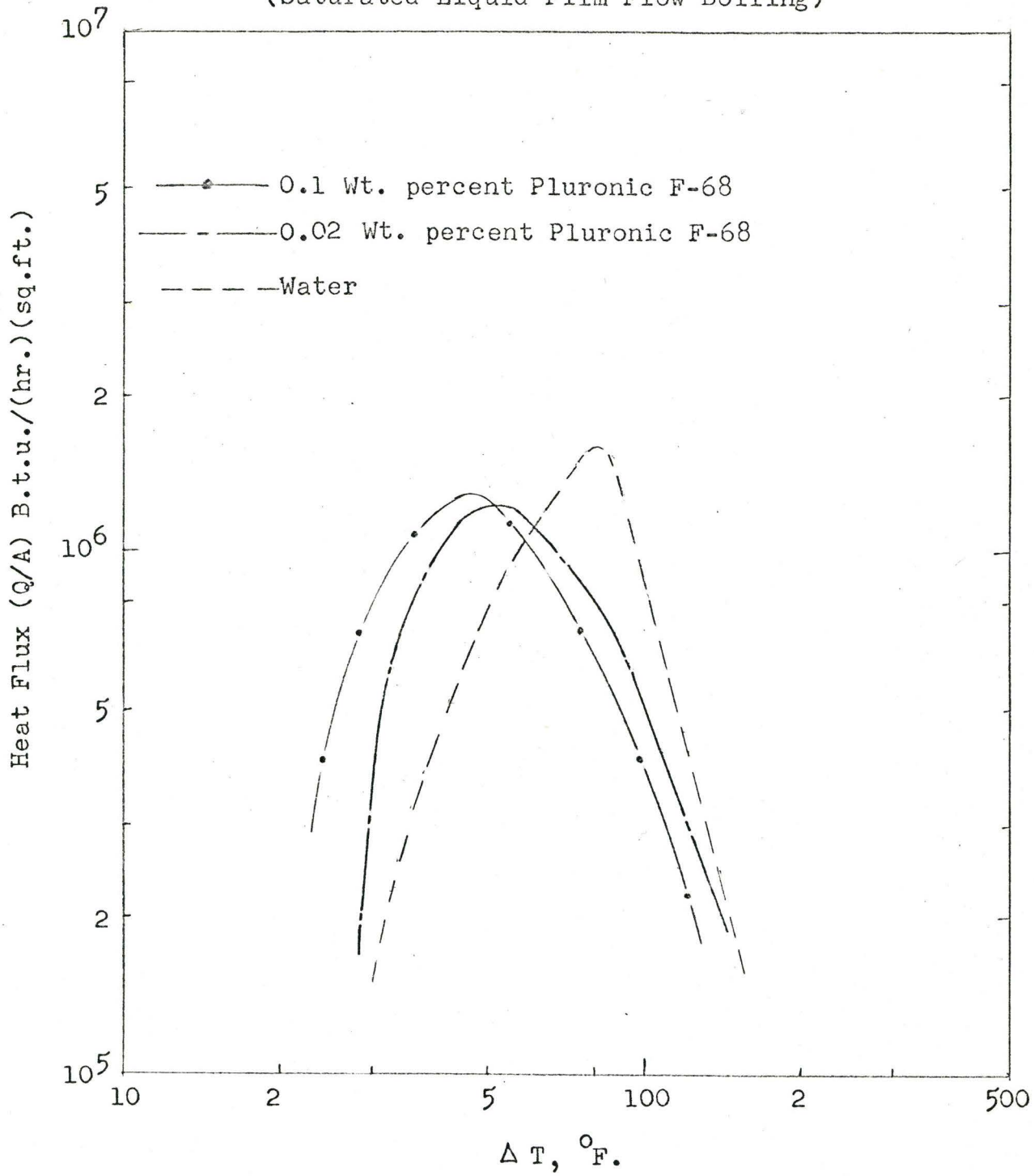

should be indicated.

These experimental observations show the same changes in maximum heat flux that were observed with these solutions in the pool-boiling experiments, i.e. changes in heat transfer according to concentration, molecular weight and hydrophobic character of the surfactant. There is also a tendency for the entire boiling curve in the nucleate boiling regime to shift to lower temperature differences for the same heat flux and hence higher heat transfer coefficients result.

5.5 Temperature and Heat Flux Fluctuations

The temperature and heat flux meter tracings from visicorder provide some additional information other than the boiling curve. The fluctuations in heat flux and temperature are shown for water in Figures 5.15 and 5.21; quite different behaviour is evident when surfactant solutions are used (Figures 5.16 to 5.20). The early studies of Moore and Mesler[M1] and Sharp[S1] have pointed out the importance of temperature fluctuation of the heat transfer surface in determining the boiling characteristics of a given surface and of a particular boiling regime. These temperature fluctuations should provide some qualitative information on boiling and indicate some of the wetting and stability characteristics of the thin interfacial films that exist during nucleate boiling.

The heat-flux meter with the thin disc showed greater fluctuations than the thick disc as expected from their respective

FIGURE 5.15

VISICORDER TRACE OF SATURATED LIQUID FILM BOILING OF WATER
(Unsteady State)

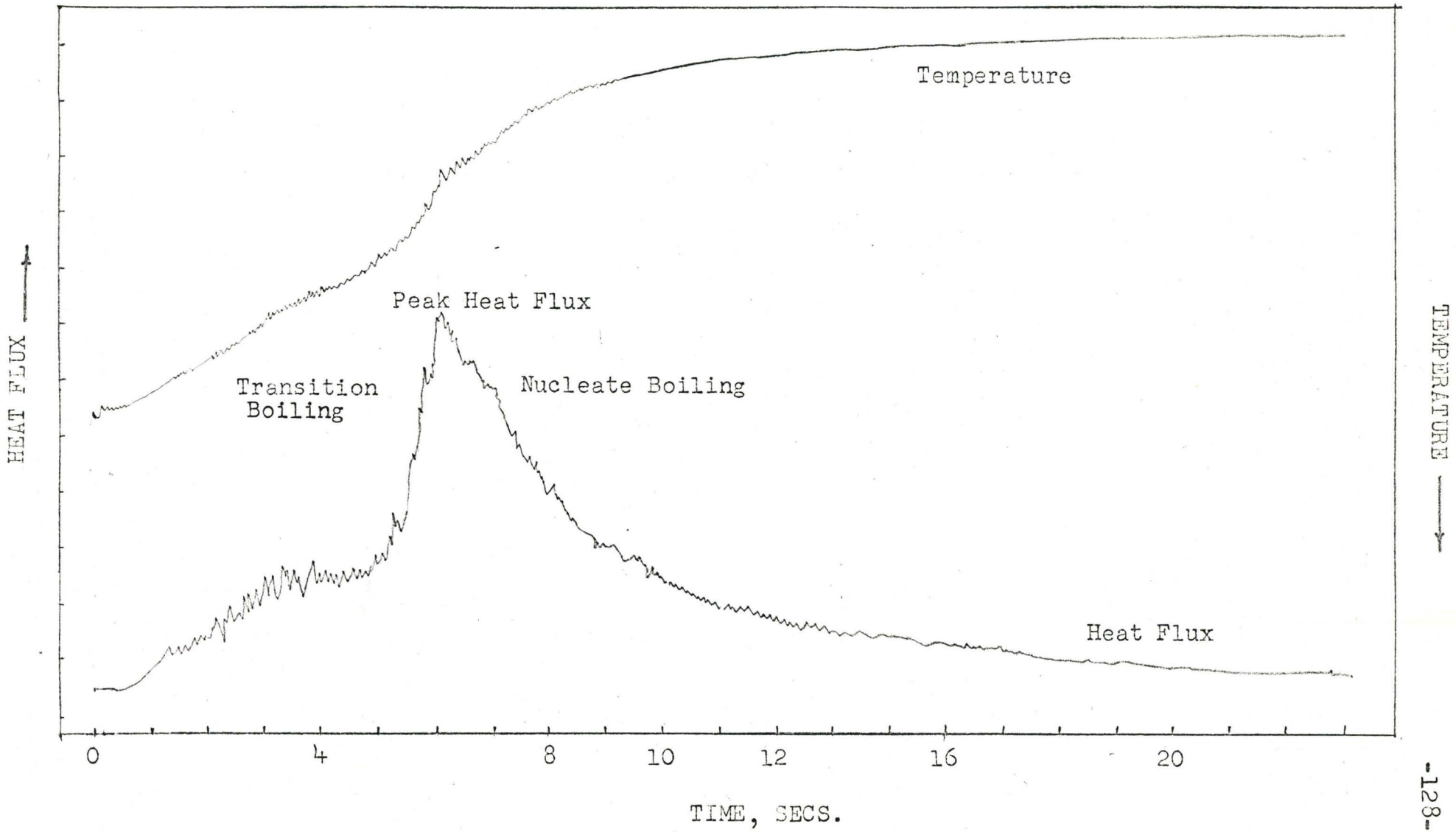

FIGURE 5.16

VISICORDER TRACE OF SATURATED LIQUID FILM BOILING OF AEROSOL-OS SOLUTION

(Unsteady State, Concentration - 0.1% by weight)

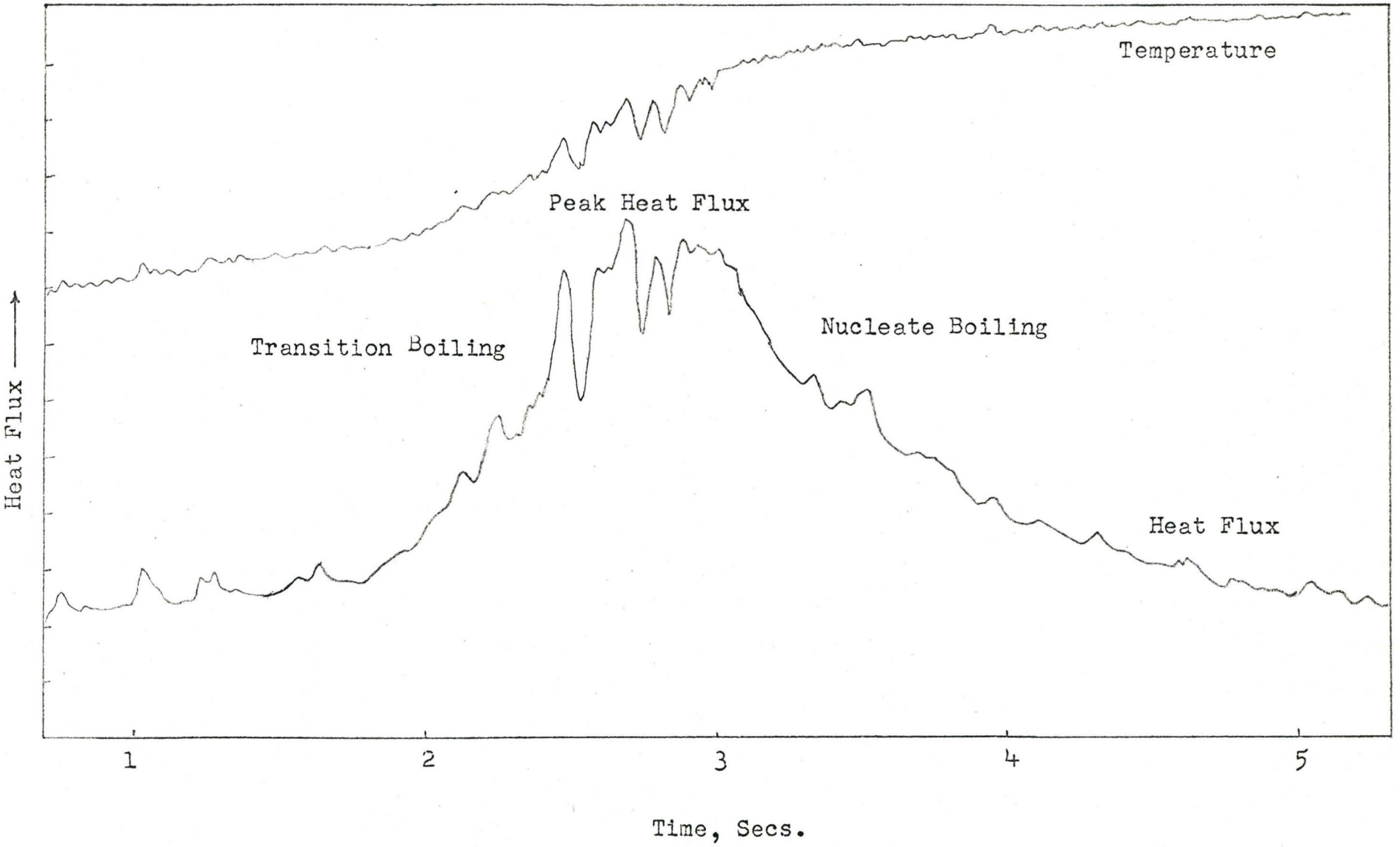

FIGURE 5.17

VISICORDER TRACE OF POOL BOILING OF PLURONIC F-68 SOLUTION

(Unsteady State - Concentration 1.0% by weight)

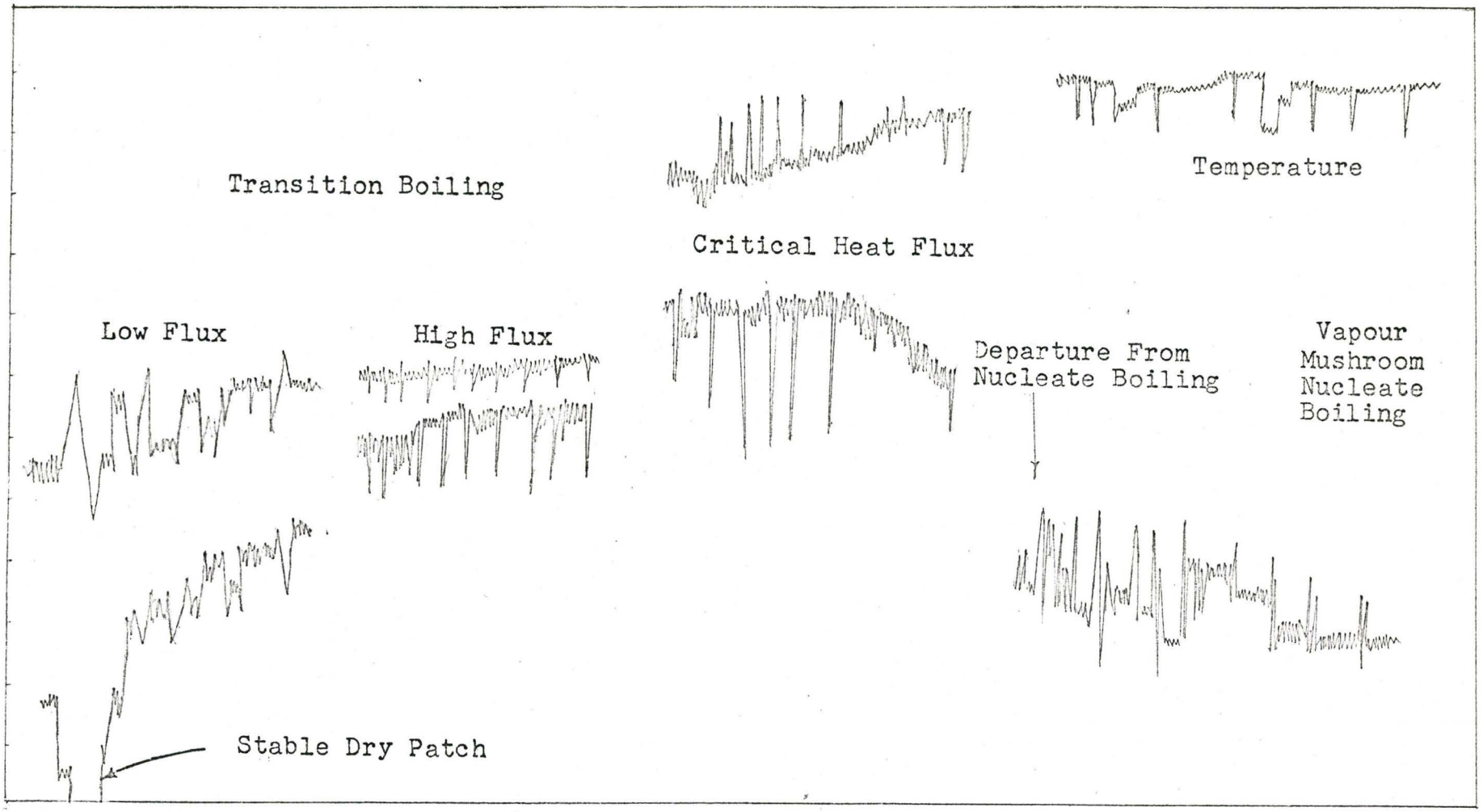

FIGURE 5.18

POOL BOILING, UNSTEADY STATE, PLURONIC L-62 1% BY WEIGHT

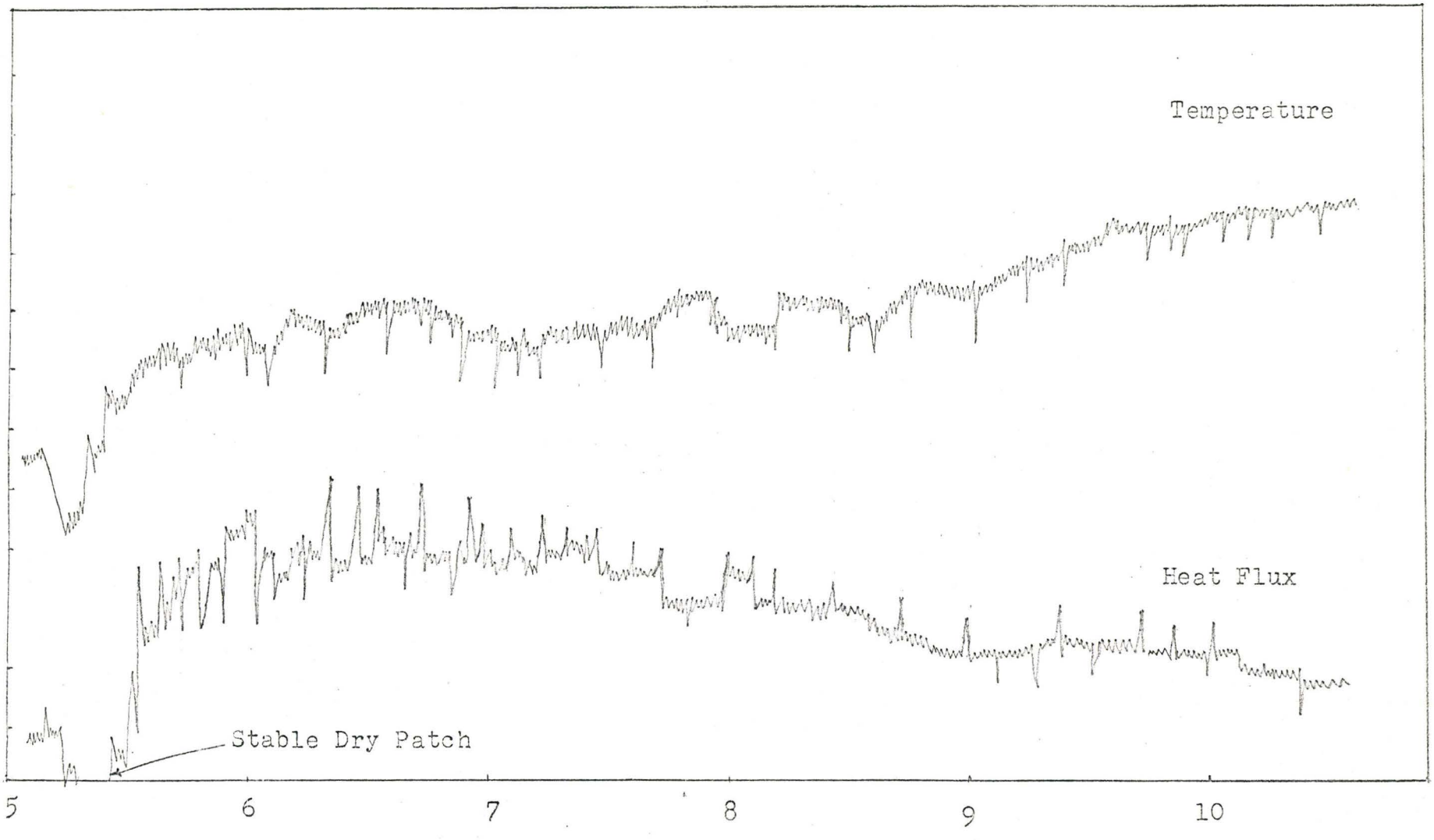

FIGURE 5.19

VISICORDER TRACE OF POOL BOILING OF AEROSOL OT SOLUTION

(Unsteady State - Concentration 0.75% by weight)

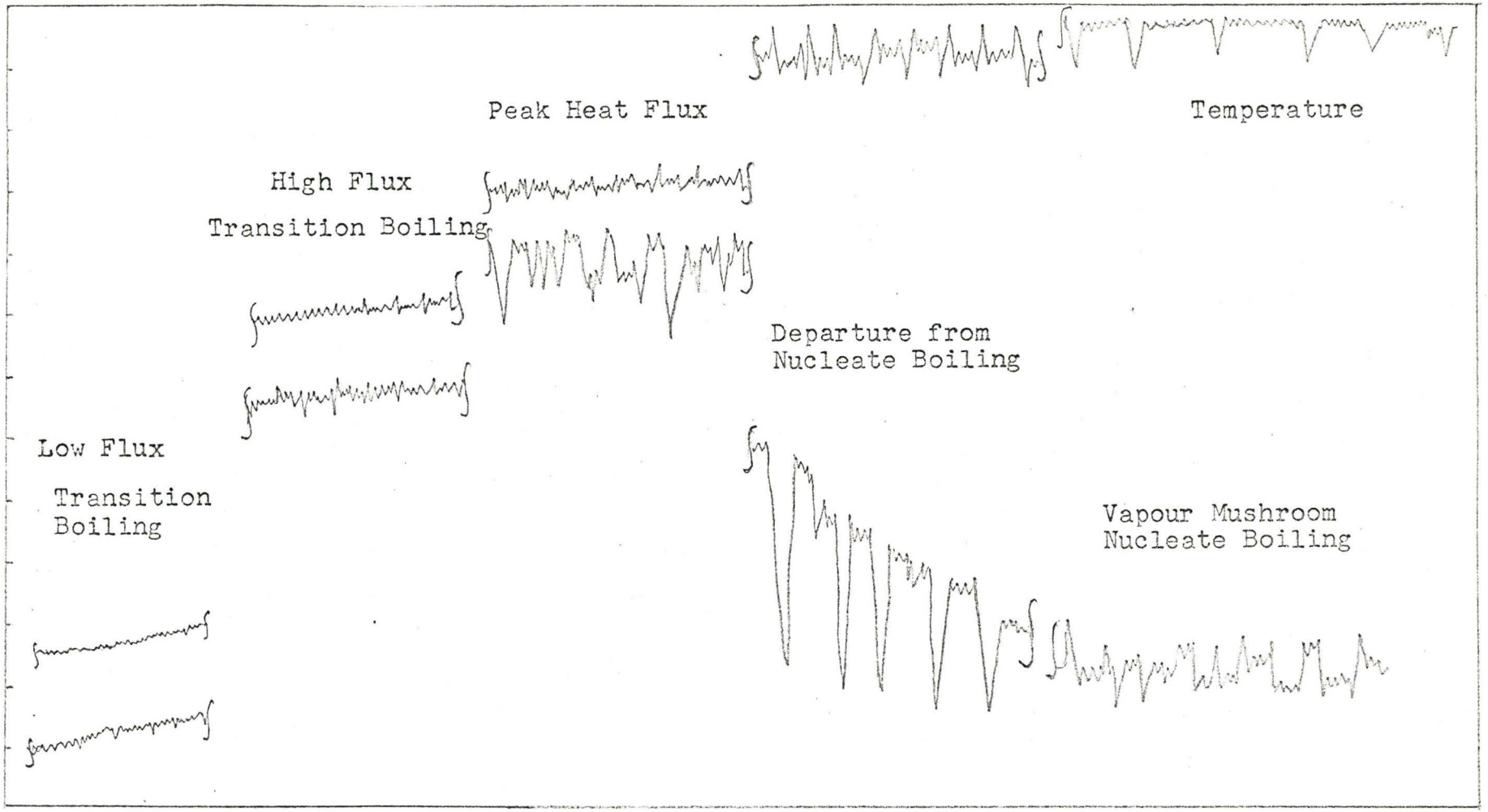

FIGURE 5.20

POOL BOILING, UNSTEADY STATE, AEROSOL-OS, CONDENSED TIME SCALE

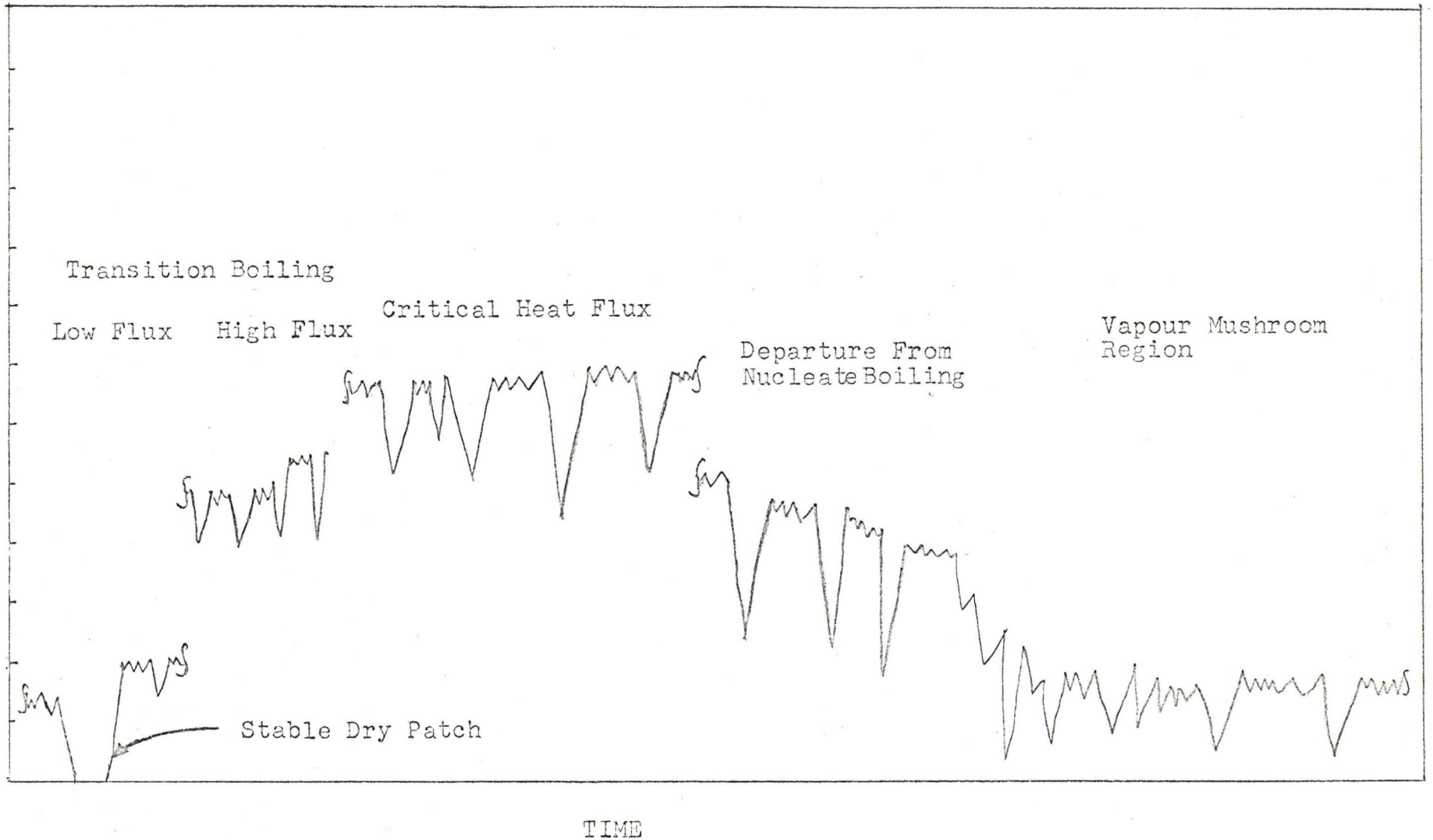

FIGURE 5.21

POOL BOILING, UNSTEADY STATE, WATER, CONDENSED TIME SCALE

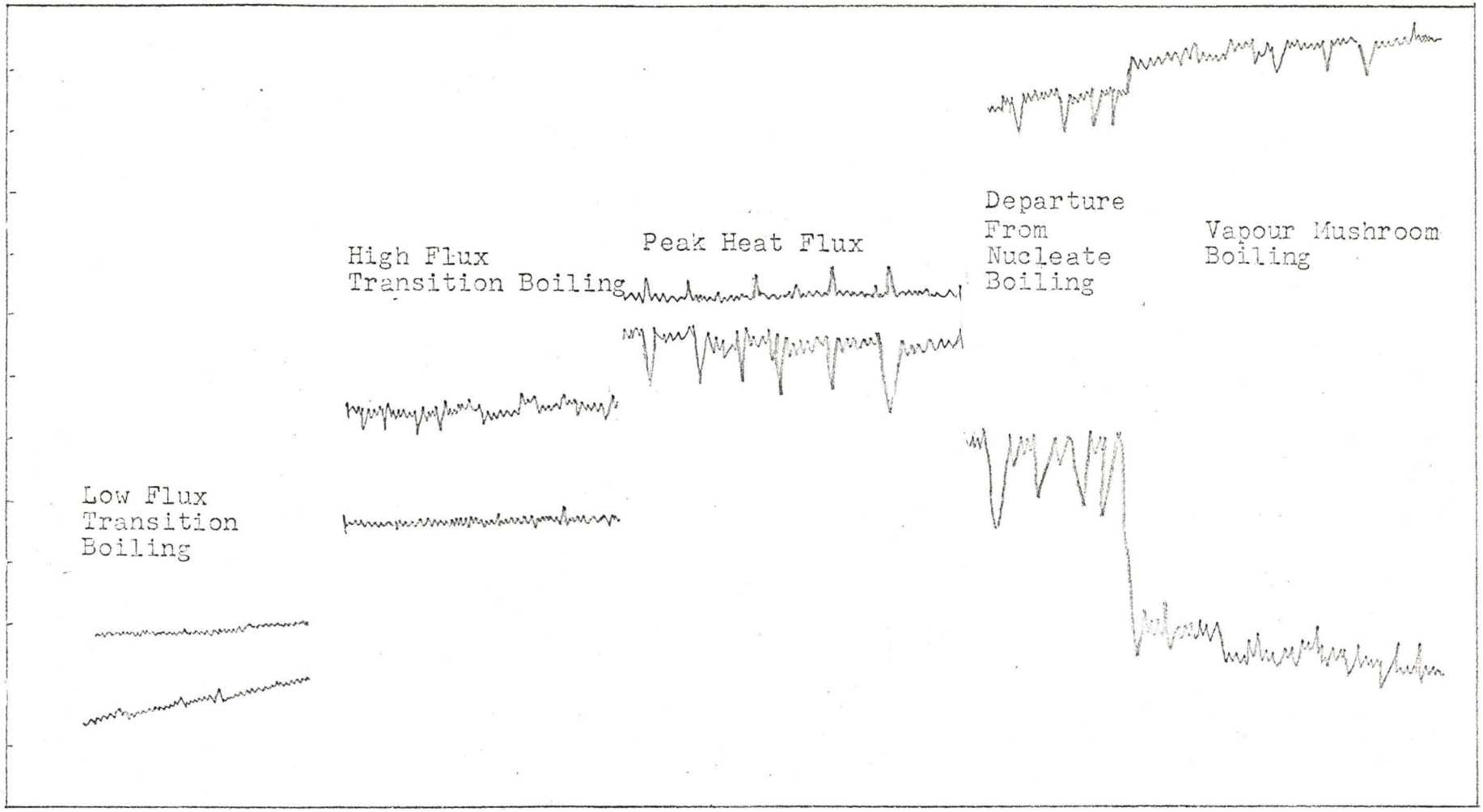

FIGURE 5.22

SPREADING COEFFICIENT OF SURFACTANT SOLUTIONS

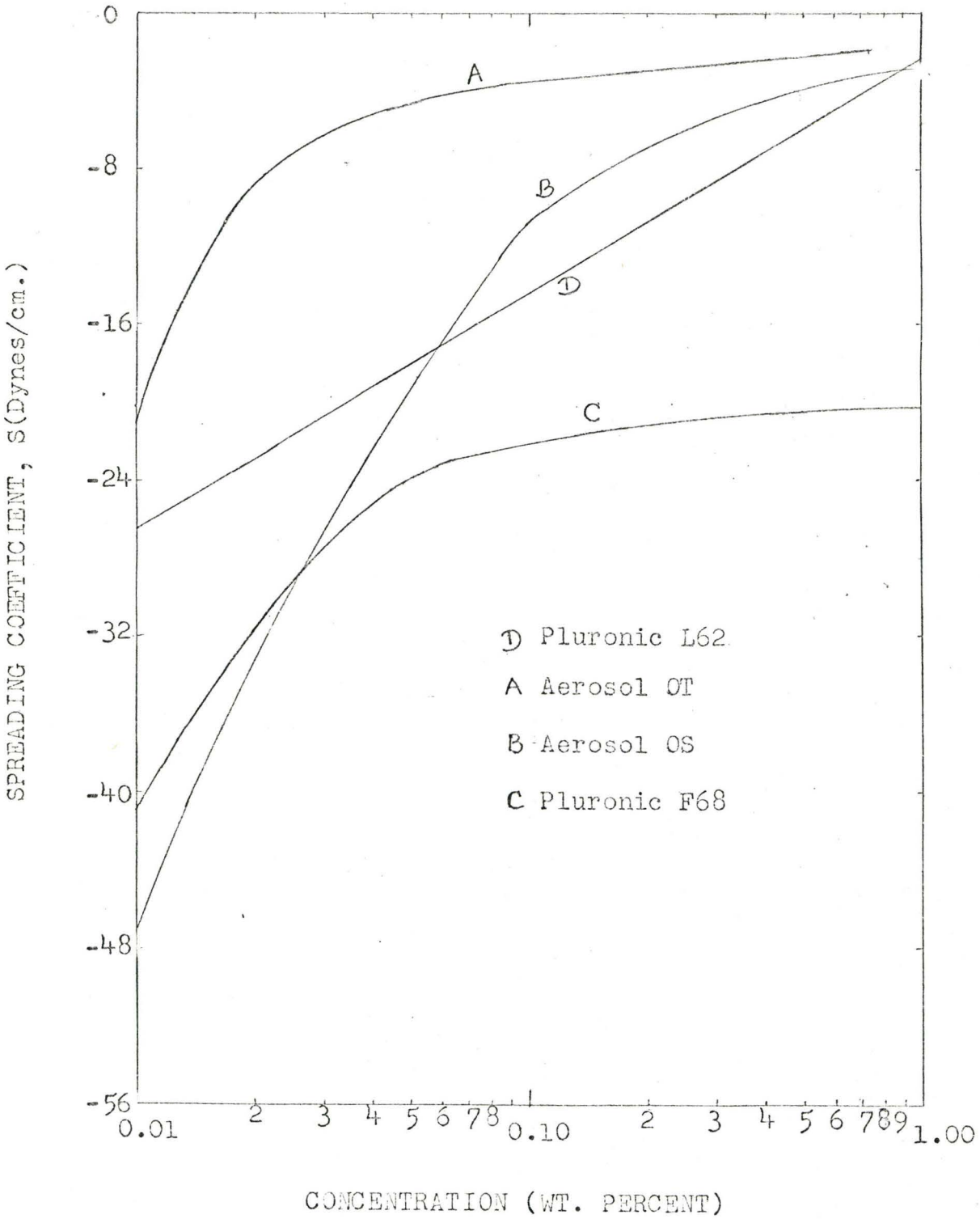

FIGURE 5.23

ADHESIVE FORCE OF SURFACTANT SOLUTIONS

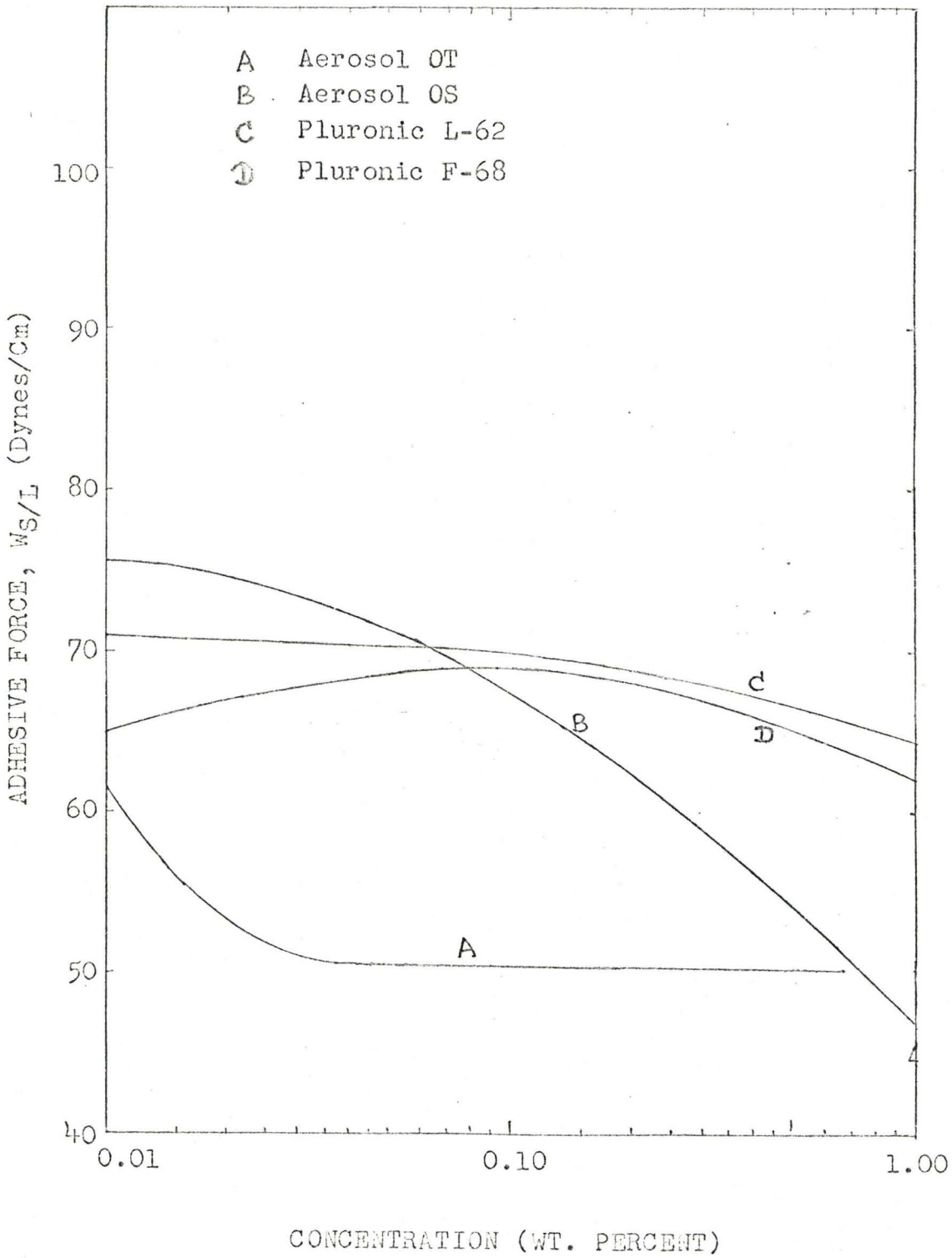

FIGURE 5.24

INTERFACIAL TENSION OF SURFACTANT SOLUTIONS

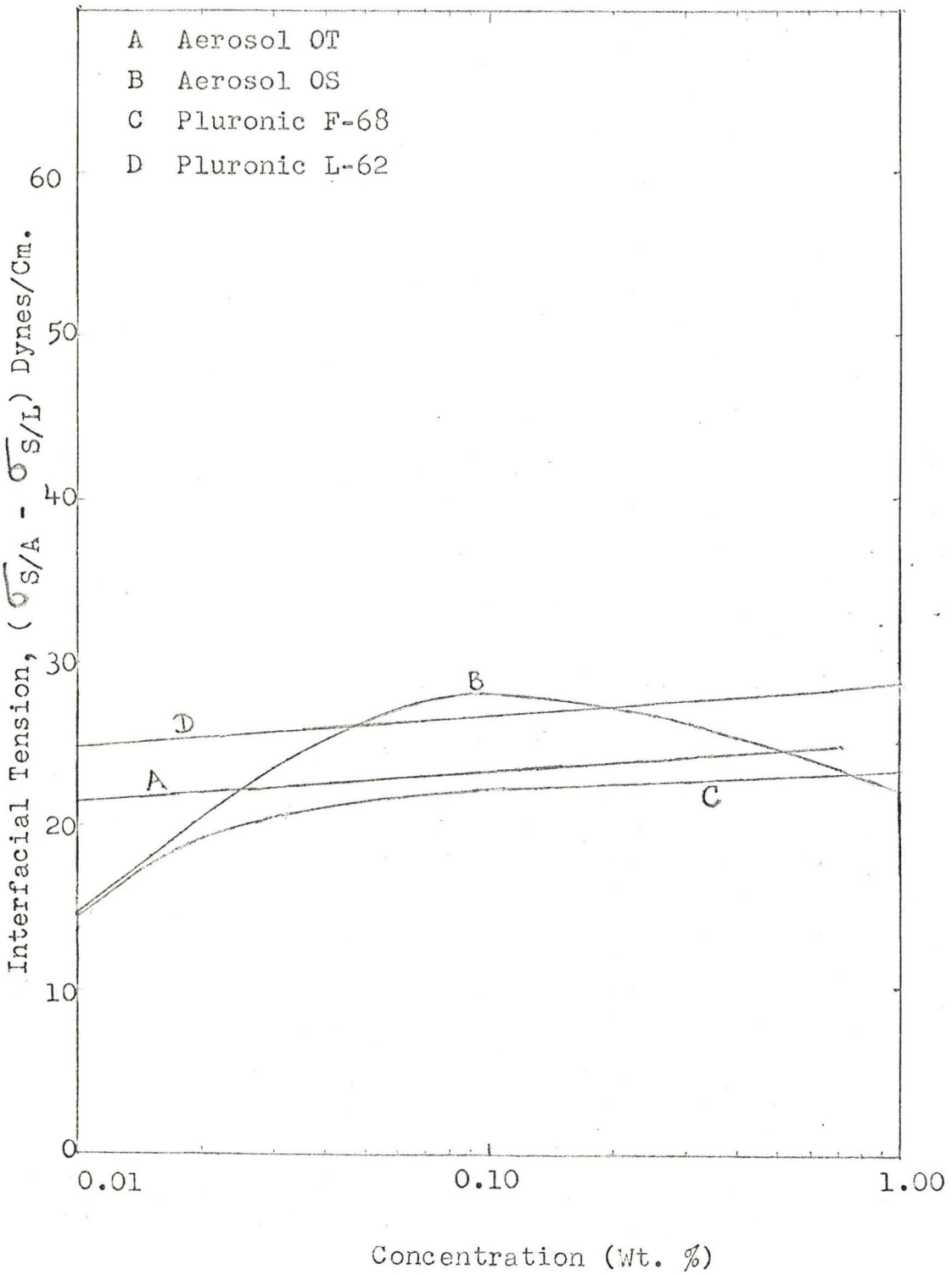

thermal capacities. The visicorder tracings indicated similar patterns and fluctuations for a particular solid-liquid combination in all runs.

The fluctuation frequency and magnitude differed considerably for a different type and concentration of surfactant. All solutions showed lesser fluctuation in the transition boiling regime. This observation became more apparent at higher concentrations of surfactants.

Observations particular to specific surfactants are noted: variations in temperature were higher in Aerosols than in Pluronics at the same concentration; F-68 showed higher fluctuations than L-62 solutions in all regimes except near the maximum heat flux; Aerosol OS indicated higher fluctuations among all the surfactant solutions in all regimes except in the region of maximum heat flux through to the point of departure from nucleate boiling; Aerosol OT showed nearly the highest fluctuation of any around the Departure fron Nucleate Boiling. In the transition regime, Aerosol OT indicated slightly larger fluctuations than Pluronic L-62 at the same concentration.

The frequency and rate of cooling and recovery also suggest a different behaviour for these solutions. Frequency of fluctuation is very high for pluronics, especially at the highest concentration; F-68 shows a higher frequency than L-62; Aerosol OS show higher frequency than OT. It also shows a very slow rate of cooling and recovery. All these temperature and heat flux fluctuations show considerable consistency.

5.6 Bubble Characteristics and Bubble Dynamics

These observations were mostly confined to high heat fluxes (greater than 70% $(Q/A)_{MAX}$) though limited observations were possible at lower heat fluxes (less than 20% $(Q/A)_{MAX}$). The detailed study of the bubble shape and behaviour needs a high-speed photographic study which was not within the scope of the present studies.

(a) Liquid Film Boiling

Large bubbles were formed at high heat fluxes and were highly unstable. Representative pictures of the top view of boiling films are given in Plates 4 and 5 and can be compared with the films of water observed by Dernedde[D1]. Plate 3 shows the effect of concentration at high heat flux. There seems to be a stabilization of liquid film with increase in concentration from 0.05% to 0.1% (by weight). There also seems to be a tendency to form dry patches in the case of the Aerosol OS solutions at high heat flux and lower concentration. This may be due to its low molecular weight and low wetting ability.

An observation was common to all boiling surfactant solutions, that is a noticeable reduction in splashing of drops of liquids in comparison to water. The large amount of splashing which was observed with water is illustrated in Plate 4. This can only be attributed to the higher wetting of these solutions. Turbulence on the surface was observed in all the studies. Liquid spikes were observed at higher heat fluxes and low concentrations.

PLATE 4

BOILING OF LIQUID FILMS AT HIGH HEAT FLUX

(Aerosol-OS in Water at 10 lb./min. and 30° incline)

0.1% Concentration

0.05% Concentration

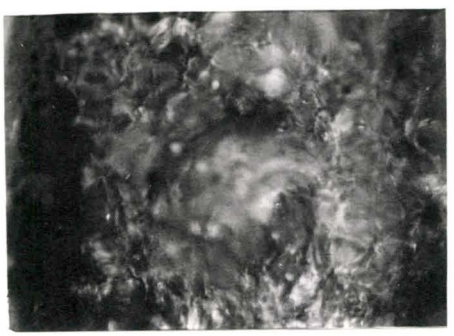

0.01% Concentration

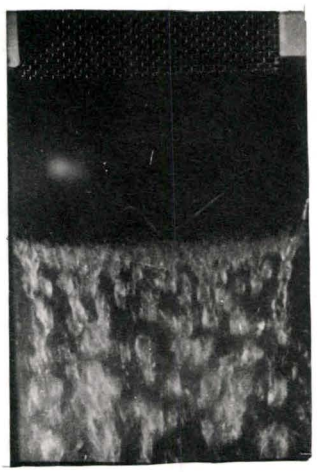

Water at 4.3 lb./min.
(Ref. D1, Plate 4)

This is obvious from the higher vaporization rate observed at low concentrations. There seem to be vapour masses almost like mushrooms which are highly unstable during the high flux boiling.

A significant increase in the thickness of flowing boiling liquid film around the region of destruction was observed. This increase was sometimes as much as ten times. This increase in thickness was due to the large number of small bubbles that were formed at lower heat fluxes.

A few observations of the bubble characteristics were made at lower heat fluxes; these are shown on Plate 5. There is a swarm of bubbles which are held together instead of the isolated bubbles observed in pool boiling. The thickness of the film increases very rapidly by virtue of these agglomerated bubbles. This shows that the bubbles which would have normally collapsed have the tendency to remain stable. There seems to be a significant effect of flow in changing the shapes of bubbles (Plate 5). The bubbles at the surface not only show an eccentricity due to flow, but also show increased eccentricity due to concentration.

(b) Pool boiling

Some observations were possible on the bubble shape and departure in the pool boiling. Due to high activity, it was not possible to observe the bubble shapes and departures at high heat fluxes, but some comparison with the predicted bubble shapes was possible. At about 1% concentration by weight and at lower heat fluxes, bubbles were small and were spherical for all surfactants. High wetting Aerosol OT and Pluronic L-62 showed larger bubbles

PLATE 5

BOILING OF LIQUID FILMS AT LOWER HEAT FLUX

(Aerosol-OS in Water at 10 lb./min. and 30° incline)

0.1% Concentration

0.05% Concentration

0.01% Concentration

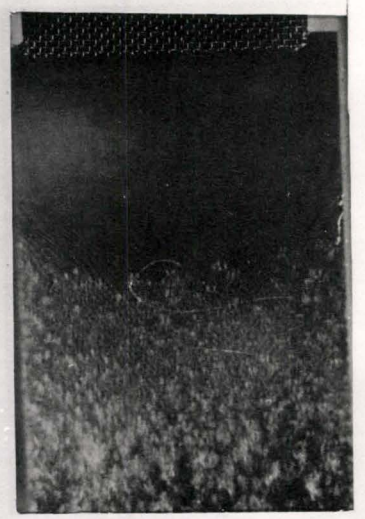

Water at 4.3 lb./min.
(Ref. D1, Plate 4)

but departure was sluggish. F-68 and Aerosol OS showed higher frequency of smaller bubbles at this concentration. At high heat fluxes most of the bubbles had the shape of bubbles suggested by Kirby[K3] as Type III. But the size and frequency of release of these vapour masses varied. The vapour release looked as though the vapourization takes place from a thin film into a large vapour mass in the case of all the solutions except Pluronic L-62. Pluronic L-62 especially at high concentrations showed vapour masses which are very sluggish. The size of the vapour masses increased considerably with the heat flux. Aerosol OT showed very large number of vapour masses released at a faster rate. The vapour masses in general were all irregularly shaped. The size and frequency of the bubble depends on the rate of vapourization. The shape and agitation of these bubbles may be important in varying the heat transfer as can be seen from the earlier discussions on the micro convection in thermal boundary layer. Bubble density was higher and vapour masses smaller in the case of Aerosols compared to Pluronics. The bubble shape and behaviour seem to indicate that it depends on the heat flux and the foam stability, while the bubble frequency varies significantly with the solid-fluid combination.

6. DISCUSSION

The experimental observations in this study demonstrate most conclusively surface active agents affect the boiling heat transfer of water in both pool and forced-flow boiling. The shape of the boiling curve is affected over the entire nucleate boiling and transition boiling regimes. Moreover, the maximum heat-flux is changed considerably by the addition of surfactants. The effect in each case is concentration-dependent, (Fig. 6.1 to 6.4), indicating an increase in heat flux at low concentrations and a decrease at higher concentrations. The actual differences also seem to be quite sensitive to the type of surfactant employed.

In trying to relate this behaviour to the basic mechanisms of the boiling phenomenon, this discussion will be concerned with two aspects of the problem.

(i) the compatability of the present observations with current theories and for models of the boiling process, and

(ii) the mechanism by which surfactants affect the boiling process.

6.1 Comparison of Observed Data with that Predicted From Existing Models

According to the hydrodynamic stability model of Zuber and Tribus[Z6], i.e. equation (4), the critical heat flux should vary as the (surface tension of the liquid)$^{0.25}$. Figure 6.5

FIGURE 6.1

EFFECT OF CONCENTRATION ON MAXIMUM BOILING HEAT FLUX

(Pool Boiling)

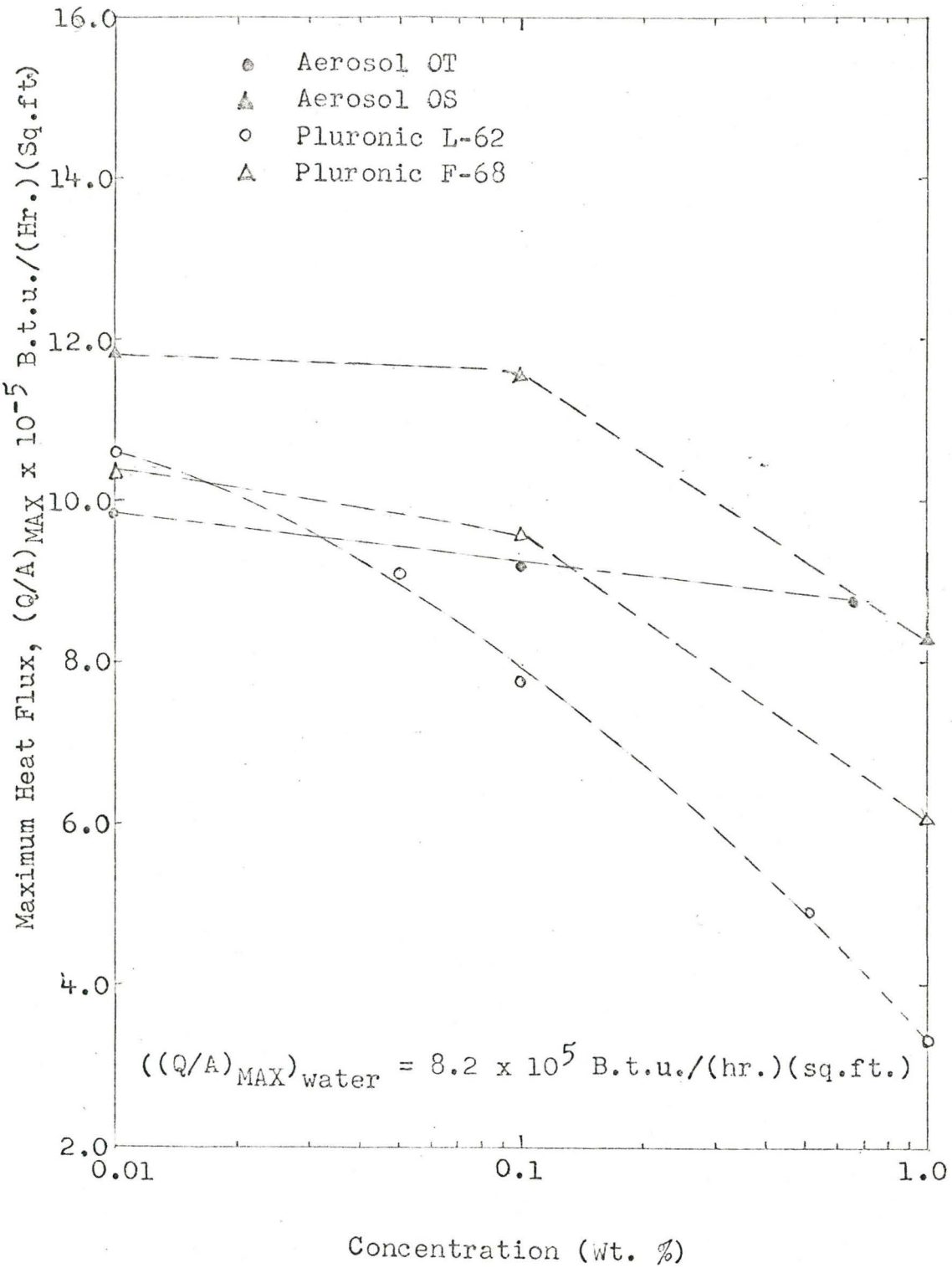

FIGURE 6.2

EFFECT OF CONCENTRATION ON CRITICAL HEAT FLUX

(Saturated Liquid Film Flow Boiling)

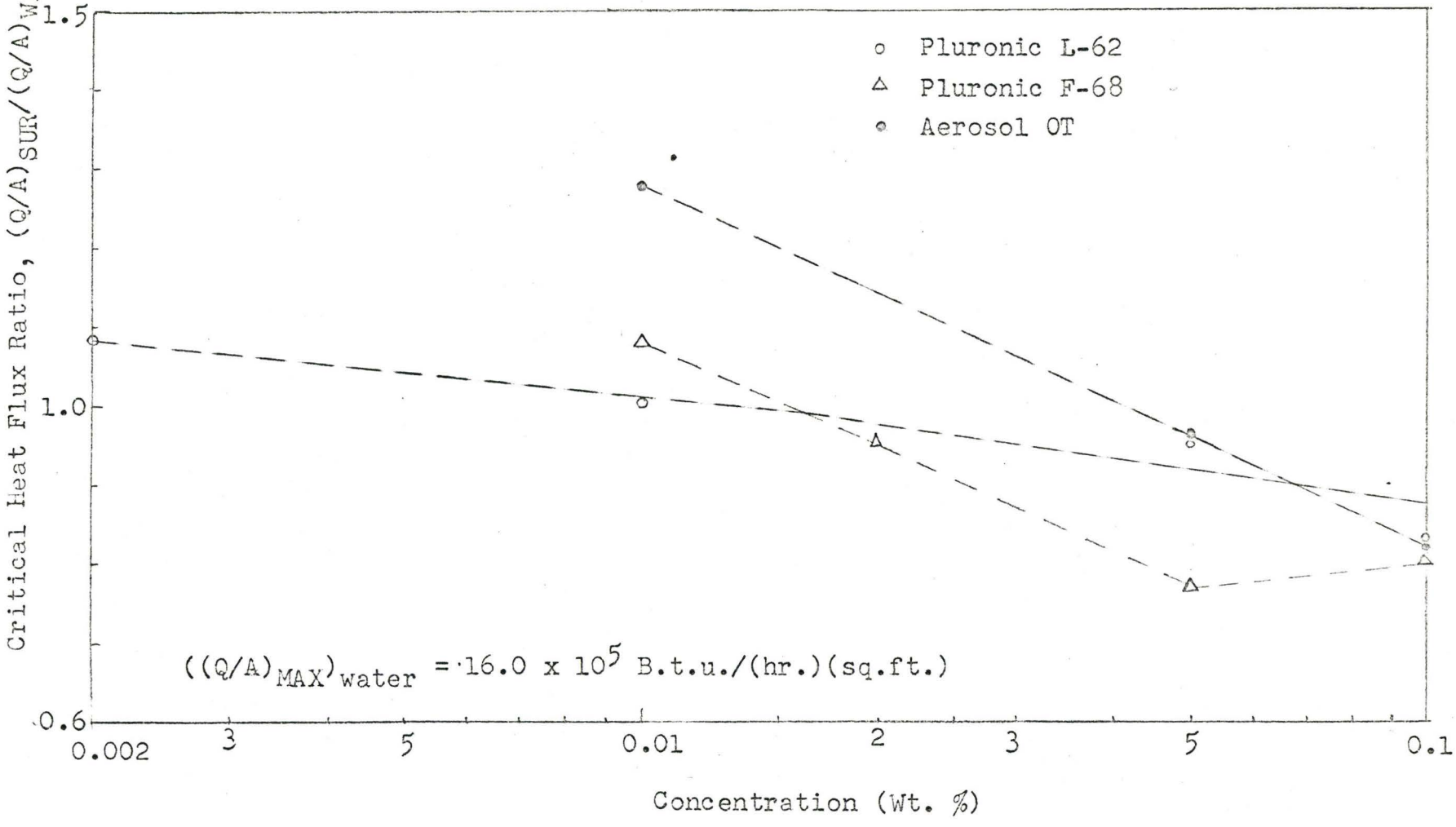

FIGURE 6.3

EFFECT OF SURFACTANT CONCENTRATION

HEAT TRANSFER COEFFICIENT AT MAXIMUM HEAT FLUX

(Pool Boiling)

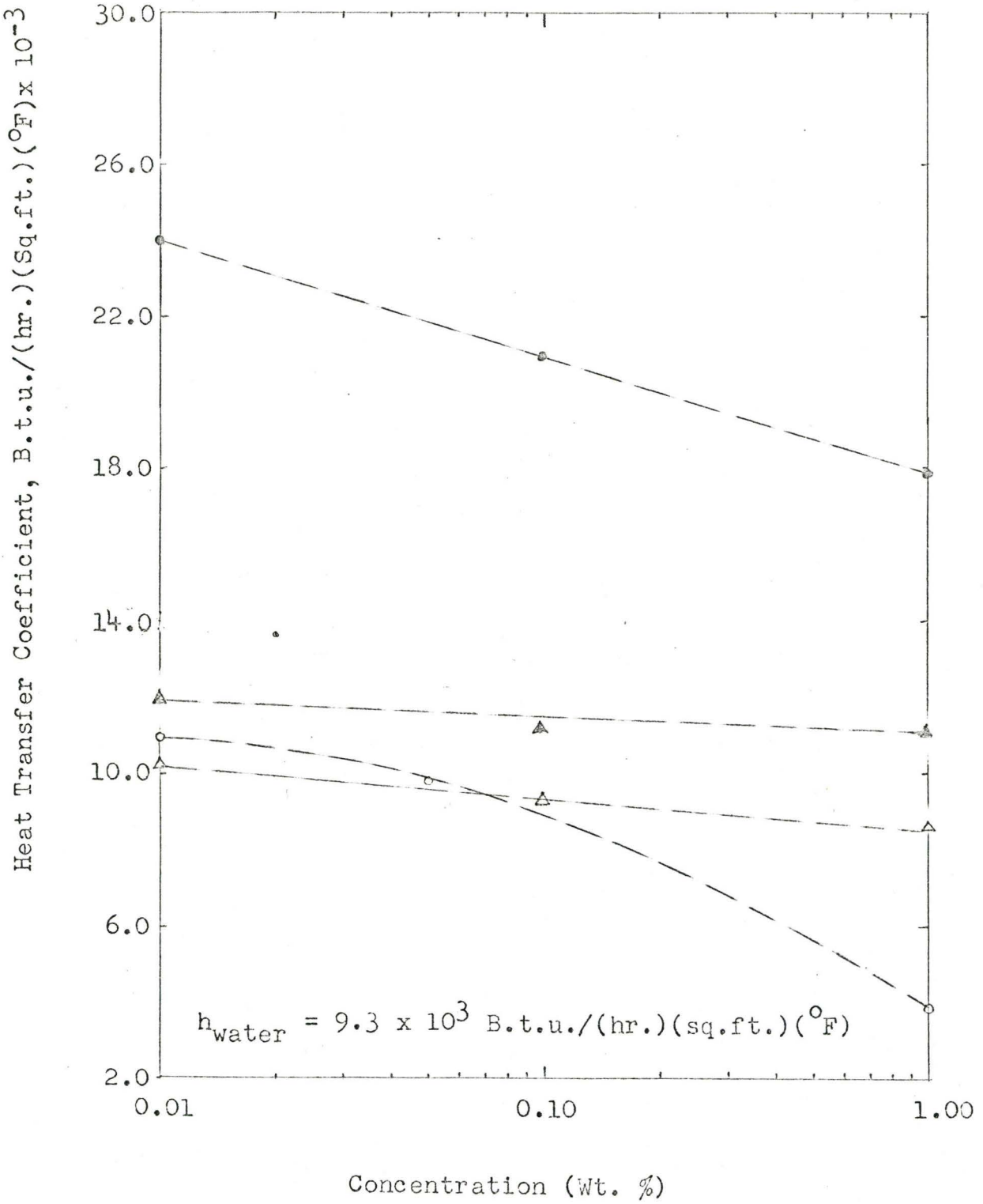

FIGURE 6.4

EFFECT OF SURFACTANT CONCENTRATION-HEAT TRANSFER COEFFICIENT AT MAXIMUM HEAT FLUX

(Saturated liquid film flow boiling)

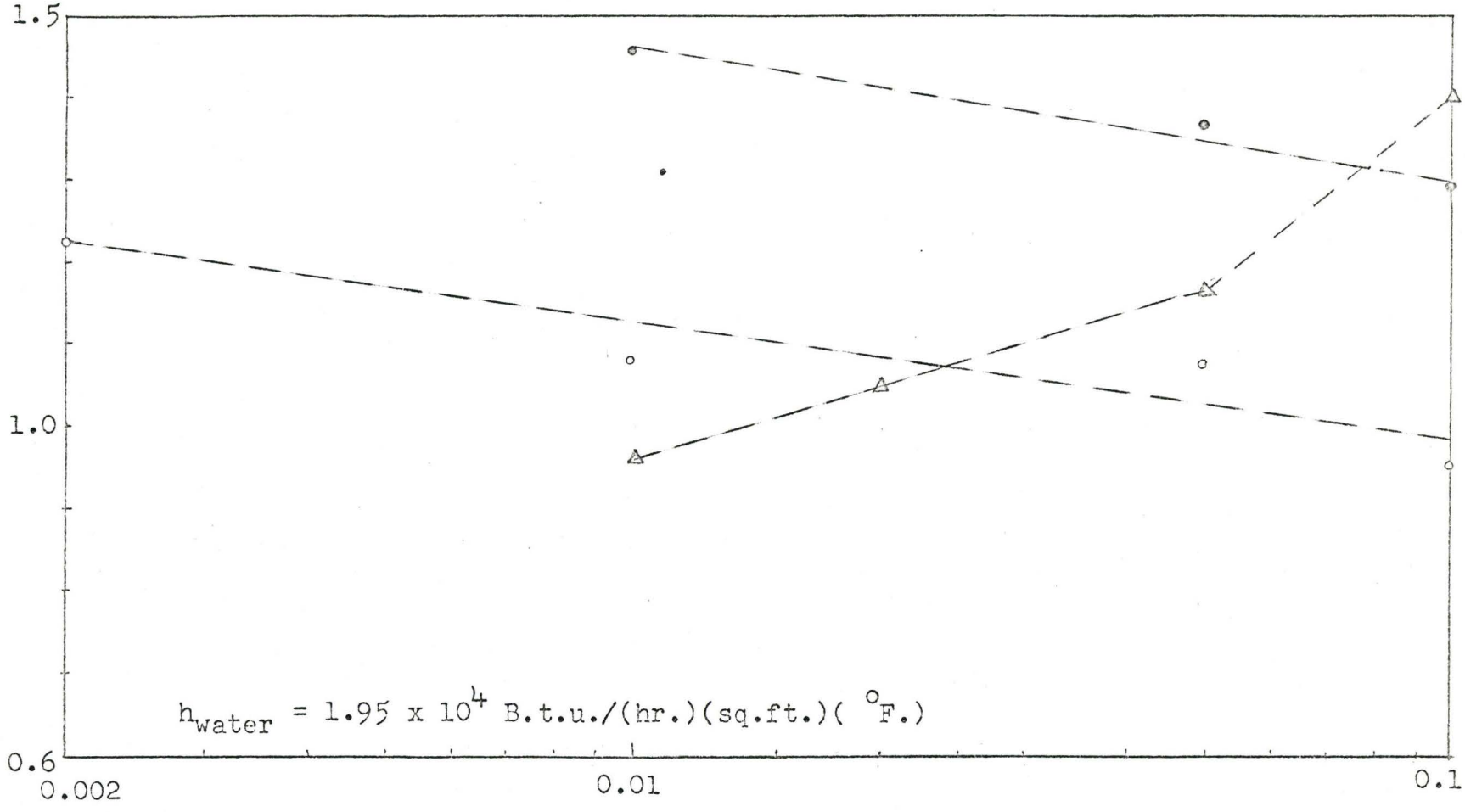

FIGURE 6.5

EFFECT OF SURFACE TENSION ON CRITICAL HEAT FLUX

(Pool Boiling)

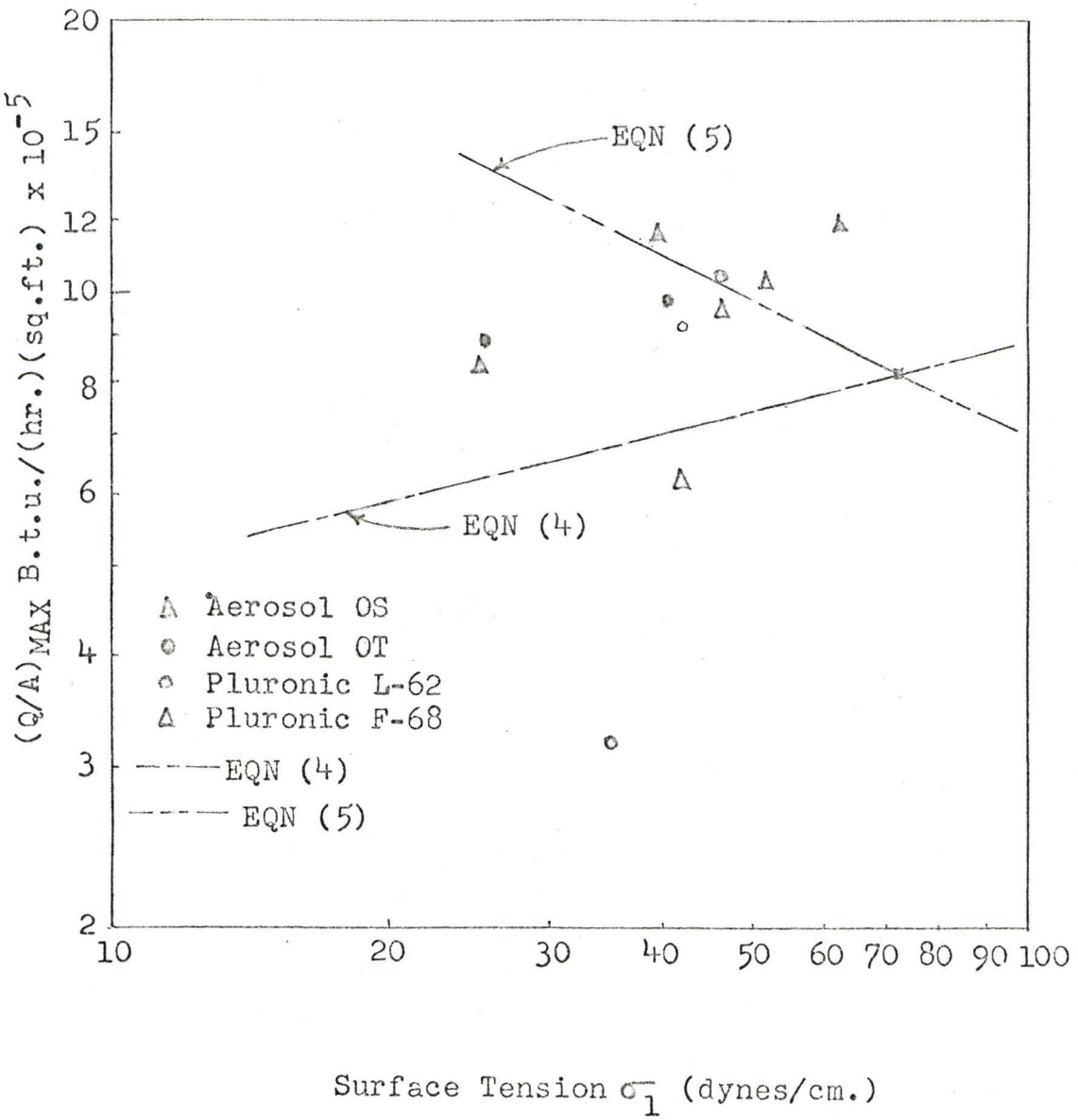

illustrates quite dramatically that the critical heat flux can be as much as 40% greater although the surface tension is decreased and all other properties are essentially constant. Equation (5) has suggested that the maximum heat flux should increase as the surface tension decreases. Figure 6.5 indicates that the inverse square root dependence does not hold either. Indeed, the critical heat flux increases as surface tension decreases and then decreases at higher concentrations of surfactants where the surface tension is decreased even further. Therefore the observations suggest that there does not seem to be any simple relation between surface tension and critical heat flux.

The effect of contact angle (equilibrium value) on critical heat flux has been predicted by Rohsenow[R3] and Diessler[D7]. The results presented on Figures 6.6 and 6.7 illustrate that the critical heat flux is neither proportional to θ or $\theta^{\frac{1}{2}}$. Each surfactant solution shows a unique curve.

6.2 Comparison with Previous Observations

Dunskus and Westwater[D5] observed a similar increase in critical heat flux with the addition of a number of surfactants to isopropanol. They found that increasing the molecular weight of the additive of the same homologous series (Igepals, in this case) increased the critical heat flux even more. They explained this on the basis of increased surface viscosity resulting from concentrating the surfactant in the liquid film under the vapour masses. This increased viscosity was said to lead to an increased

FIGURE 6.6

EFFECT OF CONTACT ANGLE ON CRITICAL HEAT FLUX

(Pool Boiling)

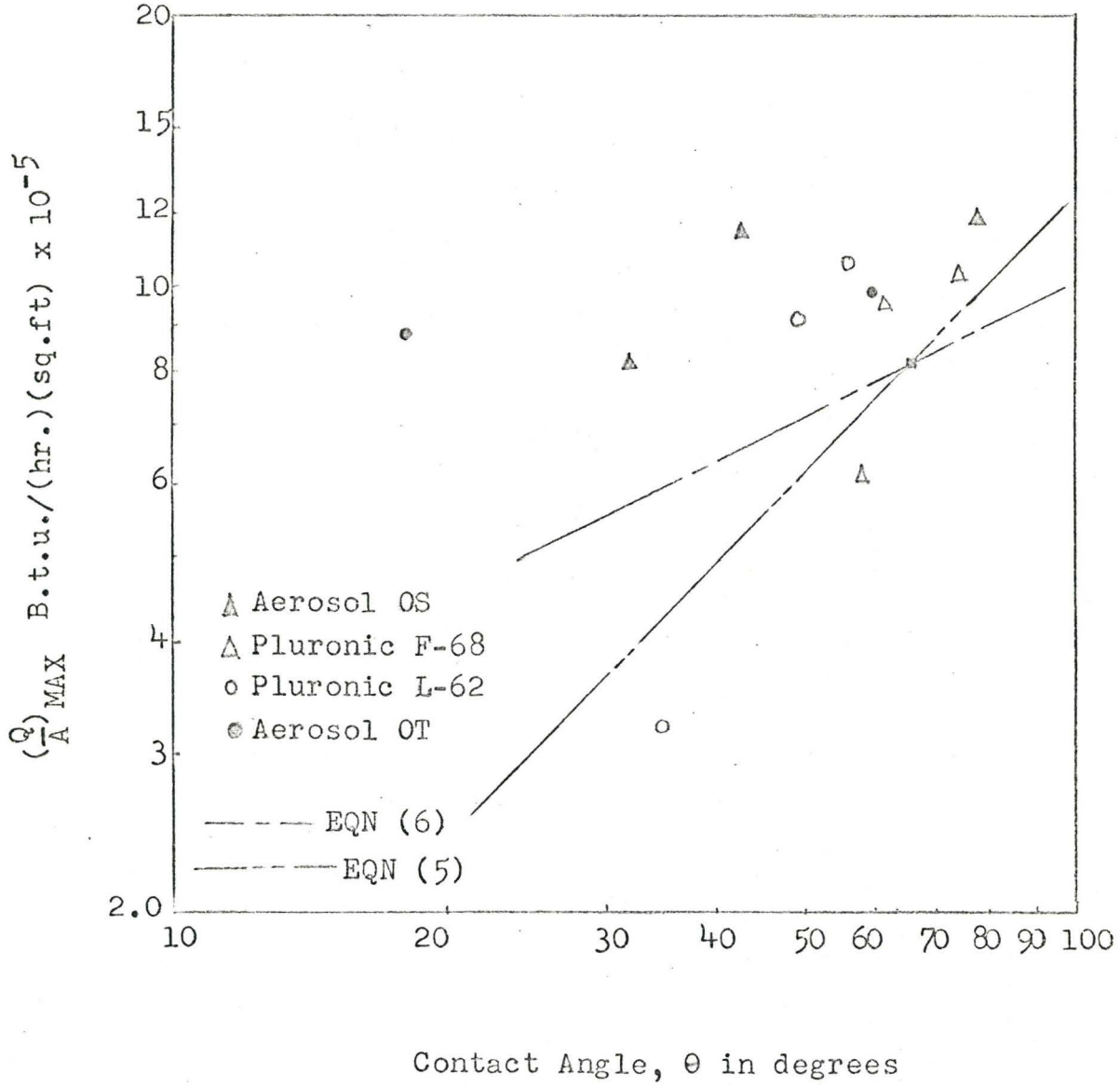

FIGURE 6.7

COMPARISON OF DIESSLER'S AND ROHSENOW'S EQUATION

(Pool Boiling)

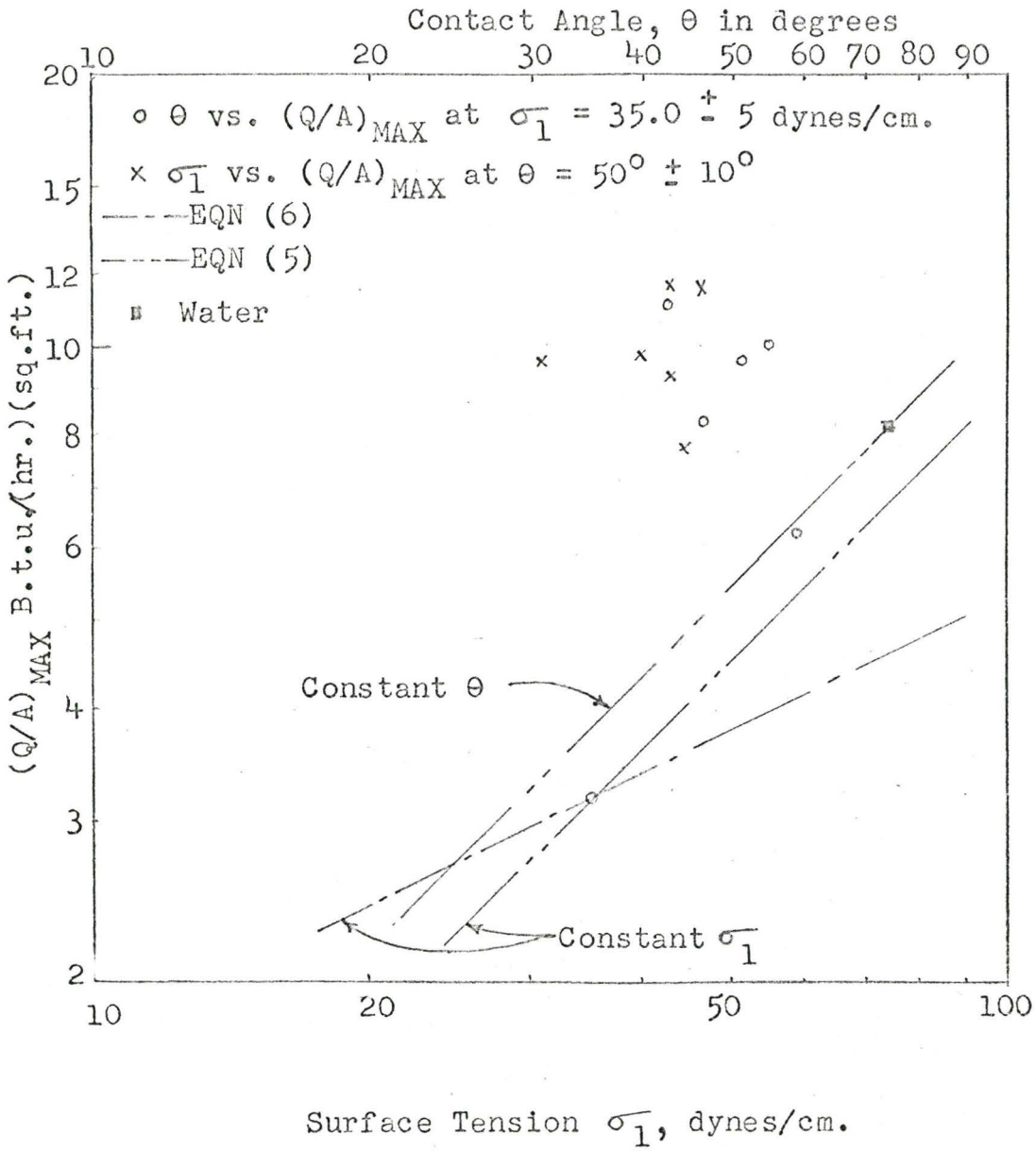

stability of these films and hence a greater resistance to the disrupting forces. In the present case, the highest molecular-weight additives, Pluronics, did not indicate a higher critical heat flux than the lower molecular weight surfactants. In fact at the higher concentrations the critical heat flux was less. Furthermore at any given wall temperature the Pluronic additives indicated a lower heat flux than that of water whereas the Aerosols indicated a higher heat flux in most cases. Therefore, stability of the liquid film, due to surface viscosity, does not seem to play a major part in the present case. Similarly their observation of a higher temperature difference corresponding to the critical heat flux is not borne out here since Aerosol OT solutions show a dramatic decrease in the temperature at which the maximum heat flux occurs.

Lowrey and Westwater[L6] suggest that organic molecules of surfactants may form nuclei and increase the heat transfer rate at any surface temperature in the same way as the teflon-spotted surfaces of Young and Hammel[Y2] do. The behaviour of Aerosol OT solutions in the nucleate boiling region makes them suspect. However, close examination of the surface after a boiling test did not show any local deposition.

Costello and Frea[C17] suggest that deposition of material from tap water should increase wettability as well as create artificial sites and increase the nucleate boiling flux and the maximum heat transfer rate. Ivey and Morris[I1] also state that wettability of the surface should affect the heat flux as well,

pointing out that oxidized (low energy) surfaces yield higher heat fluxes than clean metallic (high energy) ones. Berenson[B5] performed tests with a high-energy surface which had been roughened to various degrees and found little effect on the critical heat flux, although in this case the roughness may not have affected wetting to any significant degree. The present tests with the contaminated surface (Figure 5.10) illustrates that wetting of the surface is very important in determining the maximum heat flux since the amount of surfactant left on the surface is not expected to yield any appreciable concentration even if it were dissolved completely in the liquid used in the test.

Thus there is strong evidence to support the belief that the critical heat flux is controlled by factors other than those relating to hydrodynamic stability. Furthermore, these factors seem to be associated with surface phenomena, either at the solid-liquid-gas or the liquid-gas interface.

The effect of the surface active agent is to reduce the surface tension of the fluid, increase the spreading and adhesive tendency of the liquid and reduce the interfacial tension at the solid-liquid-vapour interface. Other effects that must be considered are deposition or adsorption of organic material on the heat transfer surface (contamination) and effects arising out of differences in the concentration of surfactants at different parts of the interface (Marangoni forces). Obviously some of these characteristics are directly measureable; others can only be speculated upon since no direct measurement is possible with

existing equipment.

6.3 A Suggested Mechanism By Which Surfactants Affect The Boiling Process

(a) The Critical Heat Flux

The present observations of critical heat flux are not consistent with the predictions based on the hydrodynamic models and some of the observations of others regarding the effect of surfactants discussed in previous sections. Therefore, additional effects must be hypothesized to account for the present observations; obviously these effects must be consistent with what is already known of the boiling phenomenon. The qualitative model which follows is offered to explain these additional effects.

Let us consider the phenomena occurring during nucleate boiling since these phenomena must be occurring at or near the critical heat flux as well. The existence of a microlayer of liquid under a vapour bubble, mushroom or jet has been established by Sharp[S1]. Attachment of these vapour masses to the wall occurs only at specific spots, as observed by Gaertner[G5], Kirby and Westwater[K3] and by Westwater and Gaertner[W6] in their electroplating experiments. This microlayer vapourizes continually at the liquid-gas interface by virtue of the heat transfer from the wall across it to the interface. Therefore, liquid must continually move from the periphery of the vapour mass to all parts of the liquid film. The film then is expected to vary in thickness according to the distance from the main liquid source.

At high heat-fluxes (near the maximum), increasing the surface temperature will increase the heat transfer (and vapourization) by virtue of the increased driving force and possibly decreased film thickness. However, increasing amounts of the surface may become dry because the liquid flow rate may not be great enough to provide the necessary liquid to cover the surface with a microlayer of liquid. Therefore any change in the system which will affect the flow of liquid over the surface is expected to affect the heat flux, especially the critical heat flux.

Up to the present time, it has been assumed that the hydrodynamic instability which develops between the upward vapour and downward liquid flow has caused the liquid to be separated from parts of the surface for short periods of time. This in turn has led to decreased liquid coverage of the surface and hence decreased heat flux. Although such a stability problem may exist, the present results indicate that other phenomena may be controlling the critical heat flux or microlayer coverage of the surface. These effects must be associated with all phenomena that may be affected by surfactants.

By their very nature, surfactants will accumulate at the interfaces. An additional concentrating effect will occur in the liquid microlayer under the vapour masses since the more volatile solvent (water) is continually being evaporated from this film. A higher concentration of surfactant leads to a lower surface tension in these regions. The surface tension

gradient that will result from the concentration differences will cause flow of liquid from the regions of higher surface tension to the regions of lower surface tension (Marangoni effect). The temperature gradients existing in these regions will magnify these effects. In addition, the shear forces arising out of the vapour movement will cause liquid to flow into or out of the microlayer. This complicated liquid flow coupled with the vapourization of solvent will determine the concentration of surfactant at every point in the microlayer. The concentration of the surfactant in the bulk of the solution will also play an obvious role. The concentration of solute is expected to be much greater in the film than in the bulk.

This increased concentration in the microlayer will affect both the surface and transport properties in that region. As a result, the liquid should wet the surface much more readily and spread more easily over the surface. Figure 5.23 indicates that the adhesive energy does not seem to be changed appreciably. But Figure 5.22 shows that spreading changes considerably. This greater spreading ability should act to increase the critical heat flux since there should be a greater driving force to cause the liquid to spread over the surface. On the other hand, the higher concentration of surfactant should increase the viscosity of the thin liquid film and decrease its thermal conductivity. The increased viscosity will mean a higher resistance to liquid flow and therefore act to reduce the extent of the microlayer coverage. Decreased thermal conductivity will cause less heat

transfer across the liquid film (less vapourization) for any given temperature and film thickness.

This model serves to explain the present experimental results as well as those of others. In the present case, a small quantity of a given surfactant serves to increase the wettability of the surface but does not offer a large increase in resistance to heat transfer. At higher concentrations, the much higher concentration at the interface offers a large resistance to heat transfer and hence causes the decrease in heat flux.

Although the general trend of the critical heat flux with increasing concentration is the same for the different surfactants, the magnitude of the effects is different for each. For example, the wetting characteristics of Aerosol OT and Pluronic L-62 are extremely high and of about the same magnitude yet the critical heat flux and general behaviour in the nucleate boiling regime is quite different. Since the molecular weight of these materials is very different (Pluronics high and Aerosols low), the viscosity of the concentrated thin film is expected to be higher for the F-68. Furthermore, the diffusion and bulk transfer of F-68 from this film is expected to be less.

These effects serve to explain the observations of others as well. Dunskus and Westwater observed an increase in the critical heat flux of isopropanol with the addition of various Igepals. They found that the higher the molecular weight of the additive the greater the heat flux. Since the thermal conductivity of these organic materials will not be very much different, the

change from one material to the next may be determined mainly by the wetting properties of these materials. It would be of interest to know whether the higher molecular weight Igepals rendered the surfaces more easily wettable without creating a highly viscous solution.

(b) Nucleate Boiling

The above discussion concerning wetting and the additional resistance to heat transfer is applicable to the entire nucleate boiling regime. In addition, visual and photographic observations in section 5.6 indicate that the vapour dynamics are affected considerably by the addition of surfactants, solutions of each surfactant having a unique behaviour.

The best manifestation of this behaviour is the variation of the heat transfer coefficient over the entire regime for the various solutions. Since the heat fluxes are nearly the same, large changes in heat transfer coefficients indicate a substantial shift in the boiling curve either to lower or higher temperature differences.

In agreement with the increased resistance hypothesis, the heat transfer coefficient is observed to decrease with increased concentration of surfactant in every case. Figure 6.3 shows the effect of concentration on heat transfer coefficient. The Aerosol OT solutions indicate large heat transfer coefficients; this is consistent with the observed behaviour with this solution. Why Aerosol OT should produce such high boiling fluxes at low temperature differences is not known except that it may be

speculated that it may be due to its low molecular weight and high wetting resulting in a comparatively high spreading and thermal conductivity and low film thickness and surface viscosity. In the case of L-62, which exhibits very low coefficients, the accumulation of a relatively thick, oily film on the surface may be offering a fairly large resistance to heat transfer.

For the liquid film boiling, the observations are essentially the same (Figure 6.4) except that of Pluronic F-68. No explanation can be offered for this behaviour of Pluronic F-68.

(c) Transition Boiling Regime

Aerosol OT and Pluronic L-62 solutions show higher negative slopes in the transition boiling regime. These are very good wetting agents. In addition, for the few runs which were observed, the minimum heat flux seems to be higher than that for pure water. In this case the hydrodynamics must be playing a part, but wetting also seems to have considerable influence.

One of the interesting observations was the "dry-patch" formation on the meter near the point where film boiling begins (Figures 5.16 to 5.20). This phenomena develops because of the lower temperature on the heat flux meter and the fact that the heat flux increases with reduced temperature. In this way the liquid on the meter evaporates very quickly and since very little liquid exists on the plate around it, a dry-patch results for a short period of time. With no liquid on the meter, the temperature increases quickly and soon the outside temperature (boiling still occurring there) is lower than the central one.

This accounts for the negative readings on the Visicorder. It also suggests that the dry-wall phenomenon can be a very local one.

(d) Film Boiling

Although the present study was primarily interested in and geared to the above two boiling regimes, some observations were possible in the film boiling regime. In line with the observation of others (H3), the minimum heat flux was observed to be greater than that of water thus indicating a greater stability of the vapour layer next to the heat transfer surface. This increased flux is not predicted from existing hydrodynamic stability analyses although dynamic effects may be clouding the picture. Berenson's[B10] suggestion that the only effect of surfactants is to make the surfaces more wettable and therefore behave more uniformly does not seem to be borne out in the experiments reported here. Certainly visual observation would suggest quite dramatic changes in the dynamics of vapour masses.

6.4 Effect of Concentration

(a) Pool Boiling

Figures 5.6 to 5.9 and 6.1 show that the maximum heat flux increases considerably over that for pure water for all surfactant solutions when the concentration is less than 0.1% (by weight). As the concentration is increased the maximum heat transfer rate decreases although this decrease is smaller for the Aerosol solutions. Pluronic L-62 shows a substantial decrease; Aerosol OS and Pluronic F-68 indicate a drop at in-

termediate concentrations (0.1 to 1.0%).

The concentration levels were not decreased to the point where the critical heat flux started to decrease and approach that of pure water. This may occur only at extremely low concentrations. Some indication of this is suggested by the boiling curve observations with distilled water over surfaces contaminated with Aerosol OT and Pluronic L-62 (clean-up runs). These data are shown on Figure 5.10 and indicate a 50% increase in the normal heat flux for pure water. Since both of these materials are very good wetting agents, the increase must be attributed in part to this property.

(b) Liquid-Film Boiling

Similar effects were observed here (Fig. 5.12 to 5.14 and 6.3) as in the pool boiling case in that the critical heat flux was greater than that for pure water only at low concentrations of surfactants. At the higher concentrations this flux was less. Furthermore, the relative effect of surfactant addition is less pronounced with the liquid-film boiling. Similar observations were made of the temperature fluctuations. Pluronic F-68 and Aerosol OT exhibit essentially the same behaviour as their concentration is increased. However, L-62 indicates smaller changes with concentration. This variation of heat flux with concentration cannot be explained by the change in surface tension since Aerosol OT and Pluronic L-62 solutions have low surface tensions but the change in critical heat flux is quite different.

6.5 Effect of Solid-Liquid Interface

The interface properties of a boiling system can in general be characterized by using the surface tension and contact angle measurements. Figures 5.22 to 5.24 illustrate the variation of these interfacial properties with surfactant concentration. These variables are more useful in illustrating the effects of spreading wetting.

Figure 6.5 indicates that the maximum heat flux seems to pass through a maximum as the surface tension is lowered by the addition of surfactants. This is the same effect as observed with concentration. The plot of this flux against contact angle will also show this behaviour. The critical heat flux decreases as the wetting of the heat transfer surface gets better. Since Figures 5.23 and 5.24 indicate that the adhesive energy and interfacial tension does not change appreciably, the liquid requires about the same energy to remove it from the surface. In the light of the microlayer mechanism of boiling heat transfer, one would expect that better spreading wetting with the same adhesion would lead to a situation which would favour higher heat fluxes. To explain in more detail: the situation can be visualized where the microlayer is evaporating under the bubbles, mushrooms or jets; attachment of these masses of vapour to the wall occurs only at specific spots (as photographed by Gaertner[G5] and Kirby and Westwater[K3]. This microlayer is being fed continually from thicker liquid films at the periphery. Up to the DNB point more nucleating sites provide for more of

these microlayers and hence the increasing flux. At higher and higher heat fluxes, beyond the DNB point the size of the dry area increases but this is offset by a thinner liquid film, which will allow greater transfer of heat to the upper evaporating interface. This implies a dynamic balance of supply and demand of liquid for vapourization at the bubble base. The imbalance allows a dry wall condition at higher temperature. The decrease in flux in the transition regime arises because of the "dry-wall" condition as the temperature increases. Hence, some consideration must also be given to the solid-liquid interface and the so-called "dry-wall" condition that is going to exist at the vapour attachment points in nucleate boiling and in the transition and film boiling regime. As discussed in section 2.6, for any liquid-solid combination, a polymolecular, residual liquid film will exist on a surface provided the surface temperature is below some given value. This liquid film will determine the surface energy and affect the wetting characteristics of the surface. That such a film exists has been clearly demonstrated by the experiments with contaminated surfaces which are illustrated on Figure 5.10. Without this stable film there would have been no effect of surfactants on the boiling curve. Dernedde[D1] observed similar effects when he studied the boiling of water on a surface which had been wiped with a benzene-soaked cloth at a high temperature ($> 400^{\circ}F.$). Temperature and heat flux fluctuations on the boiling surface noted in section 5.5 seem to indicate qualitatively the thickness, wetting and stability

characteristics of the interfacial film. Surfactant solutions whose residual film is expected to be thicker due to the molecular weight and adhesive wetting, show higher resistances to heat transfer and lower fluctuations. This is evident from the lower fluctuations and higher surface temperatures in pluronics as a contrast to higher fluctuations with Aerosols especially at higher concentrations. Such fluctuations can only be expected from bubble dynamics or microlayer dynamics. Moreover the thickness and properties of the microlayer of these various solutions is expected to be different and this will lead to different resistances to heat transfer and flow of liquid. How these film thicknesses and properties are related to the measureable properties of the surfactants is unknown.

7. CONCLUSIONS

The addition of small amounts of surfactants can affect the boiling phenomenon significantly. In particular, the vapour dynamics are affected; the critical heat flux is increased at low concentrations and decreased at higher concentrations; and the boiling curve of water is changed dramatically so that the heat transfer coefficient is increased considerably. There is reason to believe that increasing the wetting characteristics of a liquid on a surface causes an increase in heat flux. It is also suggested that the addition of surfactants causes an increase in thickness and viscosity and a decrease in thermal conductivity of the microlayer of liquid which forms over the surface during nucleate boiling. These effects lead to a reduction in the heat flux.

The existing equations to predict the critical heat flux which are based on hydrodynamic stability considerations are inadequate. Similarly those models of the boiling phenomena based on bubble agitation do not account for the surface phenomena adequately.

Different surface active agents cause different effects in boiling. There is no simple way of predicting the performance of a given surfactant from its measurable properties. Even a thin interfacial film of a surfactant solution indicates considerable and dramatic changes in the boiling curve. Different thickness and properties of microlayer, resulting from different

surfactant solutions (even during "dry-wall" conditions) is expected to be the cause of these different effects in boiling.

The heat flux meters which have been developed during this series of investigations are excellent devices to study the boiling heat transfer. These are quite convenient to investigate the effect of additives on the boiling process. Some refinements are still necessary to allow more accurate quantitative data and to withstand the rigours of high temperature operation.

8. RECOMMENDATIONS

The studies on the boiling heat transfer of water and surfactant solutions lead to some interesting results, regarding the concentration of surfactants, solid-liquid interface, boiling phenomenon and operation of boiler and heat flux meters. These lead to the following ideas for future experimental studies and modifications in the apparatus.

(a) The most interesting experimental study would be the effect of surface active agents at very low concentration; with a view to find the maximum of concentration versus maximum heat flux curve. The study of Aerosols should be of primary interest.

(b) Thin interfacial films of surfactant solutions (with measured thickness) would be of considerable interest in the pool and liquid film-flow boiling. These films may be characterized initially, by measuring surface viscosity and contact angle.

(c) High speed photographic studies of nucleation sites and bubbles on the heat flux meter area should contribute significantly to the use of heat flux meter for better quantitative measurements. High speed photographic studies with surfactant solutions coupled with fine wire thermocouples should contribute significantly to the understanding of bubble and microlayer dynamics.

(d) Present studies were mostly confined to changing the interfacial behaviour by surfactant solutions. It should be of great interest to study boiling heat transfer of surfactant

solutions with different boiling surfaces having varying nucleating characteristics. It would also be of interest to use films of varying volatility characteristics.

(e) It would be of interest to extend the present studies to subcooled pool and film boiling studies.

(f) The calibration of heat flux meters during the entire heat flux range of pool boiling of water under steady state conditions would improve considerably the quantitative measurements. This would be possible by designing a new boiler surface of a smaller area.

(g) Present studies showed considerable improvement in the heat-flux meter thermocouple sensitivity and resistance to oxidation and stresses in comparison to the earlier studies (D1). But length of service and quantitative measurements still need considerable improvement. Hence, modifications in the fine wire thermocouple joint with the parent metal by soldering under reducing atmosphere at low pressure followed by high temperature test and calibration should improve the quantitative measurements and length of service of heat flux meters.

(h) Thick disc meters used in the present studies (0.030 in. thick) seem to be adequate for subcooled and saturated film flow boiling studies. However, for saturated film flow boiling studies, 0.020 in. thick heat flux meters would give better quantitative measurements.

BIBLIOGRAPHY

A1 Andreas, J. M., et al., Fifteenth Colloid Symposium, Cambridge, Massachusetts, P. 1001, June (1938).

A2 Anick, E., and Davidson, L., Amer. Inst. Chem. Engrs. J.,2, P. 336, (1956).

A3 Averin, E. K., Izv. Akad. Nauk. SSSR, dd. Teckhn Nauk, No. 3, P. 116, (1954).

A4 Ibid, Int. Dev. Heat Transfer, ASME, D-84, August, (1961).

A5 Adams, J. M., NSFG -19697, Univ. of Washington, Seattle, (1962).

A6 Adams, N. K., "The Physics and Chemistry of Surfaces", Oxford University Press, London, (1944).

B1 Berg, J. C., and Acrivos, A., Chem. Engg. Sci., 20, P. 737, (1965).

B2 Bikerman, J. J., Surface Chemistry for Industrial Research, Academic Press, New York, (1948).

B3 Baker, H. E., et. al., Temperature Measurement in Engineering Volume 1, John Wiley & Sons, Inc., New York, (1963).

B4 Bankoff, S. G., and Mehra, V. S., Ind. Engg. Chem., Fundamentals, 1, P. 38, (1962).

B5 Berenson, P., Sc. D. Thesis, Mech. Engg. Dept., Mass. Inst. Tech., Cambridge, Mass., (1960).

B6 Bergles, A. E., Ph.D. Thesis, Mech. Engg. Dept., Mass. Inst. Tech., Cambridge, Mass., (1962).

B7 Bell, S. H., J. Oil Colour Chem. Assn., 35, P. 373, (1952).

B8 Benjamin, T. B., Arch. Mech.Stos., 16, 615,(1964).

B9 Bankoff, S. G., and Mason J. P., Amer. Inst. Chem. Engrs. J., 8, P. 30, (1962).

B10 Berenson, P. J., Int. J. Heat and Mass Transfer, 5, P. 985, (1962).

B11 Borshianskii, V. M., Zuhrn. Teckh. Fiz., Vol. 26, P. 452, (1956).

B12 Bromeley, L. A., and Motte, E. I., Ind. Engg. Chem., 49, P. 1921, (1957).

B13 Bennett, J. A. R., et al., Trans. Inst. Chem. Engg., London, 39, P. 113, (1961).

B14 Bernath, L., Chem. Engg. Prog. Symp. Series., 56, P. 95, (1959).

B15 Bonilla, C. F., Grady, J. J. and Avery, G. W., Chem. Engg. Prog. Symp. Series, 57, 61, P. 280, (1965).

B16 Bonilla, C. F., and Perry, C. W., Trans. Am. Inst. Chem. Engrs., 37, P. 685, (1941).

B17 Berenson, P. J., and Stone, R. A., Chem. Eng. Prog. Symp. Series, 57, 61, P. 214, (1965).

B18 Benard, H., Ann. Chem. Phys., (7), 23, P. 62, (1901).

C1 Costello, C. P., and Adams, J. M., Amer. Inst. Chem. Engrs. J., 9, 5, P. 663, (1963).

C2 Colver, C. P., M.S. Thesis, University of Kansas, Lawrence, Kansas, (1958).

C3 Chen, J. C., 63-HT-24, ASME- AIChE Heat Transfer Conf., Mass., August, (1963).

C4 Clark, J. A., and Rohsenow, W. M., Trans. ASME 73, P. 609, (1951).

C5 Corty, C., and Foust, A., Chem. Engg. Prog. Symp. Series, 17, 51, P. 1, (1955).

C6 Costello, C. P. et al., Chem. Engg. Prog. Symp. Series, 59, 61, P. 27, (1965).

C7 Chandrasekhar, S., "Hydrodynamic and Hydromagnetic Stability", Oxford Press, London, (1961).

C8 Cess, R. D., and Sparrow, E. M., J. Heat Transfer, 83, P. 337, (1901).

C9 Collier, J. G., et al., Trans. Inst. Chem. Engrs., London, 42, P. 127, (1964).

C10 Collier, J. G., Nuclear Power, 6, P. 61, June (1964).

C11 Chang, Y. P., ASME Paper No. 61-Hyd-182, (1961).

C12 Chang, Y. P., J. Heat Transfer, P. 89, May, (1963).

C13 Costello, C. P., Discussions in C12 by Y. P. Chang, J. Heat Transfer, P. 89, May, (1963).

C14 Carne, M., and Charlesworth, D. H., Chem. Engg. Prog. Symp. Series, 64, 62, P. 24, (1965).

C15 Costello, C. P., Discussions, Int. Dev. in Heat Transfer D-73, ASME, Boulder, Colorado, August, (1961).

C16 Carne, M., and Charlesworth, D. H., Chem. Engg. Prog. Symp. Series, 59, 61, 281, (1965).

C17 Costello, C. P., and Frea, W. J., Chem. Engg. Prog. Symp. Series, 57, 61, P. 258, (1965).

D1 Dernedde, E., Master's Thesis, McMaster University, Hamilton, Ontario, (1966).

D2 Deryagin, B. V., Research in Surface Forces, Consultants Bureau, New York, P. 8, (1966).

D3 Donald, M. B., and Haslam, F., Chem. Engg. Sci., 8, p. 287, (1958).

D4 Dergarbedian, P., Journal of Appd. Mech., 20, P. 537 (1953).

D5 Dunskus, T., and Westwater, J. W., Chem. Engg. Symp. Series, Buffalo, 32, 57, P. 173, (1961).

D6 Dukler, A. E., Ph.D. Thesis, University of Delaware, Delaware, (1951).

D7 Diessler, R. G., Heat Transfer Symp., Columbia University, New York, (1954).

E1 Ellion, M., JPL memo 20-88, Pasadena, California, March, (1954).

E2 Edwards, D. K., M.S. Thesis, Univ. of California, Los Angeles, (1956).

F1 Fuks, G. I., Research in Surface Forces, Consultant Bureau, New York, P. 79, (1966).

F2 Fritz, W., Physik Zeitschrift, Vol. 36, P. 379, (1935).

F3 Fritz, W., and Ende, W., Physik Zeitschrift, Vol. 37, P. 391 (1936).

F4 Fischer Scientific Co., Don Mills, Ontario, Private Communication, Dec. (1966).

F5 Freundlich, H., Kapillar Chemie, 1, P. 65, (1909).

F6 Fulford, G. D., Advances in Chem. Engg., Academic Press, New York, 5, P. 151, (1964).

F7 Forster, N. K., and Zuber, N., Conference on Nuclear Engg., U.C.L.A., Los Angeles, April, (1955).

F8 Forster, K. E., Grief, R., ASME Paper, 58-HT-11, (1958).

G1 Gaertner, R. F., Journal Heat Transfer, P. 17, February (1965).

G2 Gaertner, R. F., General Electric Research Lab. report, No. 63-RL-3449C, September, (1963).

G3 Grey, V. R., Chemistry and Industry, 968, June, (1965).

G4 Gardon, R., Review of Sci. Insts., 24, 5, P. 366, May (1953).

G5 Gaertner, R. F., Chem. Engg. Prog. Symp. Series, 41, 59, P. 52 (1963) and G. E. report 63-RL-3357C, Schenectady, New York, Dec. (1963).

G6 Griffith, P., and Wallis, J. D., ASME-AICh.E. Heat Transfer Conf. August, (1959).

G7 Gunther, F. C., and Kreith, F., Progress Report, 4-120, Jet Propulsion Lab., Pasadena, California, (1950).

G8 Gunther, F. C., Trans. ASME, 73, 2, P. 115, (1951).

G9 Gibbs, J. W., Collected Works, Vol. 1, Yale University Press, New Haven, P. 219, (1948).

G10 Gaertner, R. F., Paper presented at ASME Symposium, on two Phase flow, Philadelphia, (1963).

H1 Harrison, W. B., and Levine, Z., Paper 57-HT-29, AICh.E., (1957)

H2 Hendrix, C. D., M.S. Thesis, University of Tennessee, Knoxville, Tenn., (1960).

H3 Hosler, E. R., and Westwater, J. W., ARS Journal, 32, P. 553 (1962).

H4 Hsu, Y. Y., and Graham, R. W., NASA, TND-594, (1961).

H5 Hansen, W. D., Ind. Engg. Chem., P. 38, March and P. 18, April, (1965).

H6 Hoffman, T. W., Private Communication from Dernedde, E., regarding Heat Flux Meter Analysis, Sept. (1966).

H7 Hartley, D. E., and Murgatroyd, W., Nuclear Engg. Lab. Memo, Q-5, Queen Mary College, Univ. of London, Sept. (1961).

H8 Hewitt, G. F., and Lacey, P. M. C., Int. J. Heat and Mass Transfer, 8, P. 781, (1965).

H9 Hsu, Y. Y., et al., Chem. Engg. Prog. Symp. Series, Sept.,(1963)

I1 Ivey, H. J., and D. J. Morris, AEEW-R-176, (1962).

J1 Jakob, M., "Heat Transfer", Vol. I, P. 633, John Wiley & Sons, Inc., New York, (1958).

J2 Jakob, M., and Fritz, W., Physik. Zeitschrift, Vol. 36, P. 651, (1935).

J3 Jontz, J. D., and Myers, J. E., Amer. Inst. Chem. Engrs. J. 6, 1, P. 34, (1960).

K1 Kinzie, P. A., and Sosa, E. N., Review of Scientific Instruments 37, No. 5, P. 599, May, (1966).

K2 Kirk, R. E., and Othmer, D. F., Encyclopedia of Chemical Technology, Vol. 13, P. 513, Interscience Encyclopedia, Inc., New York, (1954).

K3 Kirby, D. B., and Westwater, J. W., Chem. Engrg. Prog. Symp. Series, 57, 61, P. 238, (1965).

K4 Kintner, R. C., et al., Can. J. Chem. Engg., 39, P. 235, Dec., (1961).

K5 Kutateladze, S. S., et al., Int. Chem. Engg., 5, P. 474, (1965).

K6 Kurihara, H. M., and Myers, J. E., Amer. Inst. Chem. Engr. J., 6, 1, P. 83, (1960).

K7 Kurihara, H. M., Ph.D. Thesis, Purdue University, Lafayette, Indiana, (1956).

K8 Knuth, E. L., Memo No., 20-85, Jet Propulsion Lab., Cal. Inst. Tech., Pasadena, California, (1953).

K9 Kinney, G. L., et al., Nat'l. Advisory Committee, Rept. 1087, (1952).

L1 Lozhkin, A. N.,Izraelit, I.G., J. Tech. Physics, (U.S.S.R.) 9, 2174, (1939).

L2 Langmuir, I., J. Amer. Chem. Soc., 59, P. 2405, (1937).

L3 Leinhard, J. H., Schrock, V. E., J. Heat Transfer, 85, P. 261, (1963).

L4 Leppert, G., et al., Trans. ASME., P. 1395, Oct., (1958).

L5 Langmuir, I., and Langmuir, D. B., J. Phys. Chem., 31, P. 1719, (1927).

L6 Lowrey, A. J., and Westwater, J. W., Ind. Engg. Chem., 49, P. 1445, (1957).

M1 Moore, F. J., and Mesler, R. B., Amer. Inst. Chem. Engrs. J., 7, 4, P. 620, (1961).

M2 Mixon, F. O. Jr., et al., Chem. Engg. Prog. Symp. Series, 56, 30, P. 75, (1960).

M3 Myers, J. E., and Roll, J. B., Amer. Inst. Chem. Engrs. J., 10, 4, P. 530, (1964).

M4 Moissis, P., and Berenson, P. J., J. Heat Transfer, P. 221, August, (1963).

M5 McEligot, D. M., Discussions, Int. Dev. in heat transfer, Conference, Boulder, Colarado, ASME, D-78, (1961).

M6 Mesler, R. B., et al., Amer. Inst. Chem. Engrs. J., 12, 2, P. 211, (1966).

N1 Nishikawa, K., Trans. Soc. Mech. Engrs., Japan, 20, P. 808, (1954).

N2 Norman, W. S., and McIntyre, V., Trans. Inst. Chem. Engrs., London, 38, P. 301, (1960).

O1 Osipow, "Surface Chemistry, Theory and Industrial Applications", Reinhold Publishing Corporation, New York, (1962).

O2 Ostrach, S., and Koestel, A., Amer. Inst. Chem. Engrs. J., 11, P. 294, (1965).

O3 Ostrach, S., and Koestel, A., Chem. Engg. Prog. Symp. Series, Boston, August, (1963).

P1 Paddy, J. F., "Third International Congress of Surface Activity", Cologne, Vol. I, P. 223, Academic Press, New York, (1960).

P2 Plesset, M. S., and Zwick, S. A., J. App. Phys., 25, P. 493, (1954).

P3 Pearson, J. R. A., J. Fluid Mech., 4, P. 489, (1958).

R1 Rideal, E. K., and Davies, J. T., "Interfacial Phenomenon", Academic Press, New York, 1961.

R2 Rohsenow, W. M., and Choi, A. Y., "Heat, Mass and Momentum Transfer", Englewood Cliffs, N. J., Prentice-Hall, Inc., (1961).

R3 Rohsenow, W. M., "Developments in Heat Transfer", M.I.T. Press, Cambridge, Mass., P. 174, (1964).

R4 Rohsenow, W. M., and Griffith, P., AIChE. and ASME. Heat Trans. Symp., Louisville, Ky., March, (1955).

R5 Roll, J. B., Ph.D. Thesis, Purdue Univ., Lafayette, Ind., (1962).

R6 Rohsenow, W. M., et al., Discussions on paper by Zuber, N., ASME. Trans., P. 716, April, (1958).

S1 Sharp, R. R., NASA TN D-1997, October, (1964).

S2 Scherbakov, L. M., "Research on Surface Forces", Consultants Bureau, New York, P. 19, (1966).

S3 Stock, B. J., Report ANL-6175, Argonne Nat'l Lab., Reactor Engg. Divn., June, (1960).

S4 Stucke, B., Chemie-Ingenieur-Technik, 33, P. 173, (1961).

S5 Stoicopolus, D. N., J. Colloid Science 17, P. 439, (1962).

S6 Sabersky, R. H., Ch. on "Survey of Problems in Boiling Heat Transfer in "Turbulent Flows and Heat Transfer" by Lin, C. C., P. 313, Princeton, (1959).

S7 Snyder, N. R., and Edwards, D. K., Memo 20-137, Jet Propulsion Lab., June, (1956).

S8 Sharp, R. R., and Hendricks, R. C., NASA TN D-2290, April (1964).

S9 Staub, F. W., and Zuber, N., AEC report, GEAP 4367, (1963).

T1 Treschev, G. C., A. A. Armand, ed., Grozenergoizdat, Moscow, Russia, (1959).

T2 Tong, L. S., "Boiling Heat Transfer and Two Phase Flow", John Wiley & Sons, Inc., New York, P. 35, (1965)

T3 Tippets, F. E., J. Heat Transfer, 86, P. 23, (1964).

V1 Varley, C., Trans. Soc. Arts. Manufacturers Commerce, 50, 190, (1836).

W1 Westwater, J. W., "Advances in Chem. Engg.", Vol. I, Academic Press, New York, (1956).

W2 Whitaker, S., Ind. Engg. Chem., Fundamentals, 3, P. 132, (1964).

W3 Whitaker, S., and Jones, L. O., Amer. Inst. Chem. Engrs. J., 12, 3, P. 421, (1966).

W4 Wenzel, R. N., Ind. Engg. Chem., 28, P. 988, (1936).

W5 Wyandotte Chemicals, Private Communication and Bulletin from Dept. 297, Wyandotte, Michigan, (1961).

W6 Westwater, J. W., and Gaertner, R. F., Chem. Engg. Prog. Symp. Series, 30, 66, P. 39, (1960).

W7 Westwater, J. W., Buehl, W. M., Amer. Inst. Chem. Engrs. J., 12, 3, P. 571, (1966).

W8 Westwater, J. W., Petro./Chem. Engr., 33, 9, P. 40, (1961) and 33, 10, P. 53, (1961).

Y1 Yamagata, K., et al., Memoirs of Faculty of Engg., Kyushu Univ., Japan, Vol. 15, (1955).

Y2 Young, R. K., Hummel, R. L., Chem. Engg. Prog., 60, P. 53, (1964).

Z1 Zisman, W. A., and Fox, H. W., J. Phys. Chem., 7, P. 431, (1952).

Z2 Zuber, N., Appd. Mech. Rev., 17, 9, P. 663, (1964).

Z3 Zuber, N., Int. J. Heat and Mass Transfer, 2, P. 83, (1961).

Z4 Zuber, N., ASME. Trans., P. 710, April, (1958).

Z5 Zuber, N., J. Heat and Mass Transfer, 6, P. 53, (1963).

Z6 Zuber, N., and Tribus, M., AEC Report, AECU 3631, (1958).

Z7 Zuber, N., Ph.D. Thesis, Univ. of California, Los Angeles, California, (1959).

APPENDIX 1

1. BOILER AND HEAT FLUX METERS

Some of the essential details have already been discussed in Chapters 3 and 4. Here the rest of the description that is necessary to understand the problems in the boiler operation (sec. A-1.1) and heat-flux meters (sec. A-1.2) is considered. The boiler consists essentially of a heavy copper block as the source of heat, into which Kanthal heating strips are imbedded. Power is supplied to these Kanthal strips at a maximum of 30 volts, to generate the heat necessary for boiling. Figure A.1 shows the heater assembly and power connections. Figures A.5, A.4 and 3.1 show the sideview, plan and elevation of the boiler assembly with the copper block and heaters. These are essentially the same as those used earlier by Dernedde[D1]; major modifications were mentioned in section 3.3. The copper block is connected by soft solder to a 1.0" thick copper plate to even out the heat distribution. This copper plate has a $\frac{1}{4}$" thick copper plate inserted into it. The copper plate with $\frac{1}{4}$ in.insert plate is shown in Figure A.2. The top surface of the insert plate is the boiling surface. The insert was used to facilitate the assembly of heat-flux meters.

Figure A.2 also shows the lay-out of the heat-flux meters and surface thermocouples. There are five thick-disc heat-flux meters (0.030 in. thick), two thin-disc heat-flux meters (0.010 in. thick) and eleven surface thermocouples. Assembly and preparation

FIGURE A.1

COPPER BLOCK WITH KANTHAL HEATERS

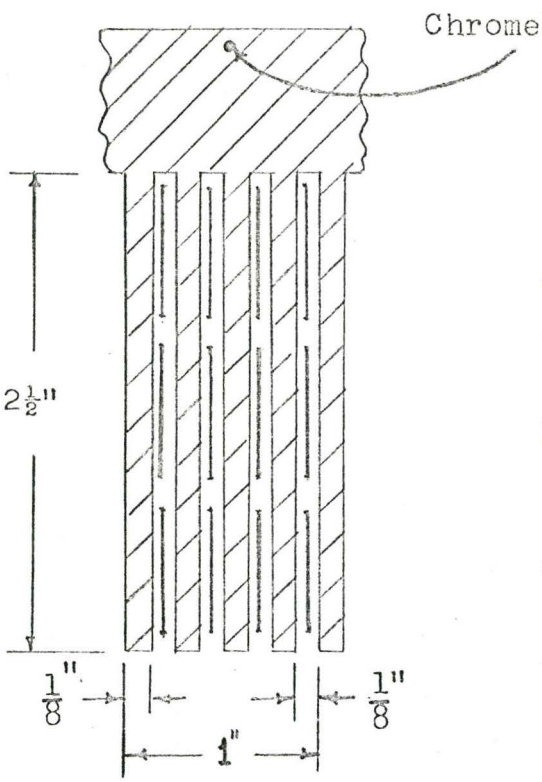

Side View

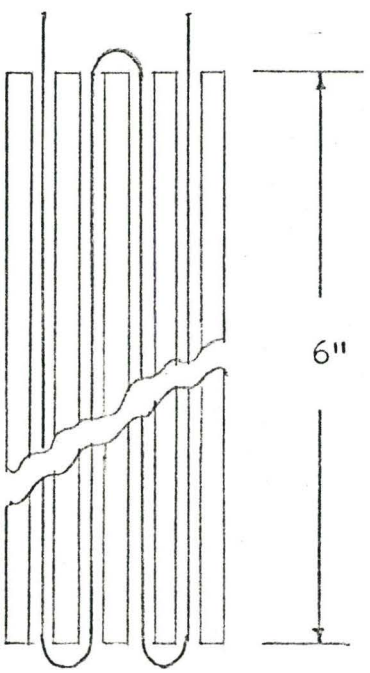

Top View

Kanthal Windings

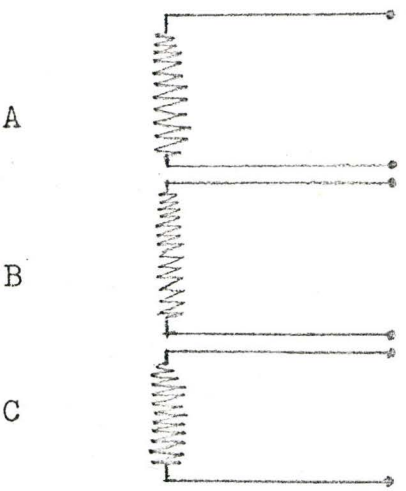

Heater Connections

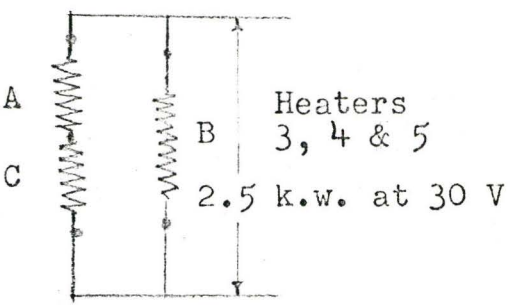

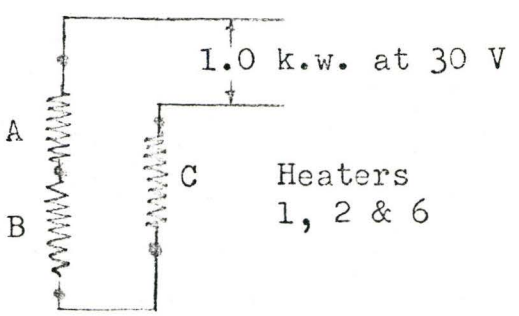

FIGURE A.2

LAY OUT OF HEAT FLUX METERS AND SURFACE THERMOCOUPLES

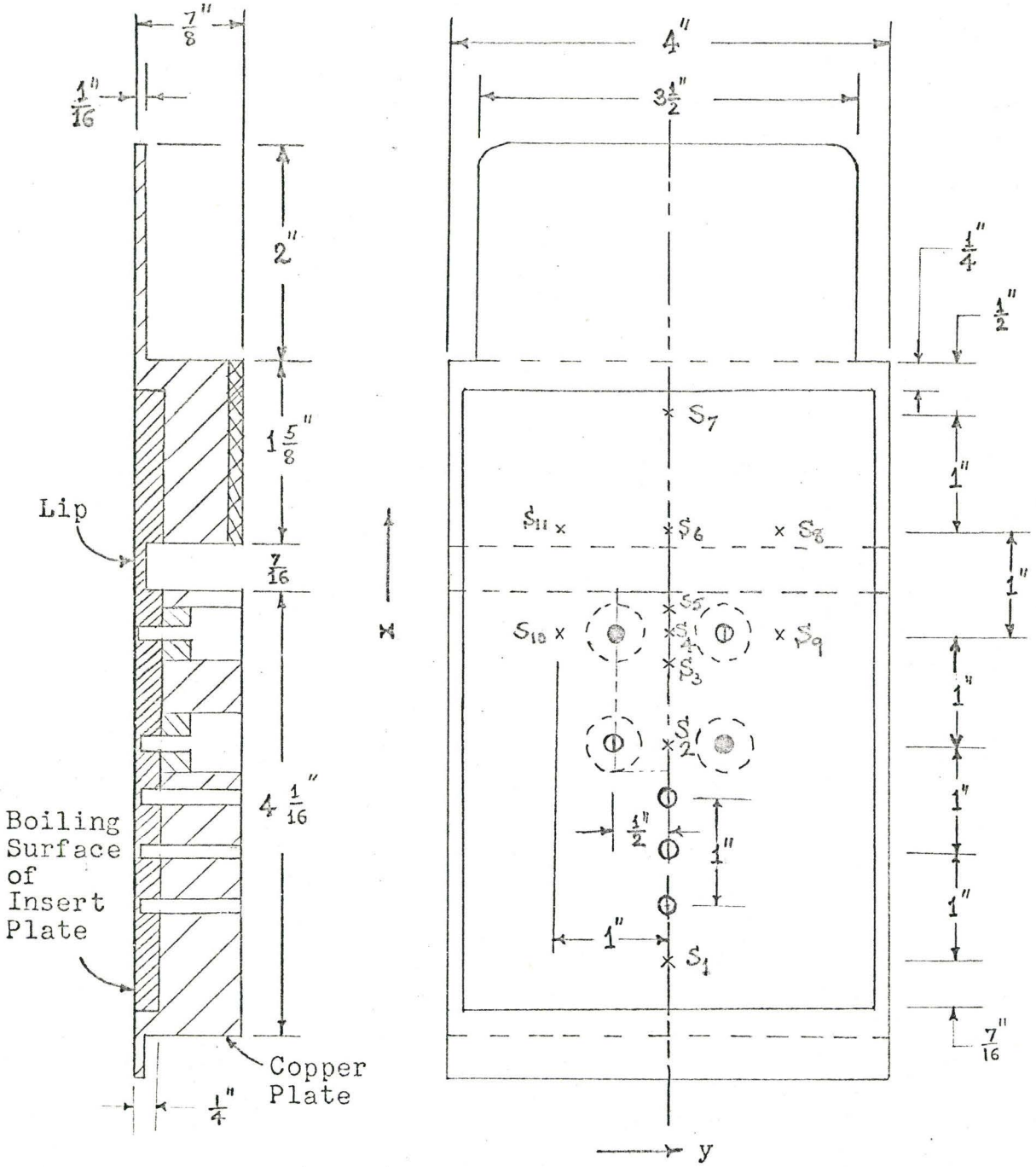

x Surface Thermocouples (S_1 to S_{11})

● 0.156 in. dia. 0.010 in. thick, Heat Flux Meter (Thin Disc)

⊙ 0.156 in. dia. 0.030 in. thick, Heat Flux Meter (Thick Disc)

FIGURE A.3

HEAT FLUX METER AND SURFACE THERMOCOUPLE

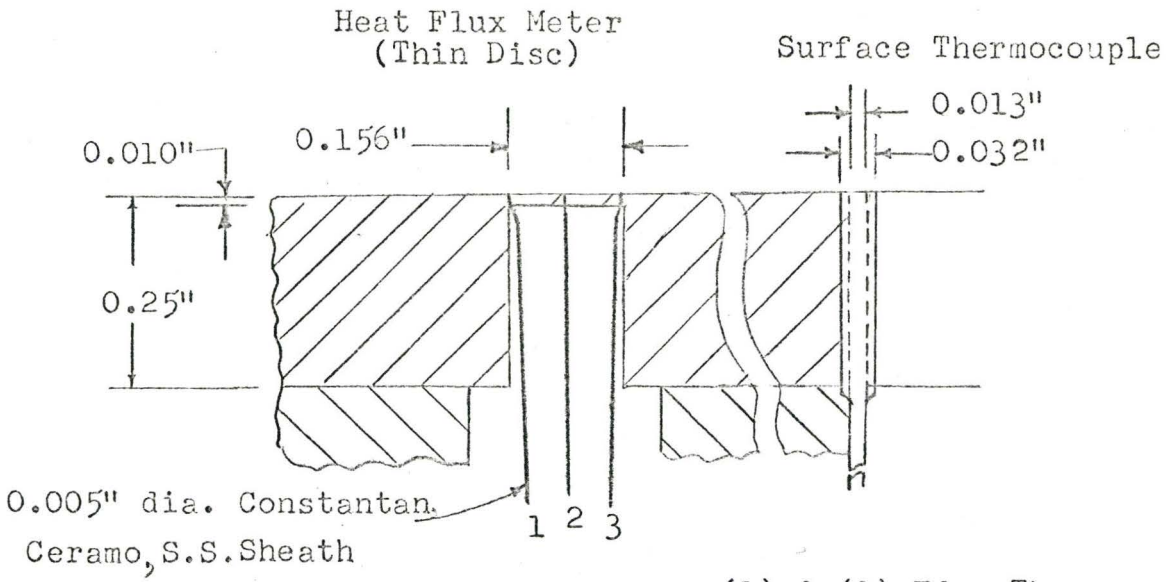

(1) & (3) Edge Thermocouples
(2) Centre Thermocouple

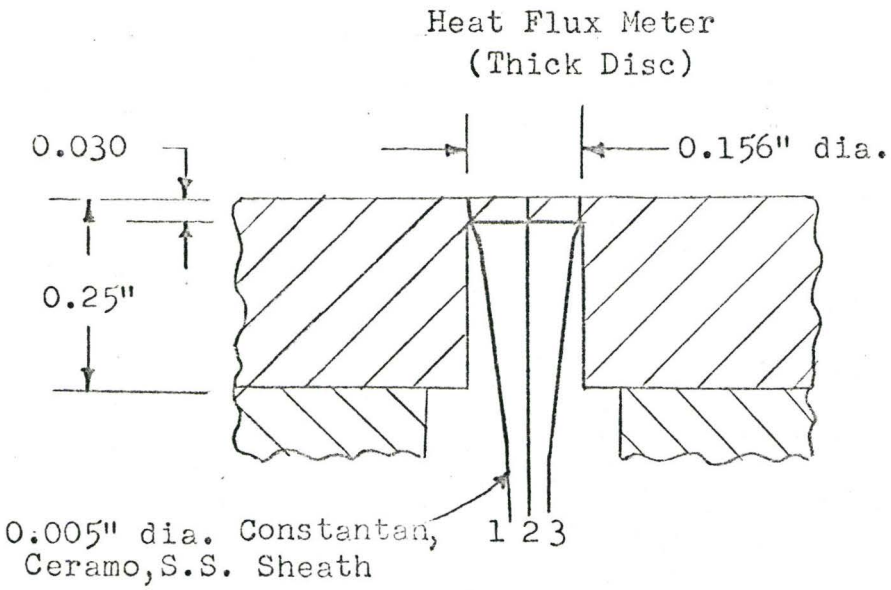

(1) & (3) Edge Thermocouples
(2) Centre Thermocouple

BOILER ASSEMBLY
(PLAN)

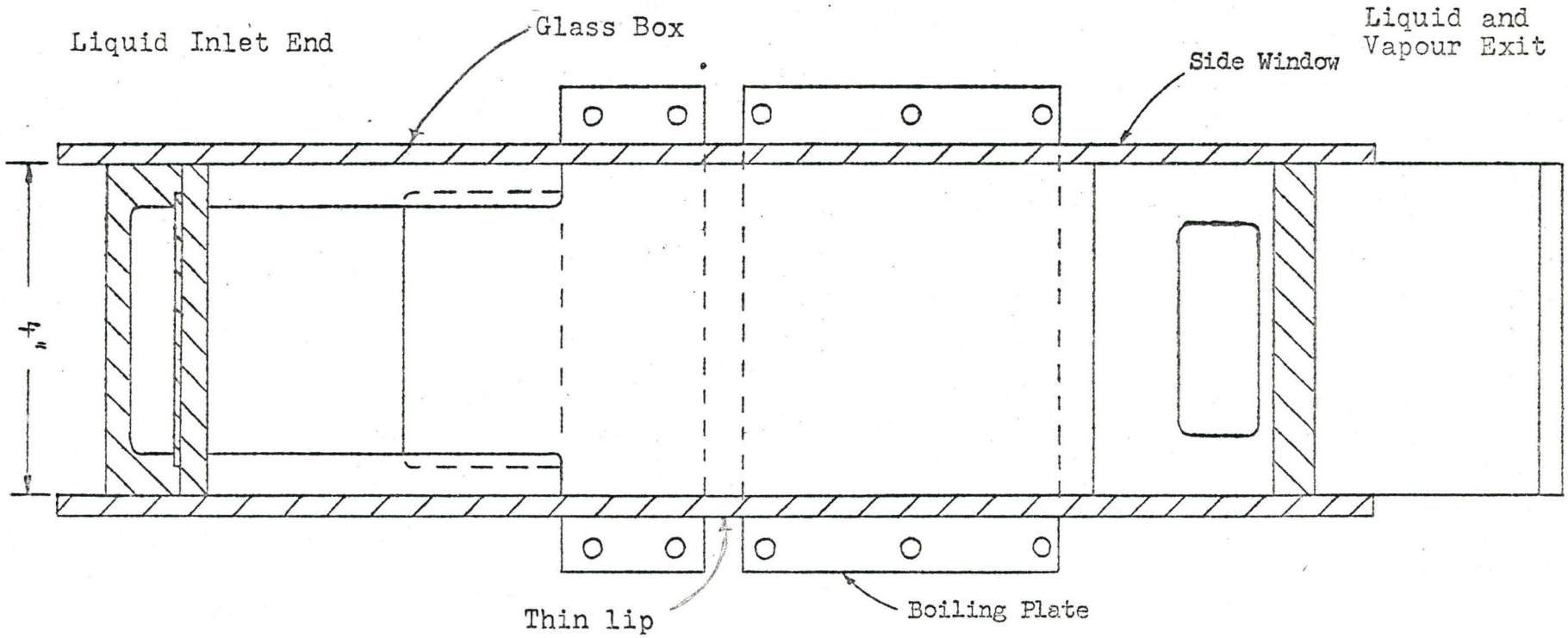

FIGURE A.4

BOILER ASSEMBLY
(END ELEVATION)

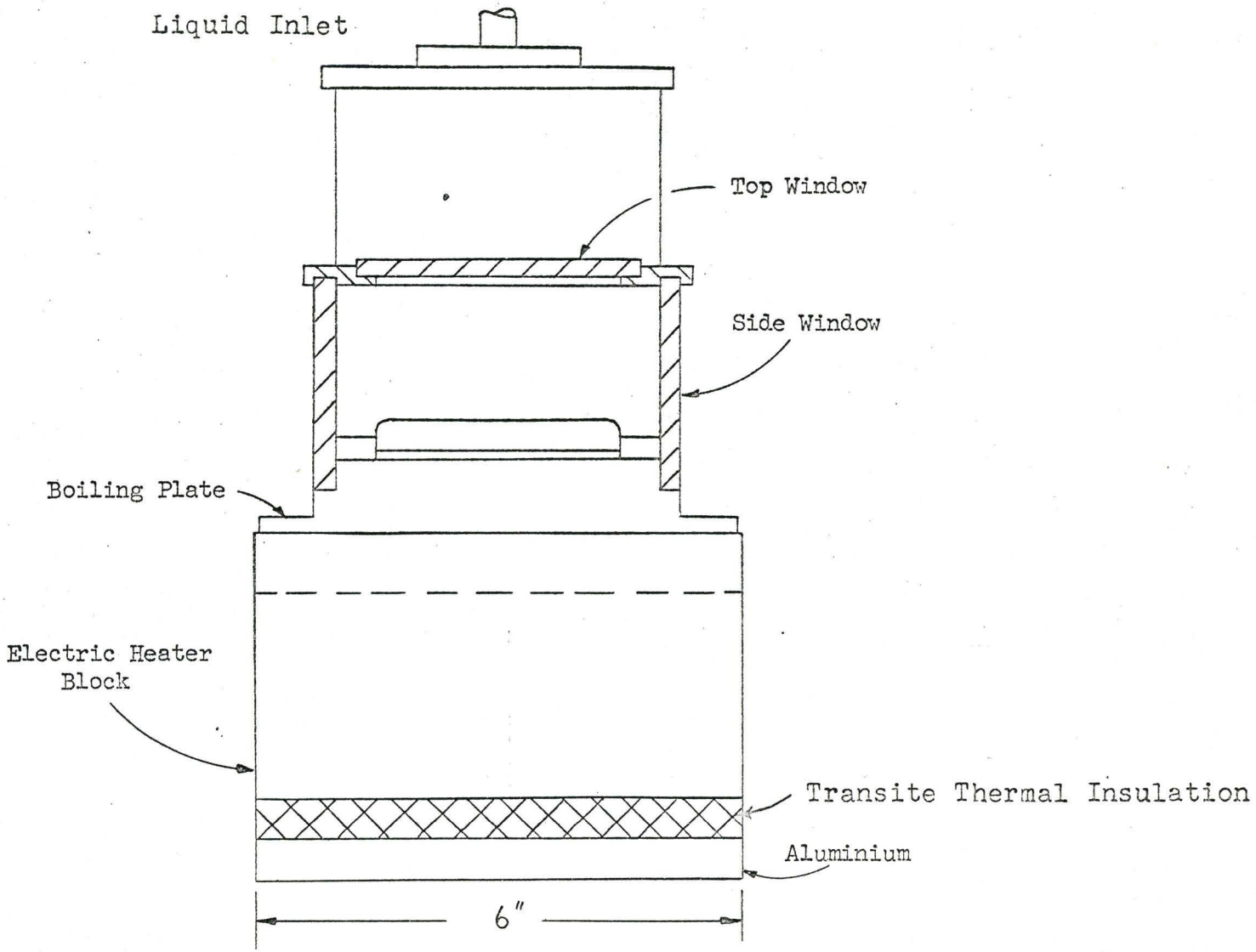

FIGURE A.5

procedure for the heat-flux meters and surface thermocouples are essentially the same as used earlier by Dernedde[D1]. Figure A.3 shows a thick disc and a thin disc heat-flux meter and a surface thermocouple. The thermocouples (insulated and sheathed) pass through convenient channels made in the copper plate and are connected to a junction box, from which they are connected to a visicorder or a Honeywell recorder. Typical connections of heat-flux meters and surface thermocouples are shown in Figure A.6.

1.1 Boiler Operation

Major problems in the operation of boiler was the frequent breakdown in the electrical circuit used for heating (shown in Figure A.1). High contact resistances were developed at the joints connecting the Kanthal strips to copper power leads. These connections needed replacement from time to time. Further this contact resistance caused the heat input to the boiler to be reduced considerably with usage. The Kanthal strips used for heating showed excellent durability and performance. However, some poorly welded contacts got disconnected. There was also very small leakage of current from the Kanthal strips to the copper block through the insulating heat transfer cement. This leakage was eliminated from the boiler system by proper earthing. The operation of the steady-state pool boiling of water in the entire range needs considerably large power input than what can be provided at present.

1.2 Heat Flux Meter Operation

Heat Flux meter is an essential tool for these boiling

FIGURE A.6

INSTRUMENT CONNECTIONS FOR THERMOCOUPLES

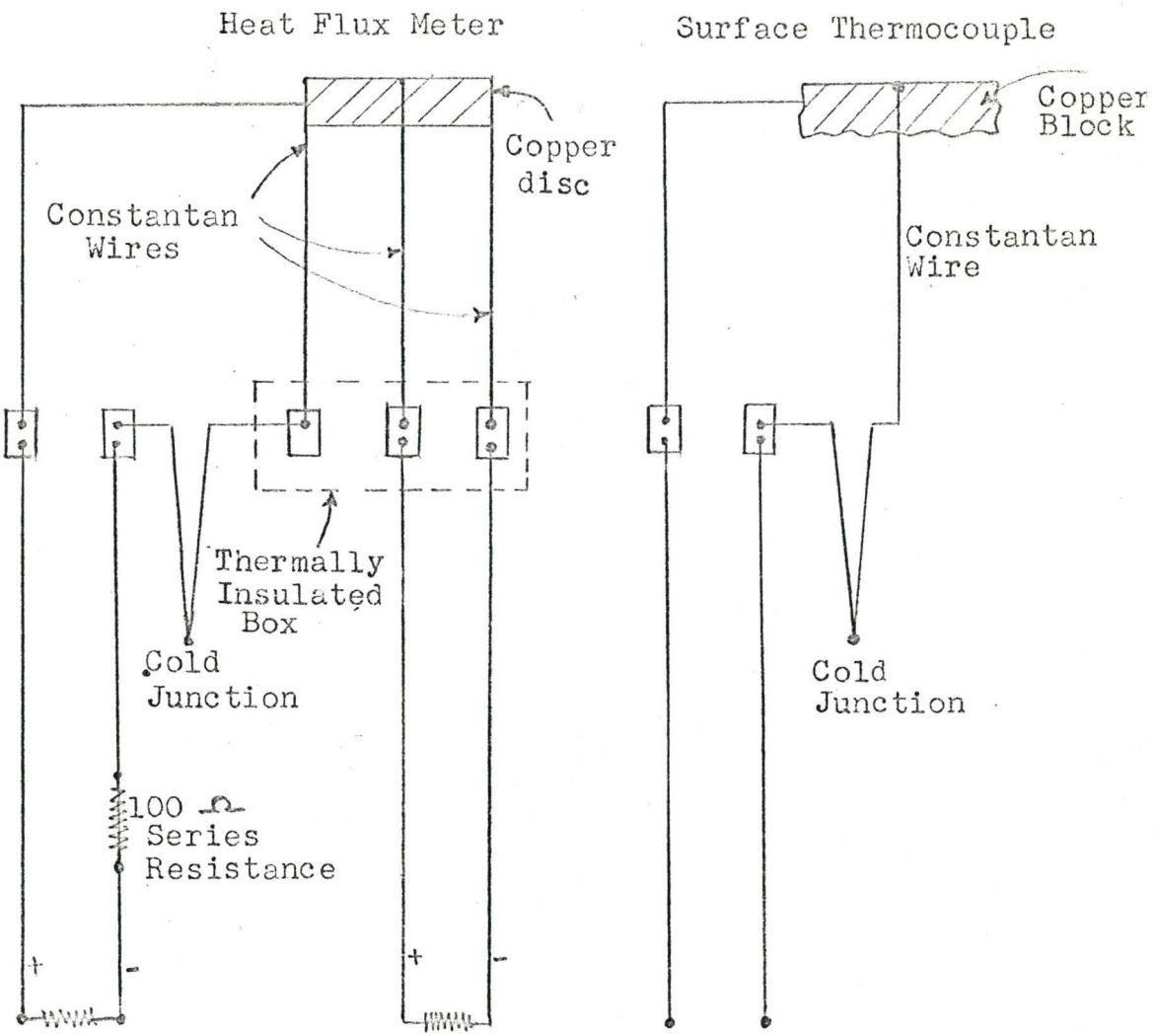

heat transfer studies. Essentially the same procedure used successfully by Dernedde[D1] in his measurement of boiling heat flux of thin liquid films was followed, for measurement of heat fluxes. The temperature of the boiling surface was measured by a separate edge thermocouple. The present analysis of the problems associated with the use of the heat-flux meter is a continuation of the magnitude of error analysis and problems considered earlier by Dernedde[D1]. Problems associated with the measurement of heat flux and temperature are several. Of them only a few are significant. These can in general be considered by the following theoretical and experimental considerations:

(a) temperature distribution

(b) thermocouples

(c) visicorder

(d) surface characteristics.

(a) Temperature distribution

(i) Theoretical Study - The temperature distribution in three dimensions in a cylindrical disc of the heat-flux meter (Figure A.7) is given by:

$$\frac{\partial^2 T'}{\partial r^2} \quad \frac{1}{r} \quad \frac{\partial T'}{\partial r} \quad \left(\frac{R_o}{t}\right)^2 \quad \frac{\partial^2 T'}{\partial z^2} \quad \frac{\partial T'}{\partial \theta} \qquad \ldots(A1)$$

where T = temperature at any point (r', z')

$r = r'/R_o$

$z = z'/t$

$\theta = \alpha\, \theta'/R_o^2$

Considering the heat flux meter as shown in Figure A.7 the following boundary conditions apply to equation (A1), for a constant heat flux over the entire heat flux meter area.

$$r = 0, \frac{dT}{dr} = 0, \quad \text{radial symmetrical temperature distribution} \qquad \ldots(A2)$$

$$z = 0 \quad \frac{dT}{dz} = 0, \quad \text{no heat loss from the underside of the disc} \qquad \ldots(A3)$$

$$z = 1, \quad \frac{dT}{dz} = \frac{(Q/A)\ t}{K}, \quad \text{uniform heat flux away from the disc} \qquad \ldots(A4)$$

where $T = T' - T_w$

Assuming a constant edge temperature (T_w), $T = 0$, at $r = 1$ steady and unsteady analysis of the temperature distribution at the center of heat-flux meter was carried out by Dernedde[D1]. He concluded from his analysis that the average temperature at the center of the disc coupled with the two-dimensional analysis of Gardon[G4] with the same boundary conditions agree with the heat flux predicted by three-dimensional analysis. The equation resulting from the two-dimensional equation is given as

$$\frac{Q}{A} = \frac{4\ K_o\ t}{R_o^2} \quad (T_w - T_c) \quad \left[1 + \frac{\alpha}{2} \left(\Delta T_w + \Delta T_c \right)\right] \qquad \ldots(A5)$$

where $K = K_o(1 + \alpha . \Delta T)$ is the thermal conductivity of the material of

the heat flux meter disc and t is the thickness of the disc. Substituting for temperature difference in terms of thermocouple E.M.F. ($E = \beta T + \gamma T^2$), equation (A5) can be written as

$$\frac{Q}{A} = \frac{4 K_o t}{R_o^2} \cdot \frac{\Delta E}{C} \qquad \ldots(A6)$$

where C is the heat flux meter constant given by

$$C = \frac{(\beta + 2 \gamma \Delta T_w)}{(1 + \alpha \Delta T_w)} \qquad \ldots(A7)$$

$\alpha = -0.00005$, $\beta = 0.0212$ and $\gamma = 0.137 \times 10^{-4}$ if ΔT_w is the temperature difference between wall and reference junction in ^oF. The equation (A6) has been used in determining the heat flux from the voltage output recorded by the visicorder. Variation of C with temperature indicated by the edge thermocouple (T_w) is shown in Figure A.7a

The analysis of Gardon[G4] and Dernedde[D1] discussed earlier however assumes two boundary conditions that may not be met in practice, namely the heat flux is constant over the entire heat-flux meter area and that the edge temperature is constant along the thickness of the heat-flux meter. Recently Hoffman and Dernedde[H6] considered the effect of the temperature gradient that must exist at the edge of heat flux meter. Dernedde solved equation (A1) using finite-difference methods and the three boundary conditions mentioned earlier. There seems to be considerable

FIGURE A.7

HEAT FLUX METER ANALYSIS

Two Dimensional Analysis

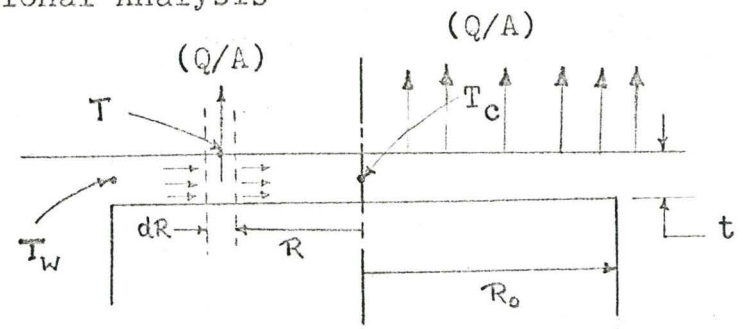

Equation (A5); (Q/A) = Constant, for all R

Equation (A8); $(Q/A) = \text{Constant} \times (\Delta T)^n$

Three Dimensional Analysis

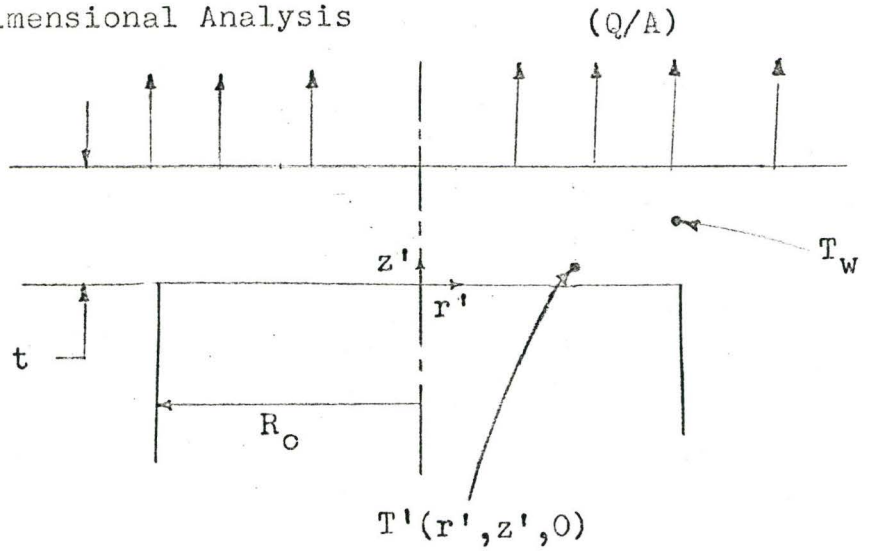

Equation (A1); T_w and Q/A are constants (Ref. D1)

Steady State and (Q/A) Constant (Ref. H6)

FIGURE A.7a

HEAT FLUX METER CONSTANT

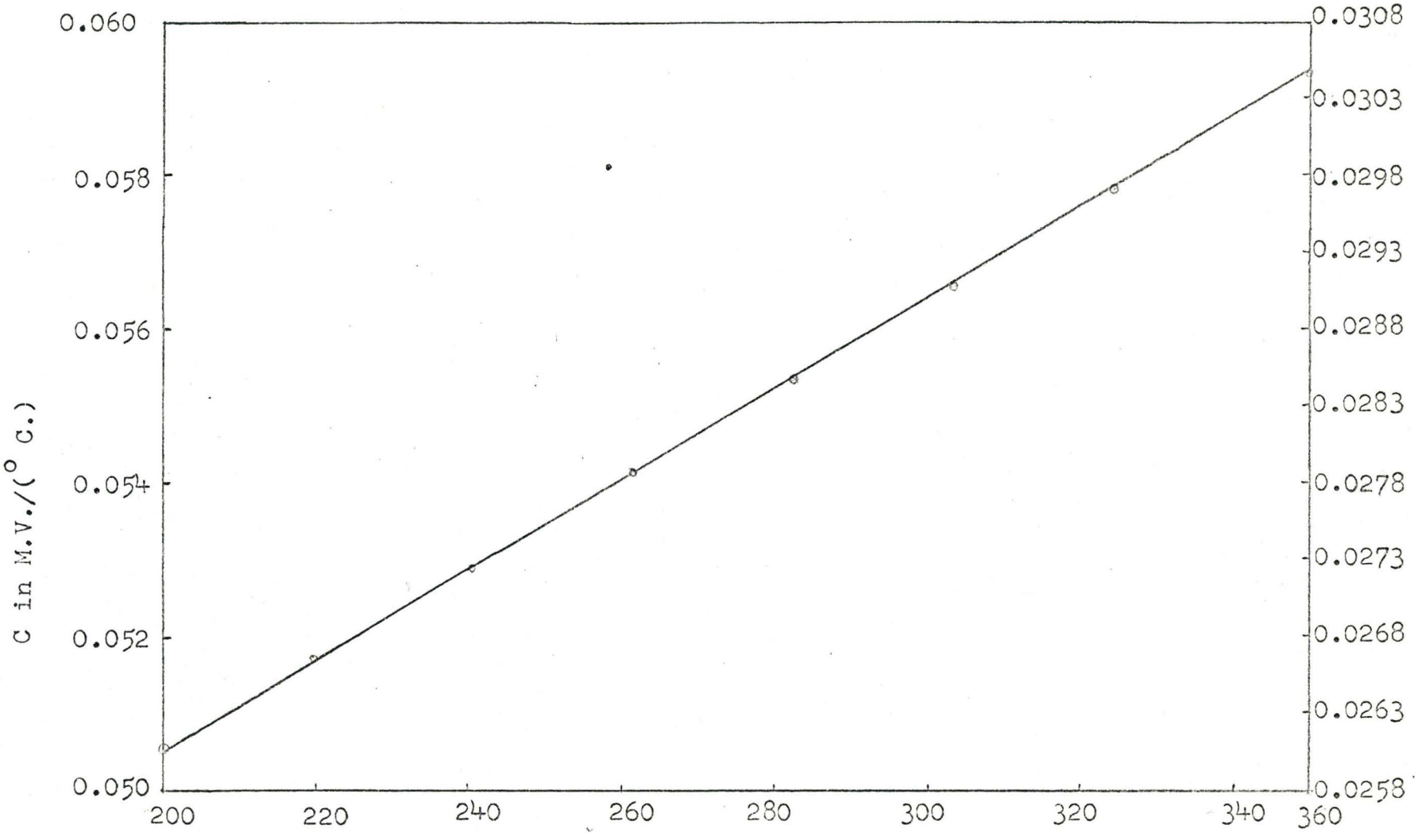

gradient especially at high heat fluxes and typical results of the order of magnitude error in heat flux measurement is given in Figure A.8. Because of this increased edge temperature the measured heat flux should be higher. This agrees well with the observations of higher heat fluxes corresponding to literature pool boiling curves shown in Figure 5.2.

The following analysis assumes that heat flux at any point on the heat flux meter, varies with the temperature according to the relationship given by the boiling curve. The effect of surface characteristics and temperature distribution associated with boiling is essentially a two dimensional problem. Two dimensional heat conduction equations at the boiling surface for varying heat flux can be written from Figure (A.7) as

$$\frac{d2T}{dR^2} + \frac{1}{R} \cdot \frac{dT}{dR} - \frac{(Q/A)}{(K_o.t)} = 0 \qquad \ldots(A8)$$

Assuming radial symmetry the following boundary conditions can be written;

$$\text{At} \quad R = R_o \quad T = T_w \qquad \ldots(A9)$$

$$\text{At} \quad R = 0 \quad \frac{dT}{dR} = 0 \qquad \ldots(A10)$$

Here it is very important to note that since the heat flux meter is used to measure the boiling on the entire area, the edge temperature is considered as the basis.

Equation (A8) is a second-order differential equation with

FIGURE A.8

HEAT FLUX METER ANALYSIS

(Temperature Difference Variation Along The Thickness)

(Ref. H6)

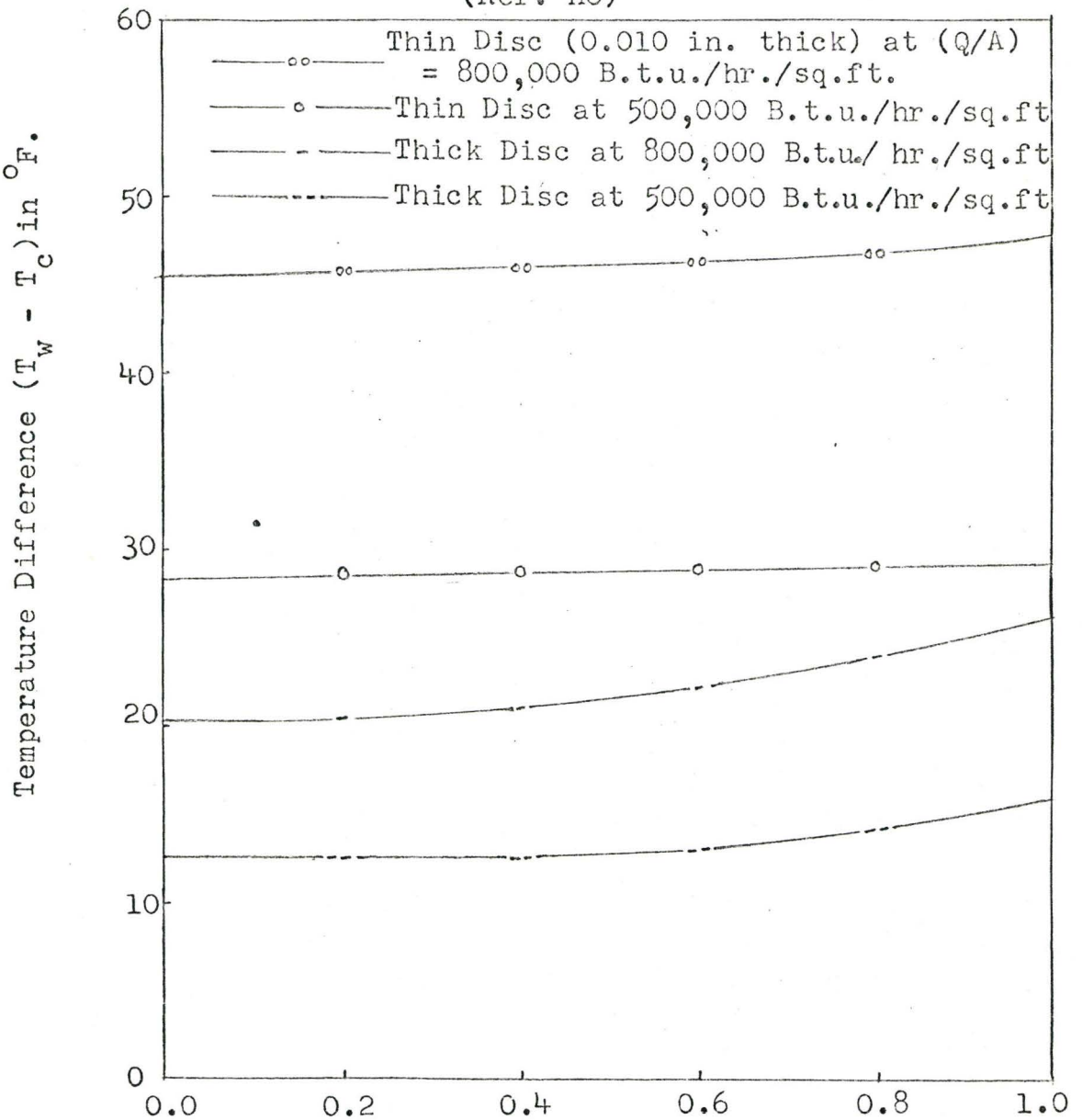

a term having (Q/A) which varies as T^n where n is the slope of the boiling curve. This equation was solved using a MIMIC program on a IBM 7040 digital computer.* The results were obtained for various temperatures at the edge of heat flux meter (252°F. to 292°F.) and are given in Figures A.9 and A.10. We find a considerable variation of heat flux predicted by this analysis in comparison to that predicted by equation (A5) for copper-water system having boiling curve characteristics shown in Figure 5.2 in the nucleate boiling region around critical heat flux. It can be seen from Figures A.9 and A.10 that the temperatures predicted by equation (A5) were lower than those predicted by the solution of equation (A8). If visicorder were to measure according to the temperature distribution given by equation (A8), then the heat flux predicted using the Gardon's equation (A6) should be lower than the actual heat fluxes. Contrary to this expectation in the region of critical heat flux, it was observed that the heat fluxes calculated using Gordon's equation (A5) and visicorder data for pool boiling of water are higher than those predicted in literature, (Figure 5.2).

(ii) Experimental Studies - Temperature distribution along the length (x) and breadth (y) of the boiling surface during steady-state pool boiling and natural-convection heat transfer to air have been plotted in Figures A.11 and A.12.

The temperature distribution of the boiling surface seems to differ considerably during boiling and natural-convection studies

* MIMIC is an executive routine which allows a differential equation to be set up as an analog problem on a digital computer. Integrations are by fourth-order Runge-Kutta integration.

FIGURE A.9

ANALYSIS OF HEAT FLUX METER

(Thin Disc)

(Radial Temperature and Heat Flux)

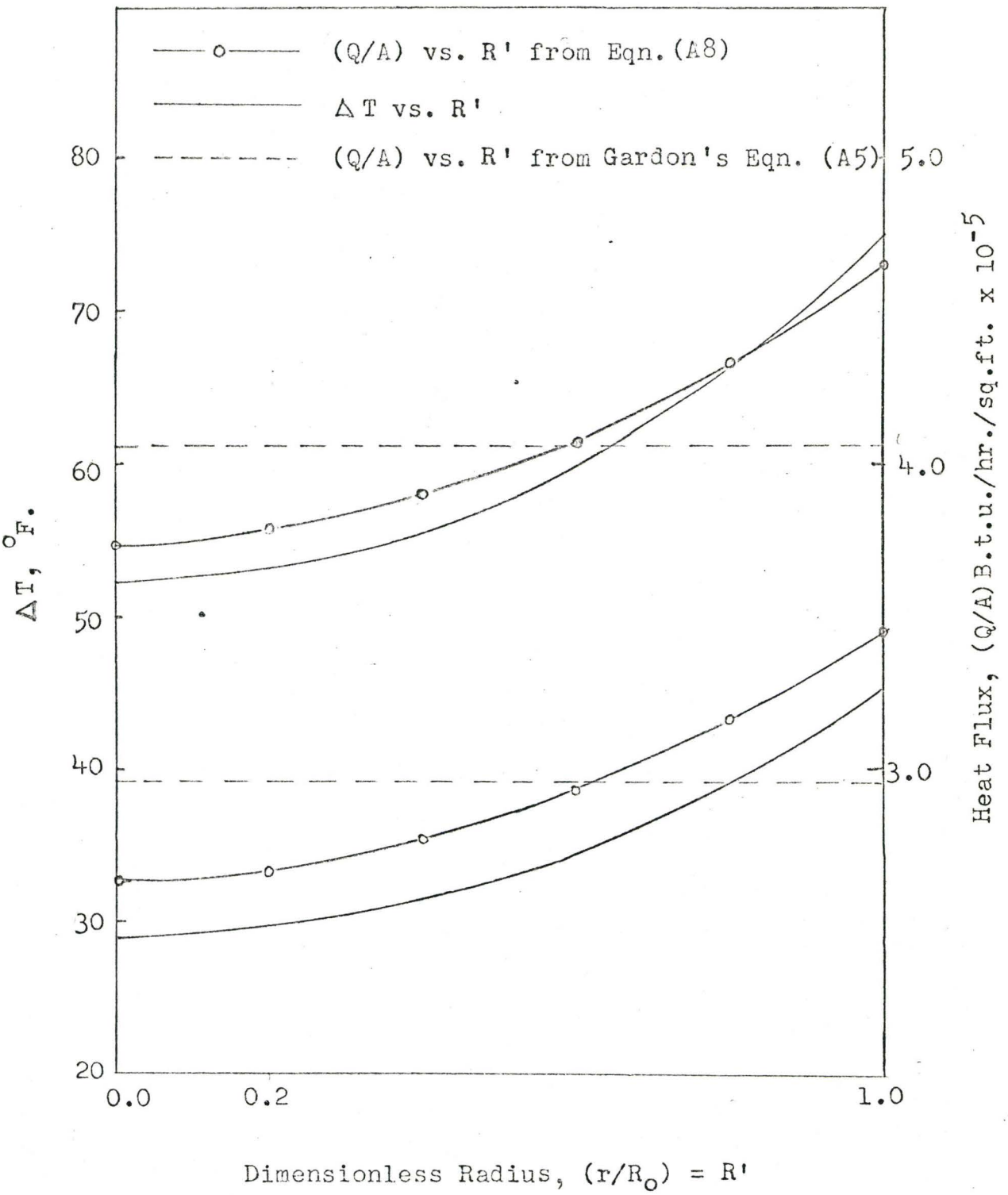

FIGURE A.10

ANALYSIS OF HEAT FLUX METER

(Thick Disc)

(Radial Temperature and Heat Flux)

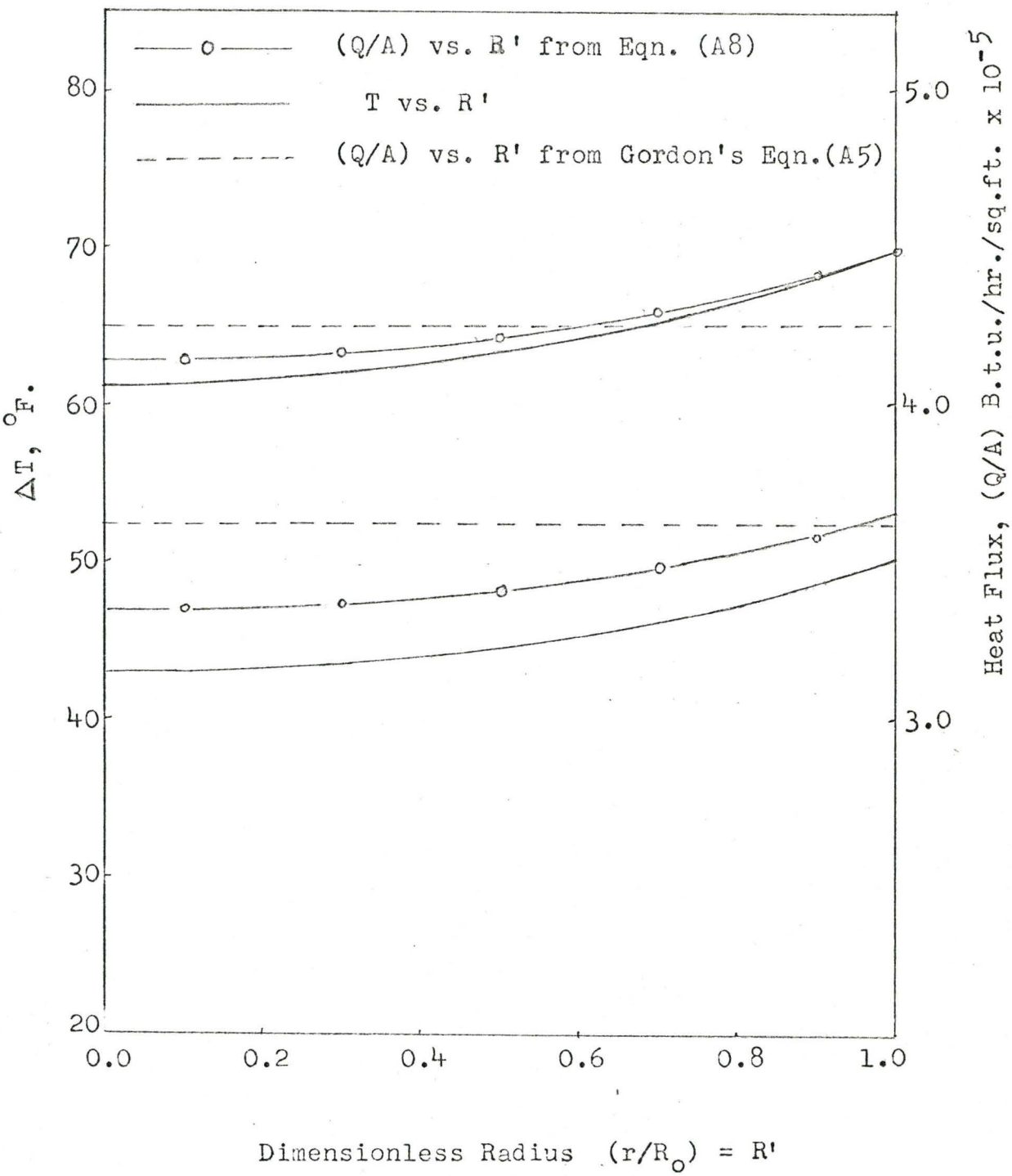

at the same reference temperature. The lower temperatures observed during boiling may be due to the preferential nucleation at the tip of some thermocouples or contact resistances at the junctions. The former can be expected mostly at the surface thermocouples, while the latter with the heat flux meter thermocouples. The magnitude of error in surface and heat flux meter thermocouples can be obtained from Figures A.11 to A.14. The heat-flux meter thermocouples were calibrated with respect to the nearest surface thermocouples S_2 and S_4 and are shown in Figure A.14.

The temperature distribution varies with the duration of operation of the boiler, and heating and cooling (Figure A.13). The effect of duration of operation may be due to oxide formation at the joint of boiler plate and copper block. The effect of heating and cooling can be expected to be due to contact resistances in the thermocouples.

(b) Thermocouples

Thermocouple errors are usually associated with:

(i) inhomogenity of the wires

(ii) parasitic voltages

(iii) high resistance to heat transfer at the junction

(iv) conduction of heat via the leads

It is impracticable and usually too small to make any sort of corrections for inhomogenity (B3). Parasitic voltages may appear due to dissimilar junctions at variable temperatures. Dissimilar junctions were avoided and thermally insulated junction boxes were used to make this effect negligibly small.

FIGURE A.11

TEMPERATURE DISTRIBUTION AT THE AXIS OF THE BOILING PLATE

(Steady State Pool Boiling)

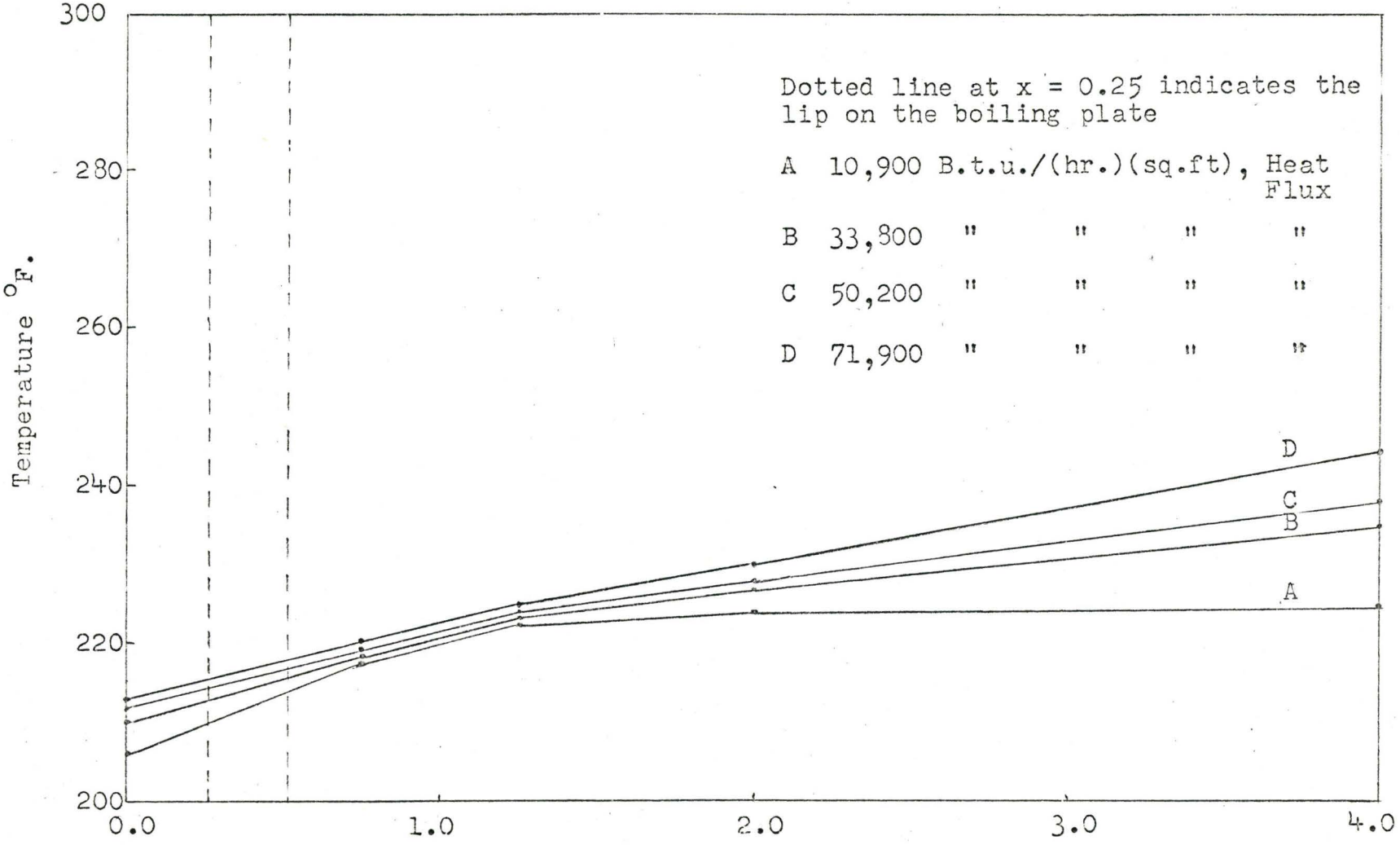

FIGURE A.12

TEMPERATURE DISTRIBUTION ALONG

THE BREADTH OF BOILING SURFACE

(Steady State Pool Boiling of Water)

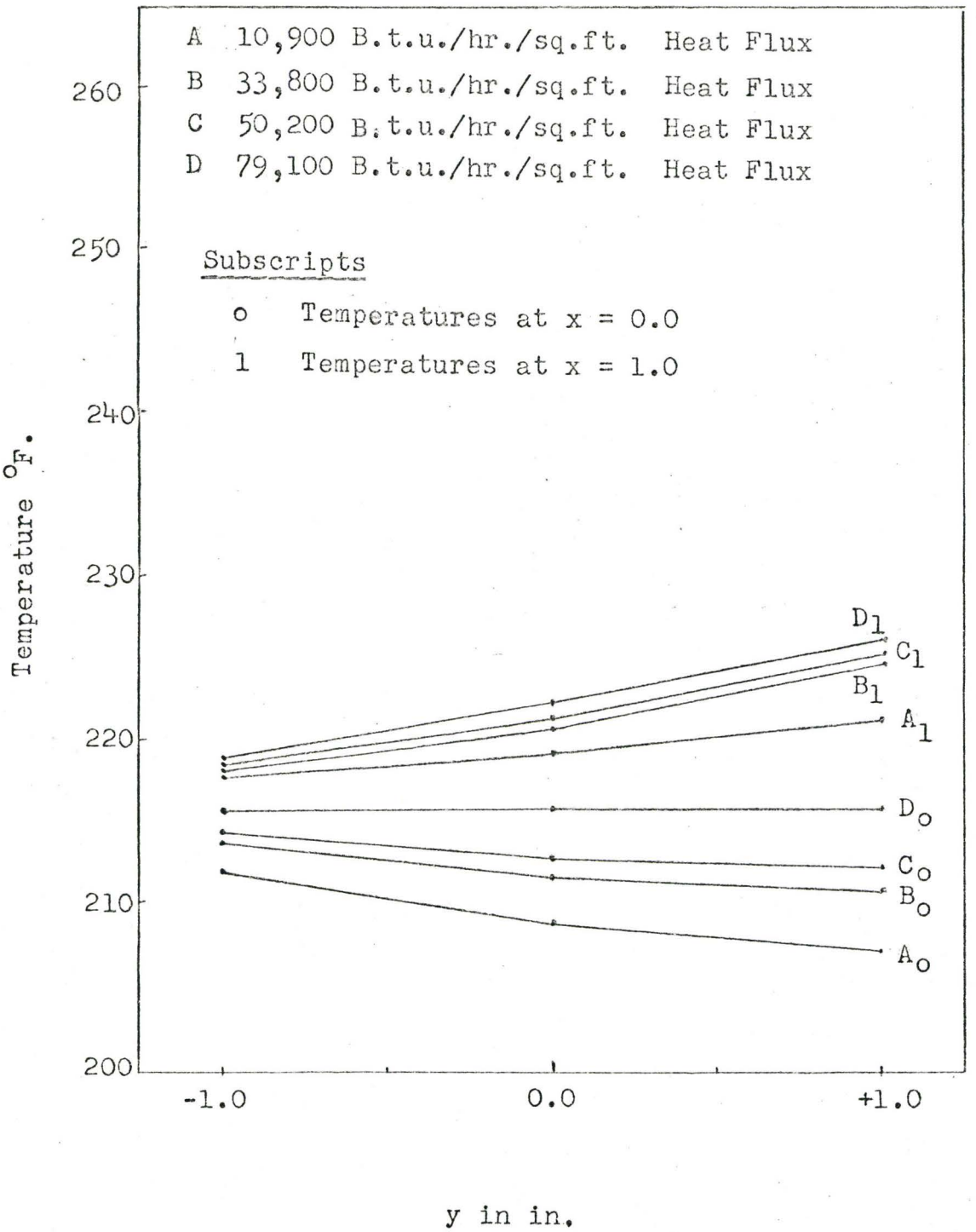

FIGURE A.13

TEMPERATURE DISTRIBUTION

(Effect of Cooling, Heating and Period)

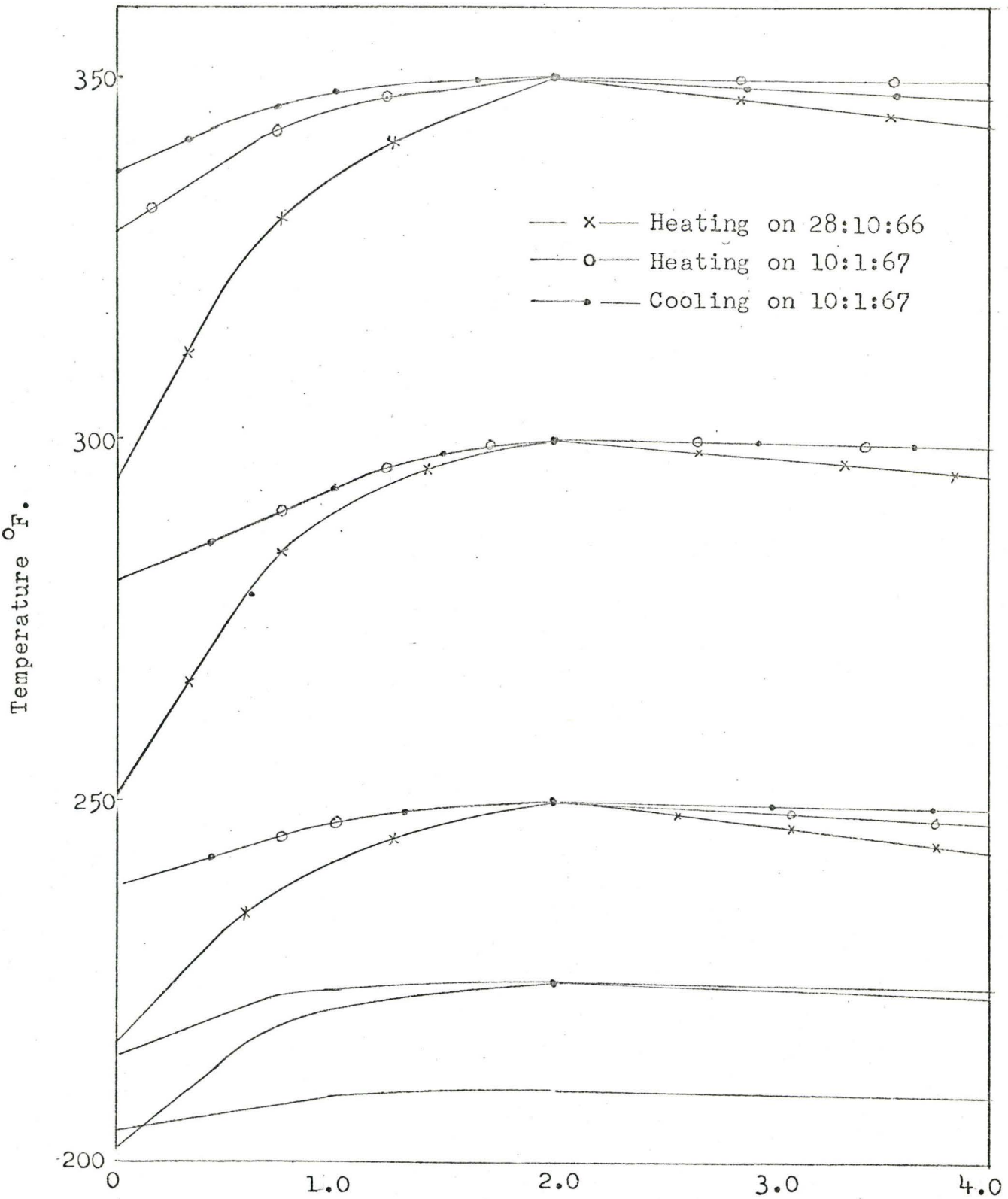

FIGURE A.14

CALIBRATION OF HEAT FLUX METER THERMOCOUPLES

(Cooling of Copper Block in Air)

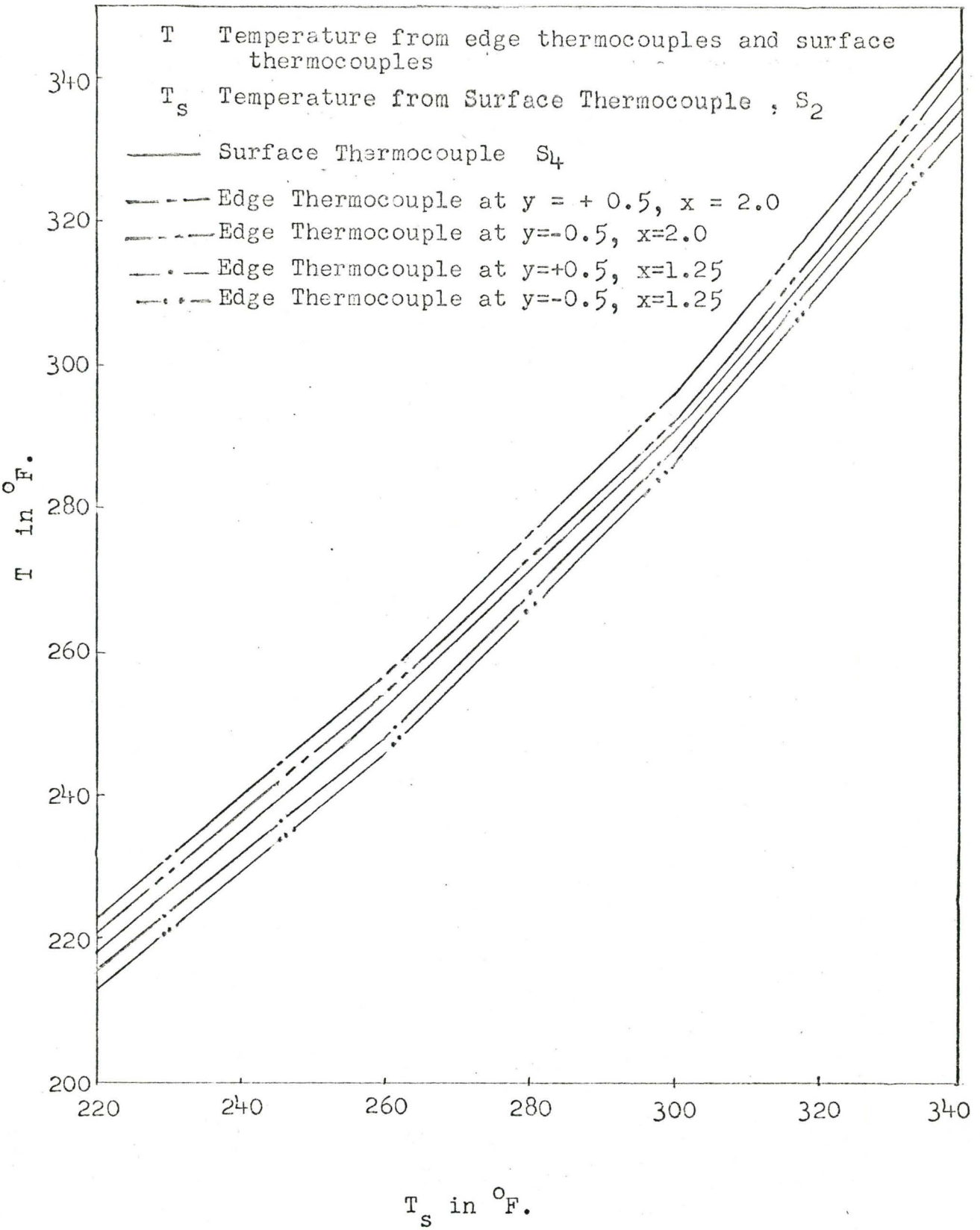

Thermal contact must be established between the sensitive element and the body to insure that temperature corresponds to actual temperature of the body. But the thermal resistance between the sensitive element and the ambient should be as high as possible so as to have negligible heat loss or gain from the surroundings. The effect due to thermal contact depends upon the thermal conductivity of the material of the body, the size of excavation and the degree of thermal contact between the body and the sensitive element. The constantan wire used as thermocouple was of very small diameter (0.005 in.) and the holes drilled are of 0.006 in. The parent material (copper) was silver-soldered to the constantan wire. Excellent thermal contact was expected. The resistance to oxidation and mechanical stresses of these 0.005" diameter constantan wires with immersion length of 0.010 to 0.030 in. is not well known. It is obvious from the experiences of earlier workers (D1,K1,G4) in the field of heat flux meters, that it is quite convenient to use these thermocouples for a sufficient length of time under the conditions that exist in the present experiments with reasonable degree of resistance to oxidation and local stresses. Contrary to the expectations, thermocouples showed very little resistance and could be verified from the disengagement of thermocouple wires from the parent metal (copper) surface. Further from Figure A.14, which shows considerable variation in edge temperature and from the fact that some of the heat flux meter thermocouples failed through oxidation or breaking away at the soldered joint, it can be concluded that the method

of fabrication has to be modified to improve resistance to oxidation and local stresses.

(c) Visicorder

Errors in visicorder can in general be due to:

(i) readability of the chart

(ii) zero reading fluctuation

(iii) sensitivity of the galvanometer.

Readability of the chart was limited to 0.1 cm. in the entire length of 15.0 cms. This amounted to 0.012 m.v. of the heat flux meter output in the range of 0-2 m.v. and 0.050 m.v. of the edge thermocouple output in the range of 4.0 to 10.0 m.v. Maximum zero reading fluctuation to the extent of 0.024 m.v. was observed in heat flux measurement. It was always positive showing higher values in heat flux at the start. This did not vary with the temperature of the boiling surface and hence it may be considered to be due to the internal stray currents. The sensitivity of the galvanometer of the visicorder is $\pm$ 1% (as per the manufacturer's catalogue). However, it varies considerably with the effective impedence of the galvanometer thermocouple circuit. Therefore, the galvanometers were caliberated using a Honeywell potentiometer. Caliberation for M-40-350 galvanometers (3&4) and M-100-350 galvanometers (5&6) are given in Figures A.15 and A.16 and the maximum deviation from the straight fit was $\pm$ 0.04 m.v. and $\pm$ 0.1 m.v. respectively. The heat flux was calculated from the m.v. output using equation (A6). The heat flux meter constant C from equation (A7) was plotted in Figure A.7a.

FIGURE A.15

CALIBRATION OF VISICORDER FOR HEAT FLUX

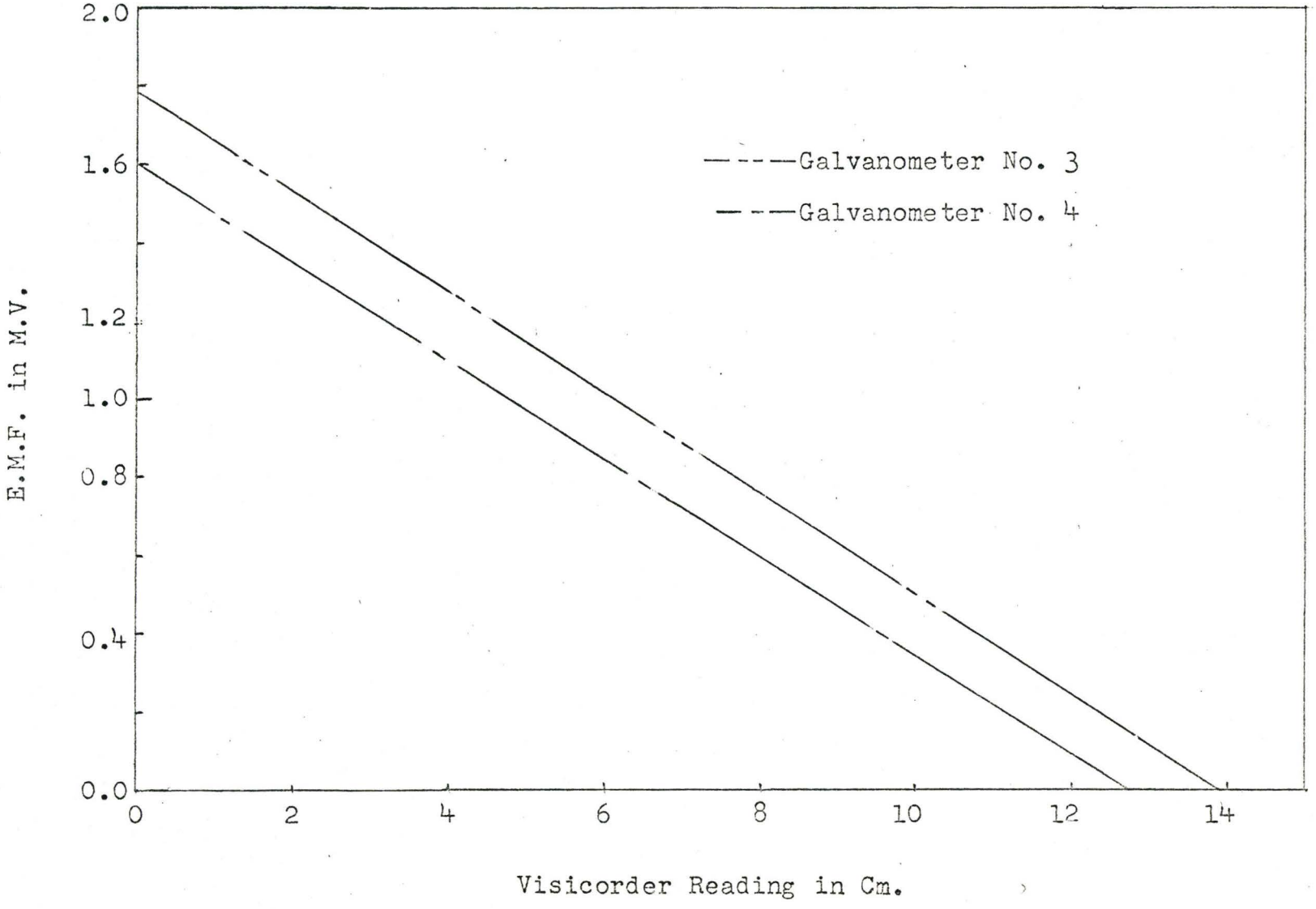

FIGURE A.16

CALIBRATION OF VISICORDER FOR EDGE TEMPERATURE

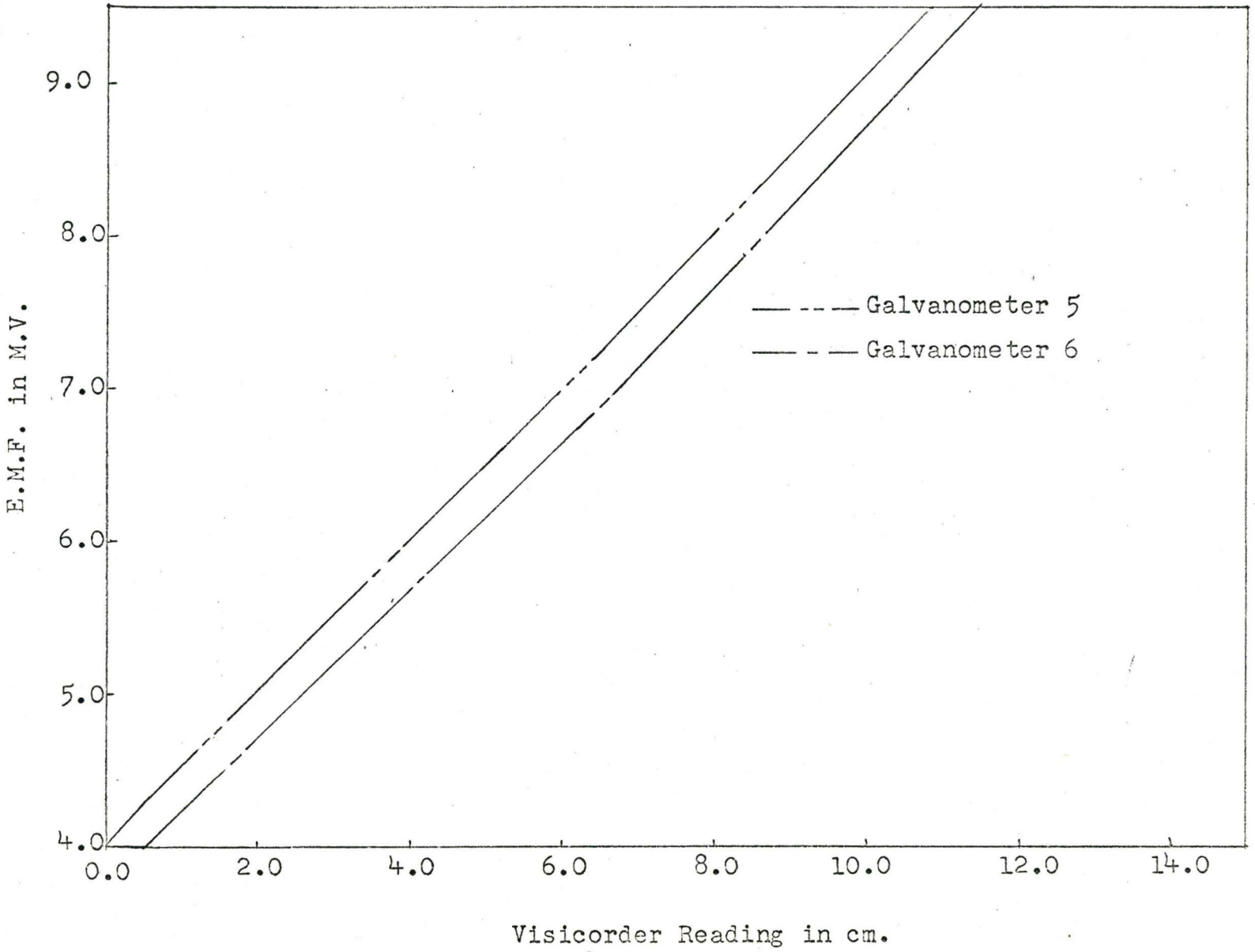

(d) Surface Characteristics

Surface characteristics may significantly alter the heat flux and temperature measurements due to change in the number of nucleating sites, size of nucleating site and contamination on the heating surface as described in detail in Chapter 2. Consideration of these variables was not possible in the present study. However, caliberation was done using the steady and unsteady state pool boiling of water.

APPENDIX II

2. MEASUREMENT OF SURFACE TENSION

Since the middle of the last century, a large number of methods have been proposed for the determination of surface tension. Paddy[P1] considered them recently in the Third International Congress on Surface Activity; an excellent review of these methods is also given by Hansen[H5]. Considering these reviews of Paddy and Hansen on merits and demerits of various methods, pendant drop method was selected. The measurement and calculations are essentially based on the method described by Andreas et al[A1]. Brief descriptions of some of the important methods for measuring surface tension along with some merits and demerits are given below.

(a) capillary rise method, (B2,A6)

(b) drop weight and drop volume method, (A6,A1)

(c) ring method or du Nuoy tensiometer method (O1,P1)

(d) pendant drop method, (A6,P1,A1)

(e) sessile drop method, (A6,S5)

(f) bubble pressure method, (A6,O1)

Among these, except for (b) and (c) which are dynamic methods (meaning that measurements are done at the time of rupture of the surface) all others are static methods in which equilibrium can be attained.

The very fact that capillary methods, ring method, and

sessile drop method involve three phase systems, brings obvious complications. In the pendant-drop and bubble-pressure methods, only the liquid and vapour phases in contact are considered. The du Nuoy tensiometer and capillary rise method have the advantage of rapidity but lack precision due to three phase contacts. This effect is further increased in the case of surface active agents at liquid-air-solid interfaces. In routine determinations where the ring of tensiometer is removed quickly, this error may be small but errors due to non-equilibrium factors may be introduced and make reproducible results difficult to obtain. Sessile drop and bubble pressure methods, may in some occasions be the only possible methods. However complicated calculation and measurement procedures are required (S 5).

All these point to the fact that pendant drop method may give better representative values of surface tension for surfactant solutions. It is very difficult to suspend a droplet of a low surface tension liquid and this makes the pendant drop method difficult to use in these circumstances. This method needed sometimes as much as a half hour for taking the picture and measuring the linear dimensions of the pendant drop which are required in the calculation of surface tension.

The details of the set up used for pendant drop photography is shown in Figure A.17. With a 100 mms lens mounted on an Exacta camera fitted with an extension of about 10 inches by a bellows and an extension tube, a magnification of 2.5X was achieved on the film. The photograph was further enlarged to

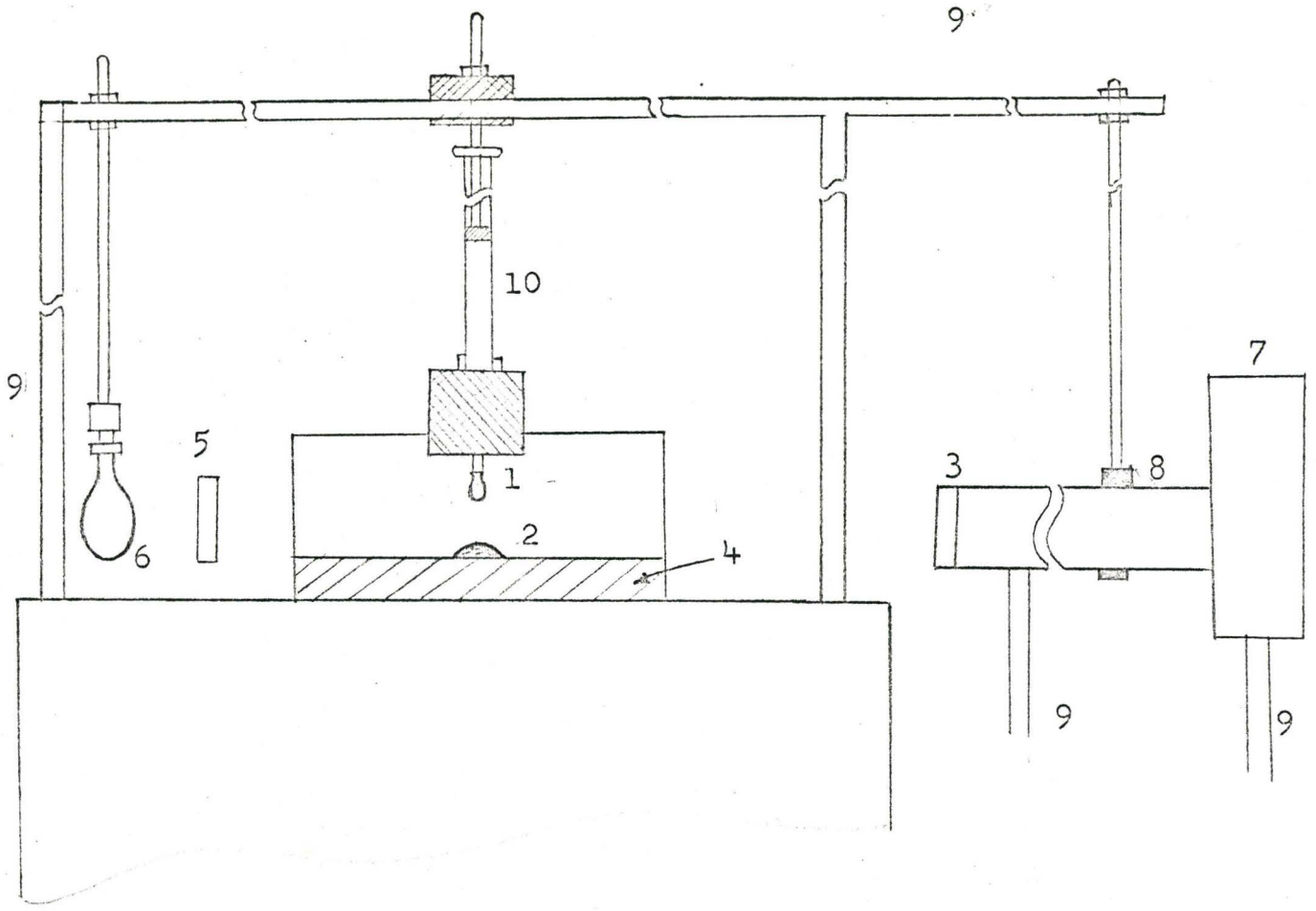

1 - Pendant drop
2 - Sessile drop
3 - Lens (f = 100 mm.)
4 - Boiler Plate
5 - Condenser Lens
6 - Lamp
7 - Exacta Camera
8 - Extension Tube
9 - Supports
10 - Syringe

FIGURE A.17

CONTACT ANGLE AND SURFACE TENSION MEASUREMENT APPARATUS

give a total magnification factor of 35. Kodak ASA 150 high speed, fine grain 35 mm film was used. The surface tension at the boiling point was measured only for a few representative surfactant solutions.

Some of the low surface tension liquids had very unstable pendant drops especially near the boiling point. The surface tension at room temperature was measured for the various surfactant solutions used in the boiling studies. Results have been plotted in Figure 5.3. Ratios of surface tension of the solution whose surface tension was measured near the boiling point, to that measured at room temperature remained almost constant and was of the same order as the ratio of surface tension of water at boiling point to that at room temperature. This is in agreement with the studies by Roll(R5) for similar type of surfactant solutions. Hence the surface tension of solutions at room temperature was considered to be representative of the surface tension at the boiling point for all liquids.

Errors in the measurement may arise out of (i) measurement of linear dimensions of drop, (ii) illumination and focusing (iii) aging of the solution. Leniar dimensions were measured to better than 1% accuracy and standardization with distilled water drops showed deviations of not more than 2%. To account for the aging, about 1 min. was allowed for the drop to attain equilibrium. Surface tension values obtained were generally lower than those obtained with ring tensiometer (R5,W5) but were of the same order.

APPENDIX III

3. MEASUREMENT OF CONTACT ANGLE

There are several methods for determining the contact angle. The application of the method in general depends on the surfaces used, the fluid used and the accuracy needed. Some of the most important methods relative to the systems encountered in boiling heat transfer are:

(i) Harkins and Jura method, (O1,G6)

(ii) Langmuir's Reflection method (L2,B2)

(iii) Zisman's Gonometer method (Z1,O1)

(iv) Poynting and Thompson method (R1,A6)

(v) Fritz's bubble method (F2,S11)

Many of these methods and their modifications are described extensively in literature (A6,B2,O1,G6,F2,S11,L2,Z1). Hence no attempt is made to give the descriptions. Most of these methods are easily applicable to low energy solid surfaces. However, high energy surfaces as encountered in boiling heat transfer presents additional limitations.

A modified form of (i) was used by Griffith and Wallis(G6) and considerable difficulties in the measurement were reported. Further this method cannot be used in our present study because the boiler surface cannot be tilted in a pool of solution. Further this gives contact angle at a particular line of contact along the boiler surface, while the present interest is in the repre-

sentative contact angle measurement in the heat flux meter area. Sessile drop methods seem to be simple and the most suitable for our studies. Hence the methods considered in the present study are (ii), (iii) and (iv). Initially Langmuir's reflection method was considered. The advantage claimed by Langmuir[L2] is a high degree of accuracy. This method was, however, found to be extremely difficult with the existing boiler surface. The difficulties of locating the reflection and adjustment of the microscope increased especially while using surfactant solutions. Using this method initial studies regarding the effect of evaporation and adsorption from sessile drops, on the measurement of contact angle were considered. The results are given in Figure A.18.

The variation of contact angle with concentration of solutions was measured using a modified form of Zisman's method[Z1]. Direct measurement of contact angle in a magnified shadow photograph of a sessile drop was made. The apparatus and procedure for photographing the sessile drop was essentially the same as used for pendant drop as described earlier in Appendix(2). The height of the sessile drop (from the shadow photograph) was used in determining the contact angle by Poynting and Thompson's method* (A6). The contact angle values from this method were used as a check with those obtained by direct measurement. Variation of

---

* which uses the relation $\text{Cos } \theta = \frac{\rho_1 g h^2}{2\sigma_1}$ where h is the height of the sessile drop.

contact angle with concentration for the surfactant solutions are given in Figure 5.4.

Determination of contact angle presents three major sources of error. They are (i) evaporation, volume and aging of sessile drops, (ii) illumination and photography, (iii) surface characteristics like roughness and contamination. Literature review of some of these aspects were considered earlier in Chapter 2. Effect of temperature on contact angle is reported to be negligible (R1). Value of $0.06^{\circ}/C^{\circ}$ was reported. Representative studies of the measurement of contact angle at $98^{\circ}C$. for some solutions, did not show an increase of more than 6°. Further, techniques for measuring contact angle at even lower temperatures need lot of improvement. Hence only a few contact angle measurements at boiling point were done to check the effect of temperature.

To have the idea of some of the problems involved in the measurement of contact angle, initial studies were done using Langmuir method and Poynting and Thompson method. Results are reported in Figures A.18 and A.19. These results give only an order of magnitude analysis. By the very nature of contact angle there may be considerable error in the measurement.

Effect of evaporation seems to be considerable. Even at $25^{\circ}C$. there seems to be considerable difference between closed and open systems for contact angle measurement. Figure A.18 shows the effect of evaporation on contact angle of water on copper surface open to atmosphere. However the effect in closed containers was considerably less and was only of the order of -2° in 5 mins.

FIGURE A.18

EFFECT OF VOLUME AND EVAPORATION

OF SESSILE DROP ON CONTACT ANGLE

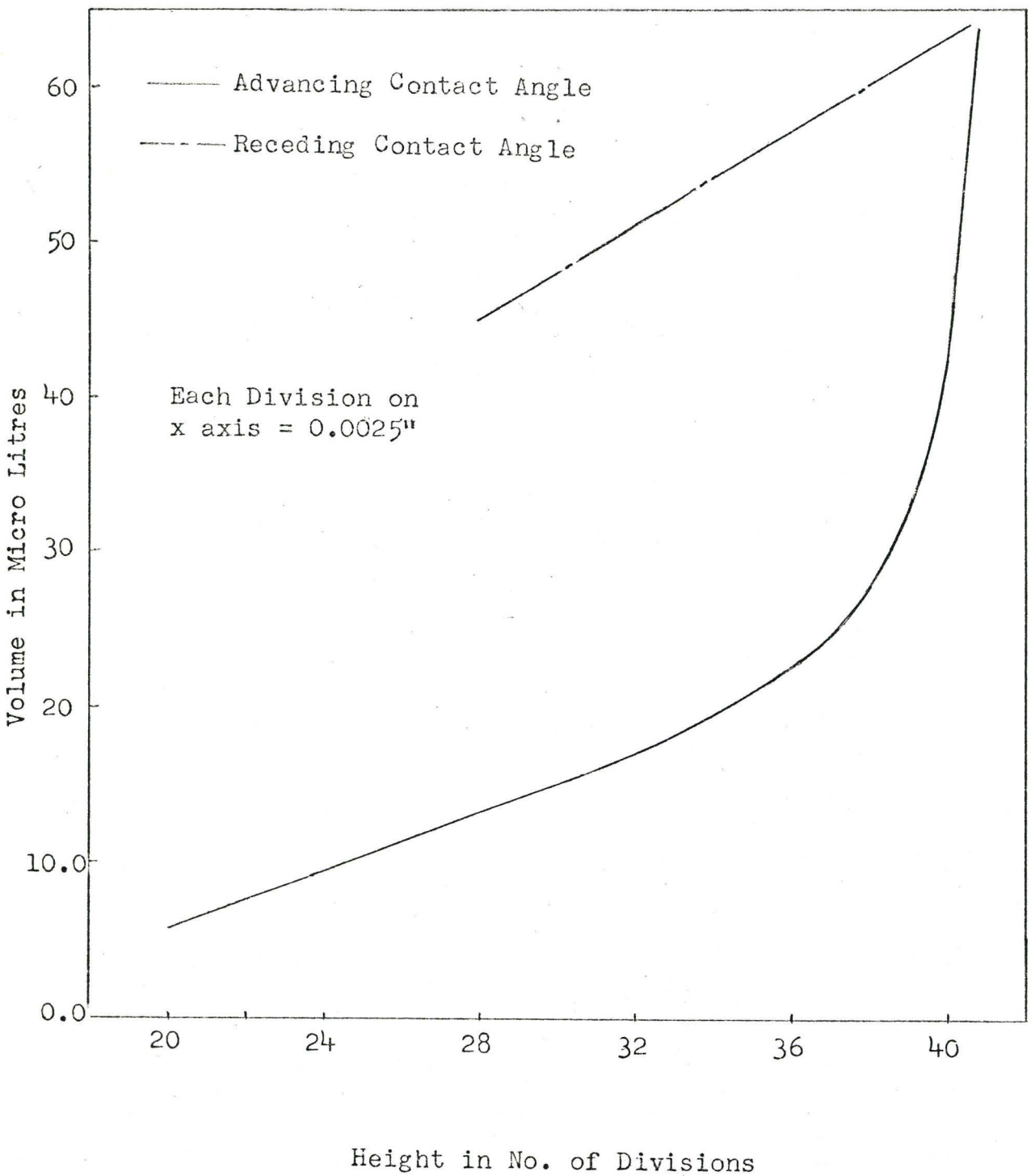

FIGURE A.19

EFFECT OF ADSORPTION AND EVAPORATION

OF SESSILE DROP ON CONTACT ANGLE

(Fresh Copper Surface - 600 Emery Finish)

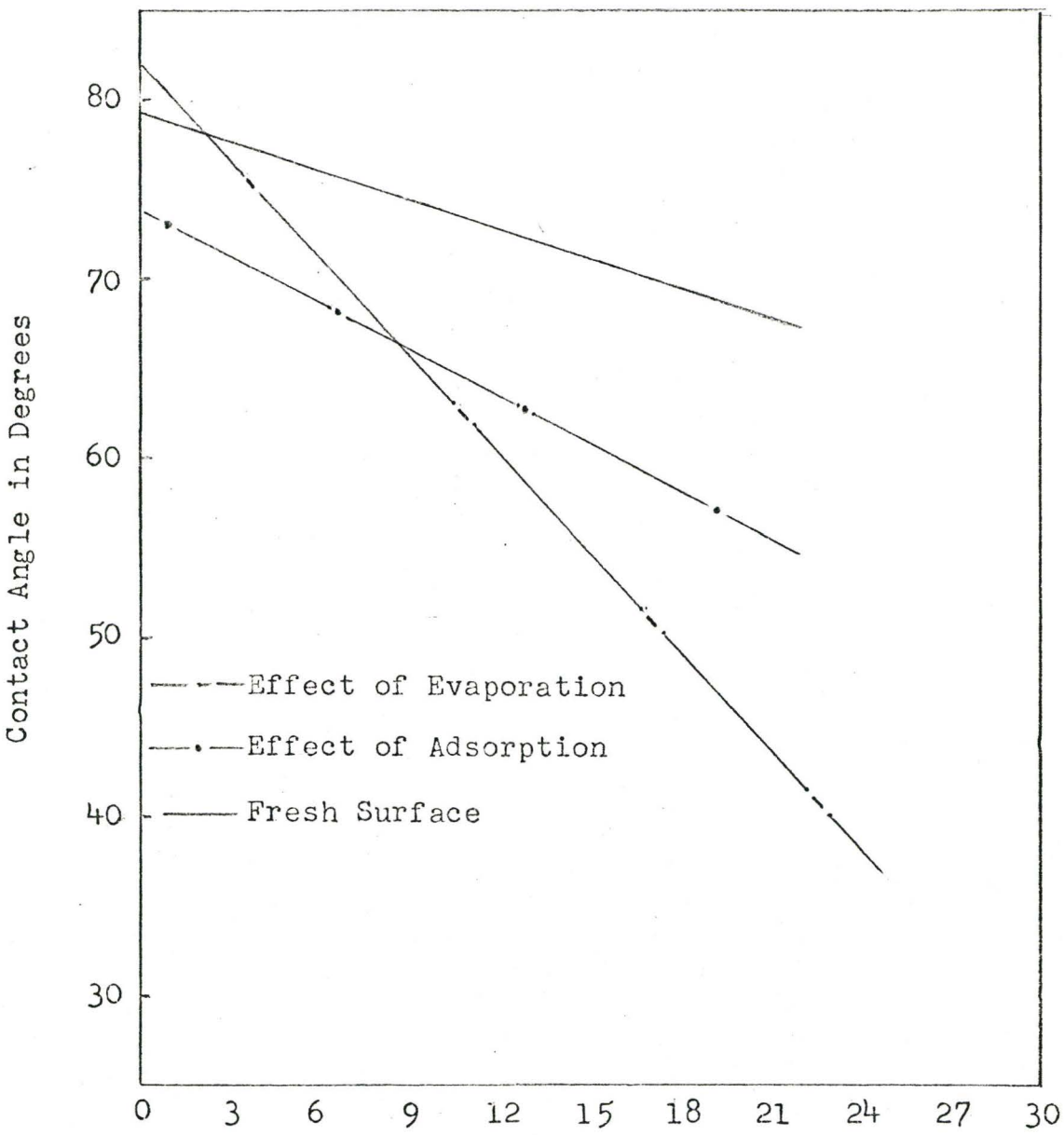

The effect of adsorption on the surface was negligible. It was too difficult to control the evaporation effects.

Errors in contact angle measurement were also observed due to advancing and receding contact angle and volume. These effects were plotted in terms of the height of the sessile drop in Figure A.19. The advancing drop formation with a volume of more than 65 micro litres of water gave stable and large sessile drops for standardization.

Aging of surfactant solutions was one of the most difficult factors (like evaporation) to control. This was a major problem at low concentrations of surfactants. To account for this problem was virtually impossible. Hence the time of measurement of contact angle was standardized at 30 secs. after placing the sessile drop.

APPENDIX IV

1. Statistical Analysis

The results of the pool boiling studies with water and aqueous surfactant solutions were analyzed to find out how much this data is subject to chance error. The t-tests were conducted to test how much of these observed differences between the sets of data for concentration is due to chance. The following table gives the data and the results (data from fig.5.6-5.9)

Average Maximum Heat Flux of Surfactant Solutions

Concentration	Aerosol OT	Aerosol OS	Pluronic L-62	Pluronic F-68
0.010	9.8	11.8	10.6	10.3
0.100	9.3	11.6	7.8	9.6
1.000	8.8	8.5	3.0	6.1
0.000	8.2	8.2	8.2	8.2
Total	36.1	40.1	29.6	34.2
Mean	9.03	10.03	7.4	8.55
Sum of Squares	1.90	11.28	10.2	10.27
s	0.796	1.94	1.84	1.85
n	4	4	4	4

Here it is assumed that the mean of each of the concentrations is u and that the variance of each type of surfactant is the same:

$$t = (x - u)/s/\sqrt{n} \qquad \ldots(A11)$$

where x is the average

u is the assumed mean

s is the standard deviation

n is the degrees of freedom

Using equation (A11) it was observed that 't' values varied from 1.9 to 4.78 at high and low concentrations. Thus with 4 degrees of freedom it can be observed that there is only less than 10% chance that there is no effect of concentration.